

# **Characterization of hyperimmunoglobulins for prevention of maternofetal Cytomegalovirus transmission**

## **Dissertation**

der Mathematisch-Naturwissenschaftlichen Fakultät  
der Eberhard Karls Universität Tübingen  
zur Erlangung des Grades eines  
Doktors der Naturwissenschaften  
(Dr. rer. nat.)

vorgelegt von  
Matthias Stefan Schampera  
aus Heilbronn

Tübingen  
2019

Gedruckt mit Genehmigung der Mathematisch-Naturwissenschaftlichen Fakultät der  
Eberhard Karls Universität Tübingen.

Tag der mündlichen Qualifikation:	07.05.2019
Dekan:	Prof. Dr. Wolfgang Rosenstiel
1. Berichterstatter:	apl. Prof. Dr. Dr. Klaus Hamprecht
2. Berichterstatter:	Prof. Dr. Hans-Georg Rammensee

# Acknowledgment

*„...versuche nicht, ein Mann des Erfolgs zu werden,  
werde stattdessen ein Mann von Wert!“*

*Albert Einstein*

I would like to show my profound gratitude to Dr. Klaus Hamprecht, Dr. Gerhard Jahn, Dr. Thomas Iftner and Dr. Matthias Germer for the opportunity to perform and finish my doctoral studies.

In detail, I would like to thank my PhD supervisor Dr. Klaus Hamprecht for his excellent scientific guidance and caring support during the preparation of my PhD thesis. I am also grateful for the provided options to increase my scientific knowledge during national and international HCMV congresses and meetings of the Society of Virology. I also appreciate the willingness and agreement of Dr. Hans-Georg Rammensee to evaluate my dissertation as second correspondent.

I thank all members of the work group for their collaborative help and I enjoyed the time, working at the Institute of Medical Virology at the University Hospital of Tübingen. At this point, I want to highlight the undoubtedly perfect assistance of the MTAs Wioleta Kapis, Irina Krotova, Veronique Baudy and Karin Kollender, who supported my scientific investigations with their laboratory experiences on the field of practical knowledge.

Furthermore, I appreciate the professional instructions of Edeltraud Faigle and Dr. Katrin Schweizer in handling of infectious material and virological methods at the beginning of my work. In this context, a special thanks goes also to my colleges Katrin Lazar and Lukas Penka for proofreading and stimulating discussions.

I am very grateful for the mental support and love of my family, who kept me on my path to reach this important step in my life which would be impossible for me without any of them.

Finally, I want to give Vanessa Bamberger a special mention in this acknowledgment for her infinite and unconditional love which gave me the strength to overcome exhausting phases. She always stayed by my side and I will spend my life to give this love back to her.

## Abstract

The primary cytomegalovirus infection is the most frequent congenital infection worldwide, potentially leading to disorders of the central nervous system and hearing loss, following maternofetal transmission to the fetus (Picone et al., 2013). In the absence of an effective vaccination against HCMV, the focus should be set on the early identification of HCMV-primary infections in pregnant women, as well as on the determination of risk factors for maternofetal transmission.

Hygiene counseling of seronegative pregnant women was shown to be a very effective tool to reduce the risk of maternal infection and transmission to the fetus by up to 50% (Revello et al., 2015). Hyperimmunoglobulins were reported to be able to reduce the risk of HCMV-transmission during pregnancy after proven HCMV-primary infection of the mother. However, HIGs are controversially discussed in literature (Nigro et al., 2005; Visentin et al., 2012; Revello et al., 2014 and Kagan et al., 2018). Intravenous HIG administrations are still the only available treatment option for women with HCMV-primary infections in combination with early hygiene counseling of both seronegative and seropositive pregnant women, who exhibit an increased risk of HCMV acquisition by intrafamiliar or professional exposure to viral shedding infants below 3 years of age (Hamilton et al., 2014). Actually, there is no recommendation for HIG treatment outside of clinical trials (Rawlinson et al., 2017).

In this PhD thesis, HCMV-specific antibodies in HIG and IVIGs which are directed against UL130 peptides and a recombinant pentameric complex, revealed strong *in vitro* neutralizing capacities (Schampera et al., 2018). Therefore, the vaccine development on the base of the viral pentameric complex could be successful which might lead to a potent vaccine in the future (Gerna et al., 2017).

In a next step, up-coming monoclonal antibodies against PC have to proof their therapeutic value in *in vivo* studies, while *in vitro* results were highly promising, regarding to viral binding, neutralization and prevention of cellular infection, compared to HIG preparation (Ha et al., 2017). The treatment with antibodies and accompanying antiviral drug therapy with VACV in second trimester of pregnancy could further improve the outcome of newborns in cases of maternofetal transmission with low viral load in fetal blood (Leruez-Ville et al., 2016).

Furthermore, the involvement of HCMV-specific CD8<sup>+</sup> T-cells might contribute in future studies of therapy-naive and HIG-treated pregnant women to identify maternal HCMV-transmitters during early pregnancy. In this context, the results in this work suggest, that determination of IFN- $\gamma$  concentration and/or IFN- $\gamma$  producing PBMCs in these mothers could be used as potential surrogate marker, using T-Track EliSPOT CMV® and QuantiFERON CMV®. This could improve the diagnostic prediction for an increased risk of HCMV transmission, after maternal HCMV-primary infection (Saldan et al., 2015).

# Publications

- 2016, Jan:** Müller NF, Schampera MS, Jahn G, Malek NP, Berg CP, Hamprecht K. Case report: severe cytomegalovirus primary infection in an immunocompetent adult with disseminated intravascular coagulation treated with valganciclovir. BMC Infect Dis. 2016 16:19.
- 2017, May:** Schampera MS, Schweinzer K, Abele H, Kagan KO, Klein R, Rettig I, Jahn G, Hamprecht K. Comparison of cytomegalovirus (CMV) specific neutralization capacity of hyperimmunoglobulin (HIG) versus standard intravenous immunoglobulin (IVIg) preparations: impact of CMV IgG normalization. J Clin Virol 2017 90:40–45.
- 2018, Jun:** Kagan KO, Enders M, Schampera MS; Baeumel E, Hoopmann M, Geipel A; Berg C; Goelz R, Wallwiener D, Brucker, S, Adler S, Jahn, G, Hamprecht, K. Prevention of maternal-fetal transmission of very early CMV primary infection by hyperimmunoglobulines. Ultrasound Obstet Gynecol. 2018 doi: 10.1002/uog.19164.
- 2018, Sep:** Schampera MS, Arellano-Galindo J, Kagan KO, Jahn G, Hamprecht K. Role of pentamer complex-specific and IgG 3 antibodies in HCMV hyperimmunoglobulin and standard intravenous IgG preparations. Med Microbiol Immunol. 2018 Sep 10.

# Index

<b>1</b>	<b>INTRODUCTION .....</b>	<b>1</b>
1.1	HUMAN CYTOMEGALOVIRUS (HCMV) .....	1
1.2	TAXONOMY .....	2
1.3	GENOME STRUCTURE AND FUNCTION.....	3
1.4	MORPHOLOGY AND VIRAL ENTRY .....	5
1.5	VIRAL REPLICATION .....	7
1.6	EPIDEMIOLOGY.....	9
1.7	TRANSMISSION AND PATHOGENESIS .....	9
1.8	CLINICAL RELEVANCE .....	10
1.9	CONGENITAL HCMV INFECTION .....	11
1.9.1	MATERNAL PLACENTA AND IGG TRANSFER.....	14
1.9.2	DIAPLAZENTAL HCMV TRANSMISSION .....	17
1.10	HCMV DIAGNOSTICS IN PREGNANCY .....	18
1.11	<i>IN VITRO</i> NEUTRALIZATION ASSAYS.....	21
1.12	PREVENTION OF HCMV PRIMARY INFECTION.....	22
1.12.1	ANTIVIRAL DRUGS.....	22
1.12.1	VACCINES AGAINST HCMV .....	24

1.12.2	HYPERIMMUNOGLOBULIN PREPARATIONS .....	27
1.13	HYGIENE-COUNSELING .....	31
1.14	MONOCLONAL ANTIBODIES AGAINST HCMV .....	32
1.15	OBJECTIVES.....	33
<b>2</b>	<b>MATERIAL AND METHODS.....</b>	<b>35</b>
2.1	TARGET CELLS .....	35
2.2	VIRUS ISOLATES .....	35
2.1	SAMPLES .....	41
2.1.1	NT ASSAY REFERENCE POOLS.....	41
2.2	IGG PREPARATIONS.....	41
2.2.1	HIG CYTOTECT® AND CYTOGAM® .....	41
2.2.2	IVIGS .....	42
2.2.3	UL130 PEPTIDES AND RECOMBINANT PENTAMERIC COMPLEX .....	42
2.3	LABORATORY SYSTEMS.....	44
2.4	REAGENTS AND MATERIALS .....	45
2.4.1	NPCR MASTER MIX FOR GB TYPIFICATION .....	46
2.4.2	BUFFERS .....	47
2.4.3	IMMUNPEROXIDASE SUBSTRATE .....	47
2.4.4	PARAFORMALDEHYDE (PFA) SOLUTION .....	48
2.4.5	GCV-DILUTION SCHEME TO DETERMINATE IC <sub>50</sub> .....	48
2.5	CELL CULTURE AND VIRUS PROPAGATION.....	49
2.5.1	CULTIVATION OF HUMAN CELLS (ARPE-19 CELLS, HFF) .....	49
2.5.2	PASSAGING OF HUMAN CELLS.....	49
2.5.3	CELL COUNTING AND CELL VITALITY TESTING .....	50
2.5.4	CRYOPRESERVATION OF HUMAN CELLS.....	51
2.5.5	REINITIALIZATION OF CRYOPRESERVED CELLS .....	51
2.5.6	VIRUS CULTIVATION .....	51
2.6	TCID <sub>50</sub> DETERMINATION .....	52
2.7	P72 IE-ANTIGEN-IMMUNPEROXIDASE STAINING (IN SITU ELISA).....	54
2.8	<i>IN VITRO</i> NEUTRALIZATION ASSAYS.....	55
2.8.1	STATISTICAL ANALYSIS.....	57
2.8.2	ANALYSIS OF ANTI-VIRAL DRUG RESISTANCE AND NT TESTING.....	57
2.8.3	HCMV-SPECIFIC ANTIBODY DEPLETION STRATEGIES.....	58
2.8.4	IGG 3 SUBCLASS DEPLETION STRATEGY .....	60
2.9	CALIBRATION OF NT ASSAYS USING A PEI REFERENCE STANDARD PREPARATION .....	61
2.10	NORMALIZATION OF THE HCMV-SPECIFIC IGG CONCENTRATION OF HIGS AND IVIGS...62	

2.11	HCMV-SPECIFIC T-CELL MODULATION AFTER HIG ADMINISTRATION OF PREGNANT WOMEN WITH PROVEN HCMV-PRIMARY INFECTION IN T1 .....	63
2.11.1	QUANTIFERON CMV® QIAGEN.....	63
2.11.2	T-TRACK ELISPOT CMV® LOPHIUS .....	64
<b>3</b>	<b>RESULTS.....</b>	<b>66</b>
3.1	STANDARDIZATION OF HCMV NEUTRALIZATION PLAQUE REDUCTION ASSAY (PRA) AND ASSAY PERFORMANCE CHARACTERISTICS .....	66
3.2	CYTOTECT® NEUTRALIZATION ACTIVITY AGAINST HCMV ISOLATES, RESISTANT TO ANTIVIRAL COMPOUNDS .....	72
3.3	CHARACTERIZATION OF CYTOTECT® NEUTRALIZATION ACTIVITIES AGAINST HCMV ISOLATES WITH DIFFERENT GB-GENOTYPES .....	74
3.4	ROLE OF PENTAMER-SPECIFIC ANTIBODIES IN HCMV HYPERIMMUNOGLOBULIN AND STANDARD INTRAVENOUS IGG PREPARATIONS.....	75
3.5	DEPLETION OF HCMV HYPERIMMUNOGLOBULIN IGG SUBCLASS 3 FROM CYTOTECT® AND ANALYSIS OF ITS FUNCTIONAL ACTIVITY .....	80
3.6	MODULATION OF THE T CELL RESPONSE BY HCMV HYPERIMMUNOGLOBULIN .....	81
<b>4</b>	<b>DISCUSSION .....</b>	<b>90</b>
4.1	STANDARDIZATION OF HCMV NEUTRALIZATION ASSAY AND ASSAY PERFORMANCE CHARACTERISTICS .....	90
4.2	CYTOTECT® NEUTRALIZATION ACTIVITY AGAINST HCMV ISOLATES, RESISTANT TO ANTIVIRAL COMPOUNDS .....	99
4.3	CHARACTERIZATION OF CYTOTECT® NEUTRALIZATION ACTIVITIES AGAINST HCMV ISOLATES WITH DIFFERENT GB-GENOTYPES .....	100
4.4	ROLE OF PC-SPECIFIC ANTIBODIES IN IGG PREPARATIONS.....	101
4.5	DEPLETION OF HCMV HYPERIMMUNOGLOBULIN IGG SUBCLASS 3 FROM CYTOTECT® AND ANALYSIS OF ITS FUNCTIONAL ACTIVITY .....	106
4.6	T CELL MODULATION VIA HIG ADMINISTRATION AFTER HCMV PRIMARY INFECTION OF PREGNANT WOMEN.....	109
<b>5</b>	<b>ZUSAMMENFASSUNG.....</b>	<b>119</b>
	DECLARATION ON OATH .....	122
<b>6</b>	<b>REFERENCES .....</b>	<b>123</b>
6.1	LITERATURES .....	123
6.2	UNIFORM RESOURCE LOCATOR.....	144

# List of figures

Figure 1: (A1) uninfected control monolayers of human foreskin fibroblasts (HFF, CRL-2429, ATCC®) 100x; (A2) CPE of HCMV-infected human fibroblasts (HFF, CRL-2429, ATCC®, Strain: H2497) 100x; (B1) uninfected control monolayers of retinal pigment epithelium cells (ARPE-19, CRL-2302 ATCC®) 100x; (B2) (A2) CPE of HCMV-infected human retinal pigmented epithelium cells (ARPE-19, CRL-2302 ATCC®, Strain: H2497) 100x..... 1

Figure 2: Diagram of HCMV genome struture; strain:AD169 (Chee et al., 1990) ..... 3

Figure 3: Overview of gene-coding regions for HCMV (Boeck et al., 2011) ..... 4

Figure 4: Model of a HCMV virion (URL: Education.expasy.org) ..... 5

Figure 5: Model and neutralizing regions of the trimer and pentameric complex (modified after Ciferri et al., 2015) ..... 5

Figure 6: Overview of HCMV replication cycle (modified after Jean Beltran et al., 2014) ..... 7

Figure 7: HCMV seroprevalence rates in adults worldwide (Adland et al., 2015) ..... 9

Figure 8: HCMV-seroprevalence compared to congenital HCMV prevalence worldwide (Manicklal et al., 2013).....11

Figure 9: A breakdown of data for maternofetal HCMV-transmission rates and resulting risk of permanent disabilities of the newborns, depending on maternal HCMV-serostatus and potential symptoms of the fetus (Buxmann et al., 2017).....12

Figure 10: Congenital HCMV cases in the EU-27 (De Vries et al., 2011).....13

Figure 11: Schematic model of maternal placenta and maternofetal blood transfer (modified after Blundell et al., 2016) .....14

Figure 12: Schematic transfer of IgG-antibodies through the placenta, using FcRn receptors (modified after Palmeira et al., 2012) .....16

Figure 13: FcRn-mediated transcytosis of IgG antibodies and HCMV virions given in 3 scenarios (Maidji et al., 2006). .....17

Figure 14: Overview of laboratory diagnostics. Blue font: Constellation of results, red font: Interpretation, green: Interventions; red border: further clarification required (modified after AWMF registration number 0093/001, 2014). .....19

Figure 15: Molecular structure of the novel antiviral drug Letermovir® modified after (Marty et al., 2017).....23

Figure 16: Results of the clinical phase II study, including gB/MF59 (Pass et al., 2009) .....25

Figure 17: Model of the pentameric complex gH/gL/UI128-131 (Ryckman et al., 2008) .....26

Figure 18: First non-randomized HIG study in pregnancy - Primary end point (modified after Nigro et al., 2005). .....27



Figure 19: A randomized controlled trail of HIG to prevent maternofetal transmission. (A) 61 women received HIG. (B) 62 women received placebo (modified after Revello et al., 2014).....	29
Figure 20: (A) Visualized binding sites of generated monoclonal antibodies, separated in 4 immunogenic regions (IRs) using an EM 3D reconstruction of pentameric complex; (B) IC <sub>50</sub> concentrations of generated monoclonal antibodies against the pentameric complex on ARPE-19 and MRC-5 cells (modified after Ha et al., 2017) .....	32
Figure 21: Phylogenetical tree which displayed and confirmed the gB types of the selected HCMV strains.....	38
Figure 22: Example for TB40E-L7 infected HFFs on 1, 3, 5 day post infection (dpi); 200x TCID <sub>50</sub> ; 100x. Light microscope figures compared to fluorescent figures of the same microtiter well (Filter set 38 HE®: Excitation BP 470/40; Emission BP525/50 ZEIZZ).....	40
Figure 23: 6 Tube magnetic separation rack. Product documentation Cell Signaling Technology .....	43
Figure 24: (A) Visualization of death/live cells via trypan blue staining; (B) schematically model of a “Neubauer counting chamber” URL1: modified after Celeromics documents (date: 02.02.2018)” .....	50
Figure 25: Visualization of HCMV-infected cell nuclei (ARPE-19 cells) using p72 IE-antigen-immunoperoxidase staining (160x) .....	54
Figure 26: Example for read out of PFUs ≥10 after 5d incubation (25x).....	56
Figure 27: Read out scheme for the NT assay systems.....	56
Figure 28: HCMV pentameric depletion scheme: two UL130-peptides and a recombinant pentameric complex (Schampera et al., 2018) .....	58
Figure 29: Calibration of the TAN-peptide concentration, revealing the maximal reachable reduction of NT-capacity .....	59
Figure 30: IgG subclass 3 depletion (Schampera et al., 2018).....	60
Figure 31: Calibration of NT assays, using PEI Units and ECLIA Units .....	61
Figure 32: Process of antigen recognition and presenting through APC resulting in IFN-γ production. (Qiagen test principle QuantiFERON CMV® Documentation).....	63
Figure 33: EliSPOT test principle; T-Track EliSPOT CMV® (Modified after URL:Mstechno.co.jp) .....	65
Figure 34: (A1) <i>In vitro</i> NT assay (stock solutions), Target cells: ARPE-19 cells , HCMV strain: H2497-11, Cell culture incubation 5d; (A2) NT <sub>50</sub> PROBIT analysis of the tested IgG-preparations (stock solutions) on ARPE-19 cells; (B1) <i>In vitro</i> NT assay (stock solutions), Target cells: HFF, HCMV strain: H2497-11, Cell culture	

incubation 5d; (B2) NT <sub>50</sub> PROBIT analysis of the tested IgG-preparations (stock solutions) on HFF.....	66
Figure 35: Determination of the average percentage of deviation of the test-dependent <i>in vitro</i> NT-capacity (NT <sub>50</sub> ) between observed results using the NT assays protocol .....	67
Figure 36: (A1) <i>In vitro</i> NT assay (HCMV-IgG normalization), Target cells: ARPE-19 cells , HCMV strain: H2497-11, Cell culture incubation 5d; (A2) NT <sub>50</sub> PROBIT analysis of the tested IgG-preparations on ARPE-19 cells; (B1) <i>In vitro</i> NT assay (HCMV-IgG normalization), Target cells: HFF, HCMV strain: H2497-11, Cell culture incubation 5d; (B2) NT <sub>50</sub> PROBIT analysis of the tested IgG-preparations on HFF .....	68
Figure 37: Transformation of sample dilution into HCMV PEI Unit/ml .....	69
Figure 38: (A1) <i>In vitro</i> NT assay (HCMV-IgG normalization), Target cells: HFF, HCMV strain: TB40E, Cell culture incubation 5d; (A2) NT <sub>50</sub> PROBIT analysis of the tested IgG-preparations on HFF .....	69
Figure 39: <i>in vitro</i> NT assay (TB40 E variant) example figures of analyzed IgG preparations on HFF, sample dilution 1:5000, 50x; (A) HCMV-IgG+pool; (B) Kiovig®; (C) Octagam® (D) Cytotect® (E) Cytogam®.....	70
Figure 40: <i>in vitro</i> NT assay (TB40 E variant) example figures of analyzed IgG preparations on ARPE-19 cells, sample dilution 1:5000, 50x; (A) HCMV-IgG+pool; (B) Kiovig®; (C) Octagam® (D) Cytotect® (E) Cytogam®.....	71
Figure 41: GCV IC <sub>25/50/75</sub> dose analysis of both investigated resistant HCMV strain (H815-06, 40571) .....	72
Figure 42: (A) <i>In vitro</i> NT assay (stock solutions), Target cells: ARPE-19 cells , HCMV strain: H2497-11, Cell culture incubation 5d; (B) <i>In vitro</i> NT assay (stock solutions), Target cells: ARPE-19 cells , HCMV strain: 40571, Cell culture incubation 5d; (C) <i>In vitro</i> NT assay (stock solutions), Target cells: ARPE-19 cells , HCMV strain: H815-06, Cell culture incubation 5d; (D) Meta-analysis of NT <sub>50</sub> -values via JMP software, comparing selected IgG preparations on a drug-sensitive and 2 drug-resistant HCMV strains .....	73
Figure 43: (A) gB type 1 <i>in vitro</i> NT assay (stock solutions), Target cells: HFF, HCMV strain: H1241-16, Cell culture incubation 5d; (B) gB type 2 <i>in vitro</i> NT assay (stock solutions), Target cells: HFF , HCMV strain: AD169, Cell culture incubation 5d; (C) gB type 3 <i>in vitro</i> NT assay (stock solutions), Target cells: HFF, HCMV strain: H1058-10; (D) gB type 4 <i>in vitro</i> NT assay (stock solutions), Target cells: HFF, HCMV strain: H487-06; (E) Meta-analysis of all investigated HCMV strains, using NT50 values via JMP software .....	74

Figure 44: (A1) <i>In vitro</i> NT assay (stock solutions), TAN-peptide antibody depletion, Target cells: ARPE-19 cells, HCMV strain: H2497-11, Cell culture incubation 5d; (A2) NT <sub>50</sub> PROBIT analysis of the tested IgG-preparations (stock solutions) on ARPE-19 cells; (B1) <i>In vitro</i> NT assay (stock solutions), TAN-peptide antibody depletion, Target cells: HFF, HCMV strain: H2497-11, Cell culture incubation 5d; (B2) NT <sub>50</sub> PROBIT analysis of the tested IgG-preparations (stock solutions) on HFF.....	75
Figure 45: (A1) <i>In vitro</i> NT assay (HCMV-IgG normalization), TAN-peptide antibody depletion, Target cells: ARPE-19 cells , HCMV strain: H2497-11, Cell culture incubation 5d; (A2) NT <sub>50</sub> PROBIT of the tested IgG-preparations on ARPE-19 cells after TAN-peptide antibody depletion; (B1) <i>In vitro</i> NT assay (HCMV-IgG normalization), SWS-peptide antibody depletion, Target cells: HFF, HCMV strain: H2497-11, Cell culture incubation 5d; (B2) NT <sub>50</sub> PROBIT analysis of the tested IgG-preparations on ARPE-19 cells after SWS-peptide antibody depletion .....	76
Figure 46: (A1) <i>In vitro</i> NT assay (HCMV-IgG stock solutions), PC antibody depletion, Target cells: ARPE-19 cells , HCMV strain: H2497-11, Cell culture incubation 5d; (A2) NT <sub>50</sub> PROBIT analysis of the tested IgG-preparations on ARPE-19 cells after PC antibody depletion; (B1) <i>In vitro</i> NT assay (HCMV-IgG stock solutions), PC antibody depletion, Target cells: HFF, HCMV strain: H2497-11, Cell culture incubation 5d; (B2) NT <sub>50</sub> PROBIT analysis of the tested IgG-preparations on ARPE-19 cells after PC antibody depletion .....	78
Figure 47: (A1) <i>In vitro</i> NT assay (HCMV-IgG stock solutions), IgG3 depletion, Target cells: ARPE-19 cells, HCMV strain: H2497-11, Cell culture incubation 5d; (A2) NT <sub>50</sub> PROBIT analysis of the tested IgG-preparations on ARPE-19; (B1) <i>In vitro</i> NT assay (HCMV-IgG stock solutions), IgG3 depletion, Target cells: HFF, HCMV strain: H2497-11, Cell culture incubation 5d; (B2) NT <sub>50</sub> PROBIT analysis of the tested IgG-preparations on ARPE-19 cells after PC antibody depletion .....	80
Figure 48: Kinetics of HCMV-IgG and IFN- $\gamma$ production, induced by HIG administration; (A) Mother 1: QuantiFERON CMV® (blue) compared to HCMV IgG ECLIA® (black); (B) Mother 1: Results of the T-Track EliSPOT CMV® (red), compared to HCMV IgG ECLIA® (black); (C) Visualization of T-Track HCMV® IFN- $\gamma$ rPBMCs in microtiter plate with controls and sample .....	82
Figure 49: Kinetics of HCMV-IgG and IFN- $\gamma$ production, induced by HIG administration (A1/B1/C1) Mother 2/3/4: QuantiFERON CMV® (blue) compared to HCMV IgG ECLIA® (black); (A2/B2/C2) Mother 2/3/4: T-Track EliSPOT CMV® (red) compared to HCMV IgG ECLIA® (black) .....	84

Figure 50: Kinetics of HCMV-IgG and IFN- $\gamma$ production, induced by HIG administration (A1/B1) Mother 5/6: QuantiFERON CMV® (blue) compared to HCMV IgG ECLIA® (black); (A2, B2) Mother 5, 6: T-Track EliSPOT CMV® (red) compared to HCMV IgG ECLIA® (black).....	85
Figure 51: Kinetics of HCMV-IgG and IFN- $\gamma$ production, induced by HIG administration; (A1/B1) Mother 7/8: QuantiFERON CMV® (blue) compared to HCMV IgG ECLIA® (black); (A2/B2) Mother 7/8: T-Track EliSPOT CMV® (red) compared to HCMV IgG ECLIA® (black).....	86
Figure 52: Kinetics of HCMV-IgG and IFN- $\gamma$ production, induced by HIG administration (A) Mother 9: QuantiFERON CMV® (blue) compared to HCMV IgG ECLIA® (black); (B) Mother 9: T-Track EliSPOT CMV® (red) compared to HCMV IgG ECLIA® (black); (C) Visualization of T-Track HCMV® IFN- $\gamma$ rPBMCs in microtiter plate with controls and sample.....	87
Figure 53: Longitudinal monitoring of all HCMV Non-Transmitters during the initial 3 HIG applications: (A) Estimated average course of IFN- $\gamma$ concentration (blue); (B) Estimated average course of IFN- $\gamma$ reactive PBMCs (red); (C) Estimated average course of HCMV-specific IgG (black).....	89
Figure 54: Results of the Tuebingen HIG study (Kagan et al., 2018).....	90
Figure 55: Percentage of infected cells (normalized) under the usage of HIG on 4 cell types. Cytogam® was incubated with the low-passage clinical HCMV strain VR1814 (Fouts et al., 2012).....	92
Figure 56: Neutralizing activity of HIGs (Cytotect®▲, Cytogam®■) versus vaccination (gB/MF59; Towne), described as IC <sub>50</sub> titers on fibroblasts (F) and epithelial cells (E) (Cui et al., 2008).....	93
Figure 57: Neutralization titers of HIG preparations Cytotect®/Cytogam® and IVIG preparations 1 and 2 (Germer et al., 2017). ....	94
Figure 58: (A) HCMV-specific IgG, detected by ELISA in PEI U/g IgG for HIGs and IVIGs; (B) Resulting NT activities of HIGs and IVIGs, expressed as PEI U/g IgG (modified after Miescher et al., 2015) .....	95
Figure 59: Comparison of NT activity of HIG and IVIG preparations against the HCMV strains AD169 <sup>wt131</sup> and TB40E-GFP on ARPE-19 (A) and MRC-5 cells (B) (modified after Wang et al., 2017).....	98
Figure 60: Inhibition of infection after Mock, gB, gH/gL or PC antibody depletion on (A) ARPE-19 cells and (B) HFF using Cytogam® (Fouts et al., 2012).....	102
Figure 61: (A) Reduction of binding activity after Mock, gH/gL and PC depletion of Cytogam®, measured in RFU (Relative Fluorescence Units) (B) Corresponding inhibition of infection in ARPE-19 cells (Loughney et al., 2015).....	103

Figure 62: (A) Visualized binding sites of PC-specific monoclonal antibodies, separated in 4 immunogenic regions (IRs) using an EM 3D reconstruction of pentameric complex; (B) IC <sub>50</sub> concentrations of generated monoclonal antibodies against the pentameric complex against 2 laboratory strains (VR1814, TB40/E) and 11 clinical isolates in comparison to HCMV-HIG on ARPE-19 (modified after Ha et al., 2017).....	105
Figure 63: (A) IgG subclass distribution in HIG and IVIGs, (B) Corresponding HCMV-specific IgG and (C) HCMV NT <sub>50</sub> values, according to Planitzer et al., 2011 .....	107
Figure 64: Overview of the functional outcome of Fc-γ receptors: From activation over inhibition to anti-inflammatory activities (modified after Schwab et al., 2013). 109	
Figure 65: <i>In vitro</i> stimulation of PBMCs with viral antigens in the present of HIG Cytotect® (A) CB8+ Cytotoxic T-cells (B) CD4+ T-helper (modified after Deml et al., 2017; ESOT2017 Barcelona Congress, Lophius).....	111
Figure 66: Unstimulated course of IFN-γ after HCMV primary infection compared with HCMV DNA viral load in blood of an immunocompetent patient (van de Berg et al., 2010) .....	112
Figure 67: (A) Correlation between HCMV low IgG avidity and high congenital transmission rate; (B) Correlation between high number of IFNγ-reactive PBMCs and high congenital transmission rate (Saldan et al., 2015).....	114
Figure 68: Comparison between QuantiFERON CMV® and HCMV EliSPOT collected data of pregnant women with and without HCMV primary infection. Bandwidth was 0.8 (modified after Saldan et al., 2016). .....	115
Figure 69: Summarized response of the immune system to HMCV and potential HIG modes of action: (A) responsible for viral neutralization; (B) potential effect on T-cell stimulation; (C) possible modulation of DC maturation; (D) Suggested impact on cytokine secretion (modified after Carbone 2016) .....	117

## List of tables

Table 1: Herpesvirus classification (modified after Davison et al., 2004).....	2
Table 2: Overview of methods is given for direct HCMV detection. When testing follow-up samples using quantitative PCR, the same starting material must always be used for DNA isolation (modified after AWMF registration number 0093/001; 2014). .....	18
Table 3: Overview of methods for the detection of HCMV-specific antibodies (modified after AWMF registration number 0093/001; 2014).....	20
Table 4: Summary of published HCMV neutralization protocols .....	21
Table 5: Overview of antiviral treatment options against HCMV .....	22
Table 6: Overview of vaccine candidates in clinical trials (modified after Poltkin et al., 2018) .....	24
Table 7: Summarized results of the studies Buxmann and Visentin 2012. ....	28
Table 8: Overview of the used HCMV strains with drug resistance, tested in NT assays .....	36
Table 9: Overview of the HCMV strains used with different gB types, tested in NT assays...	37
Table 10: Extracted UL55 sequences of gB type 1 to 4 with corresponding accession number and protein ID (upload date: 2016) (Murthy et al., 2011) .....	37
Table 11: nPCR gB primer pairs .....	38
Table 12: gB typification via enzymatic digestion after PCR. Predicted band patterns in bps for the used restriction endonucleases .....	39
Table 13: Manufacturer specifications of HIGs .....	41
Table 14: IVIGs specifications .....	42
Table 15: The UL130 peptide design on the base of Saccocio et al., 2011 .....	42
Table 16: Scheme for TCID <sub>50</sub> determination; CC = cell control; VC = virus control .....	52
Table 17: TCID <sub>50</sub> calculation example .....	53
Table 18: Biochemical specifications of the PEI HCMV-IgG reference .....	61
Table 19: Normalization of HCMV-specific IgG concentration using the HCMV <sup>+</sup> pool as reference .....	62
Table 20: Included HLA antigens which covering >98% of human population. ....	64
Table 21: ELCIA HCMV® Roche analysis; Comparison of PC-depleted samples to native samples of Cytotect® (1:15) and HCMV-IgG+pool (1:5).....	79
Table 22: Data overview of HIG-treated pregnant women, included in this study. The mothers were sorted on the number of administrated HIG applications .....	81
Table 23: Variations in Lots of HIG (A) and IVIG products (B –I), considering anti-HCMV binding activity and avidity index in comparison to the PEI reference standard 1996 (modified after Wang et al., 2017) .....	97

## List of abbreviations

AEC	3-amino-9-ethylcarbazol
ADCC	Antibody dependent cellular cytotoxicity
ADCD	Antibody-dependent complement deposition
APC	Antigen-presenting cells
ARPE-19	Adult Retinal Pigment Epithelial cell line-19
Cav	Caveosomes
CD	Cluster of differentiation
CDV	Cidofovir®
CLIA	Chemoluminescence linked immuno absorbent assay
CMI	Cell mediated immunity
CMIA	Chemoluminescence micro particle assay
CPE	Cytopathic effect
Da	Dalton
DC	Dendritic cells
dpp	Day post partum
DMEM	Medium Dulecco´s Modified Eagle Medium
DMSO	Dimethyl-sulfoxide
DNA	Deoxyribonucleic acid
dNTP	Deoxyribonucleotide triphosphate
DOT	Day of treatment
EBV	Epstein Barr Virus
ECLIA	Electro-chemiluminescence immunoassay
EDTA	Ethylenediaminetetraacetic acid
eGFP	Enhanced green fluorescent protein
ELISA	Enzyme Linked Immunosorbent Assay
FBS	Fetal bovine serum
Fc	Fragment crystallizable
FcRn	Neonatal Fc-receptor
FDA	Food and Drug Administration
FOS	Foscarnet®
g	Glycoprotein
HCMV	Human Cytomegalovirus
HFF	Human foreskin fibroblast
HHV 5	Human Herpesvirus 5
HHV 6	Human Herpesvirus 6
HHV 7	Human Herpesvirus 7

HIG	Hyperimmunglobulin
HSV	Herpes Simplex Virus
IC <sub>50</sub>	Half maximal inhibitory concentration
IE	Immediate early
IL	Interleukin
IFN	Interferon
IR	immunogenic region
IVIG	Standard intravenous immunoglobulin
GCV	Ganciclovir®
LiHep	Lithium-heparin
Mφ	Villus core macrophages
mAbs	Monoclonal antibodies
MF59	Microfluidized adjuvant
MHC	Major histocompatibility complex
MW	Molecular weight
NCBI	National Center for Biotechnology Information
NK	Natural killer
nPCR	Nested polymerase chain reaction
ns	Not significant
NT	Neutralization
ORF	Open reading frame
pABs	Polyclonal antibodies
PBS	Phosphate buffered saline
PBMCs	Peripheral blood mononuclear cells
PC	Pentameric complex
PFA	Paraformaldehyde
PFU	Plaque forming unit
POD	Peroxidase
pp	Phosphoprotein
PRA	Plaque reduction assay
rAh	Relative air humidity
RPE	Retinal pigment epithelial cells
rPBMCs	Reactive peripheral blood mononuclear cells
RT	Room temperature
SCT	Stem cell transplantation
SD	Standard deviation
T1	First trimenon
Taq	Thermus aquaticus



TBE	Tris-borate-EDTA
TBS	Tris buffered saline
TC	Trimer complex
TCID <sub>50</sub>	Tissue culture infective dose 50%
TLR	Toll-like receptor
TNF	Tumor necrosis factor
UL	Unique long
US	Unique short
USA	United States of America
UKT	University Hospital of Tuebingen
VACV	Valaciclovir®
VGCV	Valganciclovir®
VZV	Varicella Zoster Virus
WHO	World Health Organization

# 1 Introduction

## 1.1 Human Cytomegalovirus (HCMV)

HCMV was firstly described in the year 1881 by the pathologist Dr. Moritz Wilhelm Hugo Ribbert. He characterized the histo-morphology of HCMV in the year 1904 for the first time. However, the isolation of the functional virus and its DNA succeeded in cell culture by Smith, Rowe and Weller in the years 1956 and 1957, three years after the discovery of DNA itself by Watson and Crick. The age of the human-related virus is estimated at about 80 million years (McGeoch et al., 1995).

The cytomegaly (Greek: *cyto*-, "cell", and *megalo*-, "large") is an atypical enlargement of cells which are infected with HCMV. The infected cells show sloughing, endoplasmic vesicles inside the cells and detach from the cell culture matrix. (Goodpasture, 1920). The viral infection cycle may lead to a complete lysis of the cells, while the degree of the infection is described by the cytopathic effect (CPE) in cell culture (Knowles, 1979). Figure 1 illustrates the appearance of multiple CPEs in human foreskin fibroblasts (HFF) and human retinal pigmented epithelium cells (ARPE-19 cells).

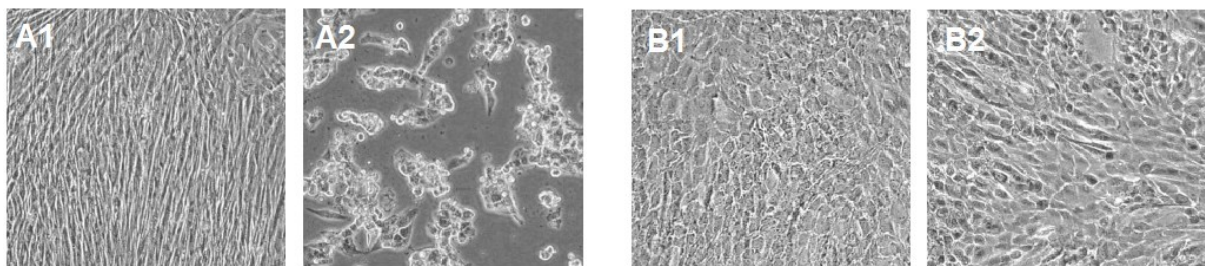


**Figure 1: (A1) uninfected control monolayers of human foreskin fibroblasts (HFF, CRL-2429, ATCC®) 100x; (A2) CPE of HCMV-infected human fibroblasts (HFF, CRL-2429, ATCC®, Strain: H2497) 100x; (B1) uninfected control monolayers of retinal pigment epithelium cells (ARPE-19, CRL-2302 ATCC®) 100x; (B2) (A2) CPE of HCMV-infected human retinal pigmented epithelium cells (ARPE-19, CRL-2302 ATCC®, Strain: H2497) 100x**

## 1.2 Taxonomy

HCMV is a member of the Herpesviridae family and is defined as human herpesvirus 5 (HHV-5) (Roizmann et al., 1992). The Herpesviridae family counts 8 members which includes Herpes-Simplex-Virus Type 1 and 2 (HSV), Varicella Zoster Virus (VZV) and Epstein-Barr-Virus (EBV), as well as HHV-6 to 8. The characteristic attribute of this virus family is the generation of life-long latency after successful infection of the host with different tissues as site of persistence like liver, kidney, lung, heart, pancreas and bone marrow (Koffron et al., 1997).

**Table 1: Herpesvirus classification (modified after Davison et al., 2004)**

Herpesvirus	Abbreviation		Genome size (kb)
	Common	Formal	
<b><math>\alpha</math>-Herpesviridae</b>			
Simplexvirus	HSV-1	HHV-1	152
Herpes Simplex Virus type 1	HSV-2	HHV-2	155
Herpes Simplex Virus type 2			
Varicellovirus			
Varicella Zoster virus	VZV	HHV-3	125
<b><math>\beta</math>-Herpesviridae</b>			
Cytomegalovirus	HCMV	HHV-5	227-236
Roseolovirus			
Human herpesvirus type 6	HHV-6	HHV-6	159-162
Human herpesvirus type 7	HHV-7	HHV-7	144-153
<b><math>\gamma</math>-Herpesviridae</b>			
Lymphocryptovirus			
Epstein-Barr-Virus	EBV	HHV-4	172-173
Rhadinovirus			
Human herpes type 8	HHV-8	HHV-8	134-138

The Herpesviridae family can be divided into  $\alpha$ -,  $\beta$ - und  $\gamma$ -Herpesviruses. These subclasses differ in several biological attributes which includes differences in replication cycle, tissue pathogenicity and host specificity. HCMV belongs together with HHV-6 and HHV-7 to the  $\beta$ -Herpesvirus family. Characteristics for this family are high host specificities and slower replications cycle compared to other herpes families ((Roizmann et al., 1981; Stinski et al., 1983; Ho et al., 1991).

### 1.3 Genome structure and function

The genome of HCMV has a linear, double-stranded DNA which consists of about 192 “open reading frames” (ORFs) with approximately 750 translational products (Stern-Ginossar et al., 2012). Therefore, it counts to the largest species among human Herpesviruses with a number of approximately 230.000 bps in general. At this point, wild type strains have to be differentiated from laboratory strains, as well as low passage *in vitro* strains like Toledo from high passage *in vitro* strains like Towne. The size and composition of the genome may differ, depending on their mutation profile, in context of cell tropism and potential drug resistance. For instance, a high passage strain adapts to *in vitro* cell culture, by spontaneous mutation of unnecessary or unused genes to improve their replication efficiency. However, they lose the ability to infect other cell types like the high passage strain AD169 which was highly propagated on fibroblasts and is unable to infect epithelial cells any more since a mutation of the specific binding receptor occurred (Wilkinson et al., 2015).



**Figure 2: Diagram of HCMV genome structure; strain:AD169 (Chee et al., 1990)**

The viral genome of HCMV can be divided into a short and a long subunit in general which are described as „unique short“ (US) and “unique long” (UL) (Fig.2). Each subunit is bordered by „terminal inverted repeats“ (TRL, TRS) and “internal inverted repeats“ (IRL, IRS). For the US segment the coding reading frames are defined as US1–US36 and for the UL segment from UL1 to UL150 (Chee et al., 1990).

In detail, 165 protein coding genes of HCMV with different functions were identified for the genome of the Merlin strain (Dolan et al., 2004). Figure 3 shows a general overview of gene-coding regions for HCMV. There are diverse genes which code for entry-related proteins, inhibitors or are associated with antiviral resistance like UL97 and UL54 (Boeckh et al., 2011; Douglas et al., 1997 and 1998).

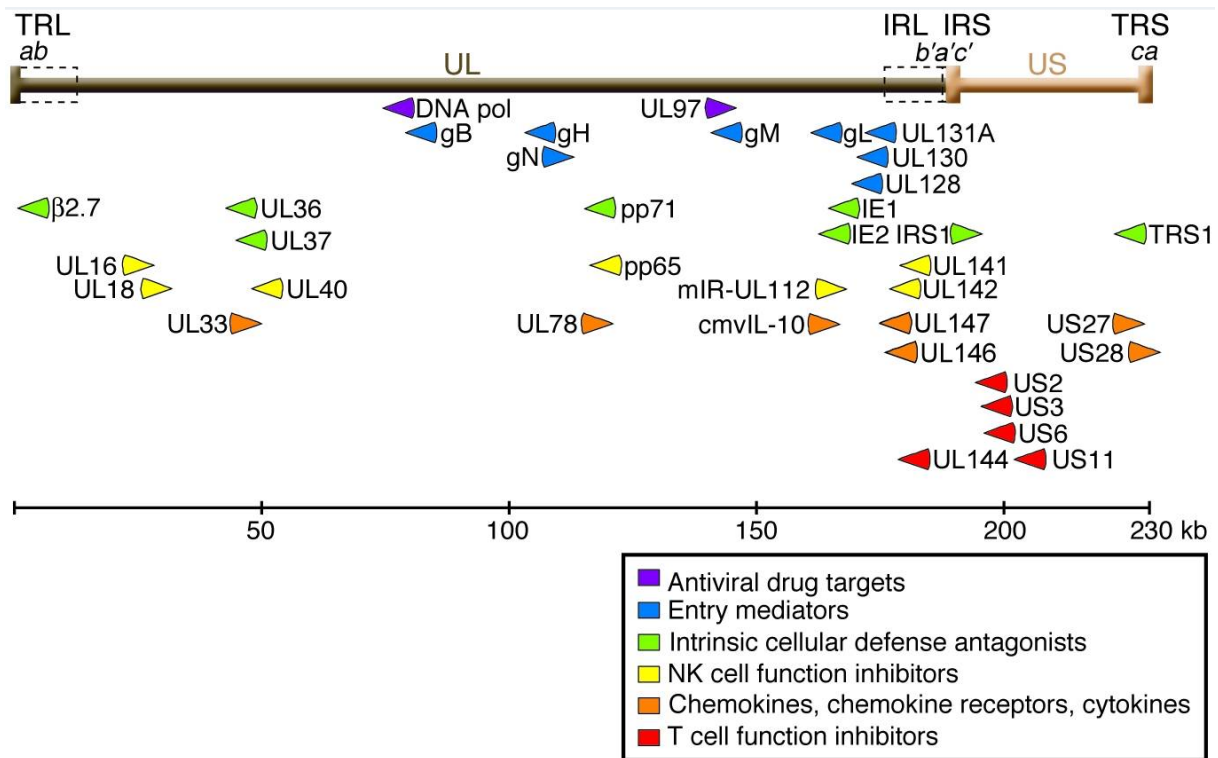


Figure 3: Overview of gene-coding regions for HCMV (Boeckh et al., 2011)

## 1.4 Morphology and viral entry

The outer diameter of HCMV is about 150 to 200 nm. Therefore, it counts to the largest known human pathogenic viruses. The genome of HCMV is enclosed by an icosahedral capsid (T16 symmetry) with an inner diameter between 100 to 110 nm and 162 capsomeres. The viral capsid is surrounded by an amorphous inner and outer tegument. It contains several phosphoproteins (pp) (Fig.4). For example, the phosphoproteins pp65, pp71 and pp150 form an essential part of those proteins (Varnum et al., 2004).

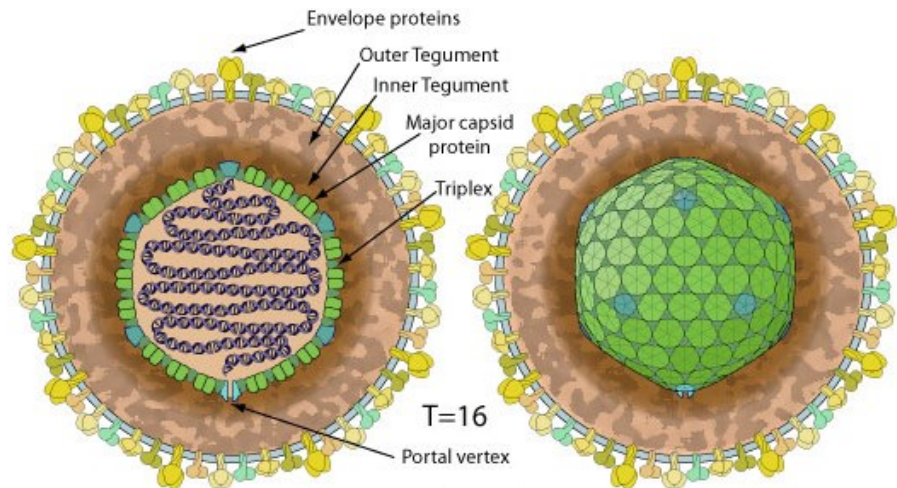


Figure 4: Model of a HCMV virion (URL: Education.expassy.org)

The typical shape of a herpes virus consists of an envelope with a lipid bilayer from the host cell. In addition, there are viral glycoproteins (g), localized on the surface of the virus. They are described as gM, gN, gO, gH, gL and gB. There are also a trimer complex (TP) and a pentameric complex (PC) which play an important role in receptor recognition and viral entry into different cell types.

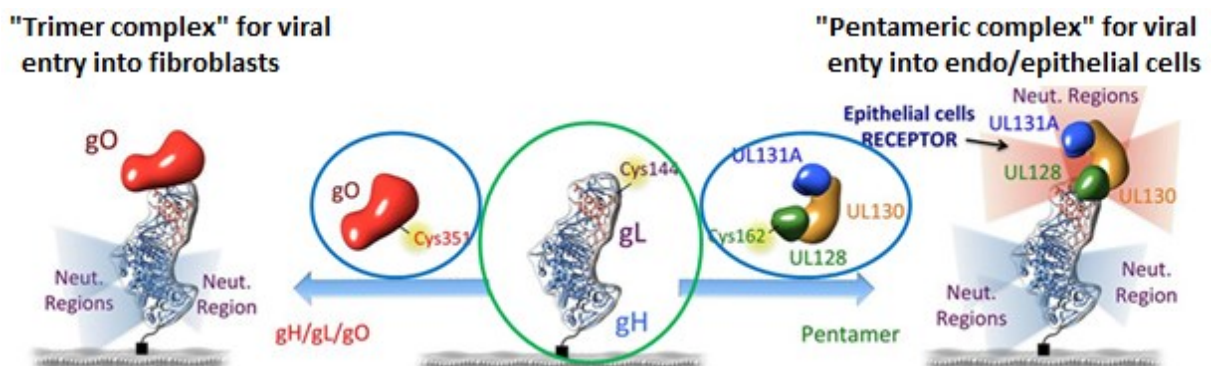


Figure 5: Model and neutralizing regions of the trimer and pentameric complex (modified after Ciferri et al., 2015)

The trimer and the pentameric complex contain the same sub unit (gH/gL) which is formed by gH and gL (green circle). The trimer complex additionally contains gO and the pentameric complex has the UL128 to 131A region (short: UL128L (L= locus)) (blue circles) (Fig.5) (Ciferri et al., 2015). The pentameric complex plays a key role in successfully entry of HCMV into both epithelial and endothelial cells, especially in context of maternofetal transmission (Tuzigov et al., 1998; Wang et al., 2005; Ryckman et al., 2008, Fouts et al., 2012). It was observed, that single mutations spontaneously occurred in the UL128-131A gene region after a few *in vitro* passages of HCMV wildtypes strains (WT) in human fibroblasts which disrupts the epithelial and endothelial tropism (Sinzger et al., 1999; Hahn et al., 2004).

Moreover, it was demonstrated, that an overexpressed gHgL-UL128-131A complex is involved in viral entry into epithelial cells which does not appear in fibroblasts, supporting the suggestion, that PC is a cell-type dependent viral complex (Wang et al., 2005; Ryckman et al., 2008; Lilleri et al., 2013). The entry into fibroblasts is mainly mediated by the trimer complex gH/gL/gO together with gB as fusion protein. (Compton et al., 1992; Li et al., 1992; Huber et al., 1998; Isaacson et al., 2009; Vanarsdall et al., 2011). The glycoprotein O has a high level of glycosylations and interferes covalently with gH and gL (Huber et al., 1997; Wang et al., 2005<sup>1</sup>).

However, latest results indicate, that the fusion protein gB (UL55) together with gH/gL/gO are generally responsible for viral entry in many different or maybe all cell types, considering comparable homologies to others herpes viruses as proof of evidence (Stegmann et al., 2017). The pentameric complex is additionally necessary for the specific entry into epithelial, endothelial and also myeloid cells, besides gH/gL/gO and gB (Connolly et al., 2011; Zhou et al., 2015; Heldwein et al., 2016). But many points of the HCMV-specific entry mechanism, especially how the pentameric complex interacts with the target cells are still unknown.

The trimer and the pentameric complex have a higher frequency on the HCMV surface than gH/gL dimers (Zhou et al., 2013). At the same time, viral structures like glycoproteins are immunogenetic points of particular importance, especially for the immune response in form of antigen presentation and antibody production (Britt et al., 1996).

The phospho-protein pp65 has been reported to possess an immunological function as an essential antigen for the cellular immune response, especially for the MHC-1 antigen presentation path way to activate CD8+ T-cells which control an HCMV infection effectively by proliferation and precisely killing of virus-infected cells (Britt et al., 1986; Jahn et al., 1987).

The phospho-protein pp71 shows comparable immunogenic properties in T-cell activation and mediates the expression of early viral genes as transactivator. The pp71-dependent induction and transcription of these „immediate early (IE) genes“ initiates the first part of the lytic replication cycle which finally ends with the release of infectious HCMV virions from the dying cell (Liu & Stinski, 1992). Furthermore, pp150 exhibit a very high amount of phosphorylations which gathers a highly immunogenic potential. Therefore, it can be used in HCMV immunoblot assays and obtains a diagnostic character, as well as the glycoprotein gB2 (Jahn et al., 1987).

## 1.5 Viral replication

While the attachment of HCMV to the target cell via viral glycoproteins to the cell receptors is well described, the mechanism of viral entry itself is not fully understood. The mediated entry depends on the target cell type, in which HCMV invades using either endocytosis or fusion at the cell membrane (Fig. 6A). In the next step, the viral proteins of the tegument facilitate the intracellular release and transport of the viral capsid to the cell nucleus, using the microtubule machinery of the cell. Then, the viral DNA is transferred into the nucleus through nuclear pores (Fig. 6B).

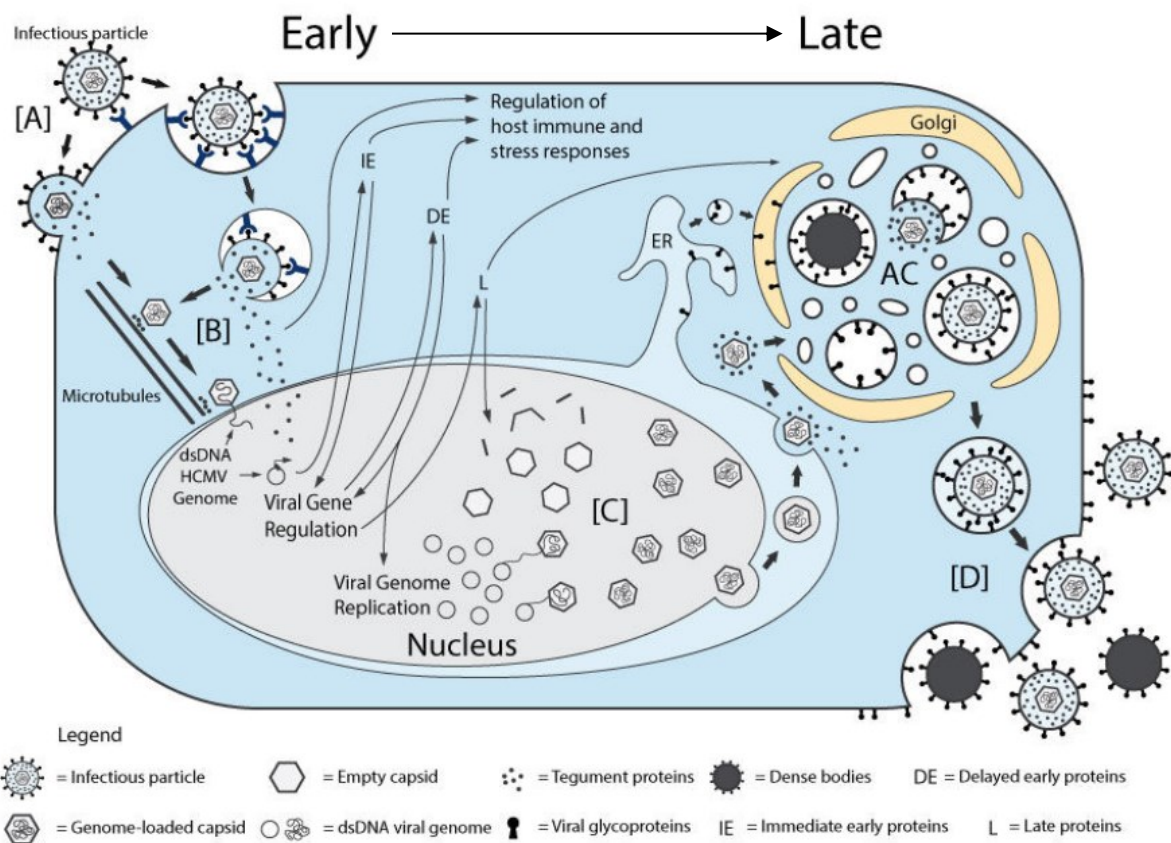


Figure 6: Overview of HCMV replication cycle (modified after Jean Beltran et al., 2014)

The replication cycle can be subdivided by time-dependent expressed genes of the virus which involve immediate early (IE), delayed early (DE) and late (L) genes. The IE and DE genes are



mainly responsible for transcriptional regulation of modulatory proteins which promote the viral DNA replication in the cell nucleus. As additional function, they also shut down the innate immune response of the host, protecting the viral replication (Fig.6C).

Interestingly, HCMV possesses its own functional DNA polymerase, but uses the cellular RNA polymerase II for viral mRNA synthesis (Snaar et al., 1999). The L genes regulate the production of structural proteins and the assembly of the capsid in the nucleus, followed by passaging through the endoplasmic reticulum (ER) into the cell plasma. On its further way from the ER and Golgi to the final release at the plasma membrane, it acquires its tegument and viral envelope which include the earlier described viral proteins (Fig.6D).

HCMV also established persistence after infection in different cell tissues which can be inactive for decades. At this point, attention should be paid to the fact, that one single individual can acquire and carry several different HCMV strains in different organs or tissues during a lifetime. The “de novo” viral replication can be triggered by various events, like oxidative stress or immune suppression after transplantation (Jean Beltran et al., 2014).

## 1.6 Epidemiology

HCMV is a ubiquitous human pathogenic virus with a seroprevalence of >95% in several countries. The percentage of the population which is infected with HCMV differs in each country and depends on manifold factors like geographic location, ethical and sexual behavior, as well as on social and economic conditions (Fig.7) (Adland et al., 2015). A general tendency to a lower prevalence of HCMV was observed in industrialized countries compared to developing countries. However, it has to be considered, that worldwide data for all countries are not available (Mocarski et al., 2007).

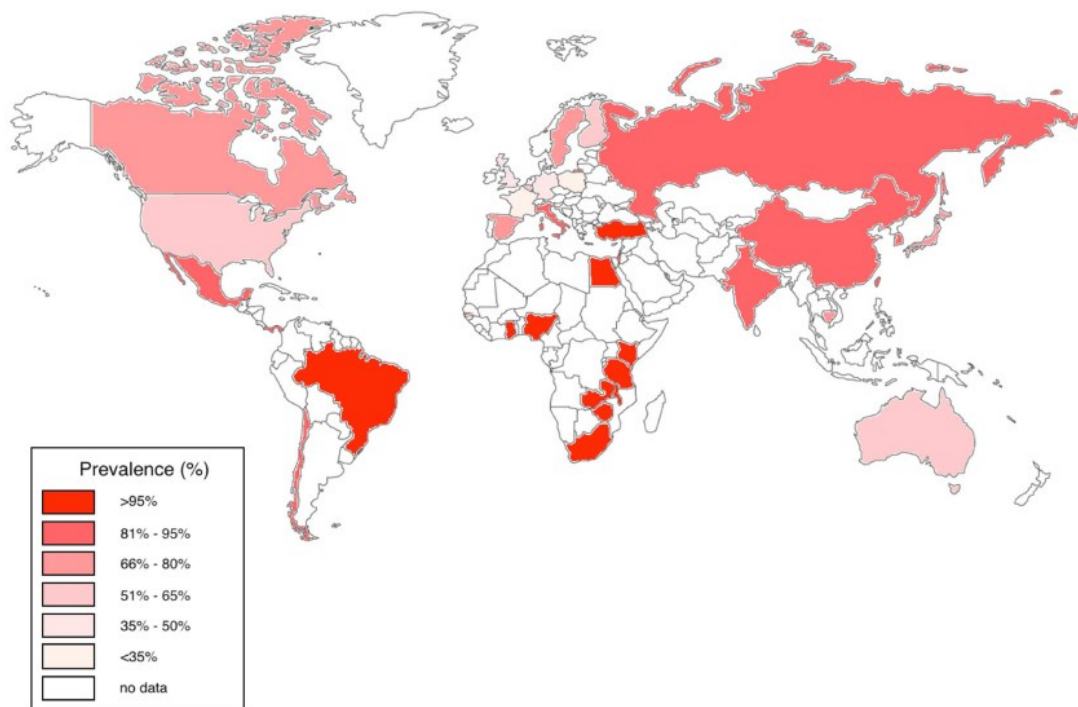


Figure 7: HCMV seroprevalence rates in adults worldwide (Adland et al., 2015)

## 1.7 Transmission and pathogenesis

HCMV cannot cross species and can be transmitted via both the horizontal person-to-person and vertical mother-to-child infection path way. The horizontal transmission needs the direct contact of “open wounds” or mucosa with infectious body fluids like blood, urine or saliva, as well as sperm and vaginal secretion. The typical entry gates for HCMV are epithelial cells of the respiratory-, gastrointestinal- and urogenital tract.

In addition, virus-contaminated blood may promote the transmission of HCMV, as well as transplantations of exogenous organs, tissue or bone marrow.

HCMV is able to invade macrophages which are part of the innate immune system (Sinzger et al., 1995 and 1996; Sinzger & Jahn, 1996). During infection, the virus shows a characteristic cell-to-cell spread, but also disseminates through the hematogenic path way (Rinaldo et al., 1977). An interesting fact is, that the viral replication rate is generally slower in epi- and endothelial cells than in fibroblasts which is typically for Herpesviruses (Kahl et al., 2000).

In contrast, the vertical mother-to-child infection may take place prenatally during pregnancy through placentally transmission, perinatally during birth over maternal blood contact to the fetus or postpartum, including breast feeding. (Reynolds et al., 1973; Lang et al., 1975 and Stagno et al., 1982). In general, the infection and reinfection with HCMV is asymptomatic in immune competent patients and pregnant women. In rare cases, symptoms of a mild cold are reported, followed by headaches, fatigue and lassitude, combined with light fever (Cohen et al., 1985; Jordan et al., 1973).

## **1.8 Clinical relevance**

HCMV holds its clinical importance in immune compromised patients after transplantation, as well as during and after pregnancy. This thesis will focus on the viral transmission during pregnancy after HCMV primary infection, especially in the first trimenon (T1). In addition, HCMV was found postpartum during lactation in breast milk of seropositive mothers in up to 85% of cases and transmitted in 35% cases to the newborns. While the viral infection of term infants is generally asymptomatic, neutropenia, thrombocytopenia and sepsis like symptoms may occur in high risk preterm infants with a birth weight of <1000g and a gestational age under 30 weeks (Vochem et al., 1998; Maschmann et al., 2001; Jim et al., 2004; Hamprecht et al., 2005 and 2008; Capretti et al., 2009).

## 1.9 Congenital HCMV infection

HCMV has an incidence of congenital infection of about 0.2-2% in all live births. The maternofetal HCMV transmission can be highlighted as most frequent intrauterine viral infection with 30 to 40% cases worldwide. During course of pregnancy, the transmission rate to the fetus increases from ~9% preconceptionally to ~65% in the last trimester of pregnancy (Picone et al., 2013). While the HCMV primary infection is mostly asymptomatic for the mother, the intrauterine transmission may cause fulminant and permanent central nervous system disabilities (Manicklal et al., 2013). However, the degree of severity of the clinical outcome depends on manifold factors like dose and time point of infection and extension period of transmission to the fetus, as well as on the immune response of the mother. In particular, the T-cell response can strongly differ between individuals, as previously reported (Jackson et al., 2014; Klenerman et al., 2016).

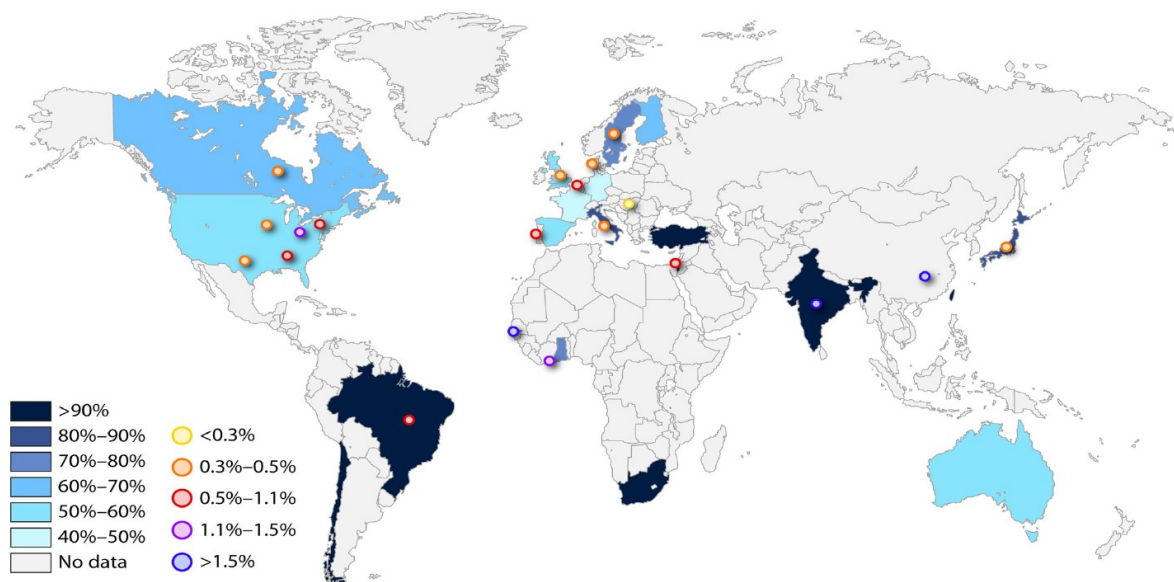


**Figure 8: HCMV-seroprevalence compared to congenital HCMV prevalence worldwide (Manicklal et al., 2013)**

While the HCMV seroprevalence can almost reach 100%, the congenital HCMV prevalence fluctuates between 0.2 to 1.5% worldwide (Fig.8). In this context, countries like India, Brazil and Japan are especially affected by maternofetal HCMV transmission which occurs despite high HCMV seroprevalence rates, maybe caused by other social or ethnical reasons (Manicklal et al., 2013).

The increased transmission rate during an HCMV primary infection is caused by a not existing preconceptional immunity of the mother. The maternal placenta is not a suitable barrier to prevent the transmission of HCMV, because of a lack of highly affine IgG-antibodies, combined with no T-cell response against HCMV. It is important to know, that early induced IgM antibodies are not able to pass the placenta to protect the fetus successfully during a HCMV primary infection (Fowler et al., 1992). The maternofetal HCMV transmission in the first trimester can lead to a termination of pregnancy in worst cases. For all other congenital infections, the mortality rate is about 8-10% for symptomatic infants at birth during the first year of life. Approximately 12% of the infected newborns show clinical symptoms like jaundice, pinpoint bleeding and hepatosplenomegaly, followed by long-term sequelae which includes mental retardation and hearing loss in the first two years of life (Mocarski et al., 2001; Landolfo et al., 2003; Mocarski et al., 2007).

In a comprehensive review of Buxmann et al., 2017 which was published in the "Deutsches Ärzteblatt", a cohort of 1000 pregnant women were investigated to exemplify the average risk for permanent disabilities, depending on the HCMV-serostatus of the mother at the beginning of pregnancy and the potential symptoms of the fetus (Fig.9).

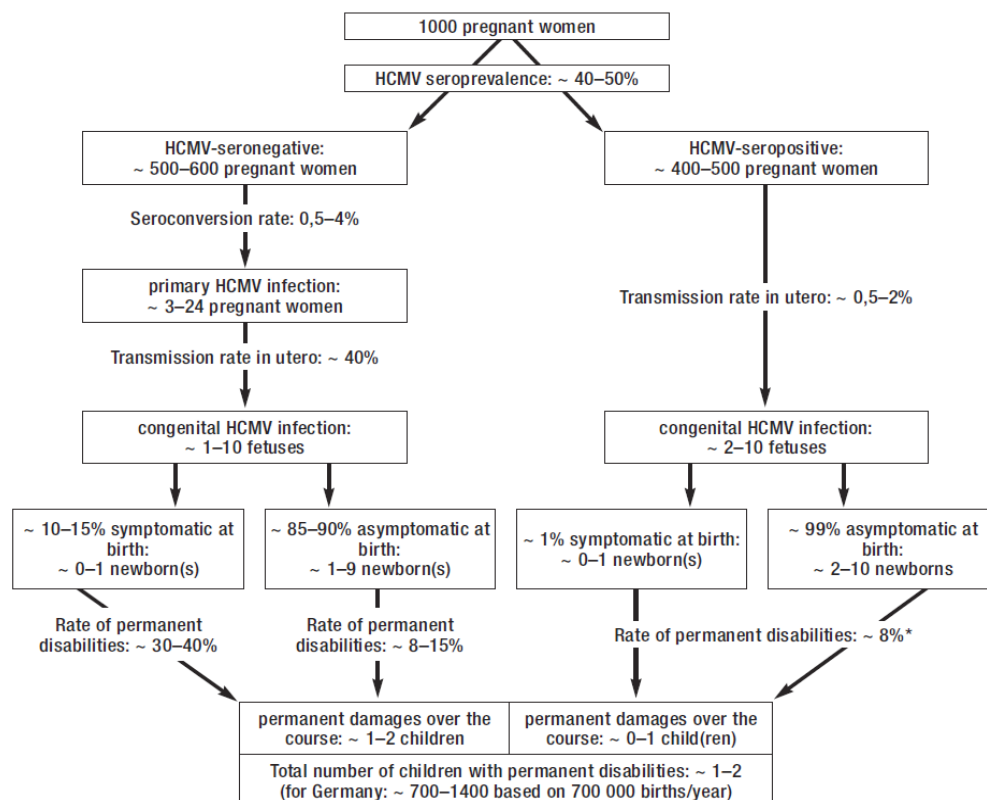


**Figure 9: A breakdown of data for maternofetal HCMV-transmission rates and resulting risk of permanent disabilities of the newborns, depending on maternal HCMV-serostatus and potential symptoms of the fetus (Buxmann et al., 2017)**

The cohort is representative for pregnant women of the Middle East of the European Union with a seroprevalence of 40 to 50%. The data of the review is based on relevant publications from the years 2000 to 2016. With 30 to 40%, the highest rate for permanent disabilities were found in HCMV-primary infected women with a symptomatic newborn which is mainly responsible for 700 to 1400 HCMV-affected births every year in Germany. Furthermore, permanent disabilities were observed in asymptomatic newborns in up to 15% of cases and the overall risk in HCMV-seropositive mothers was given with ~8%.

The data of Buxmann et al., 2017 matched with a former and independent review of De Vries et al., 2011 which showed summarized data for the risk of permanent sequelae, caused by HCMV primary and recurrent infections during pregnancy without comprehensive determination of maternal HCMV-serostatus at the beginning of pregnancy (Fig.10).

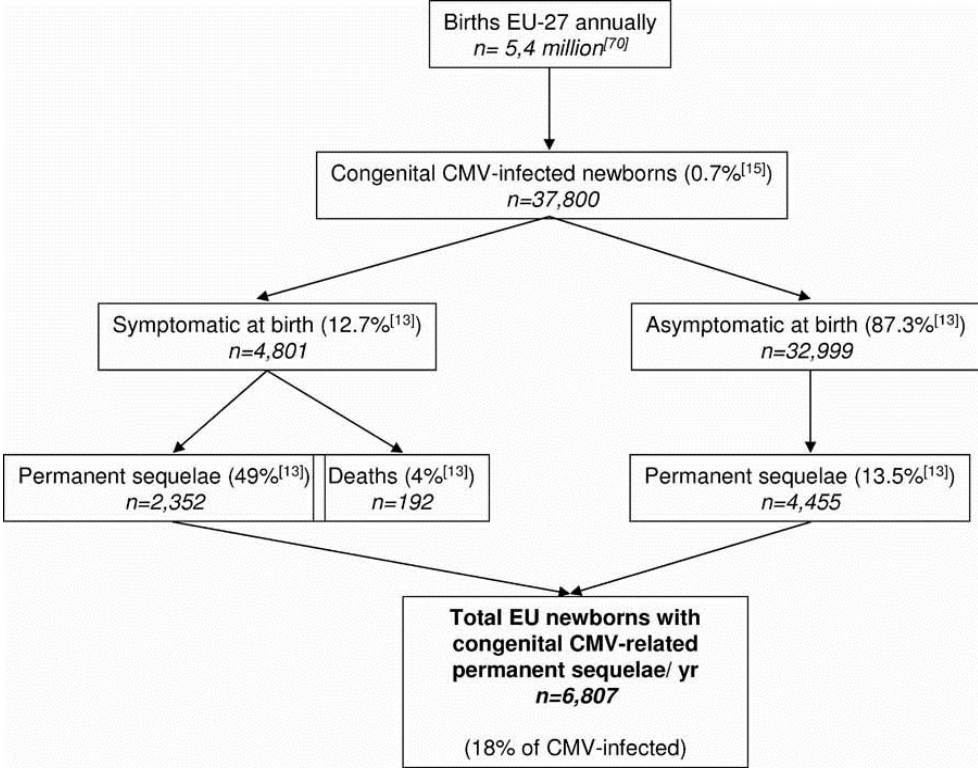


Figure 10: Congenital HCMV cases in the EU-27 (De Vries et al., 2011)

The congenital HCMV was investigated in 27 countries of the EU (Fig.10). In general, there were 0.7% HCMV congenitally infected newborns of all life births until the year 2011. The infants were in about 12% of cases symptomatic which leads to a probability of 49% for permanent sequelae and a death rate of 4%. While ~90% of the infants were asymptomatic at birth, they developed sequelae in about 13% of cases. In a summary, the overall risk to observe permanent sequelae was ~20% (De Vries et al., 2011).

### 1.9.1 Maternal placenta and IgG transfer

The successful HCMV infection of the maternal placenta is an essential precondition for the intrauterine transmission to the fetus (Mostoufi-Zadeh et al., 1984). However, not every placenta HCMV infection results in a transmission to the fetus.

An important fact is the presence and the concentration of IgG antibodies which bind and effectively neutralize HCMV virions with a high affinity by passing the placental blood barrier, in contrast to IgM antibodies (Adler et al., 1988; Pereira et al., 2006). Furthermore, the transplacental transfer of IgG subclasses 1 and 4 was significantly more efficient than IgG subclasses 2 and 3 (Garty et al, 1994).

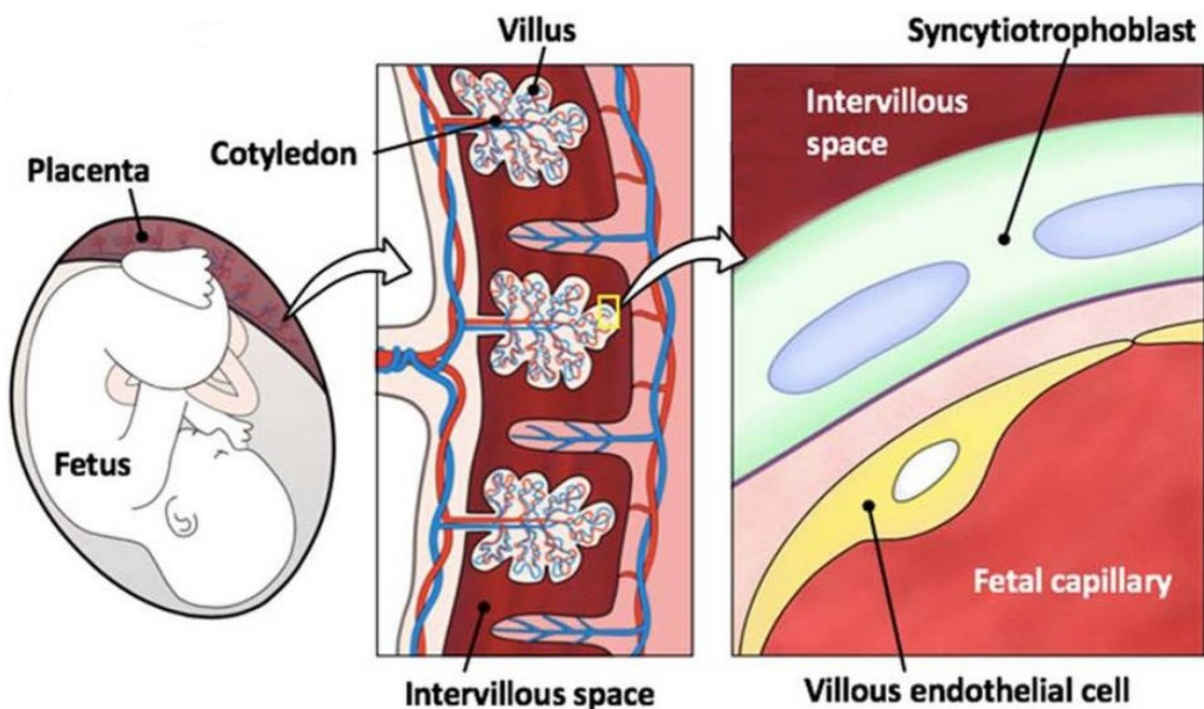


Figure 11: Schematic model of maternal placenta and maternofetal blood transfer (modified after Blundell et al., 2016)

The human placenta is built after the conception and nidation of the fertilized blastocyst in maternal uterus which can reach a diameter of about 20 cm and a weight of approximately 500 g until full maturity.

At the beginning, the placenta can be subdivided into the maternal and the fetal side which is bordered by the placental barrier and allows no direct blood transfer between the mother and the fetus.

In detail, the maternal side consists of the decidua which is the basal plate of the placenta. On the fetal side, the chorion leads to the umbilical cord and further to the fetus. The intervillous space takes its position between the decidua and the chorion which is filled with freely circulating maternal blood. The villus reaches from the fetal chorion into the intervillous space and manages the exchange of substances by connecting the maternal and fetal blood system (Fig.11). For the fetus, the provision nutrients and oxygen, as well as the elimination of wastes are the most important tasks of the placenta.

In context of immune tolerance, the separation of the maternal and fetal blood system is of particular immunological importance. The mother and the fetus are genetically heterogeneous, as well as all generated cells and resulting components. Therefore, the immune system of the mother would recognize the foreign fetal cells and would initiate an immune response against these cells which would finally result in the loss of the fetus otherwise.

The exchange of molecular weight <500 Da takes place, using 4 pathways: diffusion, facilitated diffusion, pinocytosis and receptor-mediated endocytosis. On this base, the transport of elementary substances, like O<sub>2</sub> and H<sub>2</sub>O is managed by diffusion. This is also true for drugs like alcohol which explains its fatal teratogenic potential.

On the other way, proteins like maternal IgG antibodies are transmitted with a mass of ~160 kDa by pinocytosis and constitute the passive immune protection of the fetus which is called "nest protection" in common use. The fetal immune system is not able to produce sufficient amounts of highly affine antibodies to protect itself from infections (Carlson et al., 2013).



The transfer of maternal IgG-antibodies is performed by multinucleated syncytiotrophoblasts which is illustrated in figure 12. These cells are located on the surface of the villus and bind IgG-antibodies using the neonatal Fc-receptor (FcRn receptor) from maternal blood which protects these antibodies against lysosomal degeneration in the acidic inner milieu of endosomes. Interestingly, FcRn receptors have structural homologs to the major histocompatibility complex MHC I.

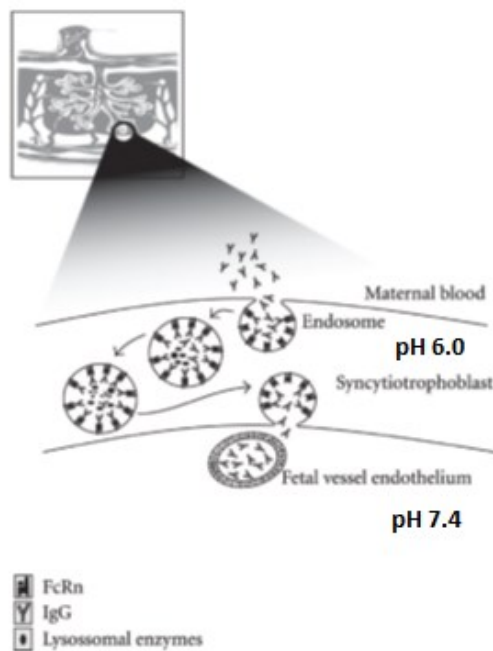


**Figure 12: Schematic transfer of IgG-antibodies through the placenta, using FcRn receptors (modified after Palmeira et al., 2012)**

After transcytosis, the endosomes melt with the membrane of cytotrophoblasts and the IgG antibodies are released from the FcRn receptors, induced by the physiological pH shift from 6 to 7.4. The FcRn receptor possesses a pH-dependent affinity for binding of IgG-antibodies, in contrast to Fcγ-receptors. This can be demonstrated in endosomes. At a pH-value of 6, the binding activity of FcRn receptors to IgG-antibodies is increased by a 100-fold, compared to the physiological pH value which triggers the antibody release on the fetal side of the placenta. However, high concentrations of IgG antibodies lead to lysosomal degeneration, initiated by oversaturation of FcRn receptors. In addition, used FcRn receptors can be delivered back to the maternal membrane and recycled for a second transcytosis of IgG-antibodies (Palmeira et al., 2012).

## 1.9.2 Diaplazental HCMV transmission

The diaplazental transmission of HCMV and the immune response can be explained in 3 different scenarios, shown in figure 13 (Maidji et al., 2006).

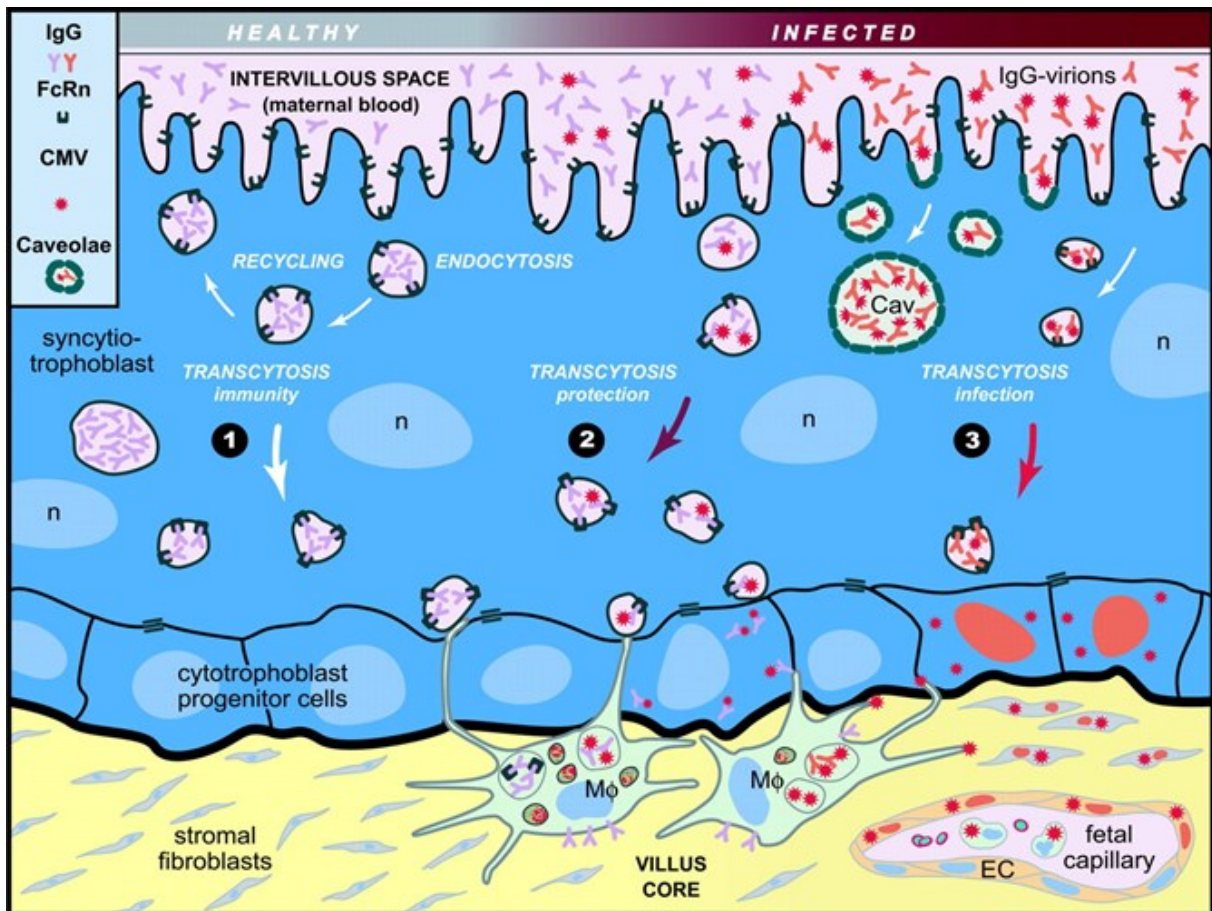


Figure 13: FcRn-mediated transcytosis of IgG antibodies and HCMV virions given in 3 scenarios (Maidji et al., 2006).

1. Latent infection: It shows the transcytosis of a healthy, HCMV-IgG seropositive ("immune") pregnant woman. IgG antibodies are delivered through pinocytosis using FcRn receptors. The transcytosis follows via endosomes to the fetal side of the placenta, as well as recycled FcRn receptors vice versa.
2. Recurrent infection: The recent infection of the placenta is suppressed in an immunocompetent latently infected mother after reactivation of HCMV (red spots) (Fig.13). At low pH value, the virus will be bound and neutralized by highly affine HCMV-specific antibodies during pinocytosis and are trapped in caveosomes (Cav) at neutral pH value. Afterwards, saturated caveosomes are transcytosed across the syncytiotrophoblasts to the membrane of cytotrophoblasts. Villus core macrophages (Mφ) capture the released virus-antibody complexes at this place and store them inside of vacuoles afterwards.

3. Primary infection: On the 3rd route through the placenta, an HCMV primary viral infection is given. IgG-antibodies with low avidity are presented in the maternal blood which are not able to bind and neutralize the virions efficiently to prevent the infection of the placental cells. Therefore, active HCMV virions are delivered to the fetal side of the placenta via endosomes. In a next step, released virions infect cytotrophoblasts and surrounding fetal fibroblasts. Furthermore, the virus invades into fetal capillaries via infected endothelial cells which is shown in a cross section in the bottom right-hand corner of figure 13 (Pereira et al., 2003 and 2006). Leukocytes will be finally infected as well which may end up in a viral dissemination and organ manifestation with a potentially critical clinical outcome, if the infection took place in the first trimester of pregnancy (Fisher et al., 2000).

### 1.10 HCMV diagnostics in pregnancy

In general, diagnosis of fetal HCMV infection through ultrasound as imaging technique is inefficient, because of its high non-specificity to detect HCMV-specific infection in the early state of pregnancy. Only about 20% can be diagnosed using ultrasound detection during pregnancy and strongly depends on the experience and interpretation of the gynecologist (Benoist et al. 2008; Guerra et al., 2008).

In Germany, the AWMF “Labordiagnostik schwangerschaftsrelevanter Virusinfektionen (AWMF Registernummer 0093/001; 2014)” regulates the diagnostics of viral infections during pregnancy. The direct HCMV detection is performed using quantitative PCR via isolated DNA and cell culture for diagnosis of active viral replication (Tab.2).

**Table 2: Overview of methods is given for direct HCMV detection. When testing follow-up samples using quantitative PCR, the same starting material must always be used for DNA isolation (modified after AWMF registration number 0093/001; 2014).**

Principle	Method	Source
HCMV-DNA detection	quantitative PCR Result: Specific genome copies/ml	Leukocytes, EDTA blood, whole blood, plasma* (determination of infection status) Urine, throat swab/flush (determination of HCMV excretion, diagnosis in newborns) Amniotic fluid, umbilical cord blood (diagnosis of fetal infection)
HCMV isolation	Propagation in cell culture (human foreskin fibroblasts) Short-term microculture for HCMV antigen detection by immunofluorescence	Urine, throat swab/flushing (determination of HCMV excretion; diagnosis in newborns) Amniotic fluid (diagnosis of fetal infection)

For further analysis, the determination of HCMV infection will be checked by analysis of HCMV-specific serology.

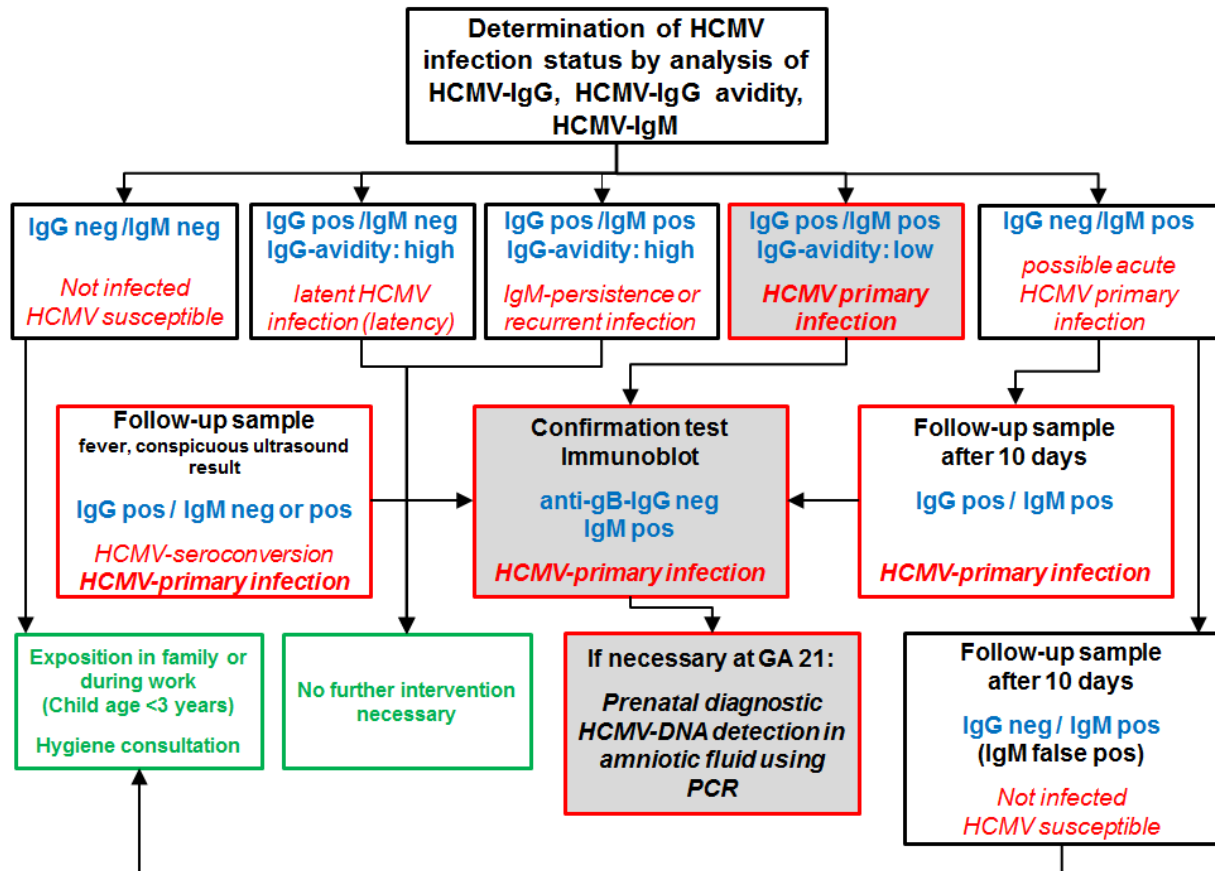


Figure 14: Overview of laboratory diagnostics. Blue font: Constellation of results, red font: Interpretation, green: Interventions; red border: further clarification required (modified after AWMF registration number 0093/001, 2014).

Figure 14 shows the general procedure of laboratory diagnostics to clarify the HCMV infection status in pregnant women, combined with optional interventions. The laboratory diagnosis of HCMV primary infection during pregnancy should be made by determining the HCMV-specific antibodies in the sense of a step-by-step diagnosis with a combination of different test systems. Table 3 gives an overview of methods for detection of HCMV-specific antibodies (AWMF registration number 0093/001, 2014).

**Table 3: Overview of methods for the detection of HCMV-specific antibodies (modified after AWMF registration number 0093/001; 2014).**

Method	Comments
Ligand assays (e.g. ELISA, CLIA, CMIA, ECLIA)	Determination and differentiation of Ig classes (IgG, IgM) in serum or plasma Simple execution, commercially available, partially automated
Immuno/ Western blot (recomLine® Immunoblot)	Determination and differentiation of IgG classes (IgG, IgM) in serum or plasma  Determination of IgG reactivities against defined HCMV proteins (anti-gB IgG not detectable in fresh HCMV primary infection)  Simple execution, commercially available
HCMV-IgG-avidity (ELISA, Immunoblot)	Differentiation between HCMV primary infection and HCMV latency/HCMV recurrence stage diagnosis for IgM detection in pregnancy
Neutralisation assays	Functional antibody test: Differentiation between HCMV primary infection and HCMV latency/HCMV recurrence primary infection: detection of neutralizing antibodies within 3-4 weeks in epithelial cell culture; within 3-4 months in fibroblast cell culture

The detection and interpretation of maternal IgM antibody index is more accurate to detect an HCMV primary infection, in combination with avidity testing and quantitative determination of HCMV-specific IgG antibodies. The detection of HCMV epitope-specific antibodies is also a useful diagnostic tool to confirm or to deny an HCMV primary infection. Therefore, several immuno assays and immunoblots are available (Guerra et al. 2008; Fabbri et al., 2011).

In general, a latent HCMV infection can be characterized by high avidity of HCMV-specific IgG antibodies and missing of IgM at the same time. However, the presence of IgM antibodies against HCMV is not a proof for an HCMV primary infection.

Both, primary and a recurrent HCMV infection may show IgM antibodies during pregnancy. Commercial antibody test systems include ELISA (enzyme linked immuno absorbent assay), ECLIA (electro chemoluminescence immuno assay), CLIA (chemoluminescence linked immuno absorbent assay) and CMIA (chemoluminescence micro particle assay). The recomLine® Immunoblot from Mikrogen is able to detect HCMV epitope-specific antibodies like p150 and gB2 by semi-quantitative scoring of epitope-specific reactivity.

### 1.11 *In vitro* neutralization assays

The serum of pregnant women can also be incubated with reference viral strains to check for specific neutralizing activity of IgG-antibodies by characterization of immunoglobulin preparations *in vitro*. A routine testing of maternal serum during pregnancy may help to narrow down the time point of infection.

In general, there are 2 different approaches of neutralization testing and different target cell were used, including human foreskin fibroblasts (HFF), human embryonic lung fibroblasts (HELFL) or retina pigment epithelial cells (RPE) (Tab.4).

Eggers et al., 2000 and Gerna et al., 2008 worked with cell-free virus strains which were shed into supernatant after several cell culture passages. Cell-free virus was preincubated with dilution series of potentially neutralizing sera. Then virus-antibody complex was transferred to non-infected target cell monolayers, using micro titer plates to determine NT<sub>50</sub>-values. Free unbound virus is able to infect target cells. The NT<sub>50</sub>-value describes the dilution of serum which is able to bind and neutralize 50% of the used viral particles via antibodies after a defined duration of time (usually 18h). After 18h incubation the single infected cell nuclei are counted, using p72 (IE1) staining.

In contrast, Frenzel et al., 2012 used cell-associated virus and a defined number of previous infected cells which are transferred to non-infected cells in a coculture of 200 infected cells/ 20.000 not infected cells. The cell-to-cell spread will be prevented by adding of diluted series of potential neutralizing sera. NT<sub>50</sub>-value will also be determined. After a defined incubation time of generally 72 h, the plates are fixed and the formed viral plaques are counted in this approach, in contrast to the first approach with single infected nuclei. In both approaches, the inactivation of complement is performed by heat incubation over time.

**Table 4: Summary of published HCMV neutralization protocols**

<b>Publication / Parameters</b>	<b>Eggers et al., 2000</b>	<b>Gerna et al., 2008</b>	<b>Frenzel et al., 2012</b>	<b>Schampera et al., 2017</b>
<b>Viral strain</b>	AD 169 cell-free	AD169 / VR1814 cell-free	AD169 / TB40 cell-associated	H2497 cell-free cell-associated
<b>Sera / Controls</b>	Pool (n = 227) pregnant women after HCMV-PI	Pool (n = 18) pregnant women after HCMV-PI	HIG, IVIG	2 Pools (n = 100) HCMV-PI / LI HIG, IVIG
<b>Target cells</b>	HFF	HFF, RPE	HELFL, RPE	HFF, RPE
<b>Serum preincubation</b>	90min, 37°C	60min, 37°C	30min, RT	90min, 37°C
<b>Centrifugation</b>	30min, 800rpm	30min, 700g	60min 16k.rpm	30min, 300g
<b>Microculture incubation</b>	16-18h, 37°C	48h, 37°C	72h, 37°C	18h-72h, 37°C
<b>Read out</b>	p72 (IE1)	p72 (IE1)	p72 (IE1)	p72 (IE1)

## 1.12 Prevention of HCMV primary infection

### 1.12.1 Antiviral drugs

Several preparations are currently licensed for antiviral therapy after acute HCMV infection in immunosuppressed patients after stem cell or organ transplantation (Tab.5).

**Table 5: Overview of antiviral treatment options against HCMV**

<b>Antiviral drug</b>	<b>Mode of action</b>	<b>Side effects / toxicity</b>	<b>in pregnancy</b>
<b>Ganciclovir®</b>	Nucleoside analog (guanine) Inhibition of viral DNA polymerase	Bone marrow toxicity Neutropenia	Ljungman et al., 2004 Puliyanda et al., 2005
<b>Valganciclovir®</b>	Nucleoside analog (guanine) Prodrug of Ganciclovir® (per oral) Valinester Inhibition of viral DNA polymerase	Bone marrow toxicity Neutropenia	Seidel et al., 2017
<b>Valaciclovir®</b>	Nucleoside analog (guanine) Prodrug of Acyclovir® (per oral) Inhibition of viral DNA polymerase	Bone marrow toxicity Neutropenia	Leruez-Ville et al., 2016
<b>Cidofovir®</b>	Acyclic Nucleoside analog (phosphonate) Inhibition of viral DNA synthesis	Nephrotoxicity	<i>No data</i>
<b>Foscarnet®</b>	Non-nucleoside analog (pyrophosphate) Inhibition of viral DNA polymerase	Nephrotoxicity	<i>No data</i>
<b>Letermovir® (current release)</b>	DNA terminase inhibitor Inhibition of viral DNA packaging	Not sufficiently investigated	<i>No data</i>

The first line of antiviral treatment options for HCMV infections in the transplant setting are Ganciclovir® (GCV) and Valganciclovir® (VGCV) which is a prodrug (Valinester) of GCV (Ljungman et al., 2004). First, both antiviral drugs have to be activated by mono-phosphorylation which is performed by the viral phosphotransferase (UL97), before they are able to inhibit the viral DNA polymerase (UL54). The successful use of GCV was confirmed in a case report to treat intrauterine HCMV infection (Puliyanda et al., 2005).

VGCV is a generic drug which revealed a 10-fold higher bioavailability (60%) than GCV in a clinical study which was reached by oral application and showed comparable antiviral treatment effects to GCV intravenously (Cvetković et al., 2005).

The study of VGCV to treat congenital HCMV infection indicates to be safe for the mother and the fetus (Seidel et al., 2017). Furthermore, no negative effects on the fetus were reported in four cases of maternal HCMV infection which described the use of GCV or VGCV during pregnancy.

In a clinical transplant setup, antiviral resistance occurred in mutations of the UL54 or UL97 gene region. Usually, mutations in UL97 were observed first, but mutations in UL54 reached higher  $IC_{50}$ -values in context of GCV resistance and showed cross-resistance to the second-line drugs Cidofovir® (CDV) and Foscarnet® (FOS) (Lurain et al., 2010; Gilbert et al., 2011). However, CDV and FOS are no treatment options during pregnancy, because of their high levels of nephrotoxicity (Enders et al., 2006; Kimberlin et al., 2005). Valaciclovir® (VACV) showed like VGCV a higher bioavailability than Acyclovir®. There is a multicenter, open-label, phase II study of congenital cytomegalovirus infection with VACV. Their results demonstrated that, VACV could be used during pregnancy by improving the clinical outcome of symptomatic HCMV-infected fetuses (Leruez-Ville et al., 2016) which was indicated by Jacquemard et al., 2007.

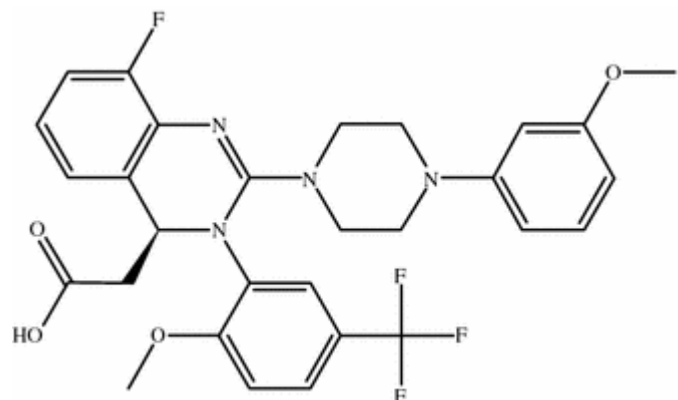


**Figure 15: Molecular structure of the novel antiviral drug Letermovir® modified after (Marty et al., 2017)**

Recently, an antiviral drug with a new mechanism of action is available for treatment recently (Fig.15). Letermovir® is a viral terminase complex inhibitor which inhibits the capsid packaging of the viral DNA (UL51 and UL56). While its mechanism completely differs from the previous described antiviral drugs, there is no known cross-resistance of Letermovir® to those DNA polymerase inhibitors (Marty et al., 2017). It was shown in a study, that Letermovir® prophylaxis resulted in a significantly lower risk of clinically significant HCMV infection than placebo in patients after allogeneic hematopoietic-cell transplantation. Letermovir® had low toxicity at the same time. Therefore, it could be a promising treatment option for HCMV infected mothers (Marty et al., 2017). But more data are necessary to evaluate Letermovir® for an “off label use” in pregnant women with an HCMV infection.



### 1.12.1 Vaccines against HCMV

There are no efficient vaccines against HCMV available up to now, but the development of a vaccine against HCMV is a major public health priority (Anderholm et al., 2016). Table 6 gives an overview of current vaccine candidates in clinical trials (Poltkin et al., 2018).

**Table 6: Overview of vaccine candidates in clinical trials (modified after Poltkin et al., 2018)**

Vaccine	Developer	Antigen			Reference
		gB	PC	pp65	
<b>Adenovirus vector</b>	Queensland Institute	X			Zhong et al., 2008
<b>Alphavirus replicons</b>	GSK	X		X	Bernstein et al., 2009
<b>Canarypox vector</b>	Sanofi			X	Berencsi et al., 2001
<b>Dense bodies</b>	Vaccine Project Management, Serum Institute, India	X	X	X	Cayatte et al., 2013 Plachter, 2016
<b>DNA plasmids</b>	Astellas, Inovio	X		X	Shedlock et al., 2012; Smith et al., 2013
<b>Lentivirus particles</b>	Variations Bio	X		X	Kirchmeier et al., 2014
<b>Live attenuated</b>	Medimmune	X		X	Adler et al., 2016; Plotkin et al., 1984
<b>Live replication-defective</b>	Merck	X	X	X	Fu et al., 2014
<b>LHCMV vector</b>	Hookipa	X		X	Schleiss et al., 2017
<b>mRNA</b>	GSK, Moderna	X			Brito et al., 2014
<b>MVA vector</b>	City of Hope	X	X		La Rosa et al., 2017
<b>Peptides</b>	City of Hope, University of Heidelberg			X	Nakamura et al., 2016
<b>Soluble pentamer complex</b>	Humabs, Redbiotech GSK		X		Kabanova et al., 2014
<b>Subunit gB</b>	Sanofi, GSK	X			Pass et al., 2009 Bernstein et al., 2016 Griffiths et al., 2011
<b>VSV vector</b>	VSV vector	X			Wilson et al., 2008

While the experiments with a life-attenuated vaccine against HCMV were not successful, another randomized, double-blind, placebo-controlled phase 2 study using recombinant vaccine gB/MF59 reached only a vaccination efficacy of 50% in healthy, postpartum women, combined with a decrease of congenital infections (Pass et al., 2009; Rieder et al., 2013 and 2014).

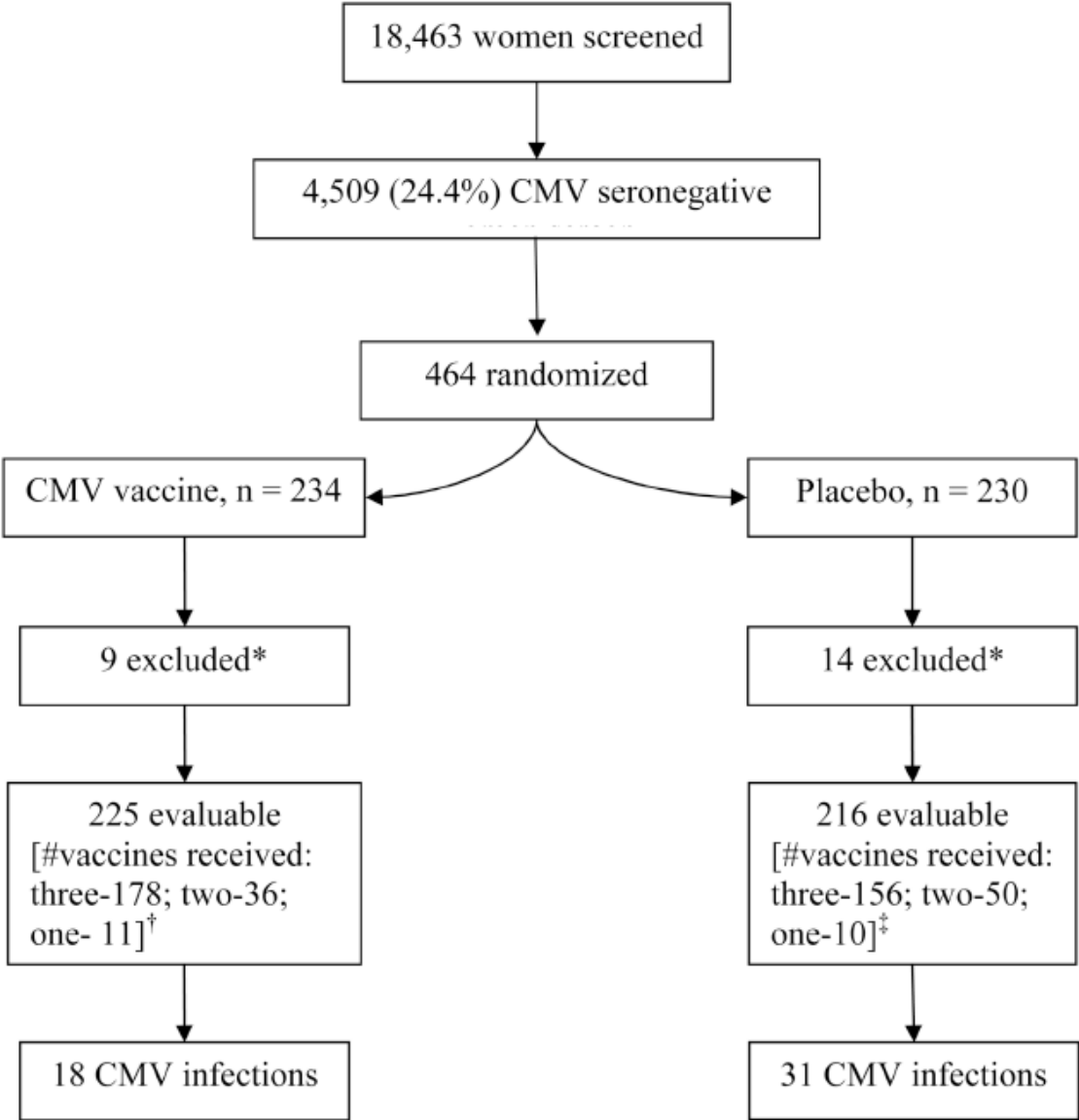
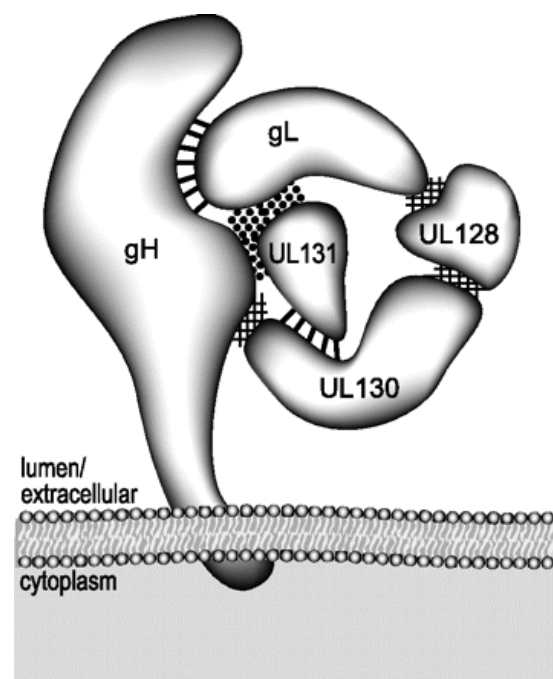


Figure 16: Results of the clinical phase II study, including gB/MF59 (Pass et al., 2009)

The study involved 225 healthy women, who were treated with gB/MF59 and 216 women got placebo (Fig.16). After vaccination, the HCMV infection rate was lower in the treated group (8%) than in the placebo group (14%). In addition, the antibody titers against HCMV were significantly higher in the vaccinated group than in the placebo group.

The next step to an effective vaccine could be the development of a pentameric complex based vaccination (Rieder & Steiniger, 2013). During the last years the potential of the pentameric complex to induce antibodies and the influence on the immune system were investigated extensively. It showed that the majority of strong neutralizing antibodies are directed against the pentameric complex (Gerna et al., 2017). These findings pushed the development of a potentially protective HCMV vaccine like the expression of recombinant pentameric complex for vaccine use in a CHO system (Hofmann et al., 2015). In terms of serology diagnostics, neutralizing antibodies to the PC could be potentially used as surrogate marker for possible reduced risk of maternofetal transmission (Lillieri et al., 2012).



**Figure 17: Model of the pentameric complex gH/gL/UL128-131 (Ryckman et al., 2008)**

Interestingly, the UL128, UL130 and UL131 genes also seem to influence the response of MHC class I and class II-restricted CD8<sup>+</sup> T-cells by inhibition of the viral epitope recognition (Hansen et al., 2013).

## 1.12.2 Hyperimmunoglobulin preparations

Hyperimmunoglobulin preparations (HIG) are pooled sera of healthy donors with high antibody titers against HCMV. The sera are collected and purified, followed by an enrichment of the HCMV-specific antibodies via ethanol-fractionation. They were generally indicated for the use in immunocompromised patients after solid organ transplantation in combination with antiviral drugs like GCV (Ljungman et al., 2004; Bonaros et al., 2008).

There are two HIGs preparation for HCMV commercially available. The HIG Cytotect® from Biotest Pharma AG has a license in the EU and its counterpart Cytogam® from CLS Behring. It has a license for the US market. In general, the long-time experience with immunoglobulins showed weak signs of side effects and a good patient compatibility, compared to antiviral drugs. Possible side effects of HIG are intermittent shivering, nausea, headache, mild fever and/or joint pains (Manufacturer specifications Cytotect®; Biotest Pharma AG, Germany).

The first study for prevention of fetal HCMV transmission in pregnancy was published in 2005 which officially introduced the “off label use” of HIGs in a non-randomized trial (Nigro et al., 2005).

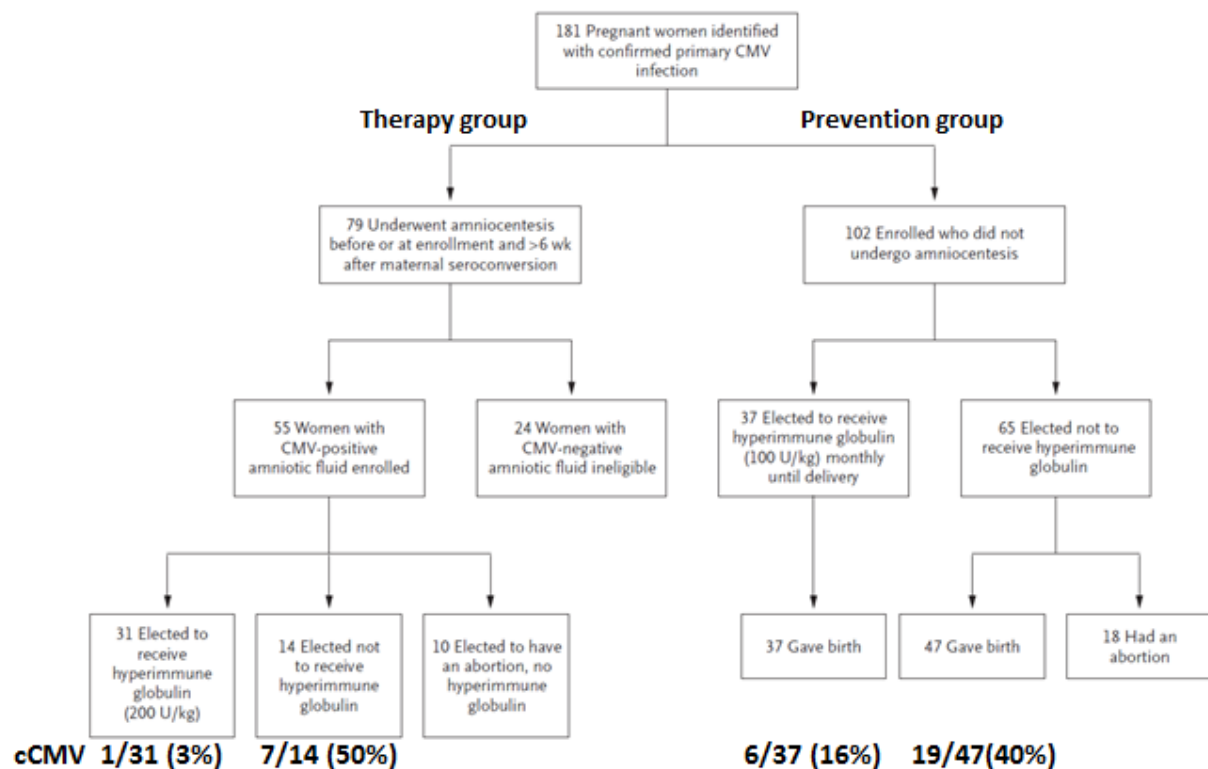


Figure 18: First non-randomized HIG study in pregnancy - Primary end point (modified after Nigro et al., 2005).

The study included 181 pregnant women with a proven HCMV primary infection (Fig.18). The women were divided into a “prevention group” of 102 members which had no amniocentesis and a “therapy group” of 79 women, who underwent an amniocentesis before or at enrollment plus <6 weeks after maternal seroconversion.

On the one side, 37 women of the prevention group received HIG (100 U/kg monthly) until delivery. 31 uninfected and 6 HCMV-infected newborns were born which corresponded with a transmission rate of 16%. The untreated part of the prevention group had a maternofetal transmission rate of about 40% which reflected a significant decrease between the treated and untreated women.

On the other side, 55 pregnant women of the therapy group were HCMV positive in amniotic fluid. 31 of the enrolled women were elected to receive HIG (200U/kg), 14 women were not treated and 10 women had a termination of pregnancy (TOP). After the treatment, only one woman had a symptomatic infected newborn at birth which correlated with an infection rate of 3% compared to the untreated 14 women. 7 of the 14 women (50%) gave birth to symptomatic HCMV-infected newborns which also revealed a significant difference between the treated and the placebo group. The recruiting standards of the Nigro study were critically discussed and a repeated enrollment of a comparable collective is no more possible, considering current ethical approvals.

Further studies of the HIG treatment of primary HCMV-infected women confirmed the improved outcome of reduced congenitally HCMV-infected infants, as well as the decrease number of newborns with sensorineural hearing loss (Buxmann et al., 2012; Visentin et al., 2012).

**Table 7: Summarized results of the studies Buxmann and Visentin 2012.**

<b>Study</b>	<b>HIG treated</b>	<b>HIG untreated (Control group)</b>
<b>Buxmann et al., 2012</b>	<u>Therapy group</u> 25% (1/4)	Not performed
	<u>Prevention group</u> 23% (9/39)	
<b>Visentin et al., 2012</b>	<u>Therapy group</u> 13% (4/31)	43% (16/37)

In the Buxmann study, 1 of 4 congenitally infected infants was symptomatic at birth in the therapy group (Tab.7). For the prevention group, 9 out of 39 were HCMV-infected, but no infant was symptomatic at birth. The study of Visentin revealed an observed absolute reduction of 30% between the HIG treated and untreated therapy group.

Almost one decade after the first HIG study of Nigro, a phase 2, randomized, placebo-controlled (RCT) study was performed to validate the importance of passive immunization during pregnancy against HCMV primary infection (Revello et al., 2014).

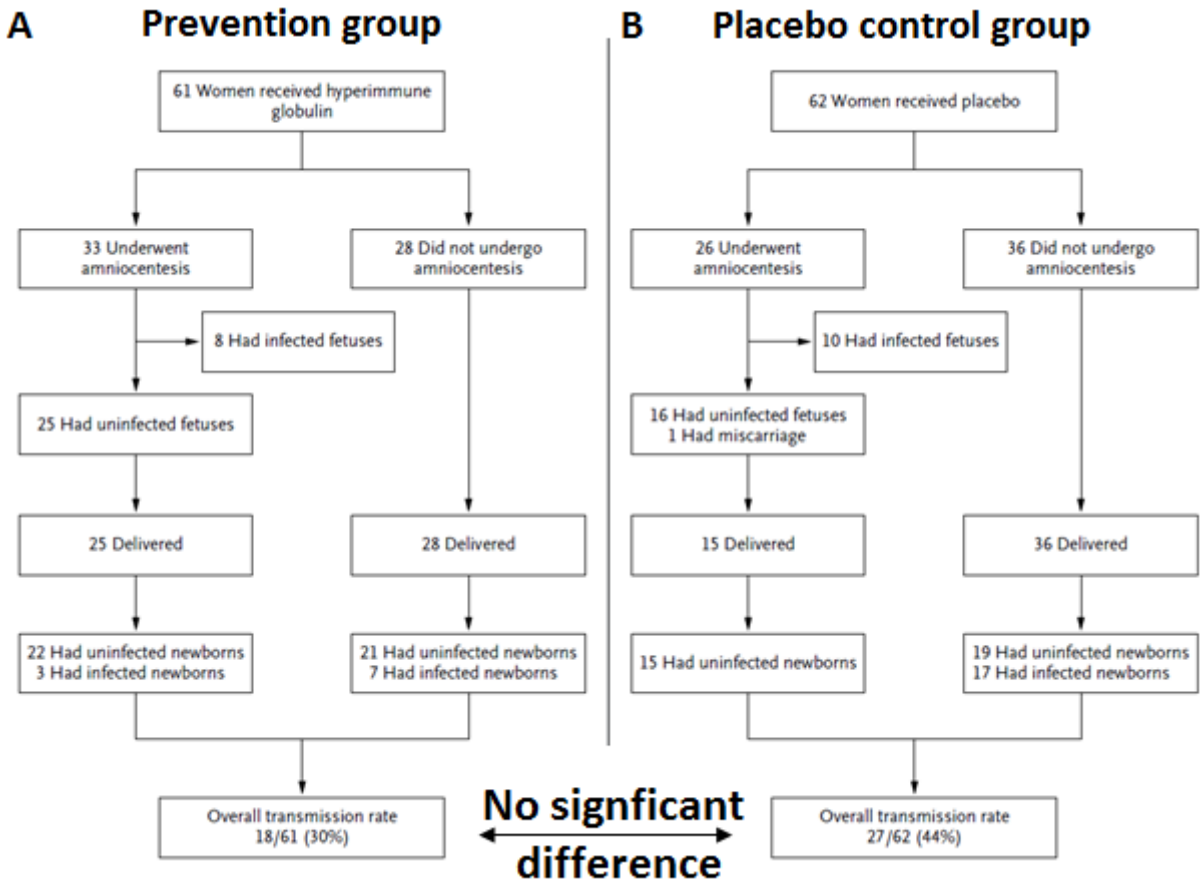


Figure 19: A randomized controlled trail of HIG to prevent maternofetal transmission. (A) 61 women received HIG. (B) 62 women received placebo (modified after Revello et al., 2014)

This study consisted of a prevention group which was subdivided into 61 women, who received HIG and a placebo group of 62 women (Fig.19). Only pregnant women were enrolled with a proven HCMV primary infection. In the treated group, 33 women underwent an amniocentesis, in which 8 infected fetuses were diagnosed. The primary end point of the study was the number of congenitally HCMV-infected newborns. The HIG treatment was discontinued in women with HCMV-positive amniotic fluid. In the placebo group, 10 infected fetuses were found during amniocentesis of 26 pregnant women. The overall transmission rate in the HIG group was 30% with 18 infected newborns out of 61, compared to 44% with 27 infected newborns out of 62. This result reached no statistically significant difference between both groups. A recent consensus review, based on the RCT study of Revello did not recommend the use of immunoglobulins in pregnant women outside of clinical trials (Rawlinson et al., 2017).

However, the underlying study design and the resulting outcome of the RCT study were controversially discussed in several “letters to the editor” in Revello et al., 2014. It can be highlighted, that both studies of Nigro and Revello, as well as the observational retrospective study of Buxmann et al., 2012 used a monthly interval for HIG administration to pregnant women with an HCMV primary infection. The time interval of HIG treatment was assumed on the base of a terminal elimination half-life of 22.4 days for total IgG antibodies (Thurmann et al., 1995). In an index case, a further single investigation of the HCMV antibody pharmacokinetics of a volunteer HCMV-primary infected pregnant woman revealed a half-life time of about 11 days after a 4-week interval HIG treatment. The shorted half-life time was paired along with strong fluctuations in epitope-specific recombinant HCMV IgG avidity and repeated decreases in neutralization activity, using ARPE-19 cells as target cells (Hamprecht et al., 2014). It is also necessary to consider, that the between-group difference in the Revello study was not significant, but the observed absolute reduction in HCMV infection was 14 % between the HIG-treated and untreated women. The 95% confidence interval ranged from -3 to 31 which does not exclude a clinically relevant effect (van Leeuwen, Letter to the editor, Revello et al., 2014). Furthermore, a meta-analysis of both studies showed a highly significant trend in a Forest plot (Blobbogram) analysis. The same study design of Nigro and Revello enabled this comparison (Rawlinson et al., 2016).

The appearing issues of the performed studies formed an interdisciplinary initiative which ended up in a novel HIG study in Tuebingen to investigate the formulated assumptions which was encouraged by authors of the Revello study (Spinillo and Gerna, response communication, letter to the editor, Revello et al., 2014).

As background, the risk for long-term sequelae after HCMV primary infection of the mother is up to 20%, depending on the gestational age at the time of maternal infection (Manicklal et al., 2013). Individual studies confirmed, that the risk for a symptomatic newborn decreases proportional to the increase of gestational age at infection and has its peak at the beginning of the first trimester (T1) of pregnancy (Enders et al., 2011; Lipitz et al., 2013 and Picone et al., 2013). Therefore, the time point of maternal seroconversion during pregnancy plays a very important role for the clinical outcome at birth and sequelae, especially in T1. In a further study, 138 children were analyzed, who underwent a congenital HCMV infection during pregnancy. An amniocentesis was performed in all pregnant women at a GA between 20 to 23 weeks, checking for viral DNA in amniotic fluid (Bilacsky et al., 2016). A correlation was found between children without long-term sequelae and no presence of viral DNA in amniotic fluid and vice versa. 14% of the children suffered from long-term sequelae and were HCMV DNA<sup>positive</sup> in amniotic fluid. In conclusion, no detection of viral DNA in amniotic fluid promises a better clinical outcome for the growing fetus.

In this context, the Tuebingen HIG study aimed for the prevention of maternofetal HCMV transmission in the first trimester of pregnancy. Therefore, a modified study design was used which based on the studies of Nigro and Revello. However, HIG (Cytotect®, Biotest Pharma AG, Germany) was administered in a biweekly interval with double dose concentration (HIGiv: 200 IU/kg maternal bodyweight), compared to both previous studies. Only women with a gestational age (GA) less than 14 weeks (T1) were included in the study cohort and were treated until week 20 or maternal mean HCMV IgG levels were above 100 U/ml, seven days after the last HIG administration. Importantly, the HIG treatment started as fast as possible after diagnosis of a proven HCMV primary infection of the mother.

The final end point of the study was an amniocentesis after the 20th week of GA. The harvested amniotic fluid was tested for viral DNA to confirm or decline the maternofetal HCMV transmission. In addition, the newborns were tested for viral DNA. For negative control, a historic cohort was used to compare the prevalence of maternal-fetal transmission. It consisted of pregnant women with a primary HCMV infection in T1 without HIG treatment. However, the results of the Tuebingen HIG study were not published at the beginning of this PhD thesis.

### **1.13 Hygiene-counseling**

In general, the infectious saliva and the urine of small children are the main sources of infection. Therefore, contaminated surfaces and the use of daily-life objects should be avoided by pregnant HCMV-seronegative women, when they have contact with potentially infected small children. The sequential hand wash, combined with virus-killing disinfection agents are simple, but effective tools to prevent a transmission of HCMV (Ross et al., 2006).

In addition to HIG treatment options, an early hygiene-counseling of pregnant women is an important tool to prevent maternofetal HCMV transmission in the first place. It was demonstrated, that objective information about HCMV infection during pregnancy, combined with followed HCMV-screening of the pregnant women could decrease the rate of seroconversion compared to no hygiene-counseling. This fact was confirmed in a 2-year and another 3-year prospective study in French hospitals (Picone et al., 2009; Vauloup-Fellous et al., 2009). However, there is no general recommendation for an HCMV antibody screening in Germany, referring to the “Mutterschaftsrichtlinien”.



## 1.14 Monoclonal antibodies against HCMV

In future, monoclonal antibodies (mABs) against the pentameric complex might be also a promising option to treat HCMV primary infections in pregnant women and therefore to prevent maternofetal-transmission. For instance, MS109 is a highly neutralizing mAB against glycoprotein H which is part of both the trimer and pentameric complex (Fouts et al., 2014). Latest studies of Fu et al., 2017 identified and characterized further mABs against different binding sides of the pentameric complex which were separated in 4 immunogenic regions (IRs 1 to 4) (Fig.20A). The  $IC_{50}$  determination of the generated mABs is shown in figure 20B on ARPE-19 and MRC-5 cells. Importantly, the mABs against IR1 (orange) revealed the most effective  $IC_{50}$  values in terms of viral binding and neutralization which consists of the UL128-131A region (UL128L).

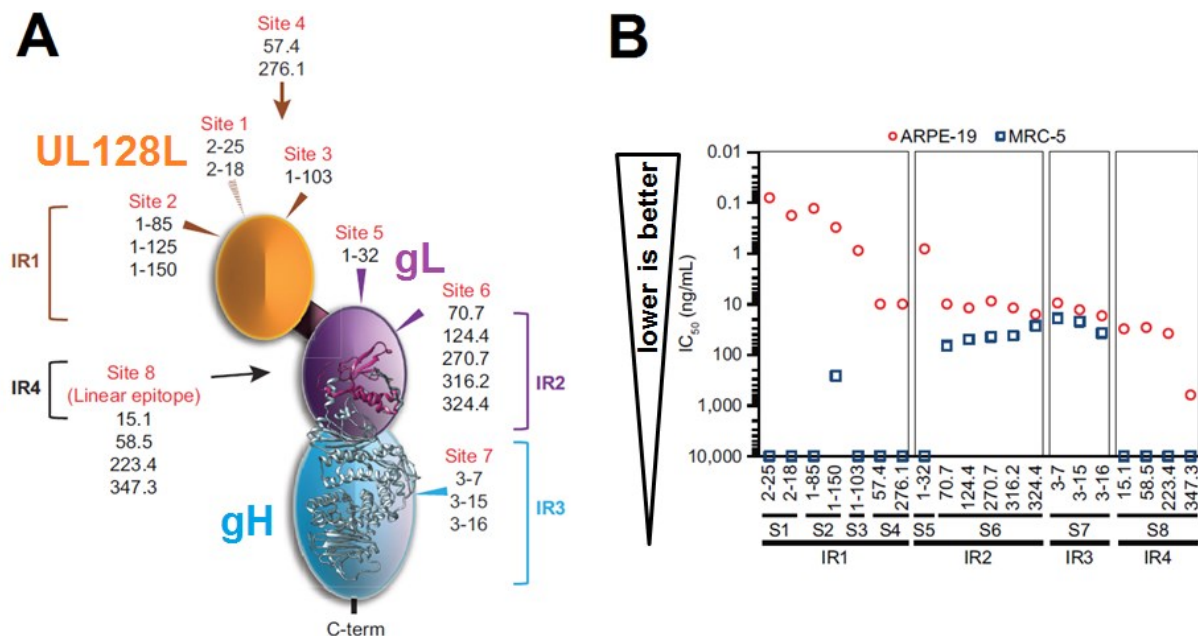


**Figure 20: (A) Visualized binding sites of generated monoclonal antibodies, separated in 4 immunogenic regions (IRs) using an EM 3D reconstruction of pentameric complex; (B)  $IC_{50}$  concentrations of generated monoclonal antibodies against the pentameric complex on ARPE-19 and MRC-5 cells (modified after Ha et al., 2017)**

In this context a former paper demonstrated that neutralizing mAbs were directed against at least a combination of two genes of the UL128L (UL128/UL130 and UL128/UL131A) (Macagno et al., 2010). In addition, the epithelial cell syncytium formation after a HCMV primary infection was prevented using mAbs against the trimer and pentameric complex, performed by the group of Gerna et al., 2016.

However, the increased risk of appearance of resistant HCMV mutants against monoclonal antibodies is to be considered which was artificially induced using the MS109 mAB in inefficient concentrations over time in *in vitro* experiments (Fouts et al., 2014). At this point, the advantage is on the usage of polyclonal HIGs instead of mABs against HCMV.

## 1.15 Objectives

The aim of the study was to characterize hyperimmunoglobulins (HIG) in the background of a novel “off label use” study design (Tuebingen HIG study) to prevent maternofetal transmission after HCMV primary infection during the first trimester (T1) of pregnancy. Scientific issues were investigated which included the validation of the HIG efficacy in *in vitro* neutralization (NT) experiments under defined circumstances, as well as the immunomodulatory effects of the treated mothers during HIG treatment.

Following scientific issues were investigated:

### 1. Standardization of an HCMV neutralization assay and performance characteristics

First, a standardized assay protocol for HCMV neutralization was established to optimize already existing NT assays and to form a base for further characterization of HIGs and Standard intravenous immunoglobulin (IVIg) preparations. Therefore, NT assay protocols in literature were considered at this point (Eggers et al., 2000; Gerna et al., 2008; Frenzel et al., 2012). Importantly, the focus was set on the performance of NT assays in routine diagnostics.

### 2. Cytotect® neutralization activity against HCMV isolates, resistant to antiviral compounds

In a second step, the established NT assay protocol was performed to compare the NT capacity of the HIG Cytotect® to other IgG preparations, using two clinical HCMV isolates with drug resistance to Ganciclovir® and Cidofovir®. As reference, a sensitive HCMV isolate was used.

### 3. Characterization of Cytotect® neutralization activities against HCMV isolates with different gB-genotypes

In next investigations, the HIG Cytotect® was further characterized by analysis its NT capacity on four HCMV isolates with different HCMV glycoprotein B genotypes (gB1, gB2, gB3 and gB4) compared to Cytogam® and two IVIGs (Kiovig® and Octagam®).

#### **4. Role of pentamer-specific antibodies in HCMV hyperimmunoglobulin and standard intravenous IgG preparations**

UL130-specific and pentamer-specific antibodies were depleted from HIG and IVIG in order to analyze their contribution to *in vitro* neutralization capacity. A modified UL130 peptide (TANQNPSPWSKLTYSKPH) was used which based on original sequence of Saccoccio et al., 2011 (SWSTLTANQNPSPWSKLTYSKPH). As depletions strategy, both UL130-peptides and a recombinant-HCMV-pentameric complex were bound via a 6-fold HisTag and anti-HisTag mAbs to magnetic beads (Schampera et al., 2018).

#### **5. Depletion of HCMV hyperimmunoglobulin IgG subclass 3 from Cytotect® and analysis of its functional activity**

In a paper of Planitzer et al, 2011, IgG subclass 3 was postulated as decisive factor for HCMV neutralization, but not IgG subclass 1 or 2. The results of Schampera et al., 2017 strongly contrast to the findings of Planitzer et al., 2011. In this context, IgG subclass 3 depletions were depleted from Cytotect®, Kiovig® to analyze their impact on *in vitro* neutralization via a modified depletion concept, using anti-IgG subclass 3 mAbs (Schampera et al., 2018).

#### **6. Modulation of the T cell response by HCMV hyperimmunoglobulin**

IgG antibodies have been reported to modulate the innate and adaptive immune response via Fcγ-receptors and IFN-γ production. Therefore, further *in vivo* investigations were performed in this PhD thesis to analyze, whether the HIG administration could beneficially induce cellular immunomodulatory effects, using IFN-γ secretions assays. Longitudinal lithium-heparin (LiHep) blood samples were collected from pregnant women with HCMV primary infection during T1, directly before and after HIG treatment. The possible immunomodulatory effect of HIG on peripheral blood mononuclear cells (PBMCs) was analyzed by their IFN-γ production upon stimulation. IFN-γ is generated during the adaptive immune response of CD4<sup>+</sup> and CD8<sup>+</sup> T cells, as well as during the innate immune response of NK cells and NK-T cells. The *ex vivo* samples were derived from women of our Tuebingen HIG study (Kagan et al., 2018).

## 2 Material and Methods

### 2.1 Target cells

For *in vitro* experiments, two different cell types were used as target cells. The neutralization capacities of IgG preparations were investigated on human foreskin fibroblasts (HFF: SCRC-1041™) and human retinal pigment epithelial cells (ARPE-19 cells: CRL-2302™). Both adherent-growing cell types were derived from ATCC® and cultivated as monolayers in T25-, T75- and T175-flasks. Cell passage numbers between 16 to maximal 28 were used for NT experiments.

ARPE-19 cells were cultivated, using a DMEM: F12 Medium (ATCC® 302006™) with 10% fetal bovine serum (FBS) and 1% Penicillin-Streptomycin. Accordingly, DMEM (1x) (Dulbecco's Modified Eagle Medium, Thermo Fisher Scientific, USA) with 10% FBS and 1% Penicillin-Streptomycin was used for HFF cultivation. These cell types were chosen, because of their presence in different human tissues and their different viral entry pathways (Fig.5).

### 2.2 Virus isolates

Several clinical isolates were used for NT assays, depending on the particular investigated scientific issue.

In general, the clinical isolate “H2497-11” was chosen as therapy-naive reference strain. It was isolated from amniotic fluid of a pregnant woman after feticide, resulting in a termination of pregnancy (TOP) in Tuebingen, 2011. One isolate was primary adapted to HFF “H2497-HFF” and the other one to ARPE-19 cells “H2497-ARPE-19”. It has to be considered at this point, that a primary adaptation of HCMV strains to ARPE-19 cells usually failed and a previous adaptation on HFF, followed by a secondary adaptation to ARPE-19 cell was necessary. The HCMV strain “H2497-11” was isolated by K. Schweizer and S. Preisetanz (Preisetanz, 2012)

For NT experiments, both H2497-HFF and H2497-ARPE-19 were treated as separated viral strains from the same source. They were separately cultivated and cell-free viral stocks of these strains were produced after viral shedding into the supernatants (passage 21 for the H2497-HFF strain and passage 22 for the H2497-ARPE-19 strain. Cell propagation was done by weekly passaging. The strains were frozen at -80°C and the infectivity of the viral stocks was determined by TCID<sub>50</sub>/ml testing, according to method point 2.6. The H2497-HFF strain reached a TCID<sub>50</sub>/ml of 6.1 and the H2497-ARPE-19 strain a TCID<sub>50</sub>/ml of 5.4.

The number of passages until cell-free a virus strain was harvested and frozen at -80°C as stock depends on the concentration of released cell free infectious virus particles into the medium supernatant of the cell culture at the end of each passage incubation. Therefore, each passage was tested with TCID<sub>50</sub> determination. Additionally, all supernatants, containing cell-free virus were centrifugalized at 50.000x g for 1h to concentrate infectious virus particles once more.

As drug-resistant HCMV strains, 2 different cell-free HCMV strains were examined (Tab.8). The strain “40571” was isolated from urine (date: 1998) after a bone marrow transplantation (BMT) and carries a resistance to Ganciclovir® (GCV) (Mutation: UL97 [A591V]). The strain was propagated to passage 24 until viral shedding (Prix et al., 1999).

**Table 8: Overview of the used HCMV strains with drug resistance, tested in NT assays**

<b>HCMV strain</b>	<b>Source</b>	<b>Patient ID</b>	<b>Patient indication</b>	<b>Viral isolate</b>	<b>TCID<sub>50</sub>/ml</b>
40571	Urine	7-year-old child (male)	BMT	Urine UL97 [A591V]	4.1
H815-06	EDTA blood	ZP (male)	SCT	Leukocytes (multi-drug resistant) UL97 [L595S] UL54 [V715M]	4.4

The strain “H815-06” was isolated from leukocytes (date: 2006) and had a multi-resistance against GCV (Mutation: UL97 [L595S]) and Cidofovir® (CDV) (Mutation: UL54 [V715M]). The passage number was 26 until viral shedding into the supernatant (Göhring et al., 2013). The generation of virus stocks and TCID<sub>50</sub> determination were performed, according to the reference strain. The TCID<sub>50</sub>/ml-value for “40571” was 4.1 and “H815-06” reached a TCID<sub>50</sub>/ml value of 4.4. Both resistant HCMV strains were cultivated in the presence of GCV unit harvest at an antiviral concentration of 6µM/ml<sup>1</sup>. The usage of CDV is not necessary for cultivation and for the NT assays, because the CDV resistance of the investigated HCMV strain “H815-06” only appears in a combination of a GCV resistance.

<sup>1</sup> HCMV strain with an IC<sub>50</sub> > 6µM/ml GCV are considered as resistant (Göhring et al., 2013)

In table 9, the in NT assays investigated HCMV strains with 4 different gB (UL55) types are displayed.

**Table 9: Overview of the HCMV strains used with different gB types, tested in NT assays.**

<b>gB type</b>	<b>HCMV strain</b>	<b>Source</b>	<b>Patient ID</b>	<b>Patient indication</b>	<b>Viral isolate</b>	<b>TCID<sub>50</sub>/ml</b>
1	H1241-16	Breast milk (dpp = 79)	EL (female)	HCMV-reactivation	Milk whey	4.5
2	AD169	Adenoid tissue (ATCC® VR538™)	7-year-old Child (female)	HCMV infection	Nasal discharge	2.2
3	H1058-10	Breast milk (dpp= 46)	SA (female)	HCMV-reactivation	Milk whey	3.9
4	H487-06	EDTA blood	ZP (male)	SCT	Leukocytes (multi-drug resistant) UL97 [L595S] UL54 [V715M]	4.3

For this purpose, an HCMV wild type strain H1241-16 from breast milk (day postpartum (dpp) = 79) was used after a local reactivation of HCMV in the breast tissue (gB type 1). The HCMV strain AD169 is a high-passaged laboratory reference isolate which was primary isolated from a 7 years old child after a HCMV infection from adenoid tissue (gB type 2). The HCMV strain H1058-10 was isolated from milk whey after a reactivation of HCMV (dpp = 46) (gB type 3). The HCMV strain H487-06 is a multidrug-resistant isolate which emerged after stem cell transplantation (SCT) in leukocytes and was isolated from EDTA blood (gB type 4) (Göhring et al., 2013). In a preliminary *in silico* sequence alignment analysis of the UL55 region, the gB types of the selected HCMV strains were analyzed by nested PCR (nPCR) and Sanger sequencing via LGC Genomics GmbH, Germany, followed by a comparison to reference sequences of gB type 1 to 4 which were extracted from the NCBI National Center for Biotechnology Information (NCBI) database (Tab.10) (Murthy et al., 2011).

**Table 10: Extracted UL55 sequences of gB type 1 to 4 with corresponding accession number and protein ID (upload date: 2016) (Murthy et al., 2011)**

<b>gB type (UL55)</b>	<b>Accession Number</b>	<b>Protein ID</b>	<b>Corresponding HCMV strain</b>
1	GU365817	ADO30523.1	H1241-16
2	GU365820	ADO30526.1	AD169
3	GU365822	ADO30528.1	H1058-10
4	GU365824	ADO30530.1	H487-06

The following alignment analysis was done via Vector NTI® program, Thermo Fisher Scientific, USA. The generated project data were transferred afterwards to the sequence analysis program Jalview®, University of Dundee, Scotland (Version 2.10.4b1) to calculate a phylogenetical tree, using the “Neighbour-Joining-Algorithm”. This specific algorithm is termed as phonetic *bottom-up* cluster method to hierarchically compare data sets via a bifurcal (2-way-crossing) resampling (Fig.21).

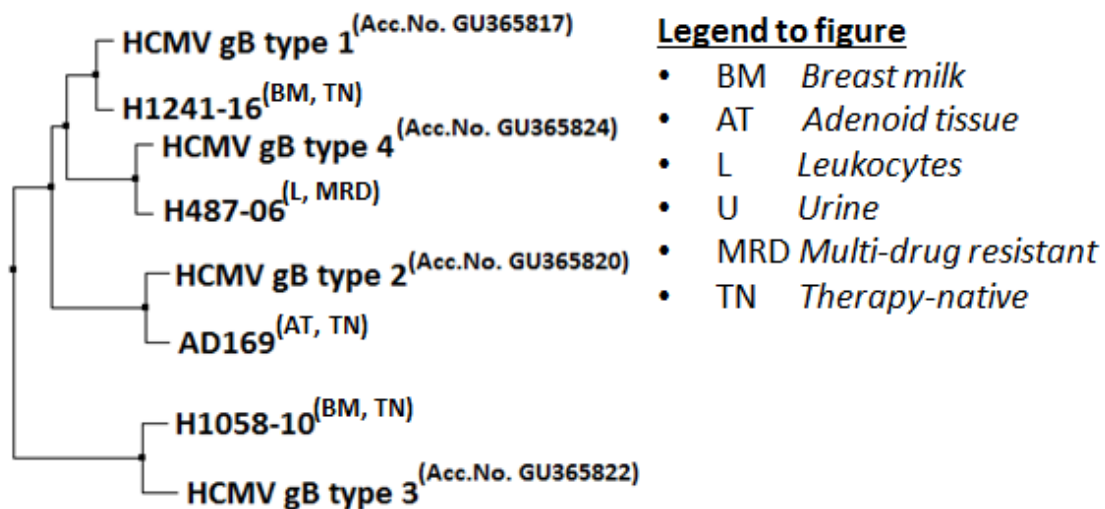


Figure 21: Phylogenetical tree which displayed and confirmed the gB types of the selected HCMV strains

The nested PCR had 2 rounds which contained 30 heat cycles (1<sup>st</sup> PCR: heat up at 94°C, 4 min; Start: 94°C, 1 min => 60°C, 1 min =>72°C, 1 min; End: 72°C, 10 min / 2<sup>nd</sup>PCR: heat up at 94°C for 4 min; Start: 94°C, 1 min => 65°C, 1 min =>72°C, 1 min; End: 72°C, 10 min). The used primer pairs are shown in table 11 (in-house protocol, modified after Chou et al., 1991). The master mix preparations are described in method point 2.4.1.

Table 11: nPCR gB primer pairs

PCR 1 gB		Type	Strand
gB1138	5`CAA GAR GTG AAC ATC TCC GA 3`	Outer	sense
gB1596	5`ÀTG GCC GAG AGA ATT GCR GA 3`	Outer	antisense
PCR 2 gB			
gB1276	5`GGT TTG GTG GTG TTC TGG CA 3`	Internal	sense
gB1524	5`CAC ACA CCA GGC TTC TGC GA 3`	Internal	antisense

The enzymatic gB typification was additionally performed which confirmed the *in-silico* sequence analysis of the UL55 region, according to Tarragó et al., 2003. Restriction endonucleases were ordered from BioLabs, New England® (Tab.12).

**Table 12: gB typification via enzymatic digestion after PCR. Predicted band patterns in bps for the used restriction endonucleases**

<b>Genotype / Enzyme</b>	<b>Alu I (R0137S)</b>	<b>Taq I (R01495)</b>	<b>Hin6 I (R108T)</b>
<b>gB1</b>	583bps, 166bps	459bps, 290bps	607bps, 82bps, 9bps, 35bps, 6bps
<b>gB2</b>	411bps, 169bps, 166bps	288bps, 271bps, 108bps, 79bps	308bps, 219bps, 82, 77bps, 35bps, 19bps, 6bps
<b>gB3</b>	583bps, 130bps, 36bps	0bps	524bps, 82bps, 77bps, 35bps, 25bps
<b>gB4</b>	583bps, 130bps, 36bps	391bps, 290bps, 63bps	311bps, 296bps, 82bps, 60bps

The digested viral DNA was separated via gel electrophoresis on a 1% agarose gel Tris-borate-EDTA (TBE) buffer, resulting in the predicted band patterns of base pairs (bps).



NT experiments in this work were also performed using the RV-TB40-BACKL7-SE-EGFP strain variant of HCMV (TB40E-L7) which was originally established by Christian Sinziger in Tuebingen and enhanced by Kerstin Sampaio (Sinziger et al., 2008; Sampaio et al., 2017). Therefore, an improved BAC cassette was inserted downstream of US34A, expressing eGFP (Green fluorescent protein – Excitation: 488 nm / Emission: 509 nm). This strain was used to offer an alternative “read out” to the performed NT assay system.

The TB40/E-L7 strain enabled an *in vitro* life observation of the NT capacity using HIGs and IVIGs from day 1 to day 5 without an end point fixation (Acetone/Ethanol), followed by visualization via p72 IE-antigen-immunoperoxidase staining.

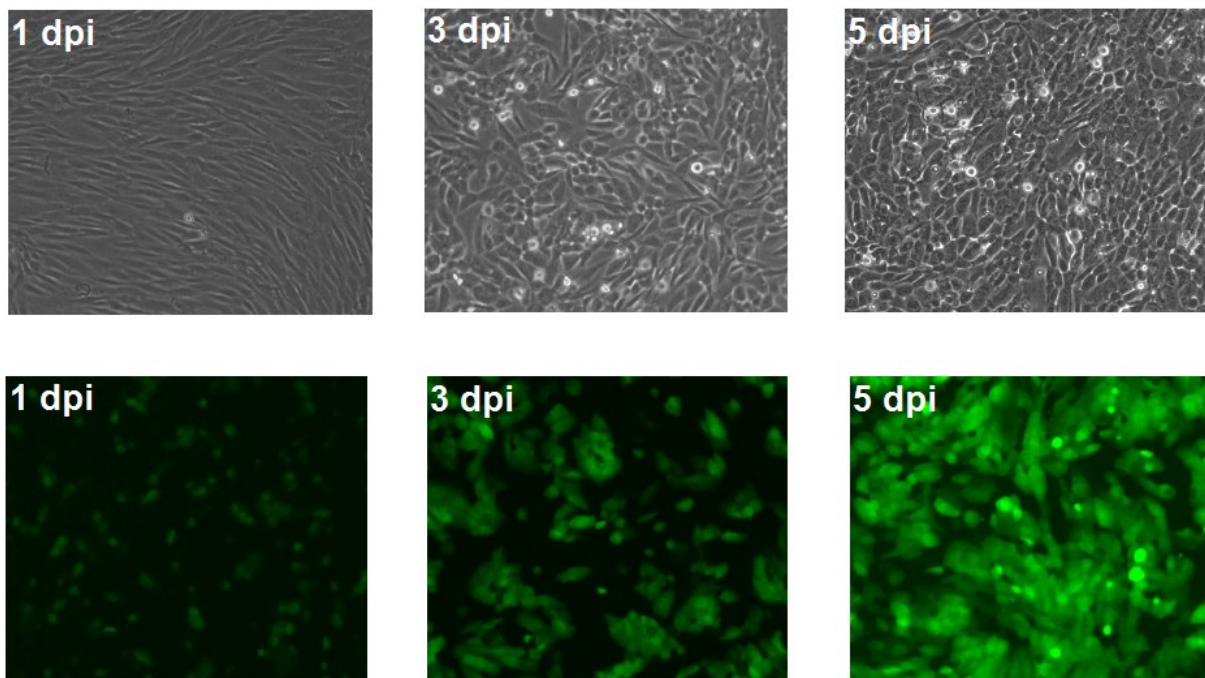


**Figure 22: Example for TB40E-L7 infected HFFs on 1, 3, 5 day post infection (dpi); 200x TCID<sub>50</sub>; 100x. Light microscope figures compared to fluorescent figures of the same microtiter well (Filter set 38 HE®: Excitation BP 470/40; Emission BP525/50 ZEISS)**

However, for better handling, the NT assay could be fixed on day 5 with 4% Paraformaldehyde (PFA)<sup>2</sup> for 10min at RT, if the “read out” analysis of infected target cells was not possible on the same day. A viral stock of TB40/E-L7 was prepared and stored at -80°C with a TCID<sub>50</sub>/ml of 4.6 until NT analysis. Figure 22 shows an example for HFFs on day 1 to 5 post infection (dpi) which were infected with cell-free TB40E-L7 with 400xTCID<sub>50</sub>/ml. The eGF-protein cumulated through virus production in the infected target cell over time which resulted in increased green glowing of these cells until day 5 post infection.

---

<sup>2</sup> A fixation of TB40/E-L7-infected cells with Acetone/Ethanol would denature the eGF-protein.

## 2.1 Samples

### 2.1.1 NT assay reference pools

For calibration of NT assays, two reference serum pools were generated as controls. The first serum pool contained sera of  $n = 100$  HCMV-IgM<sup>-</sup>/IgG<sup>-</sup> women at birth. The second serum pool was made of  $n = 100$  HCMV-IgM<sup>+</sup>/IgG<sup>+</sup> women which were HCMV-latently infected at birth. The serum samples were collected during the Tuebingen congenital HCMV study 2011 (Ethical approval EK number: 506/2015BO2). All women of this study were analyzed with 5 different HCMV serological test systems, including Enzygnost-ELISA® (Siemens), CLIA® (Diasorin) and CMIA® (Abbott), as well as ECLIA® (Roche) and ELISA® (Medac). For each pool, women were enclosed which showed concordantly equal test results in all 5 test systems. Therefore, 2 different serum pools were used which represented a comprehensive amount of 2 specific cohorts of mothers at birth. Equal serum volumes of 100 µl per sample were combined to create both pools, followed by freezing of the serum pools in 500 µL aliquots at -80°C until usage in NT assays.

## 2.2 IgG preparations

### 2.2.1 HIG Cytotect® and Cytogam®

Cytotect® and Cytogam® are hyperimmunoglobulin preparations (Tab.13). They consist of pooled sera, derived from healthy donors with high HCMV-specific IgG-titers. Cytotect® is a product of Biotest Pharma GmbH, Germany and has an official license as “Orphan Drug” in Europe and USA for intravenous application after transplantation of solid organs (2007). Besides its intended purpose, it was used via “off label use” to prevent maternofetal viral transmission after HCMV-primary infection. However, the usage is not recommended outside of clinical trials (Rawlinson et al., 2017).

In contrast, Cytogam® is made by CSL Behring, USA and has only a license for the US market. Both preparations were produced, using the same “Ethanol-fraction-process” to purify the IgG antibodies from the sera. But for sterilization, Biotest uses β-propiolacton, followed by an ultra-centrifugation and CSL Behring takes Tri(n-butyl) phosphate plus Triton X-100 in a “Solvent-detergent-process” to inactivate virus.

**Table 13: Manufacturer specifications of HIGs**

<b>Preparation</b>	<b>Manufacturer</b>	<b>Charge</b>	<b>Concentration</b>	<b>HCMV PEI Units/ml</b>
Cytotect®	Biotest Pharma	B797033	50 mg/ml	150.3
Cytogam®	CSL Behring®	4359000037	50 mg/ml	118.6

## 2.2.2 IVIGs

IVIGs are standard immunoglobulin preparations. In general, they are used after solid organ transplantation, but there is also a study which used Kiovig® in case of HCMV-primary infections in pregnant women (Pollili et al., 2012). Table 14 shows the specifications of the investigated IVIGs.

**Table 14: IVIGs specifications**

Preparation	Manufacturer	Charge	Concentration	HCMV PEI Units/ml
Kiovig®	Baxter®	LE12M265BC	100 mg/ml	42.0
Octagam®	Octapharma®	A303B853A	100 mg/ml	62.4

According to Schampera et al., 2017, all investigated IgG preparations (HIGs, IVIGs), as well as the generated HCMV-IgG<sup>+</sup>-pool showed high HCMV-specific IgG, high IgG avidity and no HCMV-specific IgM, analyzed with HCMV recomBlot®; Mikrogen, Germany.

## 2.2.3 UL130 peptides and recombinant pentameric complex

The UL130 peptide design was previously performed by Jose Arellano-Galindo (AG Hamprecht) (Tab.15). It was established by the modification of amino acid sequences and based on a UL130 SWS-peptide of Saccocio et al., 2011. The computer analysis showed, that the modified UL130 TAN-peptide showed the highest “percentage of probability” (>75%) for epitope similarity. For the antibody depletion experiments, both peptides were synthesized by Intavis Peptide Services, Germany with an additionally 6x fold HisTag on the respective C-terminus (TANQNSPPWSKLTYSKP**HHHHHHH**) for magnetic bead anti-HisTag antibody labeling.

**Table 15: The UL130 peptide design on the base of Saccocio et al., 2011**

No.	Peptide	Amino acid Position	Ratio E-B
1	<b>TANQNPSPWSKLTYSKPH</b> TAN-peptide	32-50	E= 17/19 B= 2/19
2	<b>SWSTLTANQNPSPSKLTY</b> SWS-peptide		E = 14/15 B= 1/15

*E = Exposed residue B= Buried residue*

Antigenicity scale (Yang et al., 2009)

■ 0% ■ 25% ■ 50% ■ 75% ■ 100%  
Percentage of probability

Both peptides were delivered with a concentration of 10 mg/ml and a purity of at least 90%, achieved with HPLC (214 nm). The analysis was done via MALDI-MS and RP-HPLC.

In a following NT experiment, a pentameric complex was used for antibody depletion. The investigated HCMV-PC is a recombinant product which was generated by The Native Antigen Company, Oxfordshire UK (Product Code: HCMV-PENT). This native-like PC is produced in human embryonic kidney cells (HEK293) to ensure that all proteins are properly folded and possess their native glycosylation pattern. The presence of all five proteins in the purified complex is confirmed by mass spectrometry, according to the manufacturer. There is an additional 6x fold HisTag linked to gH. The genetic sequence origin for the recombinant HCMV pentameric complex was the VR1814 strain (NativeAntigen Company, Oxfordshire UK).

For the depletion experiments of PC-specific polyclonal antibodies (pAbs), magnetic beads and anti-HisTag mAbs were used from Cell Signaling Technology, USA, as well as a 6 Tube magnetic separation rack to remove the magnetic beads after incubation (Fig.23).

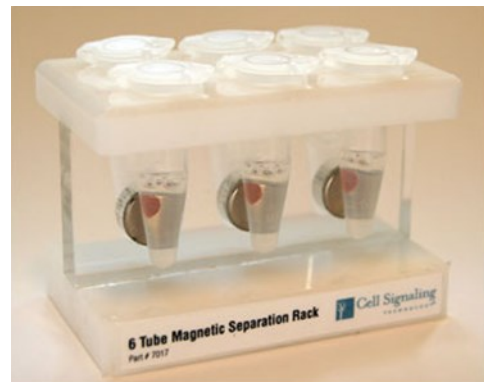


**Figure 23: 6 Tube magnetic separation rack. Product documentation Cell Signaling Technology**

Anti-IgG subclass 3 mAbs (Product code: 5247-9850, Clone: 5G12, Mouse-anti-human; BioRad laboratories, USA) were used which were bound to magnetic beads, to deplete IgG subclass 3 antibodies from Cytotect® and Kiovig®.

## 2.3 Laboratory systems

Device / Equipment	Company
Architect i1000SR®	Abbot
Camera ExwaveHAD N50®	Sony
Cell counter Z1 Beckman Coulter®	Beckman Life Sciences
Centrifuge 5417 R®	Eppendorf
Centrifuge 5804 R®	Eppendorf
Centrifuge 5810 R®	Eppendorf
Centrifuge Universal 32 R	Hettich
Cobas 6000 Analyzer®	Roche
Cold-storage room 4°C/ -20°C	NER
Extraction unit CVC 2000®	Vaccubrand
Fine scale 770®	KERN
Fridge-freezer at -20°C	Liebherr
Fridge-freezer at -80°C	Heraeus
Heat bath GFL 1086®	Memmert
Incubator 37°C; 5% CO <sub>2</sub> ; 97% rAh BBD 6220®	Heraeus
Incubator 37°C; 5% CO <sub>2</sub> ; 97% rAh C200®	Labotect
Multipette plus 8-fold® (50 µl -1200 µl)	Eppendorf
Optical microscope Axiovert 25/100®	Zeiss
pH-measuring instrument pH level 2®	inoLab
Pipette (10 µl / 100 µl / 200 µl / 500 µl / 1000 µl)	Eppendorf
Thermomixer comfort®	Eppendorf
Ultra-centrifuge Biofuge Stratos®	Thermo Scientific
Vortexer / Shaker MR 3001 K®	Heidolph
Vortexer / Shaker REAX top®	Heidolph
Workbench (laminar air flow) HS 12®	BDK/Heraeus/UntiyLabServices

## 2.4 Reagents and Materials

Material	Company
96 well microtiter plates	Nunc/Greiner
Acetone	LaboChem international
Adhesive foil Masterscreen permanent®	ERA
Cell culture medium DMEM: Medium Dulecco's Modified Eagle Medium®, 500 ml	ATCC
Cell culture medium Ham's Nutrient Mixture F-12, L-Glutamine, HEPES; 500ml	ATCC
Counting chamber C-Chip®	Digital Bio
Culture flask T25; T75; T175	Nunc
Disinfection agent DESCOSEPT AT®	Dr. Schuhmacher GmbH
Disinfection agent Sterillium®	BODE CHEMIE
DMSO	MERCK
Ethanol 99,9%	NORMAPUR
Examination gloves ProLine® powder-free, Latex	ASID BONZ
FALCON® tubes (15 ml / 50 ml)	Becton Dickinson
Fetal Bovine Serum (FBS) 500 ml, sterile filtrated (Ø 0,22 µl)	Thermo Fisher Scientific
Glass containers (250 ml / 500 ml / 1000 ml)	SCHOTT
Glycerin	ROTH
Laboratory coat (H50)	Waldner
Pancoll® (sterile filtrated)	PAN BIOTECH
Paraformaldehyde (PFA) powder 95%	SIGMA-ALDRICH
PBS: Dulbecco's Phosphate-buffered saline (-CaCl <sub>2</sub> , +MgCl <sub>2</sub> ); 500 ml	Thermo Fisher Scientific
Penicillin/Streptomycin; 100ml	Thermo Fisher Scientific
Pipette tips (10 µl / 100 µl / 200 µl / 50 µl / 1000 µl)	Eppendorf
Primary monoclonal anti-HCMV IgG-mouse-antibody E13-Klon, target IE1(UL122) anti-pp72	BioMérieux
QuantiFERON-HCMV 2 Plate Kit ELISA® 0350-0201	Qiagen
QuantiFERON-HCMV Blood Colletion Tubes® 0192-0301	Qiagen
Reaction tubes (0,2 ml / 0,5 ml / 1,5 ml / 5 ml)	Eppendorf
Secondary monoclonal anti-mouse IgG-rabbit-antibody + horseradish peroxidase (POD)	Agilent Technologies
Sterile filter MILLEX®-GS (Ø 0,22 µm, 0,44 µm)	MILLIPORE
TBE buffer 10x	Thermo Fisher Scientific
Trypsin-EDTA; 100 ml	Thermo Fisher Scientific
T-Track ELISpot kit human IFN-γ HISpecificity®	Lophius biosciences

### 2.4.1 nPCR Master Mix for gB typification

#### PCR 1: 50 $\mu$ L final volume:

- 36,75  $\mu$ L Ampuwa
- • + 0.25  $\mu$ L (0.5  $\mu$ M Primer gB1138)
- • + 0.25  $\mu$ L (0.5  $\mu$ M Primer gB1596)
- • + 0.20  $\mu$ L (100  $\mu$ M dNTP mix)
- • + 5,0  $\mu$ L Puffer Roche (10x)
- • + 0.005  $\mu$ L (0.01% Tween)
- • + 2.5  $\mu$ L Taq polymerase
- • + 2.0  $\mu$ L Template 50 ng/ $\mu$ g DNA

#### PCR 2: 100 $\mu$ L final volume:

- 86.15  $\mu$ L Ampuwa
- • + 0.05  $\mu$ L (0.1 $\mu$ M Primer gB1276)
- • + 0.05  $\mu$ L (0.1 $\mu$ M Primer gB1524)
- • + 0.20  $\mu$ L (100 $\mu$ M dNTP mix)
- • 10  $\mu$ L Puffer Roche (10x)
- • 0.01  $\mu$ L (0.01% Tween)
- • 2.5  $\mu$ L Taq polymerase
- • + 1.0  $\mu$ L Template from PCR 1 (1:50 dilution)

## 2.4.2 Buffers

### TBS-wash buffer: Tris-buffered Saline

#### Stock solution (10x):

- 60.57 g Tris-base
- • 87 g sodium chloride (NaCl)
- • solved in 800 ml ddH<sub>2</sub>O
- • pH 7.6 adjusted with 2N hydrochloric acid (HCl)
- • filled up to 1000 ml + sterile filtrated (Ø 0.22µl)

#### Ready-to-use solution: Dilution factor (1:10)

- 100 ml stock solution+900ml ddH<sub>2</sub>O+2ml Tween20

### Sodium acetate buffer (0,1 [M])

#### Stock solution (10x):

- 82.5 g sodium acetate
- • add 28.88 ml glacial acetic acid (100 %)
- • solved in 900 ml ddH<sub>2</sub>O
- • pH 4.9 adjusted with 2N hydrochloric acid (HCl)

#### Ready-to-use solution: Dilution factor: (1:10)

- 100 ml stock solution + 900ml ddH<sub>2</sub>O

## 2.4.3 Immunperoxidase Substrate

#### AEC stock solution (20x)

- 10 mg 3-amino-9-ethylcarbazol-substrat (AEC)
- • + 0.1 M sodium acetate buffer
- • solved in 2.5 ml N,N-dimethylformamide

#### Ready-to-use solution: Dilution factor (1:20)

- 100 ml stock solution + 1900ml sodium acetate buffer
- • add H<sub>2</sub>O<sub>2</sub> Dilution factor (1:1000)



#### 2.4.4 Paraformaldehyde (PFA) solution

##### PFA ready-to-use solution 4%

- 450 ml of dH<sub>2</sub>O in 1L glass vessel with screw cap
- • heated to 60°C<sup>3</sup> using hot plate with agitator + magnetic stirrer
- • add slowly 20 g PFA powder 95% to the heated water during stirring
- • add 5 single drops of 2 N NaOH in until the solution cleared up each time
- • remove from heat + add 50 ml PBS (10x)

##### Final volume 500 µL

- adjust to pH 7.2 using HCl
- • filtrate using 0,22 µM filter
- • freeze 10x50 ml aliquots at -20°C until use
- • use immediately after thawing process

Remaining PFA solution was be stored at 4°C for 2 weeks, covered from light.

The PFA solution was generated under an extractor hood, wearing gloves and protection glasses at any time.

#### 2.4.5 GCV-dilution scheme to determinate IC<sub>50</sub>

##### GCV stock solution

- Aliquots were generated at a concentration of 50 mg/ml<sup>(1)</sup>  $\triangleq$  196 mM in ddH<sub>2</sub>O

##### Dilution series (7x):

- 1 mM<sup>(2)</sup>  $\Leftrightarrow$  50 µL GCV<sup>(1)</sup> + 9750 µL MEM(+10% FCS) (Dilution factor 1:196)
- • 50 µM<sup>(3)</sup>  $\Leftrightarrow$  500 µL<sup>(3)</sup> + 9500 µL MEM(+10% FCS) (Dilution factor 1:20)
- • 25 µM<sup>(4)</sup>  $\Leftrightarrow$  5000 µL<sup>(3)</sup> + 5000 µL MEM(+10% FCS) (Dilution factor 1:2)
- • 10 µM<sup>(5)</sup>  $\Leftrightarrow$  5000 µL<sup>(4)</sup> + 5000 µL MEM(+10% FCS) (Dilution factor 1:2)
- • 5 µM<sup>(6)</sup>  $\Leftrightarrow$  5000 µL<sup>(5)</sup> + 7500 µL MEM(+10% FCS) (Dilution factor 1:2,5)
- • 2,5 µM<sup>(7)</sup>  $\Leftrightarrow$  5000 µL<sup>(6)</sup> + 5000 µL MEM(+10% FCS) (Dilution factor 1:2)
- • 0,5 µM  $\Leftrightarrow$  2500 µL<sup>(7)</sup> + 10000 µL MEM(+10% FCS) (Dilution factor 1:5)

---

<sup>3</sup>PFA is unstable at temperatures above 70°C

## **2.5 Cell culture and virus propagation**

### **2.5.1 Cultivation of human cells (ARPE-19 cells, HFF)**

In general, the cultivation of cells and microtiter plate preparation were separated from virus isolation and propagation, as well as neutralization assays. Therefore, the laboratory work took place in different lab rooms to avoid unwanted viral contamination of target cells. Furthermore, all studies were carried out under a sterile workbench using “Single-Use-Systems”, appropriate protective clothing and gloves at all times.

For cultivation, the cells were stored in intended incubators under defined culture conditions of 37°C, 5% CO<sub>2</sub> and 95% relative air humidity (rAh). T25-, T75- and T175-culture flasks Nunc® were used, depending on the needed number of cells. Afterwards, the cells were counted via Trypan blue staining and transferred afterwards to 96-well microtiter plates for NT-testing. The cells were passaged every 14 days, combined with monthly mycoplasmas testing. Only mycoplasma-free cells were used for studies. In addition, the cells were checked visually for bacterial or fungal contaminations before using in NT assays and the final passage number of the cell cultures was documented.

### **2.5.2 Passaging of human cells**

The cells were passaged after reaching 80% confluence in the culture flask. Firstly, the medium was removed, followed by a wash step of the cells with phosphate-buffered saline (PBS) +1% Penicillin-Streptomycin, Thermo Fisher Scientific, USA. Trypsin was added to the culture flask (1 ml for T25, 3 ml for T75 or 6 ml for T175) for duration of 5-8 min, remaining in the incubator. Afterwards, the culture flask was gently tapped until the cells detached from the inner surface of the flask, checked by using a microscope (solution: 100x). On demand, the cells were usually split and transferred into 2 or 3 new culture flasks, containing fresh medium (5ml for T25, 12ml for T75 or 24ml for T175). The change of medium was performed every 4 days for ARPE-19 cells and every 7 days for HFF.

### 2.5.3 Cell counting and cell vitality testing

Trypan blue was used for vital staining of cells. Trypan blue is able to penetrate the membrane of dead cells which resulted in dark blue dead cells, compared to living cells (Fig.24A). Therefore, adherent cells were detached by gently shaking with trypsin until they were present as single cells. The cells were mixed with trypan blue (1:2), transferred directly to the Neubauer counting chamber.

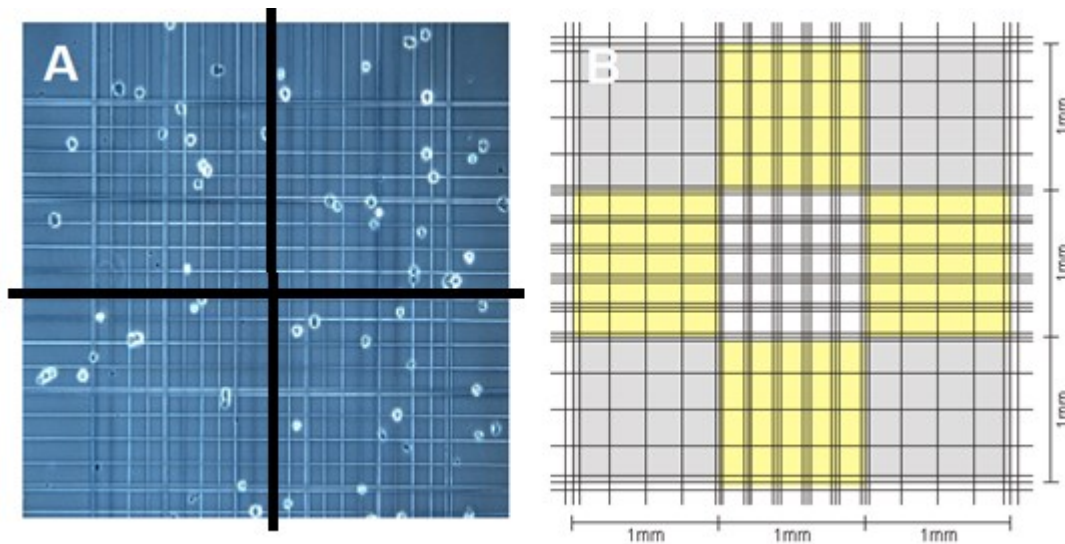


**Figure 24: (A) Visualization of death/live cells via trypan blue staining; (B) schematic model of a "Neubauer counting chamber" URL1: modified after Celeromics documents (date: 02.02.2018)"**

By using the 4 "grey" squares (Fig 24B), the cells were counted and the number of cells per milliliter were calculated using a mathematical equation (Eq.1).

**Equation 1: Calculation of cell number /ml Neubauer counting chamber**

$$\text{Cell number/ml} = \frac{\text{NIC}}{\text{NIQ}} \times \text{Df} \times 10^4$$

Legend to equation 1:

NIC = Number of counted living cells

NIQ = Number of used large square

Df = Dilution factor

$10^4$  = Chamber factor

The vitality of cells describes the ratio between dead and living cells for the counted cells and was calculated, using equation 2.

**Equation 2: Vitality of cells**

Legend to equation 2:

VC = Vitality of cells

NdC = Number of counted dead cells

NIC = Number of counted living cells

$$\text{VC} = \frac{\text{NdC}}{\text{NIC}} \%$$

#### **2.5.4 Cryopreservation of human cells**

Cryopreservation is used for long time storage of cell stocks with a low passage number. Stocks of HFF and ARPE-19 cells were prepared and frozen for this work to ensure the comparability and quality of the performed experiments. The cells were enzymatically detached from the culture flasks and transferred to fresh culture medium, followed by cell counting via trypan blue staining. After adjustment of the cell concentration to (5 million cells/ml per cryogenic vial), a centrifugation was performed at 300x g for 5 min. The supernatant was removed and the cells were re-suspended in cryomedium with a temperature of 4°C. Afterwards, the cells were transferred to marked cryo-vials. Immediately, the cells were frozen at -80°C in a fridge. The cryomedium contained additionally 5% dimethyl-sulfoxide (DMSO) and 25% FBS, compared to standard culture medium to avoid crystallization of the water during the freezing process. For infected cells, 10% glycerin and 20% FBS were used instead to preserve the viral infectivity. However, DMSO inhibits the crystallization better than glycerin.

#### **2.5.5 Reinitialization of cryopreserved cells**

DMSO shows cell toxicity at room temperature (RT). Therefore, it should be removed immediately after the thawing process. The cryogenic vials were put into a warm water bath at 37°C to ensure a quick defrost.

After thawing, the cells were transferred into fresh culture medium without DMSO and centrifuged at 300x g for 5 min. Afterwards, the medium was replaced by fresh medium. In order to remove DMSO completely from the cell culture, the wash process was repeated and the cells were finally placed in T25 culture flasks and for further cultivation into T75 or T175 culture flasks on demand.

#### **2.5.6 Virus cultivation**

HCMV replicates only in specific living and growing eukaryotic cells. Therefore, HFF and ARPE-19 monolayers were used in a culture flask with a confluence of approximately 80% for virus cultivation. The medium was removed and the cell culture was washed with PBS. At this point, cell-free virus supernatant or already infected cells were added to the cell culture. After an incubation of 10 min at 37°C, 5% CO<sub>2</sub>, cell culture flasks were filled with fresh medium and stored in an incubator at 37°C, 5% CO<sub>2</sub>. For NT experiments, the concentration of virus was defined via tissue culture infective dose 50% (TCID<sub>50</sub>)-determination.

## 2.6 TCID<sub>50</sub> determination

The determination of TCID<sub>50</sub> (tissue culture infective dose 50%) is defined as concentration which is necessary to infect half of the non-infected cells after inoculation with viral lysates in a given time, normally 18 h to 72 h at 37°C, 5% CO<sub>2</sub>. In detail, the TCID<sub>50</sub> value reflects the reciprocal logarithmic dilution which corresponds to the potency of the dilution. For the determination, 96 well microtiter plates were used with 20.000 non-infected cells in each well. Cells were previously counted and transferred to the microtiter plate until they reached adherence, usually in 4-5 h at 37°C, 5% CO<sub>2</sub>. A dilution series of cell free virus was created in  $_{\log}10$  steps from 10<sup>-0</sup> to 10<sup>-9</sup>.

**Table 16: Scheme for TCID<sub>50</sub> determination; CC = cell control; VC = virus control**

	1	2	3	4	5	6	7	8	9	10	11	12
A	10 <sup>-0</sup>	10 <sup>-1</sup>	10 <sup>-2</sup>	10 <sup>-3</sup>	10 <sup>-4</sup>	10 <sup>-5</sup>	10 <sup>-6</sup>	10 <sup>-7</sup>	10 <sup>-8</sup>	10 <sup>-9</sup>	CC	VC
B	10 <sup>-0</sup>	10 <sup>-1</sup>	10 <sup>-2</sup>	10 <sup>-3</sup>	10 <sup>-4</sup>	10 <sup>-5</sup>	10 <sup>-6</sup>	10 <sup>-7</sup>	10 <sup>-8</sup>	10 <sup>-9</sup>	CC	VC
C	10 <sup>-0</sup>	10 <sup>-1</sup>	10 <sup>-2</sup>	10 <sup>-3</sup>	10 <sup>-4</sup>	10 <sup>-5</sup>	10 <sup>-6</sup>	10 <sup>-7</sup>	10 <sup>-8</sup>	10 <sup>-9</sup>	CC	VC
D	10 <sup>-0</sup>	10 <sup>-1</sup>	10 <sup>-2</sup>	10 <sup>-3</sup>	10 <sup>-4</sup>	10 <sup>-5</sup>	10 <sup>-6</sup>	10 <sup>-7</sup>	10 <sup>-8</sup>	10 <sup>-9</sup>	CC	VC
E	10 <sup>-0</sup>	10 <sup>-1</sup>	10 <sup>-2</sup>	10 <sup>-3</sup>	10 <sup>-4</sup>	10 <sup>-5</sup>	10 <sup>-6</sup>	10 <sup>-7</sup>	10 <sup>-8</sup>	10 <sup>-9</sup>	CC	VC
F	10 <sup>-0</sup>	10 <sup>-1</sup>	10 <sup>-2</sup>	10 <sup>-3</sup>	10 <sup>-4</sup>	10 <sup>-5</sup>	10 <sup>-6</sup>	10 <sup>-7</sup>	10 <sup>-8</sup>	10 <sup>-9</sup>	CC	VC
G	10 <sup>-0</sup>	10 <sup>-1</sup>	10 <sup>-2</sup>	10 <sup>-3</sup>	10 <sup>-4</sup>	10 <sup>-5</sup>	10 <sup>-6</sup>	10 <sup>-7</sup>	10 <sup>-8</sup>	10 <sup>-9</sup>	CC	VC
H	10 <sup>-0</sup>	10 <sup>-1</sup>	10 <sup>-2</sup>	10 <sup>-3</sup>	10 <sup>-4</sup>	10 <sup>-5</sup>	10 <sup>-6</sup>	10 <sup>-7</sup>	10 <sup>-8</sup>	10 <sup>-9</sup>	CC	VC

An overview for the TCID<sub>50</sub> determination is given in table 16, whereby each 8 replica (A-H) of dilutions 10<sup>-0</sup> to 10<sup>-9</sup> are shown (column 1 to 10) on the microtiter plate in 8 replicas (A to H). 100 µL of each dilution was added to the intended wells. Cell control (CC) and virus control (VC) were additionally prepared and added. Afterwards, the microtiter plate was centrifuged for 30 min at 300x g; RT, followed by an additional incubation of 30 min at 37°C, 5% CO<sub>2</sub>. Finally, 100µL fresh culture media was added to each well, followed by an incubation for the next 17 h at 37°C, 5% CO<sub>2</sub>. After inoculation, the infected nuclei were visualized under the light microscope via p72 IE-antigen immunoperoxidase staining. Under this condition, the TCID<sub>50</sub> value is the potency of the dilution which contains 4 of 8 infected wells. One infected cell core defines infection in a well.

For calculation of the TCID<sub>50</sub>, the single dilutions were defined as class borders and values exactly between the class borders (x+ 0.5) were called “middle of class” (Tab.17). The mathematical product was calculated through the increase of the number of infected wells from dilution to dilution and the corresponding middle of class of dilution. In the next step, the products were summed up and divided through the number of replicas of each dilution, in this setup 8. This TCID<sub>50</sub>-value is equal to the logarithm (basis 10) per 100µL. The potency must be added by +1 to gain the logarithm per ml (Method after Spearman-Kaerber; Bonin, 1973).

**Table 17: TCID<sub>50</sub> calculation example**

<b>Class borders</b>	<b>-9</b>	<b>-8</b>	<b>-7</b>	<b>-6</b>	<b>-5</b>	<b>-4</b>	<b>-3</b>	<b>-2</b>	<b>-1</b>
<b>Number of infected wells</b>	0	0	0	2	4	6	8	8	8
<b>Middle of dilution class</b>		-8,5	-7,5	-6,5	-5,5	-4,5	-3,5	-2,5	-1,5
<b>Increase of infected wells</b>		0	0	2	2	2	2	0	0
<b>Product</b>		0	0	-13	-11	-9	-7	0	0

**Equation 3: Calculation of TCID<sub>50</sub> using an example**

$$\log \frac{TCID_{50}}{mL} (18h) = \left| \frac{\text{Sum of products}}{\text{Number of dilution replicas (8)}} \right| + 1 = \left| \frac{-40}{8} \right| + 1 = |-5| + 1 = 6$$

Table 17 and equation 3 explain the calculation using a chosen example. The TCID<sub>50</sub>/ml for 18h was calculated and resulted in 6. The TCID<sub>50</sub>/ml can be used as indicator for infectivity of the virus and the used concentration of cell-free virus in neutralization assays can be described as (x)-fold of the TCID<sub>50</sub>/ml value to induce 100 SICs (single infected cell cores) or 100 PFUs (plaque forming units) which were defined as n ≥10 linked infected cell cores in the negative control after a defined incubation time (18 h or 5 d) at 37°C, 5% CO<sub>2</sub>.

**Equation 4: Calculation of the (x)-fold TCID<sub>50</sub> value for NT assays**

$$(x) - \text{fold} \frac{TCID_{50}}{ml} (18h) = \frac{10^6}{800} = 1250$$

For example, of calculation, the virus supernatant corresponds in a dilution of 1:800 to a 1250-fold TCID<sub>50</sub>/ml, as shown in equation 4.

## 2.7 p72 IE-antigen-immunoperoxidase staining (in situ ELISA)

The p72 IE-antigen immunoperoxidase staining is an ELISA (Enzyme-linked Immunosorbent Assay) which is used for detection of HCMV infection in cell culture in routine diagnostics. The immediate early antigen p72 of HCMV is recognized by a monoclonal anti-p72 primary mouse antibody, BioMérieux, France in the nucleus of infected cells. After a wash step, a monoclonal secondary anti-mouse antibody, Agilent Technologies, USA conjugated with a horseradish peroxidase (HRP) binds on the Fc-part of the primary anti-p72 mAb. HRP is able to catalyze 3-amino-9-ethylcarbazole (AEC) in a redox reaction which results in a red crystalline water-insoluble color and can be detected under a light microscope by eye (Fig.25).

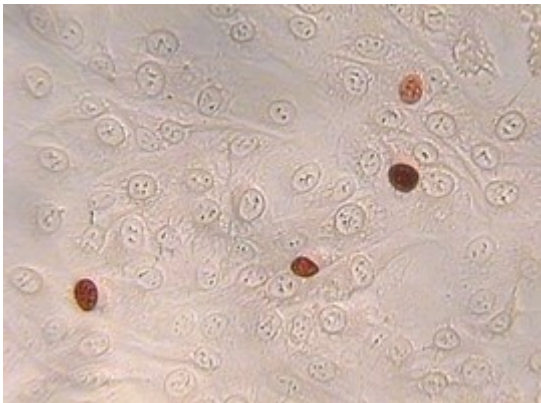


**Figure 25: Visualization of HCMV-infected cell nuclei (ARPE-19 cells) using p72 IE-antigen-immunoperoxidase staining (160x)**

The reaction needs the use of hydrogen peroxide ( $H_2O_2$ ) which will be reduced to water ( $H_2O$ ) by the enzyme.  $H_2O_2$  delivers the necessary biochemical energy to catalyze the reaction. For this purpose, the enzyme possesses a trivalent iron  $^{+3}$  cation in its active center. In a redox reaction, the substrate AEC will be oxidized and forms a red azomethine at the same time (Burstone, 1960). However, in order to perform this procedure, the infected cell culture had to be previously fixed with a 1:1 mixture of ethanol and acetone for 90 s, after removing the culture medium. For safety, the mixture was prepared under a hood.

After the incubation of 90 s, the cells were washed with 200  $\mu$ L/well tris-buffered saline (TBS) buffer and incubated with 100  $\mu$ L/well of the primary anti-p72 mAb in a concentration of 1:500. A second incubation of 1h at 37°C, 5%  $CO_2$  took place, followed by a 3 wash steps with TBS buffer to remove unbound primary mAb. Next, 100 $\mu$ L/well of the secondary anti-mouse mAb was added, used in a concentration of 1:400 to bind the primary mAb for the next 1 h at 37°C. Afterwards, the cells were washed 3-times with TBS buffer. Meanwhile, the substrate solution was prepared which included AEC and sodium acetate buffer in a ratio of 1:20. The ACE was previously solved in N, N-dimethylformamide. The generated solution contains coarse crystals which had to be removed by a 22  $\mu$ m filter.

The 100 µL of the ACE solution was transferred to each well and hydrogen peroxide was separately given to the wells to initiate the reaction. The color development was supported by a light-protected incubation for about 20 to 30 min, 37°C. After reaching the desired coloration, the reaction was stopped by removing the solution, followed by 2 wash steps with TBS buffer. Finally, the wells were filled with 200 µL PBS and the SICs/PFUs were counted under the light microscope. For storage, the plates were placed at 4°C, covered from light.

## **2.8 *In vitro* neutralization assays**

First investigations focused on *in vitro* neutralization assays to characterize the HIG Cytotect® in context of its ability to neutralize HCMV effectively. The neutralization protocols were modified after a previous work of Schampera et al., 2017 which originally based on Eggers et al., 2000 and Abai et al., 2007.

Two different approaches of NT-assays, including a short-term cell-free HCMV neutralization assays (CFNT) of 18h for binding and the prevention of viral infection of cells and a long-term cell-adapted neutralization-plaque-reduction assays (PRANT) of 3 days to demonstrate inhibition of cell-to-cell spread via plaque formation (Schampera et al., 2017).

In this work, the NT-assay protocols were multiple adapted to combine the advantages of both approaches of Schampera et al., 2017 to investigate viral infection and detect active viral cycles, as well as using less volume of the IgG preparations at the same time. In general, the performed NT-protocol used different cell-free virus strains which were incubated with dilution series of IgG-preparations (1:50; 1:500; 1:1.000; 1:5.000; 1:10.000; 1:50.000) in a ratio of 1:1 for 90 min at 37°C, 5% CO<sub>2</sub> under defined conditions, depending on the specific question (referring to 1.15.). Then, 100µL of the incubated virus-antibody solution was transferred to ARPE-19 cell and/or HFF monolayers, followed by a centrifugation at 300xg, RT for 30 min and a further incubation at 37°C, 5% CO<sub>2</sub> for 30 min.

Afterwards, all wells were filled with 100 µL of fresh culture medium and an incubation of 5 days took place at 37°C, 5% CO<sub>2</sub>. While this time, the virus had time to infect the cell culture. In preliminary test, the concentrations of each used viral strain were determined, that induce approximately 100 PFUs after 5 days of incubation in the negative reference pool. As additional control, a positive pool was used in each NT assay which represented the average NT-capacity of latently infected women at birth.



The read out was performed by p72 IE-antigen-immunoperoxidase staining. An example for a read out of 1 PFU  $\geq$  10 SICs is given after performance of a NT assay with a duration of 5 days (2 images of the virus control) (Fig.26). The reference serum pools were preincubated for 30 min, at 56°C on a heat block for complement inactivation. The used IgG-preparations contain no complement and additional heat incubations showed no effect on *in vitro* NT-capacity in preliminary NT-activity testing.

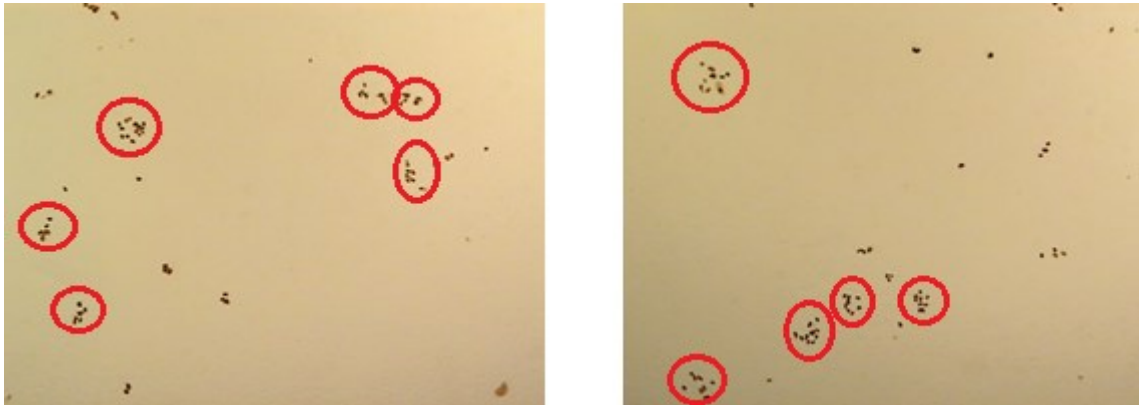


**Figure 26: Example for read out of PFUs  $\geq$ 10 after 5d incubation (25x)**

In order to standardize the “read out” of the NT assay system, each well of the microtiter plate was counted 2 times (blue and red), using defined squares and according to the scheme in Figure 27. Afterwards, the numbers between both counts were summarized and divided by 1.5. Therefore, the “field of view” of the microscope was adjusted at a resolution of 50x to the outer corners of the squares which touched the edge line of the microtiter well, marked with red circles. This read out pattern was used to reduce variabilities between the counts of different experimenters, using the same assay test system.

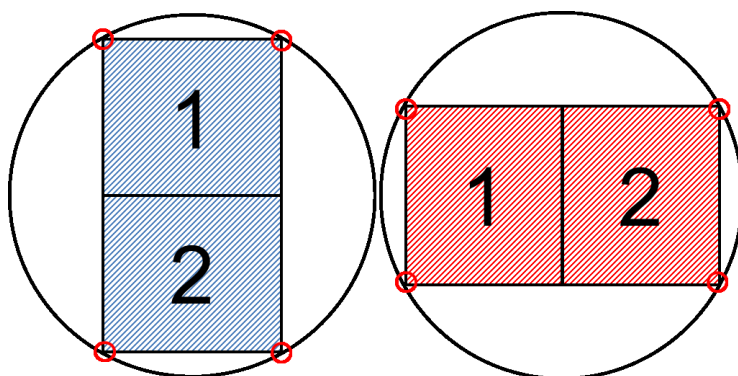


**Figure 27: Read out scheme for the NT assay systems**

### 2.8.1 Statistical analysis

The NT assays were performed to calculate NT<sub>50</sub> titers. Therefore, all compiled data were measured in triplicates, calculating mean and standard deviation (SD). For PROBIT®-analysis and statistical valuation the programs PASW-Statistics version 18 (SPSSInc® Company) and JMP-version 18 (SAS® Company) were used. The Wilcoxon-signed-rank test was used to compare quantitative values between groups. Calculated statistical p-values were visualized as follows: ns<sup>4</sup>= 0.05>p; p\*≤0.05; p\*\*≤0.01; p\*\*\*≤0.001.

### 2.8.2 Analysis of anti-viral drug resistance and NT testing

The GCV resistant strain “40571” and the multi-drug resistant strain “H815-06” were used in NT assays to analyze the impact of HCMV-specific IgG on anti-viral drug resistant strains. In this setup, the NT-capacities of IgG-preparations were investigated in the presence of GCV in increasing concentrations. The inhibitory concentration 25% (IC<sub>25</sub>), IC<sub>50</sub> and IC<sub>75</sub> of both stains were determined in preliminary tests, according to Göhring et al., 2013 and were used in the NT assays. Therefore, the GCV depended IC-values were determined by serial dilution of GCV (50 µM, 25 µM, 10 µM, 5µM, 2.5 µM, 0.5 µM) which were added to cocultures of 100 infected and 20.000 non-infected cells in triplicates, using 96 well microtiter plates. After an incubation of 5 days at 37°C, 5% CO<sub>2</sub>, the cells were fixed and PFUs were counted, followed by statistical Probit® analysis to calculate the strain-dependent IC-values. The NT results of both drug-resistant strains were compared to the drug-sensitive strain “H2497-11” as reference.

Prior to NT testing, routine-based PCRs and Sanger sequencing were performed for UL97 or/and UL54 which confirmed the already described mutations of 40571 and H815-06, resulting in drug-resistance to GCV or/and CDV (Göhring et al., 2013).

---

<sup>4</sup>ns = not significant

### 2.8.3 HCMV-specific antibody depletion strategies

Two UL130 peptides and a recombinant whole PC were used to deplete specific antibodies from IgG-preparations in order to analyze their impact on *in vitro* NT-capacity.

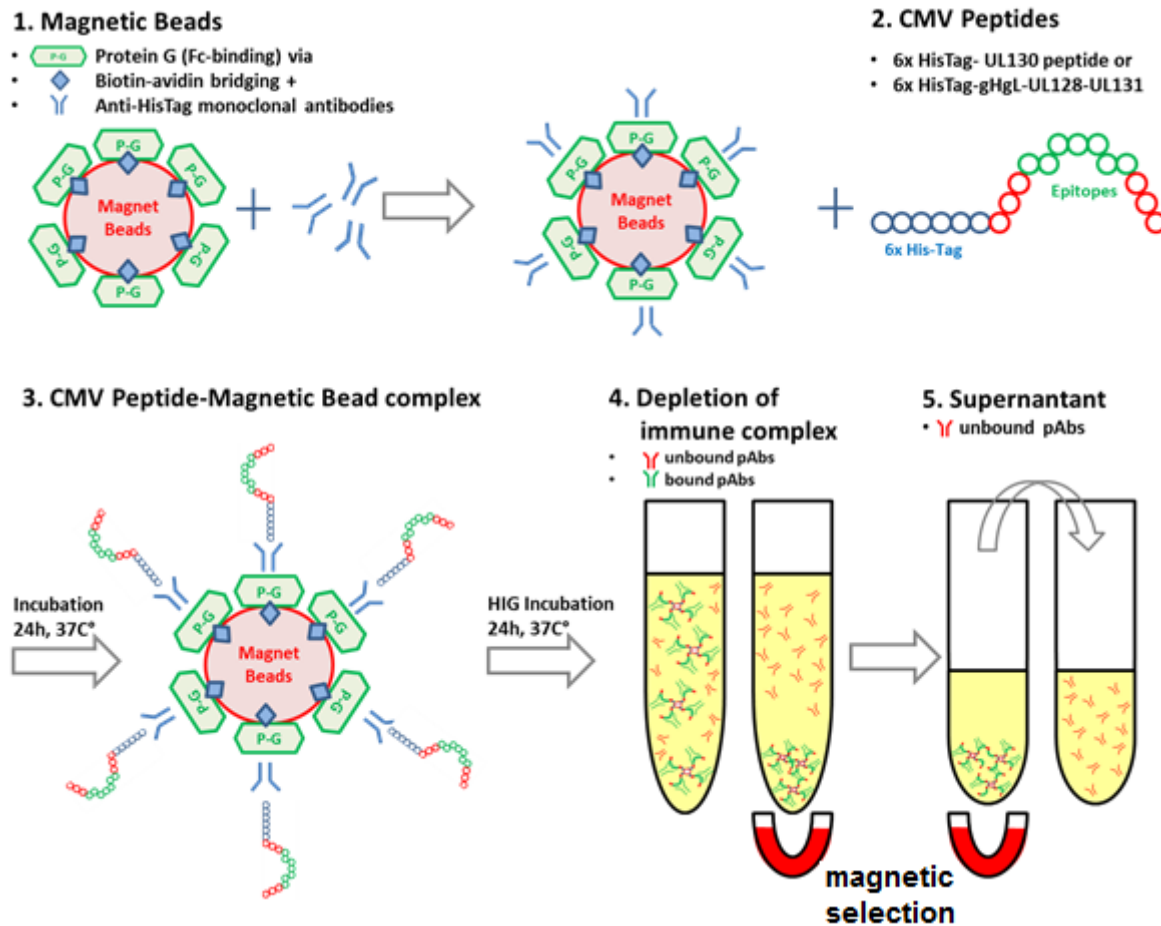


Figure 28: HCMV pentameric depletion scheme: two UL130-peptides and a recombinant pentameric complex (Schampera et al., 2018)

UL130 TAN/SWS peptide with an additional 6x fold HisTag on the C-terminus and a recombinant PC with a linked 6x fold HisTag on glycoprotein H (gH) were used. For the pAb depletion strategy, magnetic beads were coated with protein G to attach monoclonal anti-HisTag-antibodies on the bead surface (Fig.28). After incubation for 24 h at 37°C, 5% CO<sub>2</sub>, bead-fixed immune complexes were formed.

On the next step, the magnetic bead peptide complexes and samples of HCMV IgG preparations were mixed (1:2), followed by incubation for 24 h at 37°C, 5% CO<sub>2</sub>. Then a “6 tube magnetic separation rack” was used to deplete the potentially bound HCMV-specific anti-PC and anti-TAN/SWS peptide pAbs. The supernatants with unbound antibodies were transferred into new tubes (Schampera et al., 2018)

In following neutralization assays, the neutralization capacities of native samples were compared to depleted samples of the investigated IgG preparations and the HCMV IgG<sup>+</sup>/IgM<sup>-</sup>-serum pool as reference. The magnetic beads plus anti-HisTag-monoclonal antibodies (27E8), as well as the 6-tube magnet separation rack (7017) were derived from Cell Signaling Technology, UK.

In a precalibration, the TAN peptide was diluted in log<sub>10</sub> steps (0.001 to 1 mg/ml) to determinate the concentration which resulted in the maximal reachable depletion effect of *in vitro* neutralization capacity for Cytotect®, Kiovig® and HCMV IgG<sup>+</sup>pool (Fig.29).

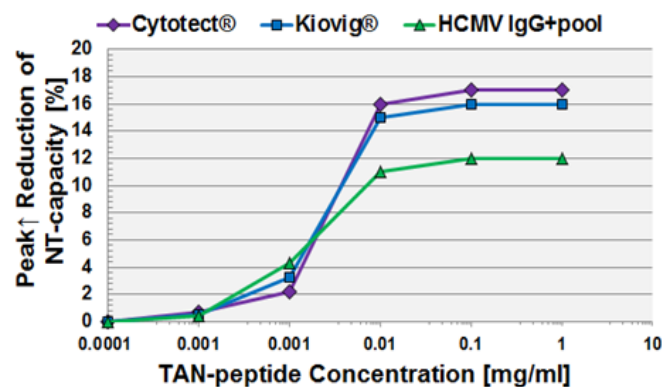


Figure 29: Calibration of the TAN-peptide concentration, revealing the maximal reachable reduction of NT-capacity

The peaks of *in vitro* neutralization reduction, taken from each NT assay revealed that the best valuable *in vitro* NT-depletion effect which was detectable at a concentration of 0.01 mg/ml without risking of unspecific depletion effects. This unspecific depletion effects are caused by protein masking - too high protein concentrations could interfere with the formed virus-antibody complex. The UL130 TAN/SWS peptide and the pentameric complex were used in a concentration 0.01 mg/ml, mixed with 1% magnetic bead solution in order to deplete specific antibodies from IgG preparations.

## 2.8.4 IgG 3 subclass depletion strategy

In a next depletion experiment, the influence of the IgG subclass 3 antibodies on *in vitro* NT-capacity was characterized. Therefore, a modified depletion concept was established (Fig.30).

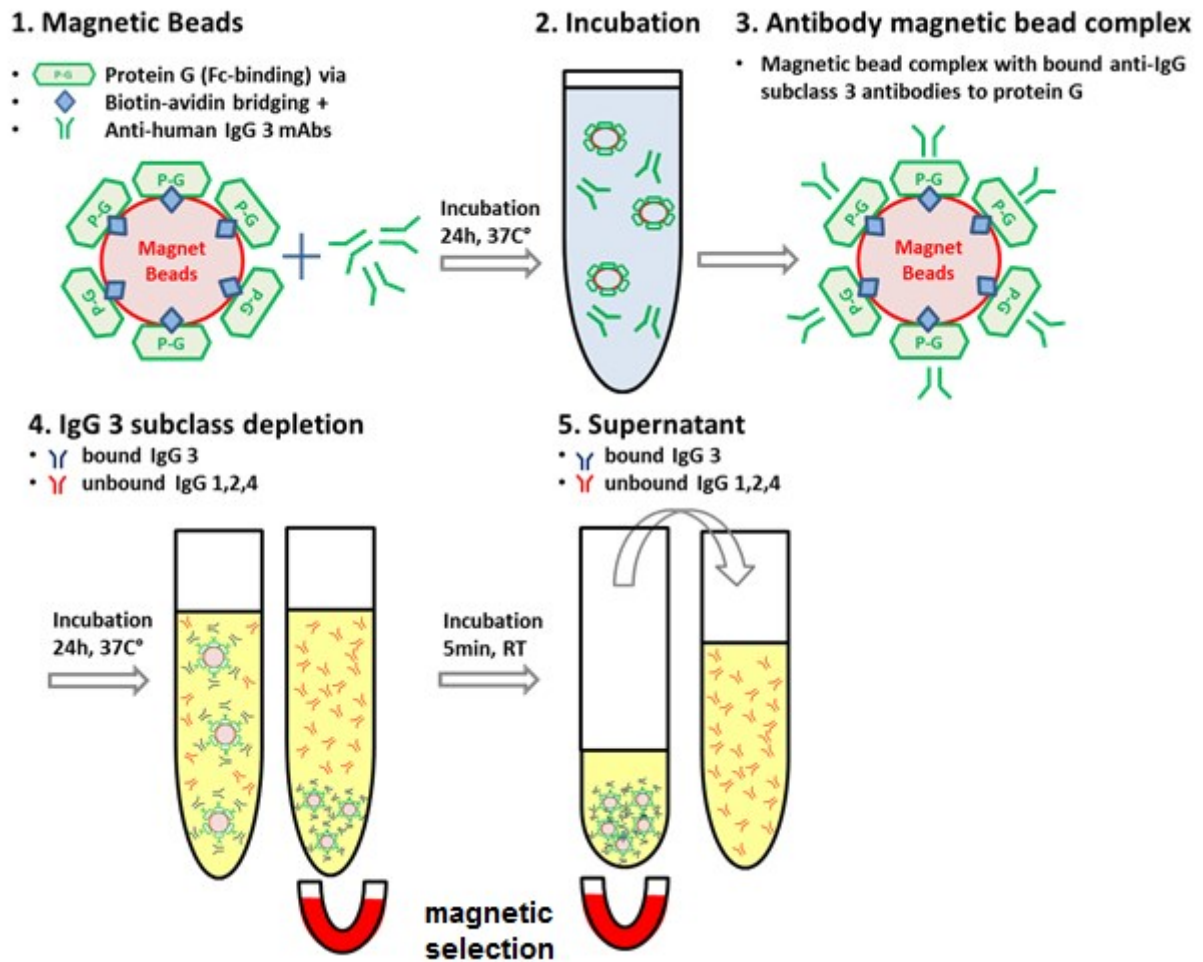


Figure 30: IgG subclass 3 depletion (Schampera et al., 2018)

Anti-human IgG subclass 3 mAbs were bound via protein G to magnetic beads to deplete IgG subclass 3 specific pAbs from IgG preparations. For control, the IgG<sup>+</sup>/IgM<sup>-</sup> reference pool was also depleted (Schampera et al., 2018).

## 2.9 Calibration of NT assays using a PEI reference standard preparation

In the absence of an international WHO unit standard and in order to increase the reliability of the NT assays, a reference preparation was used for HCMV-IgG calibration which was derived from the Paul-Ehrlich Institute, Germany. It was generated in the year 1996 and contains 110 PEI Units/ml which was measured with Enzygnost Anti HCMV/IgG® from Siemens Healthcare Diagnostics Products, Germany.

**Table 18: Biochemical specifications of the PEI HCMV-IgG reference**

Bioch. parameter	PEI standard [g/dl]	Normal serum [g/dl]
Total protein	49,3	6,1-8,1
Total IgG	47,7	0,7-1,6
Total IgA	1,49	0,04-0,23
Total IgM	0,05	0,07-0,38

The biochemical specifications were given from the Paul-Ehrlich institute (Tab.18). Compared to parameters of normal human serum, there is a clear increase of total protein which is caused by the high concentration of IgG. The concentration of IgA is also remarkably higher than in normal human serum.

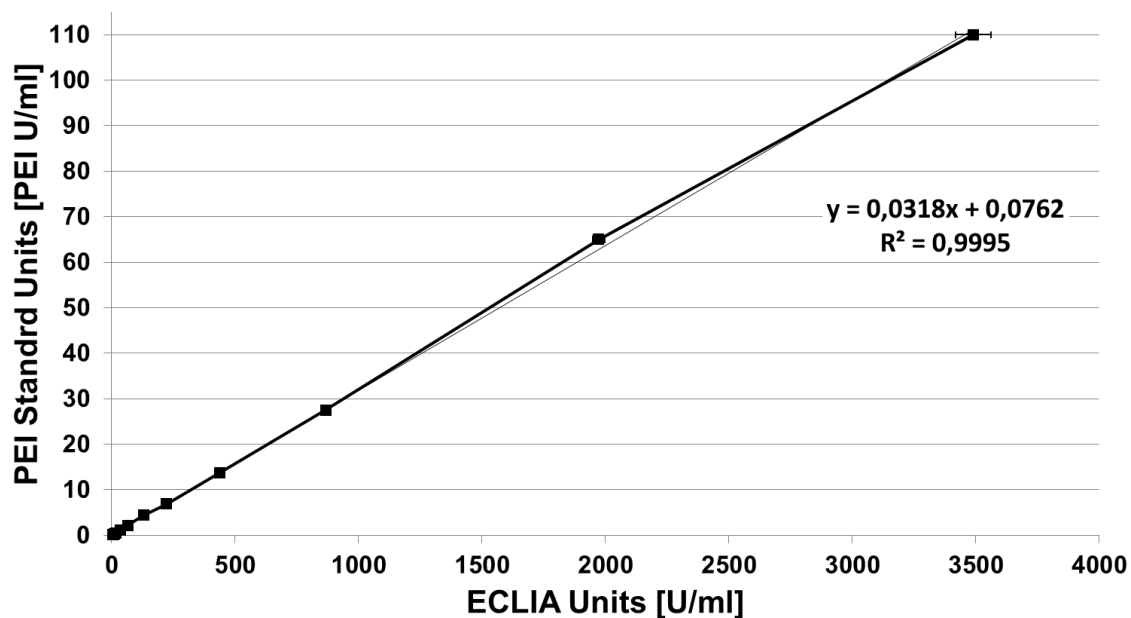


**Figure 31: Calibration of NT assays, using PEI Units and ECLIA Units**

On the base of PEI units, HIGs and IVIGs can be compared to specify HCMV-specific IgG. Additionally, the results of this work can be placed in context to other publications which already used PEI units to illustrate and interpret their data (Filipovich et al., 1992; Miescher et al., 2015; Germer et al., 2016; Schampera et al., 2017).

Therefore, in a preliminary experiment, the PEI reference standard was firstly diluted in 2-fold steps from (undiluted), 1:2, 1:4, 1:8, 1:16; 1:32; 1:64, 1:128, 1:256, 1:512 to 1:1024, then measured in triplicates with the ECLIA CMV Cobas 6000 Analyzer® from Roche to generate a dilution standard curve of HCMV-specific IgG (Fig.31).

**Equation 5: Transformation from ELCIA Units to PEI Units**

$$y[PEI U / ml] = 0,0318x[ECLIA U/ml] + 0,0762$$

The standard curve allowed the transformation from ECLIA units to PEI standard units using the mathematical equation 5 with a correlation coefficient of R<sup>2</sup>= 0.9995. The ECLIA test system is generally used in routine diagnostic of the HCMV serostatus which includes HCMV-IgG, IgG avidity (Sandwich principle) and HCMV-IgM (μ-Capture test principle) (Roche SOP documents URL2 / URL3: date: 06.04.2018).

**2.10 Normalization of the HCMV-specific IgG concentration of HIGs and IVIGs**

The investigated HIGs and IVIGs contain different concentrations of HCMV specific IgG, as previous reported (Miescher et al., 2015; Germer et al., 2016; Schampera et al., 2017). In order to compare the qualitative NT capacity, the HCMV specific IgG concentration of these IgG preparations were normalized to the HCMV specific-IgG concentration of the generated HCMV-IgG<sup>+</sup>-pool using PEI Units (Tab.19), according to Schampera et al., 2017. The normalized IgG preparations were analyzed in following NT assays with different HCMV strains.

**Table 19: Normalization of HCMV-specific IgG concentration using the HCMV<sup>+</sup>pool as reference**

<b>Preparation</b>	<b>Mean PEI Unit/ml</b>	<b>Dilution factor</b>
HCMV-IgG <sup>+</sup> pool	41.2	---
Cytogam®	118.7	1:2,9
Cytotect®	150.3	1:3,6
Kiovig®	42	1:1
Octagam®	62.4	1:1,5

## 2.11 HCMV-specific T-cell modulation after HIG administration of pregnant women with proven HCMV-primary infection in T1

The second part of this work was addressed to the impact of HIG administration on the modulation of HCMV-specific T-cells via the indirect measurement of produced IFN- $\gamma$ . Therefore, the QuantiFERON CMV® from Qiagen and the T-Track ELISpot CMV® from Lophius were performed. The whole blood samples of pregnant women were collected, who were treated with Cytotect® biweekly after a proven HCMV primary infection in T1 (under week 14 of gestational age) (Kagan et al., 2018). 4x 5 ml LiHep whole blood was drawn from treated women with their previous permission and based on the ethical approval (EK number: 506/2015BO2). The samples were taken at the beginning of the HIG administration (day of treatment (dot) = 0) and every 7 days, until GA = 21 week. In two selected cases, additional blood samples on day 2, 4, 7, 9 and 11 were collected between the first and second HIG administration.

### 2.11.1 QuantiFERON CMV® Qiagen

QuantiFERON CMV® is an *in vitro* interferon- $\gamma$  release assay which uses heparinized whole blood samples to detect cell-mediated immunity against human cytomegalovirus. Therefore, the assay quantifies immune modulatory responses to a cocktail of specific HCMV-antigens during infection by measuring levels of interferon- $\gamma$  secretion via an “Enzyme-Linked Immunosorbent Assay” (ELISA) test principle. IFN- $\gamma$  is generated during the adaptive immune response of CD4<sup>+</sup> and CD8<sup>+</sup> T cells, as well as during the innate immune response of NK cells and NK-T cells. In this context, IFN- $\gamma$  production can be a functional surrogate marker for the identification of HCMV-specific CD8<sup>+</sup> T cells and the number of HCMV-specific CD8<sup>+</sup>T cells can be predictive for the risk of developing HCMV-related diseases (Zaia et al., 1993). In general, this assay is used to monitor the immune situation of solid organ transplant (SOT) recipients (Kobayashi et al., 2017; Kwon et al., 2017).

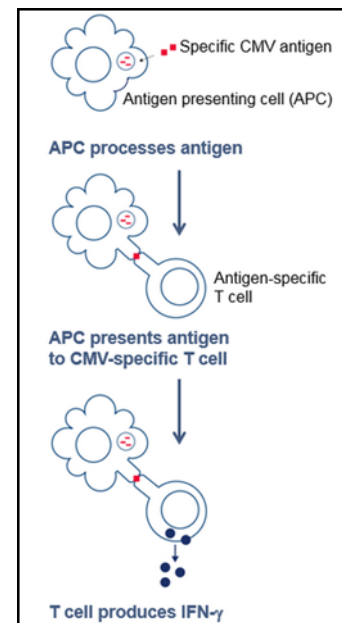


**Figure 32: Process of antigen recognition and presenting through APC resulting in IFN- $\gamma$  production. (Qiagen test principle QuantiFERON CMV® Documentation)**



The assay covers over 98% of the human population via the included HLA types (Tab.20). The whole blood samples were incubated in “Blood Collection Tubes 1 ml” which are surface-labeled inside the tubes with HCMV antigens (Giulieri et al., 2011).

**Table 20: Included HLA antigens which covering >98% of human population.**

### **Included HLA types**

---

A1, A2, A3, A11, A23, A24, A26

B7, B8, B27, B35, B40, B41, B44, B51, B52,  
B57, B58, B60

Cw6 (A30, B13) HLA Class I haplotypes

Each collected sample had its own negative and positive control tube. Mitogen was used as positive control to stimulate unspecific IFN- $\gamma$  secretion. The sample collection, incubation and ELISA assay were performed, according to the test protocols of Qiagen test kit. The OD (optical density)-values were measured via Photometer Microplate Reader, BEP-systeme Siemens AG, Germany with a 450 nm filter and a reference filter at 620/650 nm. The data analysis was performed using the calculation program Cellestic HCMV QuantiFERON Analysis Software® (version 3.03), provided from Qiagen. The quantitative determination of IFN- $\gamma$  concentrations was measured in two-fold replica by establishing an IFN- $\gamma$  standard curve via known IFN- $\gamma$  concentration solutions. Therefore, the samples were diluted 1:10 for quantification, according to the Qiagen test protocol.

#### **2.11.2 T-Track EliSPOT CMV® Lophius**

In contrast to the QuantiFERON CMV®, the T-Track EliSPOT CMV® (Enzyme-linked immunosorbent spot) CMV® from Lophius recognizes the number of IFN- $\gamma$  producing cells after purification of peripheral blood mononuclear cells (PMBCs). The whole blood was mixed with PBS (1:1) in a 50 ml Falcon® tube. Then, 15 ml of Pancoll® (density: 1.077 g/ml, at RT) was filled and in other 50 ml Falcon® tube and was slowly covered with the diluted blood, followed by a centrifugation at 880x g for 30 min, RT. During this time, an interphase was formed which included the PMBCs. The PMBCs were carefully transferred to a new tube using a pipette and were washed 2-times with PBS afterwards. The cells were washed 2-times via a centrifugation at 300x g for 10 min. Meanwhile, the microtiter plates were prepared with a negative control (medium), a positive control (PHA<sup>5</sup>; 1:10) and overlapping HCMV pp65 (ppUL83) antigens in a concentration (1:20). All samples were performed in duplicates.

---

<sup>5</sup> Phytohemagglutinin-L

After the centrifugation of the cells, the supernatant was removed and the cells were resuspended in 1ml AIM-V®+ AlbuMAX® medium from Thermo Fisher Scientific, USA. In a next step, the number of cells was adjusted to ( $2 \times 10^6$  cells/ml) using the Z1 Beckman Coulter® Life Sciences, USA (upper size border: 13  $\mu$ M, lower size border: 8  $\mu$ M).

The system was calibrated before each measurement via a cell count standard for leucocytes. 100 $\mu$ L/well of the adjusted PBMCs were transferred to the prepared microtiter plate for an incubation of 20-24 h at 37°C, 5% CO<sub>2</sub>. Afterwards, the cells were removed and the bound IFN- $\gamma$  was visualized on the surface, according to the test protocol for HiSpecificity<sup>PRO</sup>® (for research only) (Lophius).

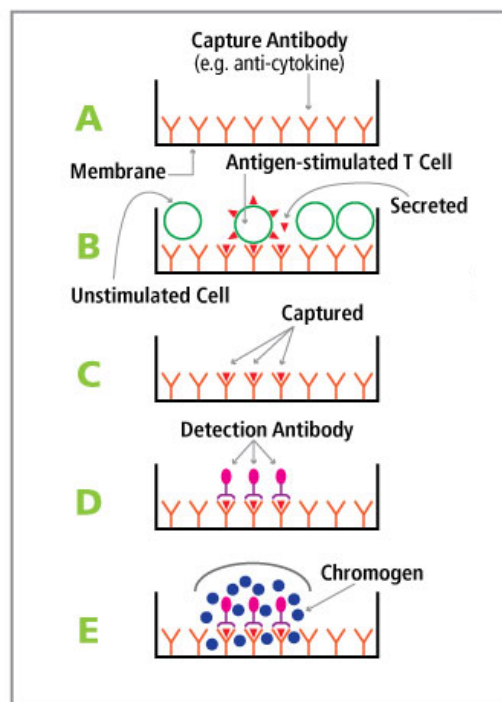


**Figure 33: ELISpot test principle; T-Track ELISpot CMV® (Modified after URL:Mstechno.co.jp)**

The ELISpot test principle uses anti-IFN- $\gamma$  mAbs which were coated on the bottom membrane of the wells (Fig.33). During incubation, stimulated cells produce IFN- $\gamma$  which is captured by the anti-IFN- $\gamma$  mAbs. After incubation, the wells were repeatedly washed. A secondary mAb bound to the IFN- $\gamma$  at a different epitope and visualized the spots through a substrate color reaction. The spots are a negative image of the removed IFN- $\gamma$  reactive PBMCs (Barabas et al., 2017; Banas et al., 2017).

### 3 Results

#### 3.1 Standardization of HCMV neutralization plaque reduction assay (PRA) and assay performance characteristics

The first step was to establish a NT assay protocol which was used for all investigation of previously determined issues in the objectives (point 1.15). The results are given for the final NT assay protocol with ARPE-19 cells (Fig.34A1) and HFF (Fig.34B1) as target cells. The clinical strain H2497-11 was used as target for viral neutralization and prevention of infection via selected IgG preparations. In this context, stock solutions of the HIGs Cytotect®/Cytogam® were compared to stock solutions of the IVIGs Octagam®/Kiovig®. Additionally, the HCMV-IgG<sup>+</sup>pool served as control reference and reflected the average NT-capacity of latently infected mothers at birth.

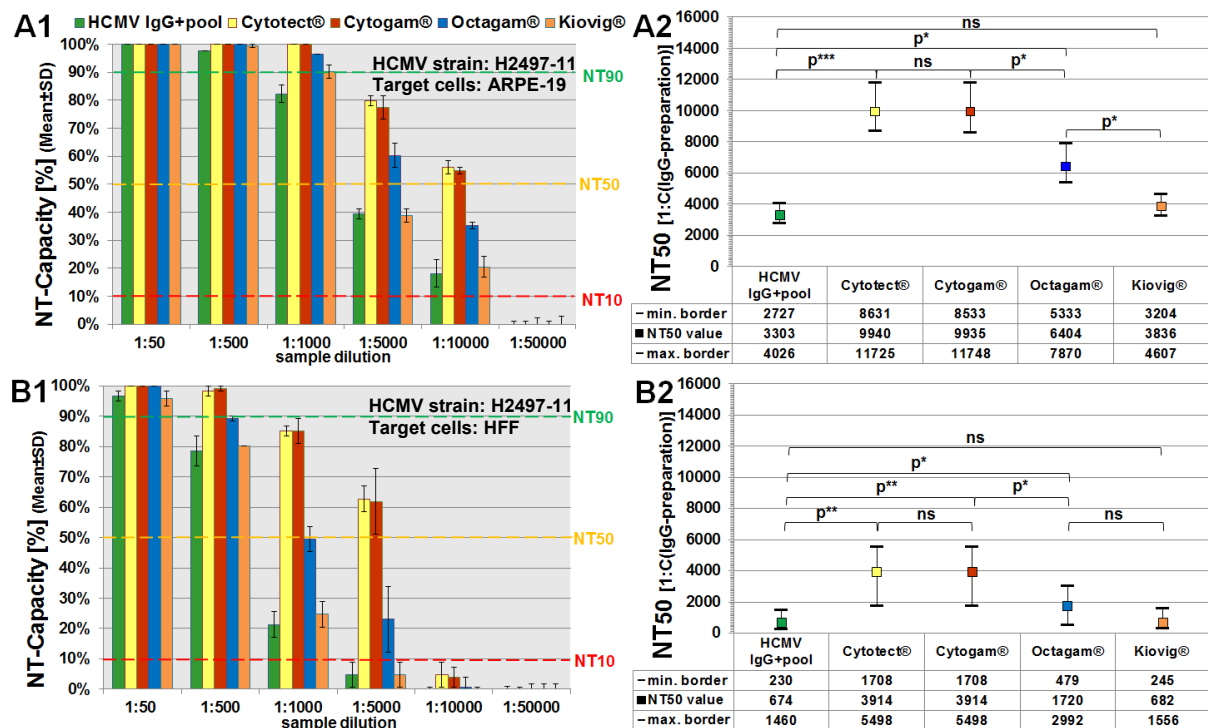


Figure 34: (A1) *In vitro* NT assay (stock solutions), Target cells: ARPE-19 cells, HCMV strain: H2497-11, Cell culture incubation 5d; (A2) NT<sub>50</sub> PROBIT analysis of the tested IgG-preparations (stock solutions) on ARPE-19 cells; (B1) *In vitro* NT assay (stock solutions), Target cells: HFF, HCMV strain: H2497-11, Cell culture incubation 5d; (B2) NT<sub>50</sub> PROBIT analysis of the tested IgG-preparations (stock solutions) on HFF<sup>6</sup>

The corresponding NT<sub>50</sub> values were shown in Figure 34A2/B2 as reciprocal value of the stock solutions which were calculated by Probit analysis. While the minimal and maximal border described the 95% confidence interval of the tested IgG-preparations, the analysis of statistical significance was performed, using JMP18® software.

<sup>6</sup> ns(not significant) 0.05>p; p\*≤0.05; p\*\*≤0.01; p\*\*\*≤0.001

The HIGs Cytotect®/Cytogam® revealed significant higher *in vitro* NT capacities than the IVIGs Octagam®/Kiovig®, while the NT capacities of both HIGs were comparable which was confirmed on ARPE-19 cells and HFF.

The HCMV-IgG<sup>+</sup>pool reached the lowest *in vitro* NT capacity in the performed NT assays. In general, the calculated NT<sub>50</sub> values of all investigated IgG preparations were significant higher (~3.5-fold) in ARPE-19 than in HFF (p>0.001) (Fig33A2/B2). For better understanding, NT<sub>50</sub> values were displayed as reciprocal value of the stock HCMV-IgG concentration of the investigated HIGs and IVIGs.

In a next step, the generated NT assay protocol was additionally performed 6 times under the same conditions at different days to validate the average percentage deviation of the test-dependent *in vitro* NT-capacity between observed NT<sub>50</sub> results of the analyzed IgG preparations (Fig.35).

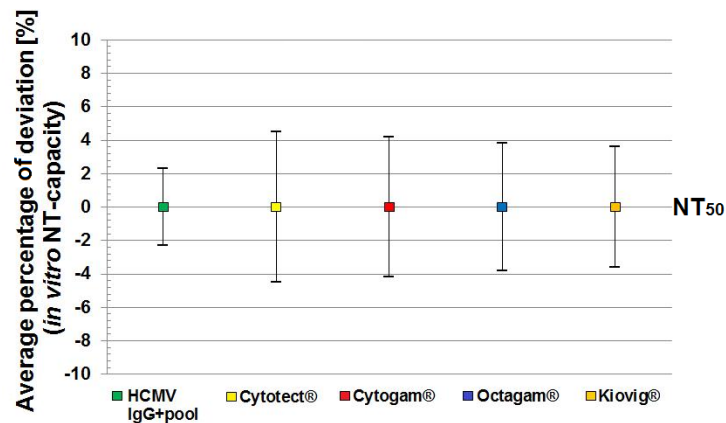


**Figure 35: Determination of the average percentage of deviation of the test-dependent *in vitro* NT-capacity (NT<sub>50</sub>) between observed results using the NT assays protocol**

The highest percentage of deviation to mean of NT-capacity was found in Cytotect® with ±4.5% and Cytogam® with ±4.2%. Octagam® had a percentage deviation to NT-capacity mean of ±3.8%, followed by Kiovig® with ±3.6%. The lowest deviation was observed in the reference HCMV-IgG<sup>+</sup>pool of 100 latently infected mothers at birth, regarding to ±2.3%. The deviations between repeated NT assay approaches were considered during interpretation of the collected data in this work.

In a next experiment, the differences in the quantitative *in vitro* NT capacity [NT<sub>50</sub>/HCMV PEI U] of the IgG preparations were investigated to answer the question, if the same HCMV-specific concentrations of the different IgG-preparations resulted in similar or different *in vitro* NT capacities against HCMV (H2497-11) (Fig.36). Therefore, the IgG preparations were pre-diluted before NT assay, according to table 19 and normalized to HCMV-specific IgG concentration of the HCMV-IgG<sup>+</sup>pool.

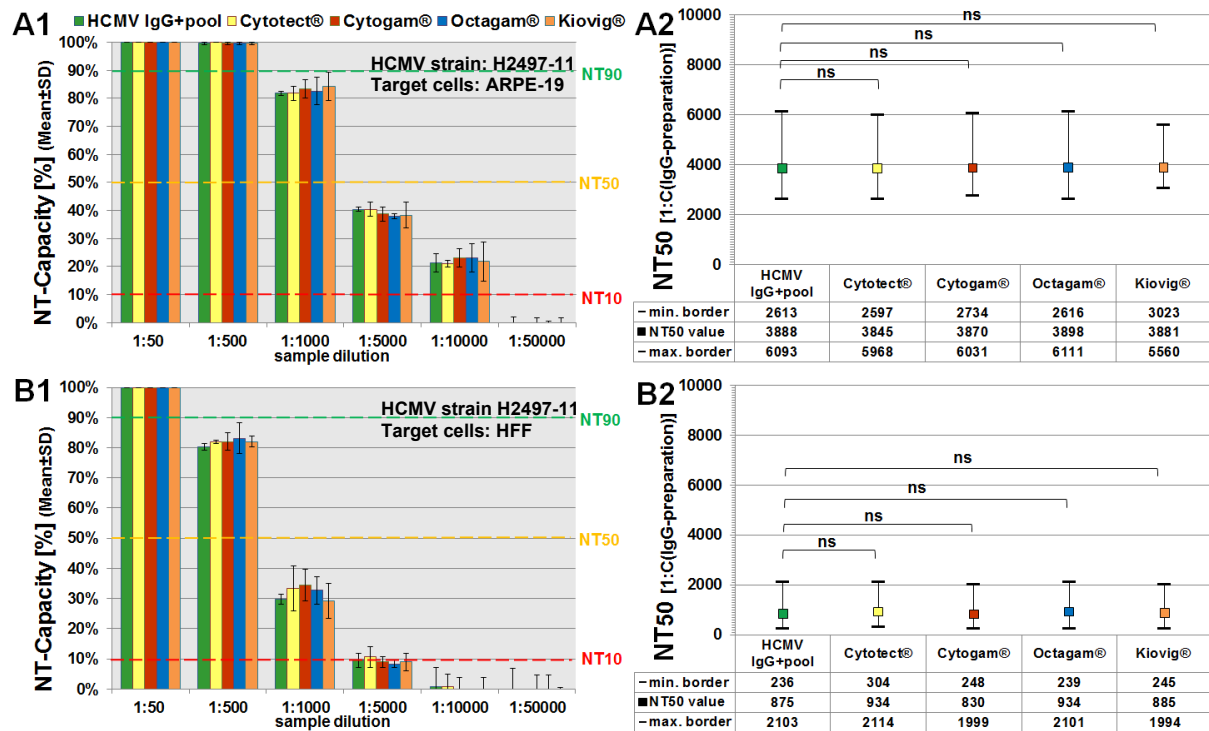


**Figure 36: (A1) *In vitro* NT assay (HCMV-IgG normalization), Target cells: ARPE-19 cells, HCMV strain: H2497-11, Cell culture incubation 5d; (A2) NT<sub>50</sub> PROBIT analysis of the tested IgG-preparations on ARPE-19 cells; (B1) *In vitro* NT assay (HCMV-IgG normalization), Target cells: HFF, HCMV strain: H2497-11, Cell culture incubation 5d; (B2) NT<sub>50</sub> PROBIT analysis of the tested IgG-preparations on HFF**

The *in vitro* NT assay was performed with the HCMV strain H2497-11 on ARPE-19 cells and HFF (Fig.36A1B1), while the corresponding NT<sub>50</sub> values were illustrated in Figure 36A2/B2. For better understanding, NT<sub>50</sub> values were displayed as reciprocal value of the normalized HCMV-IgG concentration of the investigated HIGs and IVIGs.

After HCMV-IgG normalization, all IgG preparations revealed no significant differences in *in vitro* NT-capacity, comparing of NT<sub>50</sub> values. This was observed on both used target cell type cultures. Additionally, the *in vitro* NT capacities were about 3.5-fold higher in ARPE-19 cells than in HFF which confirmed the first results with IgG stock solutions (Fig.34A2/B2).

Following HCMV IgG normalization, the sample dilutions of the IgG preparations were transformed into HCMV PEI Unit/ml, as shown in Figure 37. For better visualization, the HCMV PEI values were displayed as log<sub>10</sub> as an approximated-linearized course.

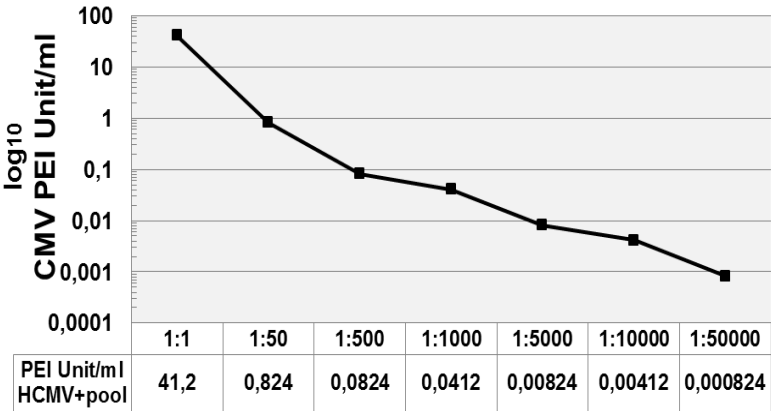


Figure 37: Transformation of sample dilution into HCMV PEI Unit/ml

The results showed no quantitative differences in *in vitro* NT-capacity per HCMV PEI Unit between the investigated IgG preparations using the clinical isolate H2497-11 on HFF and on ARPE-19 cells (Fig.37).

The NT assay protocol was additionally tested under the usage of a genetically modified HCMV-strain TB40E variant (RV-TB40-BACKL7-SE-EGFP) to establish an alternative read out system via an inserted BAC cassette at US34A downstream which intracellularly expresses GFP (Green fluorescent protein) (Fig.38).

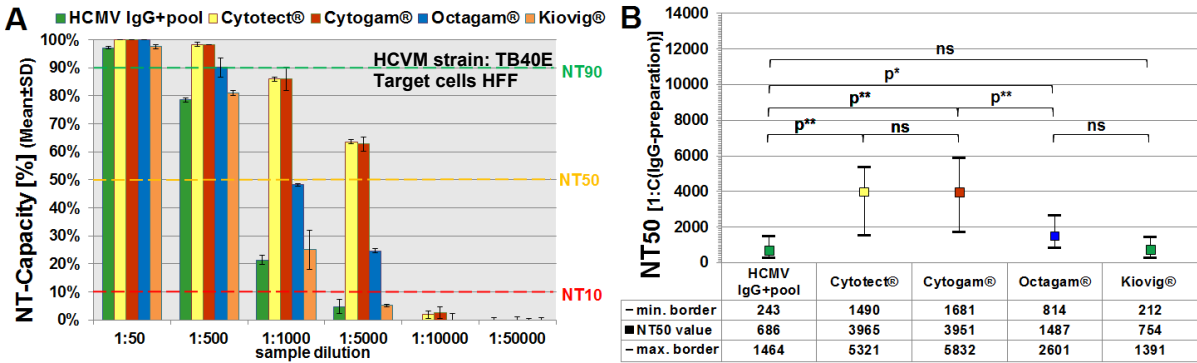
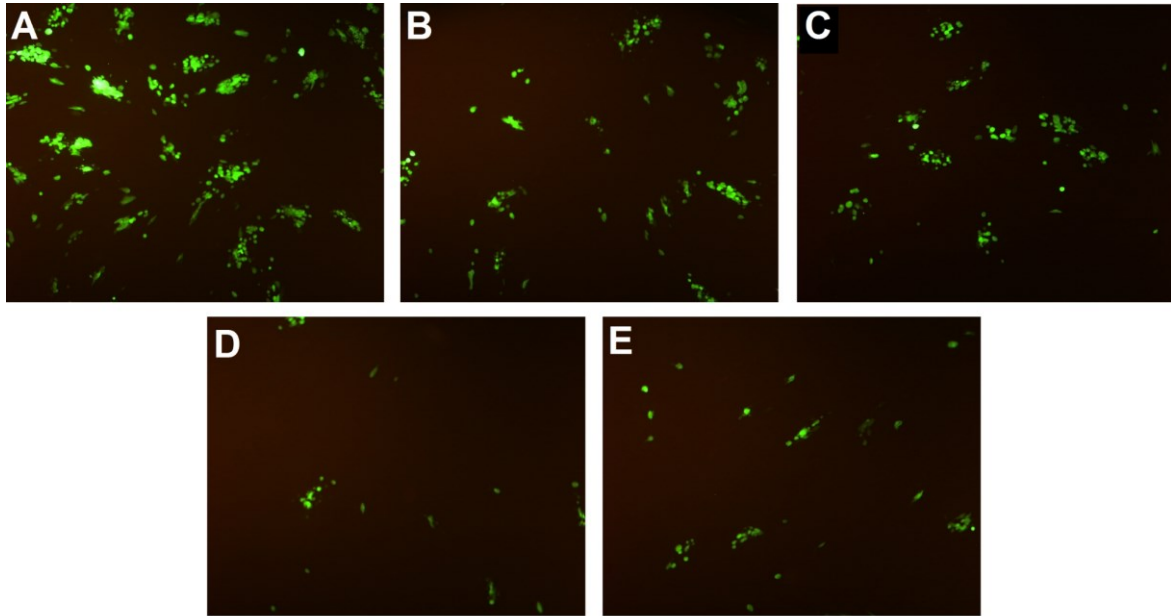


Figure 38: (A1) *In vitro* NT assay (HCMV-IgG normalization), Target cells: HFF, HCMV strain: TB40E, Cell culture incubation 5d; (A2) NT<sub>50</sub> PROBIT analysis of the tested IgG-preparations on HFF

In comparison with the clinical HCMV isolate H2497-11, all IgG preparations and the generated HCMV-IgG<sup>+</sup>pool were able to reach comparable *in vitro* NT-capacities to the H2497-HFF strain after incubation time of 5 days, using the TB40E variant on HFF (Fig.38A/B).

In addition, the usage of the TB40E variant allowed a live investigation of the viral reproduction and spread in cell culture during the NT assay from day 1 to day 5 of the experiment under a fluorescence microscope, without p72-staining via antibodies at the end of the incubation. For a better visualization of the *in vitro* NT assay using the TB40E variant, live images were taken from the corresponding microtiter plates.



**Figure 39: *in vitro* NT assay (TB40 E variant) example figures of analyzed IgG preparations on HFF, sample dilution 1:5000, 50x; (A) HCMV-IgG+pool; (B) Kiovig®; (C) Octagam® (D) Cytotect® (E) Cytogam®**

Figure 39 shows images of the HCMV-IgG<sup>+</sup>pool and each analyzed IgG preparation on HFF at a sample dilution of 1:5000. While the HCMV-IgG<sup>+</sup>pool showed the most HCMV-specific PFUs at this dilution, only few PFUs were found in the HIGs Cytotect® and Cytogam®. The number of PFUs of the IVIGs ranged between the HCMV reference pool and the HIGs.

In contrast to the successfully performed NT assay on HFF, the TB40E variant induced not enough PFU numbers in ARPE-19 cells for an evaluable NT analysis.

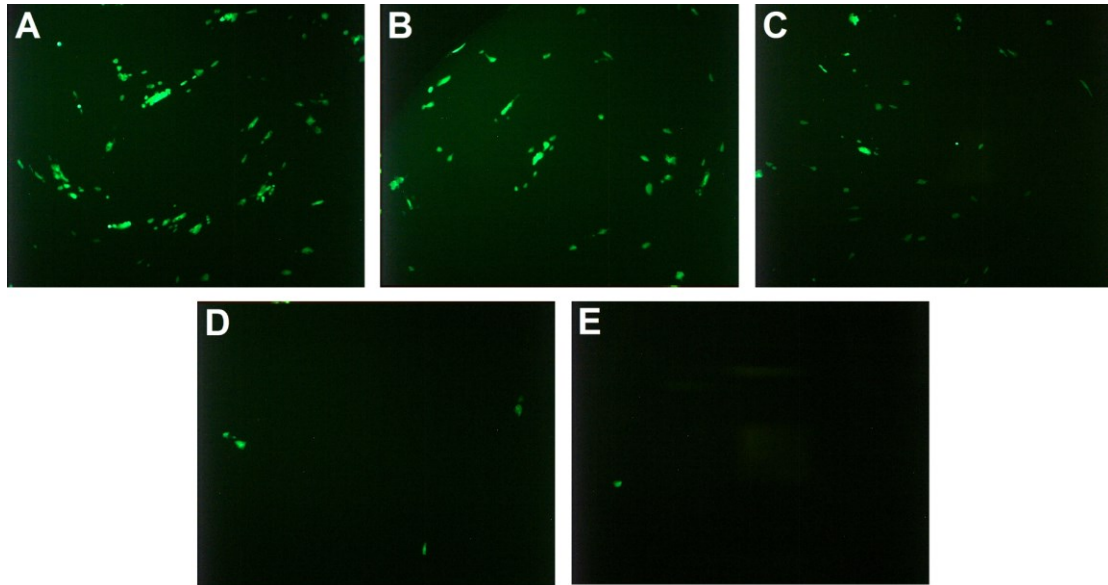


**Figure 40:** *in vitro* NT assay (TB40 E variant) example figures of analyzed IgG preparations on ARPE-19 cells, sample dilution 1:5000, 50x; (A) HCMV-IgG+pool; (B) Kiovig®; (C) Octagam® (D) Cytotect® (E) Cytogam®

Sample images were taken from NT assay, using ARPE-19 cells as target cells (Fig.40). The TB40E variant hardly tended to induce infection or viral plaque formation in ARPE-19 cells. There were few evaluable HCMV-PFUs found in the HCMV reference pool and in Kiovig, but the NT assay showed no sufficient results for Octagam®, Cytogam® and Cytotect®.

Further NT experiments on ARPE-19 cells were performed using the viral isolate H2497-11 and p72-staining as read out system.



### 3.2 Cytotect® neutralization activity against HCMV isolates, resistant to antiviral compounds

For this experiment, the GCV IC<sub>25</sub>, IC<sub>50</sub> and IC<sub>75</sub> values of the drug-resistant HCMV strains H815-06 and 40571 were determined (Fig.41).

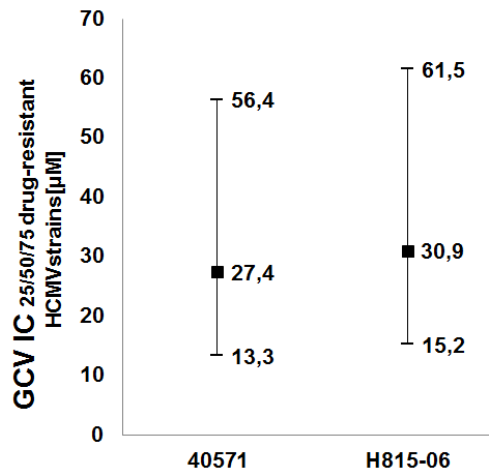
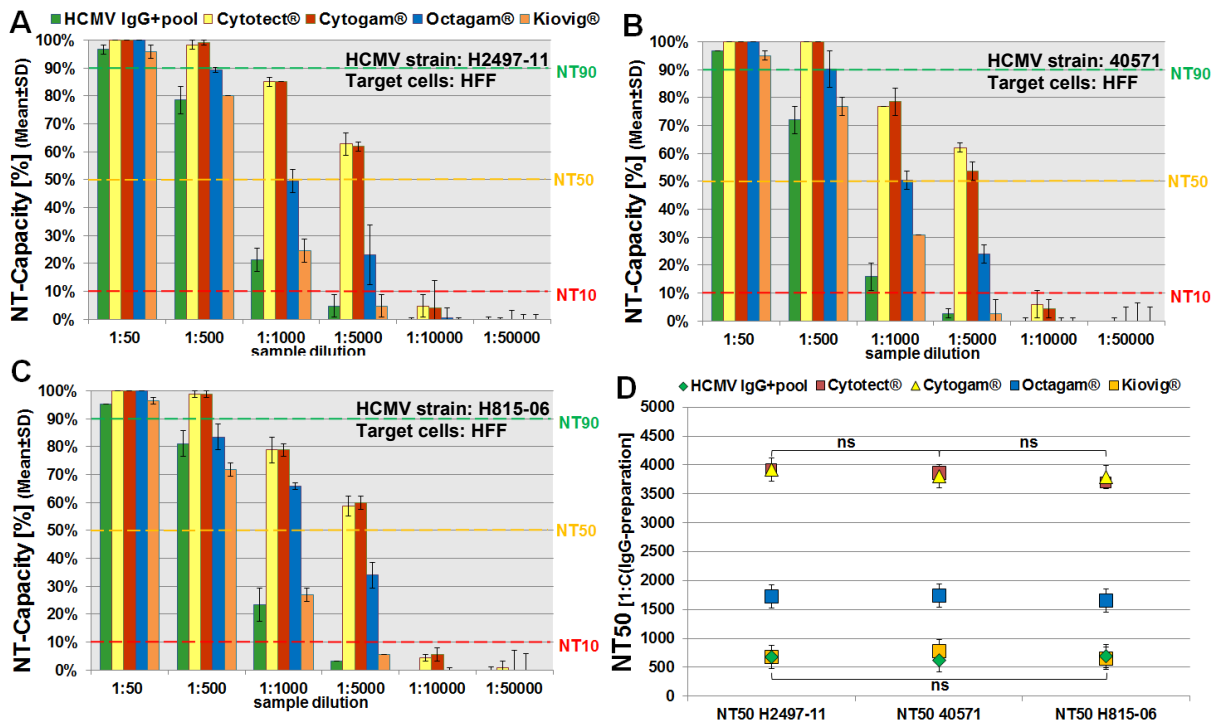


Figure 41: GCV IC<sub>25/50/75</sub> dose analysis of both investigated resistant HCMV strain (H815-06, 40571)

The analysis of the strain-dependent GCV IC<sub>50</sub> concentration confirmed, that both HCMV strains were resistant against Ganciclovir®, according to the threshold value for GCV resistance of  $\geq 6 \mu\text{M}$  (Prix et al., 1999, Göhring et al., 2013). Interestingly, both HCMV strains were comparable in context of GCV resistance, considering IC<sub>25</sub>, IC<sub>50</sub> and IC<sub>75</sub> values.

The HCMV strain 40571 and H815-06 were analyzed in PRA using the established NT assay protocol and were compared to the sensitive reference HCMV strain H2497-11. The following NT assays were performed on HFF monolayers, because the drug-resistant HCMV strains were initially isolated from primary material and cultivated exclusively on fibroblasts afterwards without adaption to epithelial cells.



**Figure 42: (A) *In vitro* NT assay (stock solutions), Target cells: ARPE-19 cells, HCMV strain: H2497-11, Cell culture incubation 5d; (B) *In vitro* NT assay (stock solutions), Target cells: ARPE-19 cells, HCMV strain: 40571, Cell culture incubation 5d; (C) *In vitro* NT assay (stock solutions), Target cells: ARPE-19 cells, HCMV strain: H815-06, Cell culture incubation 5d; (D) Meta-analysis of NT<sub>50</sub>-values via JMP software, comparing selected IgG preparations on a drug-sensitive and 2 drug-resistant HCMV strains**

In general, the HIGs Cytotect® and Cytogam® showed the highest *in vitro* NT-capacities in all 3 performed NT assays with drug-sensitive and drug-resistant HCMV isolates, followed by the IVIGs Octagam®, Kiovig® and the reference HCMV-IgG+pool (Fig.42ABC). This observation correlated with the first results in point 3.1. In a further comparison, all IgG preparations showed not similar, but comparable *in vitro* NT-capacities (Fig.42D). In a statistical analysis of NT<sub>50</sub>-values via JMP in a comprehensive meta-analysis, all 3 investigated HCMV strains revealed no significant difference in *in vitro* NT-capacity, if each HCMV strain was individually compared to all other HCMV strains (All p-values were >0.05  $\hat{=}$  ns (not significant)). This approach was repeatedly performed with no appearance of significant differences in *in vitro* NT-capacity between the HCMV strains.

### 3.3 Characterization of Cytotect® neutralization activities against HCMV isolates with different gB-genotypes

In order to continue the characterization of Cytotect®, all IgG preparations were compared in these NT assays using 4 HCMV strains with different gB types 1 to 4.

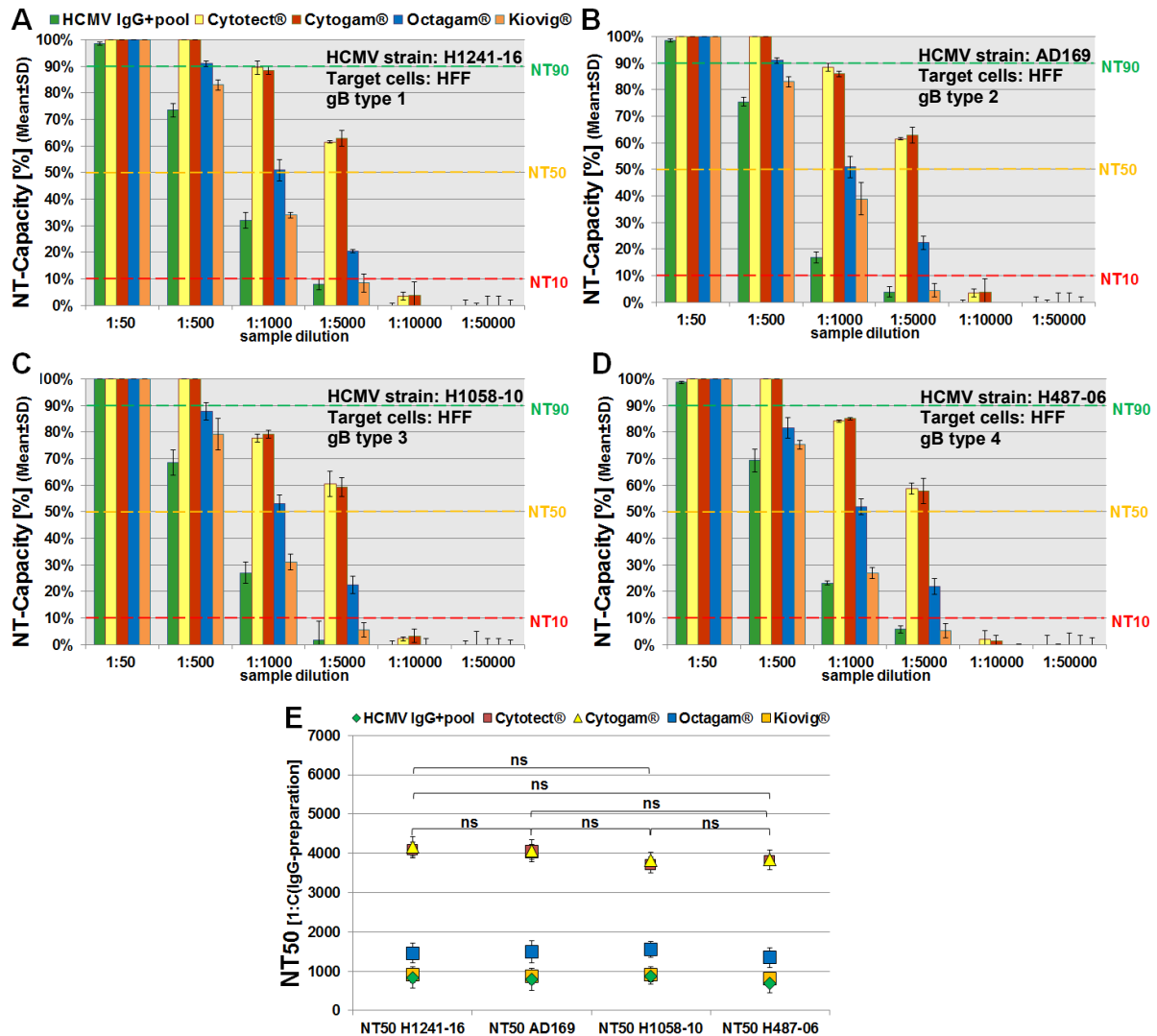


Figure 43: (A) gB type 1 *in vitro* NT assay (stock solutions), Target cells: HFF, HCMV strain: H1241-16, Cell culture incubation 5d; (B) gB type 2 *in vitro* NT assay (stock solutions), Target cells: HFF, HCMV strain: AD169, Cell culture incubation 5d; (C) gB type 3 *in vitro* NT assay (stock solutions), Target cells: HFF, HCMV strain: H1058-10; (D) gB type 4 *in vitro* NT assay (stock solutions), Target cells: HFF, HCMV strain: H487-06; (E) Meta-analysis of all investigated HCMV strains, using NT50 values via JMP software

The results for this experiment confirmed, that HIGs Cytotect® and Cytogam® reached the highest NT-capacities on all used HCMV strains, followed by the IVIGs Octagam®, Kiovig® and the generated HCMV-IgG+pool (Fig.43ABCD). The statistical meta-analysis compared the NT<sub>50</sub>-values of all IgG-preparations of one HCMV strain to each other used HCMV strain (Fig.43E). It revealed no significant differences in NT-capacity, therefore all IgG preparations performed comparable on the investigated HCMV strains, independently to gB types (All p-values were >0.05  $\hat{=}$  ns (not significant)).

During the establishment of viral stocks and NT assay protocols, differences in viral spread and morphology between the investigated HCMV isolates were observed. The HCMV strains tended differently to generate different PFUs in cell culture in terms of form and size. There were also differences in appearance time from SICs to PFU and the degree of lysis differed in speed and strength which resulted in cell-free areas in the cell monolayers. These observations complicated the “read out” via p72 staining. Under these conditions, the HCMV strain H2497-11 has shown to be suitable for NT-testing and was used for the next antibody depletions and NT assays.

### 3.4 Role of pentamer-specific antibodies in HCMV hyperimmunoglobulin and standard intravenous IgG preparations

The NT experiments in this setting focused on the impact of PC-specific antibodies in IgG preparations using stock solutions. A depletion concept was established, using magnetic bead separation. The results of NT assays are given on ARPE-19 cells and on HFF (Fig.44A1/B1) with statistical analysis of NT<sub>50</sub> and p-values (Fig.44A2/B2). The reference HCMV strain H2497-11 was used. A comparison of native and depleted samples of the IgG preparations was performed to detect the difference in resulting NT-capacities, following antibody depletion.

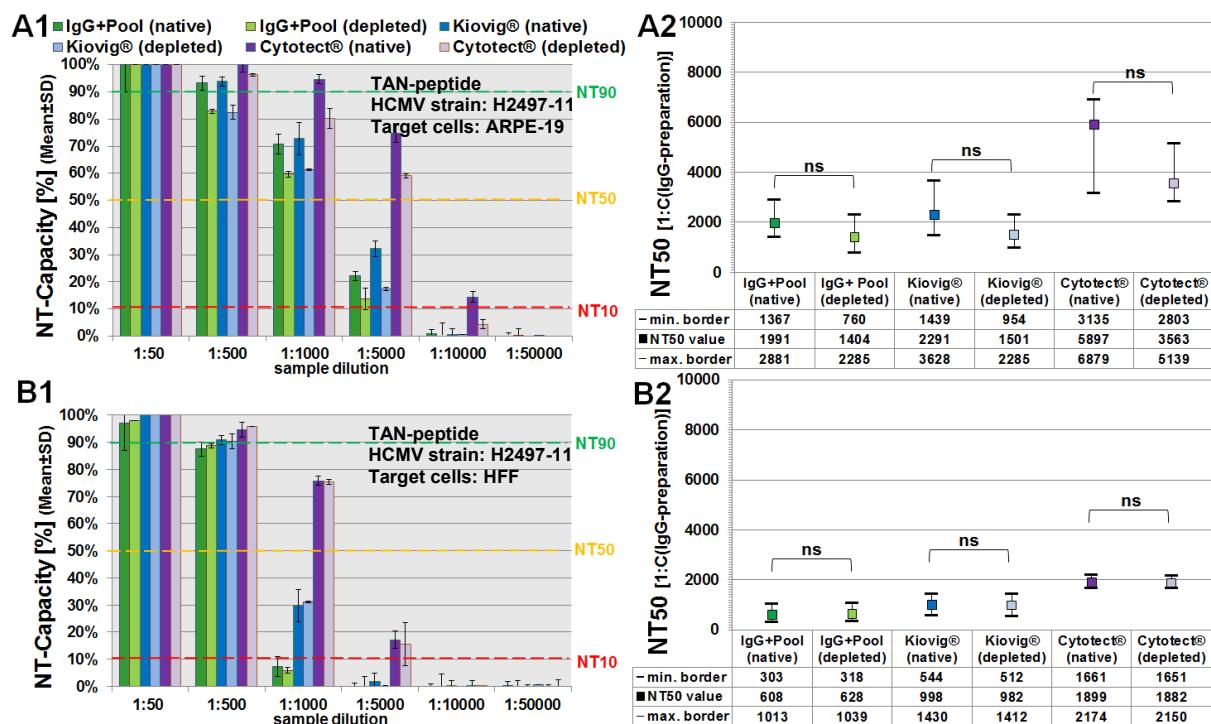
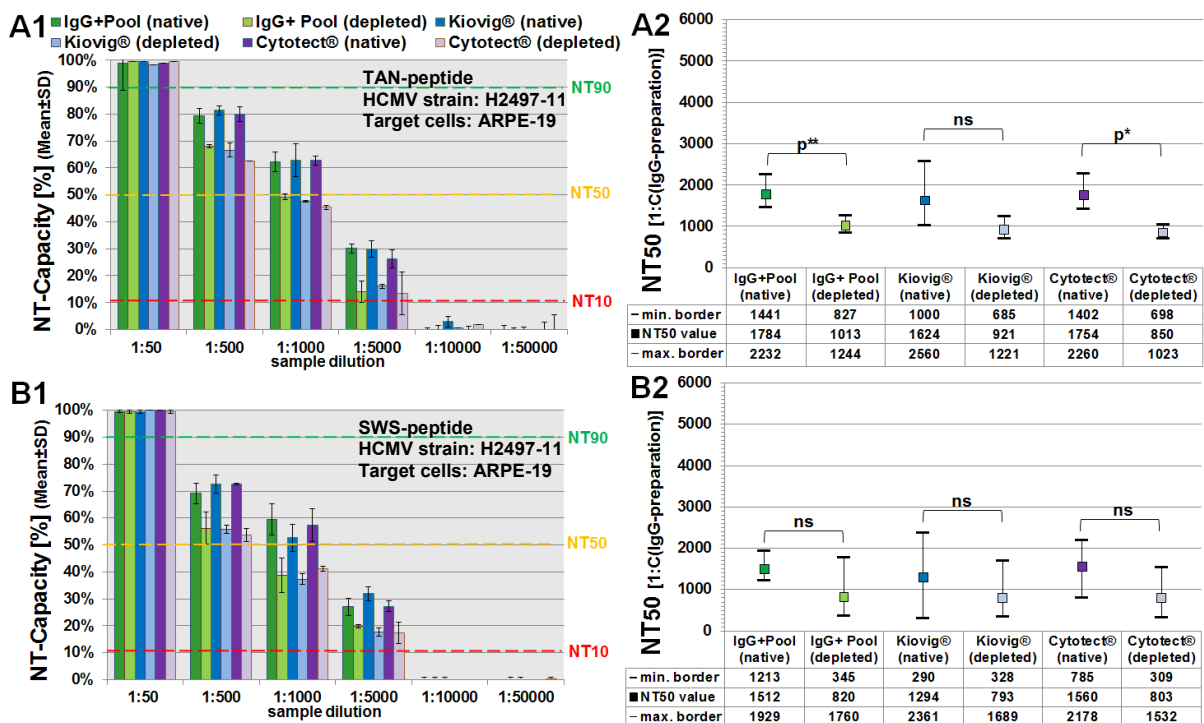


Figure 44: (A1) *In vitro* NT assay (stock solutions), TAN-peptide antibody depletion, Target cells: ARPE-19 cells, HCMV strain: H2497-11, Cell culture incubation 5d; (A2) NT<sub>50</sub> PROBIT analysis of the tested IgG-preparations (stock solutions) on ARPE-19 cells; (B1) *In vitro* NT assay (stock solutions), TAN-peptide antibody depletion, Target cells: HFF, HCMV strain: H2497-11, Cell culture incubation 5d; (B2) NT<sub>50</sub> PROBIT analysis of the tested IgG-preparations (stock solutions) on HFF (Modified after Schampera et al., 2018)

The results for the NT assay on ARPE-19 cells revealed no significant differences in *in vitro* neutralization reduction between native and HCMV antibody-depleted samples (all p-values > 0.05  $\triangleq$  ns) (Fig.44A2). However, a non-significant trend forward decrease of NT capacities was observed. In detail, the highest NC reduction effect (16%; p= 0.12) was found for Cytotect® at a dilution of 1:5000 which was equivalent to 30.1 mPEI U/ml. For Kiovig, the highest NC difference (15%; p= 0.11) was shown at dilution 1:5000, corresponding to 8.4 mPEI U/ml. HCMV IgG+ reference pool had its highest difference in NC at (11%; p= 0.11) at 1:1000 which was transformed into 41.2 mPEI U/ml.

The depletion concept, using magnetic bead separation resulted in no detectable reduction of *in vitro* neutralization capacity on HFF which was performed as proof of concept to decline unspecific reductions of *in vitro* neutralization capacities through the performance of the depletion process (Fig.43B2) (HCMV-IgG+pool p= 0.78; Cytotect® p= 0.65; Kiovig® p= 0.69). As reminder, the depletion of TAN-specific antibodies should have no impact on the *in vitro* neutralization capacity on HFF.

In a next approach, the differences in reduction of neutralization between the TAN-peptide and the original SWS-peptide of Saccoccio et al., 2011 were investigated at a concentration 0.01mg/ml, using normalized HCMV IgG concentrations of the IgG preparation Cytotect® and Kiovig®. ARPE-19 cells were used as target cells (Fig.45).



**Figure 45:** (A1) *In vitro* NT assay (HCMV-IgG normalization), TAN-peptide antibody depletion, Target cells: ARPE-19 cells, HCMV strain: H2497-11, Cell culture incubation 5d; (A2) NT<sub>50</sub> PROBIT of the tested IgG-preparations on ARPE-19 cells after TAN-peptide antibody depletion; (B1) *In vitro* NT assay (HCMV-IgG normalization), SWS-peptide antibody depletion, Target cells: HFF, HCMV strain: H2497-11, Cell culture incubation 5d; (B2) NT<sub>50</sub> PROBIT analysis of the tested IgG-preparations on ARPE-19 cells after SWS-peptide antibody depletion (Modified after Schampera et al., 2018)

In general, Cytotect® and Kiovig® showed comparable *in vitro* neutralization capacities, compared to the HCMV-IgG<sup>+</sup>pool after IgG normalization in both NT assays (Fig.45A1B1).

These results matched with previous investigations, analyzing the impact of HCMV IgG normalization on neutralization capacities in different IgG preparations. In contrast to the first depletion experiments, using the TAN peptide with IgG stock solutions, a statistically significant difference in NC reduction was observed between the native and depleted samples in Cytotect® (p=0.02) and HCMV-IgG<sup>+</sup>pool (p= 0.01) (Fig.42A2) which was not found via SWS-peptide for HCMV-specific IgG depletion Cytotect® (p=0.11) and HCMV-IgG+pool (p= 0.13) (Fig.45B2). The reduction of NC was not significant for Kiovig® in both approaches. However, the data showed a non-significant trend forward decrease of NC after IgG depletion for the SWS-peptide. In comparison, the maximal reduction of resulting *in vitro* NC was about 15% for both analyzed UL130 peptides at a sample dilution of 1:1000 or 41.2 mPEI U/ml.

In following experiments, HCMV-specific antibodies were depleted from Cytotect® under the usage of a recombinant pentameric complex at a concentration of 0.01mg/ml and the established depletion concept. The PC (gH/gL-UL128L) contains an increased amount of potential neutralizing-involved and epitopes which are also non-linear in comparison to the analyzed UL130 peptides. The NT assays were performed on ARPE-19 cells and HFF with IgG stock solution of Cytotect®. The HCMV-IgG+pool was depleted as control reference.

The results of the NT assay with native and depleted samples, resulting in differences in *in vitro* NT-capacity are given in figure 46.

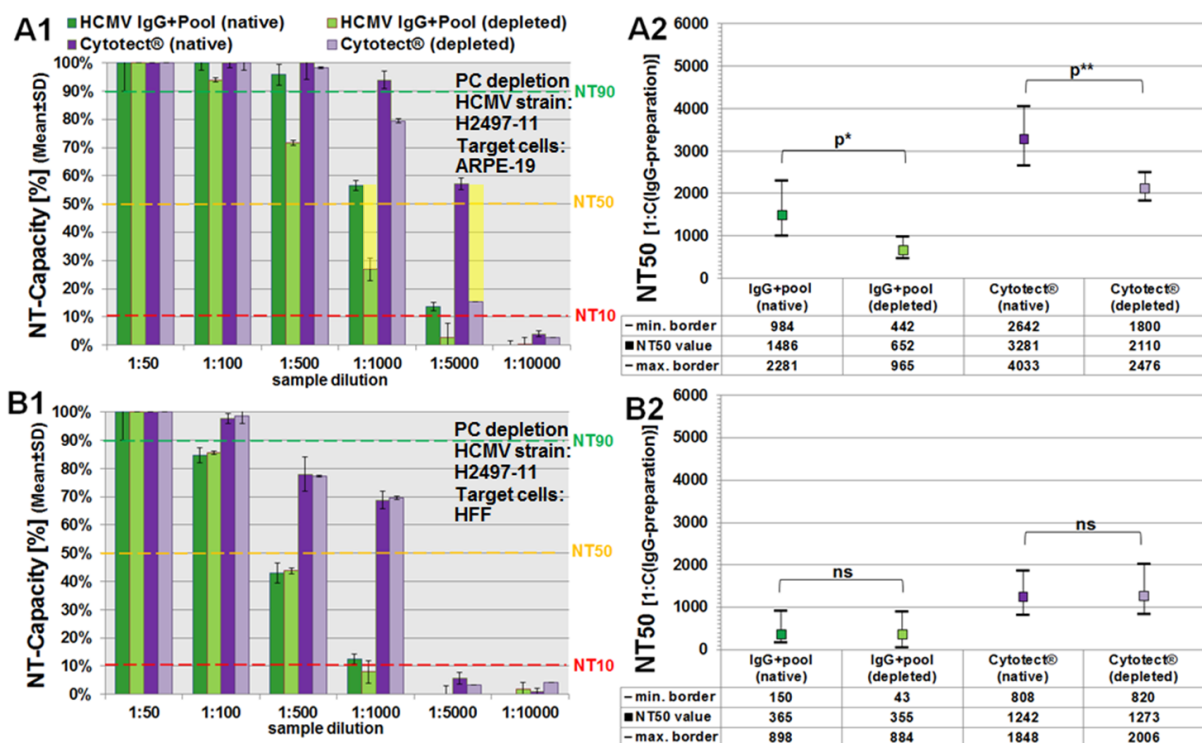


**Figure 46: (A1) *In vitro* NT assay (HCMV-IgG stock solutions), PC antibody depletion, Target cells: ARPE-19 cells, HCMV strain: H2497-11, Cell culture incubation 5d; (A2) NT50 PROBIT analysis of the tested IgG-preparations on ARPE-19 cells after PC antibody depletion; (B1) *In vitro* NT assay (HCMV-IgG stock solutions), PC antibody depletion, Target cells: HFF, HCMV strain: H2497-11, Cell culture incubation 5d; (B2) NT<sub>50</sub> PROBIT analysis of the tested IgG-preparations on ARPE-19 cells after PC antibody depletion (Modified after Schampera et al., 2018)**

The results showed a significant difference in the reduction in *in vitro* NT-capacity between native and PC-depleted samples for the HCMV-IgG<sup>+</sup>pool (30%, p= 0.03) at a 1:1000, corresponding to 41.2 mPEI U/ml, as well as for the HIG Cytotect® with a difference of 42% and a p-value of 0.01 (Fig.46A1/A2). The strongest difference *in vitro* NT-capacity in Cytotect® was determined at a dilution of 1:5000 which correlated with 30.06 mPEI U/ml. The reductions in *in vitro* NT-capacity were additionally highlighted, using yellow marks (Fig46A1). For HFF, the usage of PC to deplete HCMV-specific antibodies from Cytotect® and the HCMV-IgG<sup>+</sup>pool had no noticeable effect on reduction of HCMV-related NT-capacity (p>0.05; 0.68/0.87) (Fig46B1/B2).

It can be highlighted that the PC-related antibody depletion reached a 2- to 3-fold higher reduction in NT-capacity against HCMV than the approach using single UL130 peptides (TAN/SWS) in ARPE-19 cells.

The PC-depleted samples were additionally compared to the native stock solutions in the ELCIA HCMV test system® of Roche. Interestingly, the ECLIA was not able to detect differences in HCMV-specific IgG (Tab.21).

**Table 21: ELCIA HCMV® Roche analysis; Comparison of PC-depleted samples to native samples of Cytotect® (1:15) and HCMV-IgG+pool (1:5).**

<b>ELCIA HCMV® Roche [U/ml]</b>	
<b>HCMV-IgG+pool (native)</b>	105
<b>HCMV-IgG+pool (depleted)</b>	99.4
<b>Cytotect® (native)</b>	312.3
<b>Cytotect® (depleted)</b>	322.8



### 3.5 Depletion of HCMV hyperimmunoglobulin IgG subclass 3 from Cytotect® and analysis of its functional activity

In the last antibody depletion experiments, the impact of IgG subclass 3 antibodies on the NT-capacity against HCMV was analyzed using a modified depletion strategy. IgG 3 antibodies were removed from stock solutions of Cytotect® and Kiovig® via anti-IgG 3 antibodies and magnetic bead separation. The results and the statistical analysis of the NT assays are shown in the figure 47.

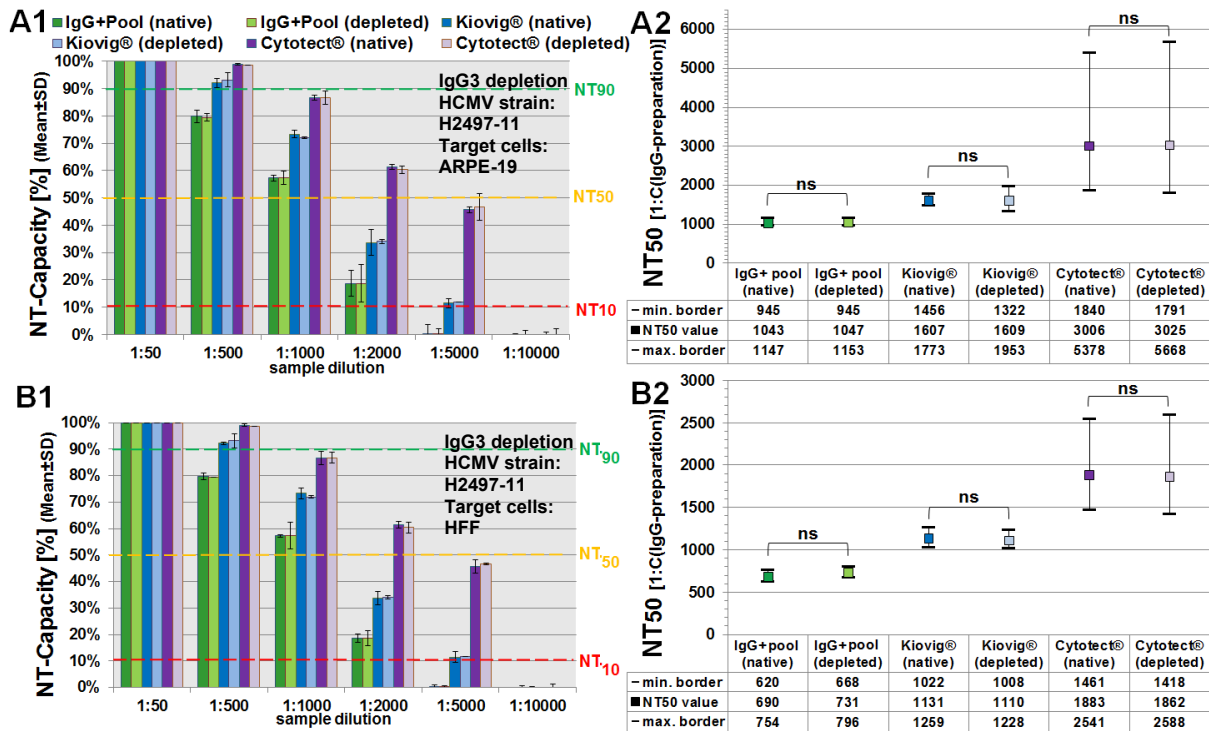


**Figure 47:** (A1) *In vitro* NT assay (HCMV-IgG stock solutions), IgG3 depletion, Target cells: ARPE-19 cells, HCMV strain: H2497-11, Cell culture incubation 5d; (A2) NT<sub>50</sub> PROBIT analysis of the tested IgG-preparations on ARPE-19; (B1) *In vitro* NT assay (HCMV-IgG stock solutions), IgG3 depletion, Target cells: HFF, HCMV strain: H2497-11, Cell culture incubation 5d; (B2) NT<sub>50</sub> PROBIT analysis of the tested IgG-preparations on HFF cells after PC antibody depletion (Modified after Schampera et al., 2018)

After the IgG subclass 3 depletion, no significant differences in reduction of NT-capacity were found between native and depleted samples of the IVIG Kiovig®, HIG Cytotect® and the HCMV-IgG<sup>+</sup>pool (all p-values were >0.05  $\triangleq$  ns (not significant)). These results were confirmed on ARPE-19 cells as well as on HFF. The depletion of the IgG subclass 3 had no impact on the *in vitro* neutralization activity of Kiovig® and Cytotect® under the chosen depletion concept via magnetic bead separation.

### 3.6 Modulation of the T cell response by HCMV hyperimmunoglobulin

In the second part of this study, the immunomodulatory effects of repeatedly given HIG administrations on the cellular immune response were analyzed in pregnant women with a proven HCMV-primary infection in the first trimester of pregnancy. These women were included in the cohort as part of the Tuebingen HIG study (Kagan et al., 2018). LiHep-Blood samples were longitudinally taken from women before and after HIG treatment, who achieved Cytotect® in a biweekly interval until gestational age of 21 weeks. The secretion of IFN-γ via stimulated PBMCs or whole blood was determined with two different detection systems. The collected blood samples were processed and analyzed via the QuantiFERON CMV® from Qiagen and the EliSPOT CMV® assay from Lophius, according to their derived process protocols.

**Table 22: Data overview of HIG-treated pregnant women, included in this study. The mothers were sorted on the number of administrated HIG applications**

No	ID	HIG applications	Age	GA	Gravida/Para
<b>HCMV Non-transmitter</b>			32±4	10.5±2.3	
1	ZeJe	3	29	13.3	G3P1
2	BrBa	3	29	14.6	G1P0
3	IbKa	3	32	14.3	G4P2
4	StRe	4	36	9.5	G5P1
5	AIDa	5	33	9.5	G2P1
6	YuNi	5	35	9.4	G2P1
7	ScSa	6	26	8.2	G1P0
8	RaCa	6	31	8.5	G2P1
<b>HCMV Transmitter</b>					
9	HaSa	5	41	8.6	G5P1

Table 22 shows an overview of HIG-treated pregnant women, who were included and analyzed in this part of the study. The women achieved different numbers of HIG applications, depending on the time point of enrollment into the Tuebingen HIG study and the time range of GA= 21 weeks until the therapy was stopped and amniocentesis was performed.

Mother 1 was investigated with both HCMV-specific IFN- $\gamma$  detection systems. In this selected case, the first 2 weeks were longitudinally analyzed, using narrow time points for blood collection (day of treatment (DOT) = 0, 2, 4, 7, 9, 11, 14) to analyze kinetics of IFN- $\gamma$  production and validate the results between the first and second HIG application.

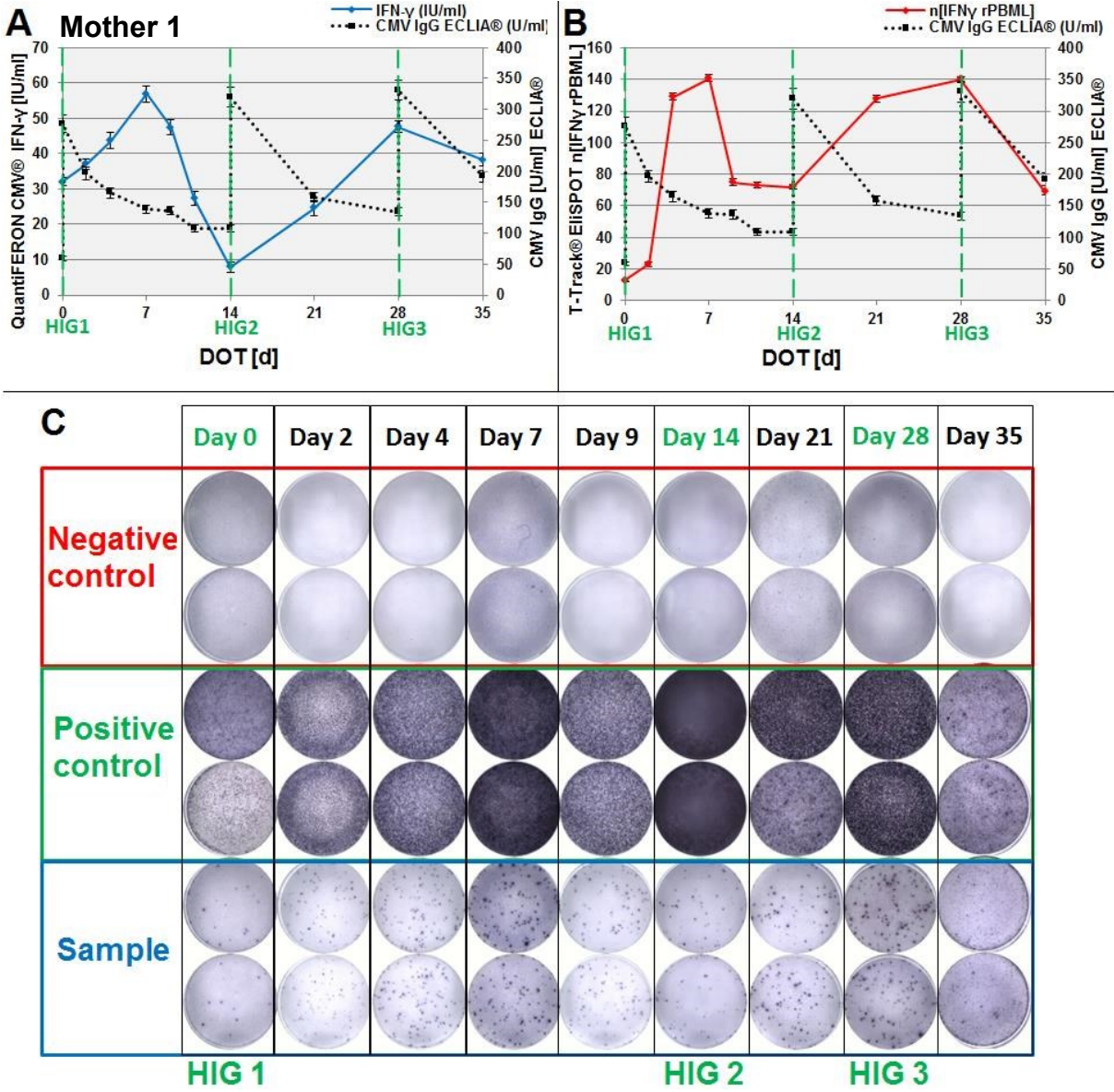


Figure 48: Kinetics of HCMV-IgG and IFN- $\gamma$  production, induced by HIG administration; (A) Mother 1: QuantiFERON CMV® (blue) compared to HCMV IgG ECLIA® (black); (B) Mother 1: Results of the T-Track EiiSPOT CMV® (red), compared to HCMV IgG ECLIA® (black); (C) Visualization of T-Track HCMV® IFN- $\gamma$  rPBMCs in microtiter plate with controls and sample

The HCMV-specific IgG was visualized as black-dashed line which, showed a recurring increase after each HIG application. After the first intravenous HIG administration of Cytotect®, the HCMV-specific IgG increased from a baseline of ~10 U/ml to a peak level of ~290 U/ml, using the HCMV ECLIA® assay after 2h, followed by a constant drop to the second HIG application on day 14 (Fig.48AB).

The results of the QuantiFERON CMV® showed an increased baseline of IFN- $\gamma$  concentration at the beginning of the first HIG administration, compared to the T-Track HCMV® EliSPOT (Fig.48A/B). Both tests had a peak on day 7. The level of IFN- $\gamma$  shortly decreased thereafter until day 14 and showed a repeated increase after the second HIG application and lasted to the third HIG dose on day 28 until the concentration of IFN- $\gamma$  dropped again. In contrast, the number of IFN- $\gamma$  reactive PBMCs<sup>7</sup> which were measured with the T-Track HCMV® EliSPOT showed a comparable kinetic pattern to the IFN- $\gamma$  concentration of the QuantiFERON HCMV®, except for the proportional lower number IFN- $\gamma$  rPBMCs at the start point of HIG treatment than the relative high concentration of IFN- $\gamma$  (Fig.48B). In addition, the following reduction of IFN- $\gamma$  level was stronger than the number of corresponding IFN- $\gamma$  producing PBMCs until day 14. The fluctuation in IFN- $\gamma$  reactive PBMCs was illustrated in figure 48C, showing an image of the T-Track EliSPOT sample wells (blue) with controls (red and green).

---

<sup>7</sup> Peripheral blood mononuclear cells

The IFN- $\gamma$  results of mother 2, 3 and 4 were summarized in figure 46. The second and third woman achieved three applications of HIG like the first investigated women and the fourth woman got four doses of Cytotec® every 14 days.

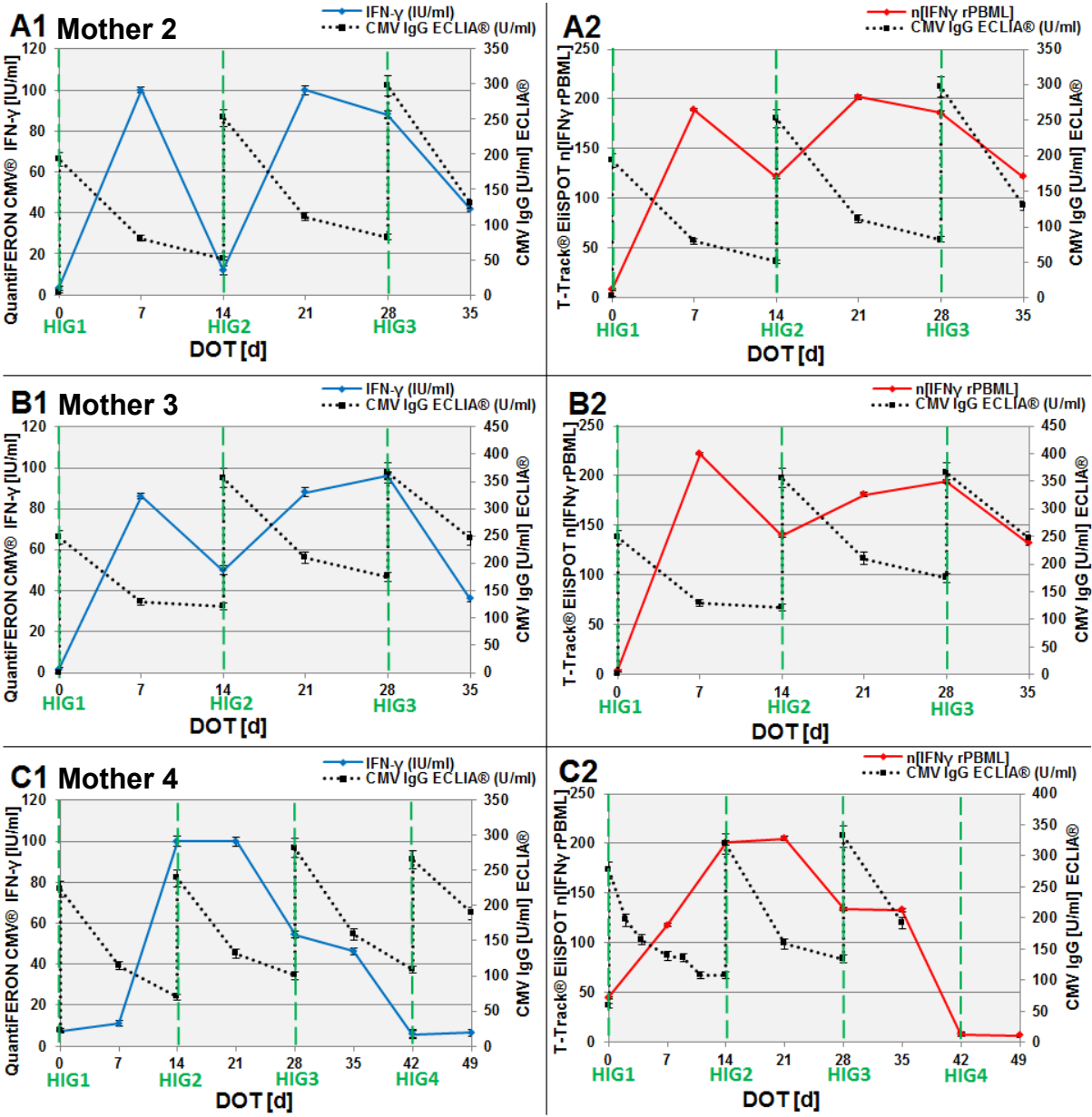


Figure 49: Kinetics of HCMV-IgG and IFN- $\gamma$  production, induced by HIG administration (A1/B1/C1) Mother 2/3/4: QuantiFERON CMV® (blue) compared to HCMV IgG ECLIA® (black); (A2/B2/C2) Mother 2/3/4: T-Track EliSPOT CMV® (red) compared to HCMV IgG ECLIA® (black)

In a first comparison to mother 1, the second and third woman revealed similar kinetic patterns of IFN- $\gamma$  and IFN- $\gamma$  reactive PBMCs (Fig.49A1/A2–B1/B2). However, differences were found in mother 4 (Fig.49C1/C2). The fourth woman had only one major IFN- $\gamma$  related peak at the time point of the second HIG application.

The IFN- $\gamma$  levels and the number of IFN- $\gamma$  reactive cells constantly decreased, except for day 35 which formed a short-lasting plateau in the T-Track HCMV® EliSPOT, but showed slower decreasing IFN- $\gamma$  levels in QuantiFERON HCMV®.

The fourth application to mother 4 seemed to have no further impact on IFN- $\gamma$  secretion at all. In a general consideration, both IFN- $\gamma$  based detection systems showed comparable results and confirmed the observation, taken from mother 1.

In the next data set of IFN- $\gamma$  results, the mothers 5 and 6 were combined and presented in figure 50. Both women were treated with fifth HIG administrations until the last application on day 56.

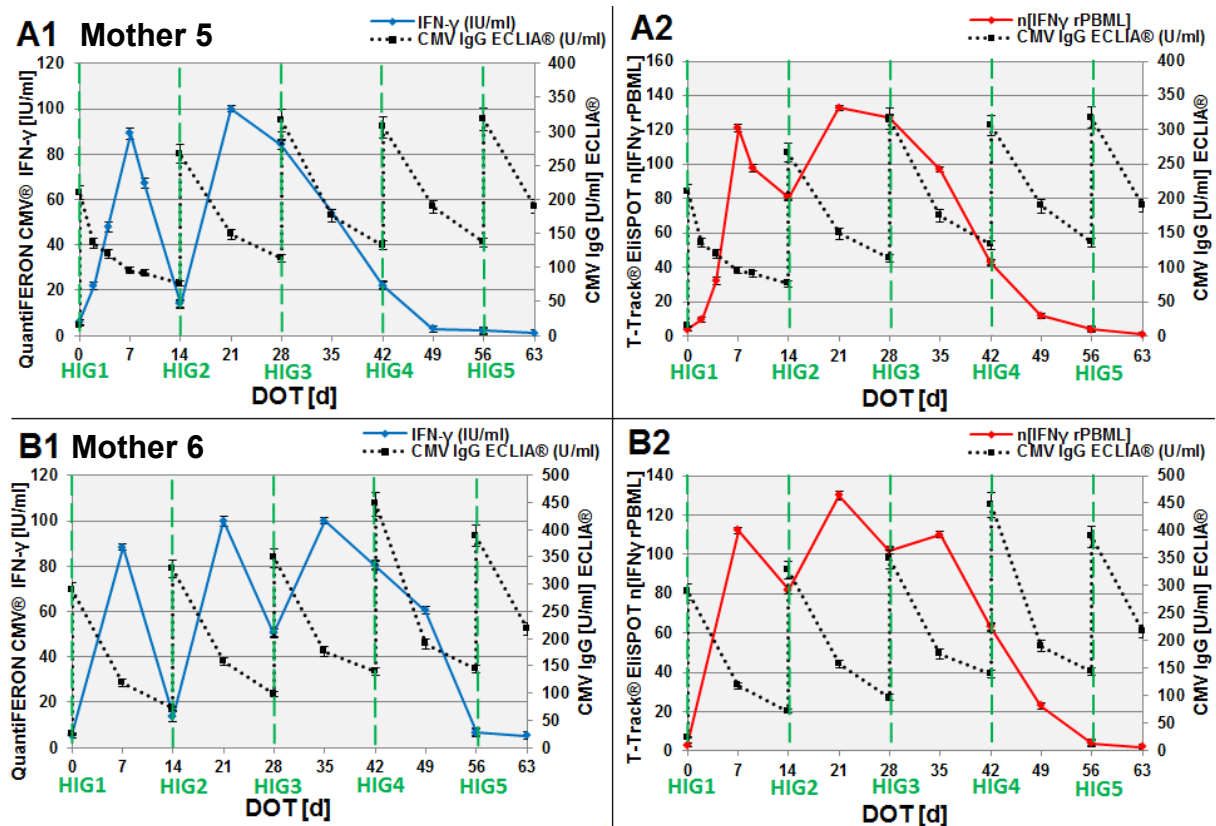
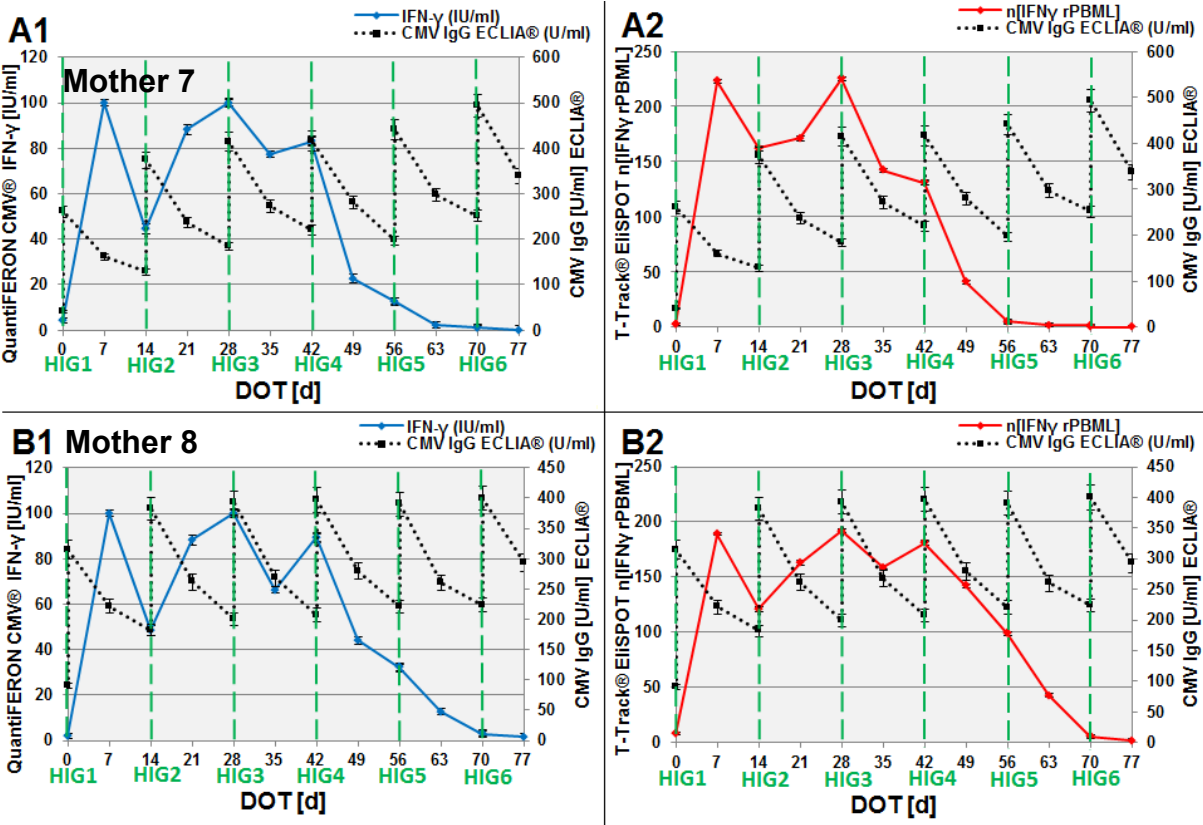


Figure 50: Kinetics of HCMV-IgG and IFN- $\gamma$  production, induced by HIG administration (A1/B1) Mother 5/6: QuantiFERON CMV® (blue) compared to HCMV IgG ECLIA® (black); (A2, B2) Mother 5, 6: T-Track EliSPOT CMV® (red) compared to HCMV IgG ECLIA® (black)

For mother 5, it was possible to perform the same IFN- $\gamma$  kinetics between the first and second HIG administration like in the selected case of mother 1 (Fig.50A1/A2). The proportional course of IFN- $\gamma$  reactive PBMCs and the concentration of produced IFN- $\gamma$  were similar to the investigated women in both IFN- $\gamma$  detection systems. Interestingly, the fourth and fifth HIG application induced no further IFN- $\gamma$  secretion which confirmed results of mother 4.

In contrast, three peaks of IFN in both tests were detected during HIG treatment of mother 6 on day 7, 21 and 35 (Fig.50B1/B2). However, the fourth and fifth HIG application also showed no re-stimulation of IFN- $\gamma$  activity like in mother 4 and 5.

In a next analysis, Mother 7 and 8 got six doses of Cytotect® until 70th dot every 14 days.



**Figure 51: Kinetics of HCMV-IgG and IFN- $\gamma$  production, induced by HIG administration; (A1/B1) Mother 7/8: QuantiFERON CMV® (blue) compared to HCMV IgG ECLIA® (black); (A2/B2) Mother 7/8: T-Track EliSPOT CMV® (red) compared to HCMV IgG ECLIA® (black)**

Mother 7 and 8 showed comparable kinetic patterns in the QuantiFERON CMV® (Fig.51A1/B1), compared to the results of T-Track EliSPOT CMV® of both mothers (Fig.51A2/B2). In both women, the number of IFN- $\gamma$  reactive PBMCs and resulting IFN- $\gamma$  concentrations reached their first peak on day 7 which was observed in the most HIG-treated mothers, followed by a decrease and a second longer-lasting increase of IFN- $\gamma$  levels and IFN- $\gamma$  reactive cells in both detection systems. In summary, both women had three peaks during the treatment with HIG and the investigations revealed that more than 3 to 4 applications of Cytotect® resulted in no recurring IFN- $\gamma$  stimulations in almost all mothers.

In context of HCMV-specific IgG, cumulative effects were noticed in all treated women, considering the rising baseline from the first HIG application to the last HIG application. In the exceptional case of mother 8, the woman reached the steady state for HCMV-specific IgG almost after the first HIG administration and only a small increase was observed during further HIG treatment.

In the last case, the analysis of a 41 years old woman is described, who was the oldest woman in this collective and the only HCMV-transmitter to the fetus which resulted in an asymptotically HCMV-infected newborn. The results of mother 9 were given in the figure 52.

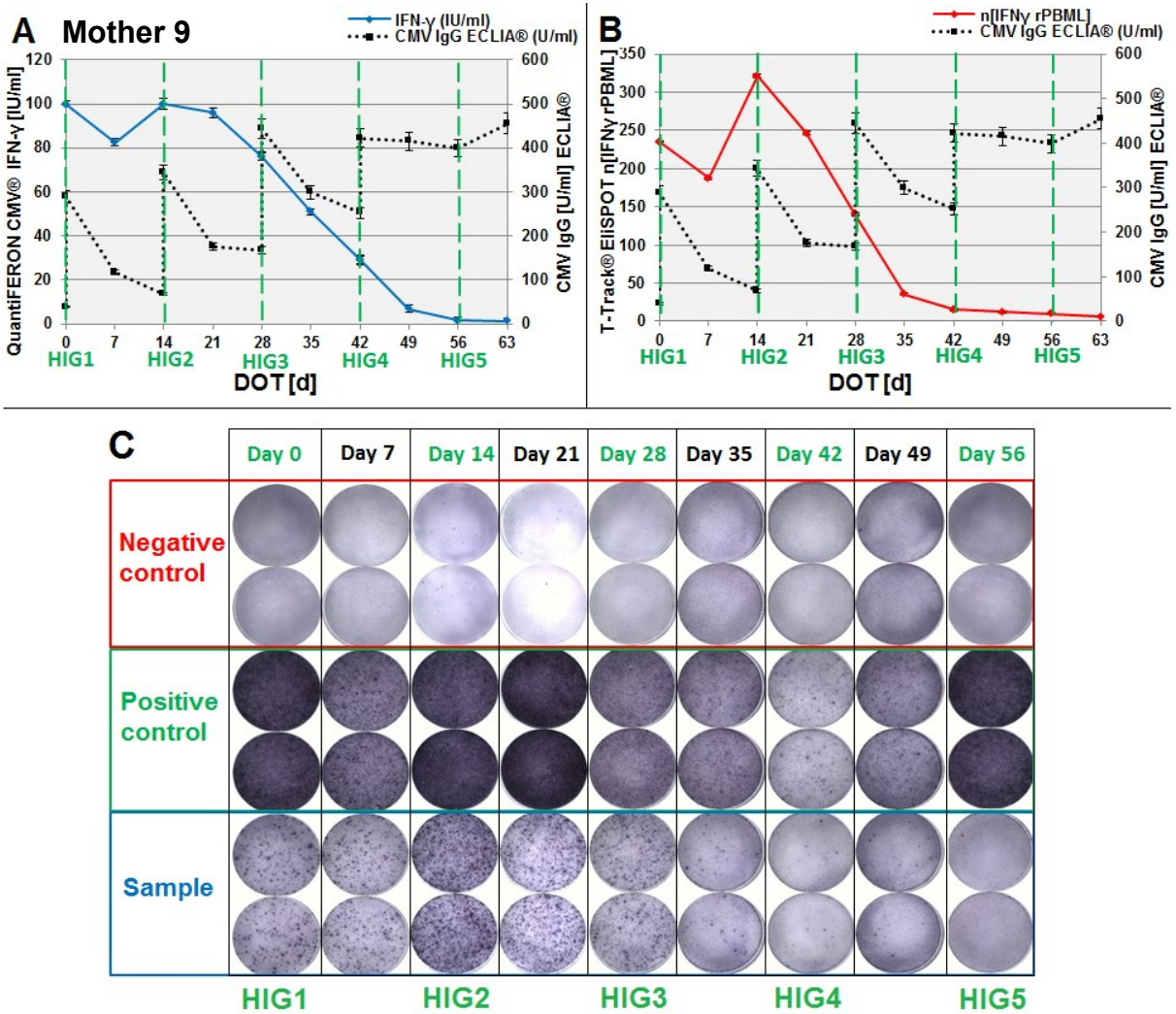


Figure 52: Kinetics of HCMV-IgG and IFN-γ production, induced by HIG administration (A) Mother 9: QuantiFERON CMV® (blue) compared to HCMV IgG ECLIA® (black); (B) Mother 9: T-Track EliSPOT CMV® (red) compared to HCMV IgG ECLIA® (black); (C) Visualization of T-Track HCMV® IFN-γ rPBMCs in microtiter plate with controls and sample

It has to be noticed, that the kinetic courses of IFN-γ concentration and the number of IFN-γ reactive PBMCs of maternofetal HCMV-transmitter strongly differed from all other investigated women in this cohort (Fig.52A/B).



The woman possessed already high levels of IFN- $\gamma$  and a high number of IFN- $\gamma$  producing cells at the beginning of the HIG treatment which decreased after HIG1. Then, an increase of IFN- $\gamma$  activity was detectable which surpassed the number of IFN- $\gamma$  rPBMCs of the T-Track EliSPOT CMV® at starting point, but not the IFN- $\gamma$  concentration. The QuantiFERON CMV® was already at its peak level at the start of the investigation (QUANTI<sup>max</sup> = 100 IU/ml). After its peak, a constant decrease was observed in both IFN- $\gamma$  detection assays, independent of the following three HIG administrations until day 63. For visualization of T-Track EliSPOT CMV®, figure 52C illustrated the analyzed wells of the blood samples (blue) plus controls (green/red). Single spots were shown in this figure which represented the countable IFN- $\gamma$  reactive PBMCs from a high count on HIG1 to constantly dropping numbers of these cells until HIG5. In addition, there was a slight deviation of HCMV-IgG concentration during the fourth and fifth HIG application.

In a further overall comparison, the collected kinetic IFN- $\gamma$  data of QuantiFERON CMV® and T-Track EliSPOT CMV®, as well as the detected HCMV-specific IgG ECLIA CMV® were summarized by box plots of all investigated HCMV Non-transmitter during the first three HIG applications (Fig.53). An estimated average course was calculated for each analyzed blood parameter. During the HIG treatment of the HCMV primary infected women, there were fluctuations detectable in concentrations of IFN- $\gamma$  between each individually investigated mother, mainly caused by single outliers.

However, in average, there was a clear proportional increase of the mean of IFN- $\gamma$  concentration after the first and second HIG application in the most treated mother. The estimated course of means of IFN- $\gamma$  reactive PMBLs reflected the observation of the means of IFN- $\gamma$  concentrations.

In contrast, there were fewer single outliers in the T-Track EliSPOT CMV® than in the QuantiFERON HCMV®. Furthermore, the numbers of IFN- $\gamma$  reactive PMBLs were more stable and underlay fewer fluctuations during HIG treatment than the detected IFN- $\gamma$  concentrations. For the HCMV-specific IgG, two samples were collected during each HIG application on the same day. The first sample was taken 15 min before the administration of Cytotect® and the second sample was harvested 2 h after each woman achieved the HIG dose. In average, the means of HCMV-specific IgG showed a repeated rise after each HIG application and the described cumulative effect of HCMV-specific IgG enrichment was already noticed after the first three HIG applications in the investigated women. Comparing IFN- $\gamma$  data and HCMV-specific IgG, the IFN- $\gamma$  reactive cells responded with a delay in producing IFN- $\gamma$  after the first HIG administration and further applications of Cytotect® were needed to maintain the production of IFN- $\gamma$  in most cases. The analyzed IFN- $\gamma$  related parameters were not affected by later HIG applications.

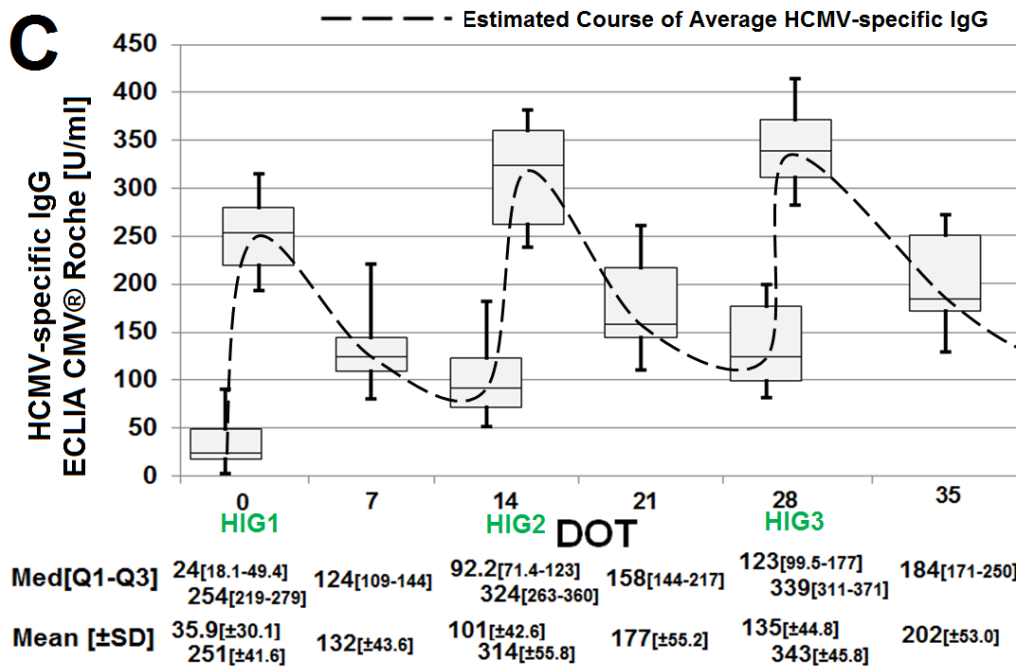
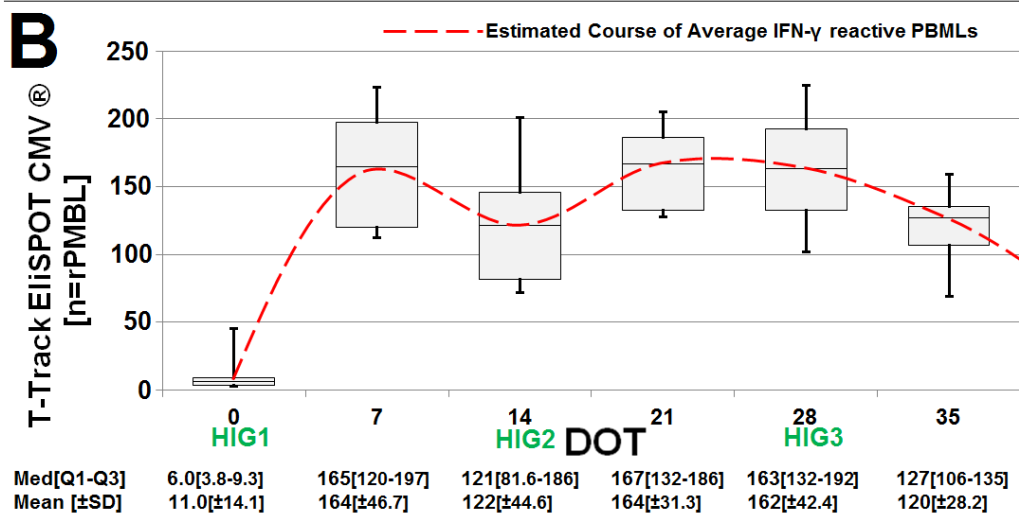
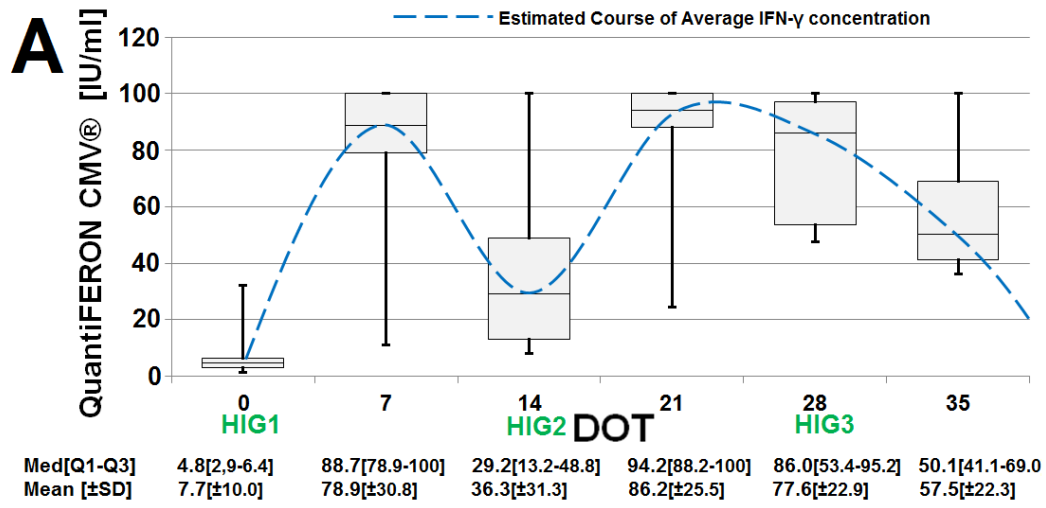


Figure 53: Longitudinal monitoring of all HCMV Non-Transmitters during the initial 3 HIG applications: (A) Estimated average course of IFN- $\gamma$  concentration (blue); (B) Estimated average course of IFN- $\gamma$  reactive PBMLs (red); (C) Estimated average course of HCMV-specific IgG (black)

## 4 Discussion

### 4.1 Standardization of HCMV neutralization assay and assay performance characteristics

The investigated scientific issues in this work were based on discordant results of Nigro et al., 2005 and Revello et al., 2014, as well as on a currently published paper of Kagan et al., 2018. The studies of Nigro and Revello used the same study design in order to analyze the impact of HIG treatment on HCMV primary infected women during pregnancy. While the first study of Nigro achieved a success in therapy of HCMV infection as well as in prevention of HCMV transmission to the fetus under the usage of HIG, the RCT study of Revello did not find a significant difference between the placebo and the investigated prevention group. In a later formulated consensus review, no general recommendation was given for the treatment of HCMV primary infected pregnant women with hyperimmunoglobulins outside of clinical trials (Rawlinson et al., 2017). However, both studies revealed a trend towards reduction of HCMV transmission to the fetus in the HIG-treated group (Fig.54). Furthermore, currently available results of the Kagan study demonstrated a clear causal relation between a shorter interval of HIG applications and the prevention of maternofetal HCMV transmission under strict virologic inclusion parameters for the pregnant women with HCMV-primary infection in the first trimenon.

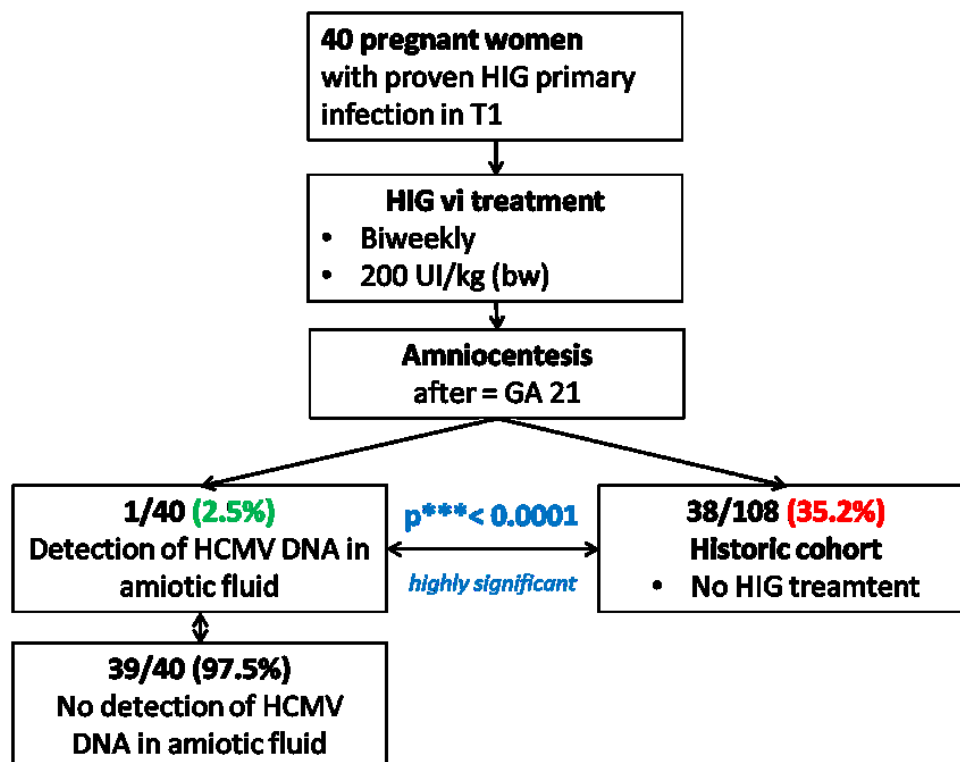


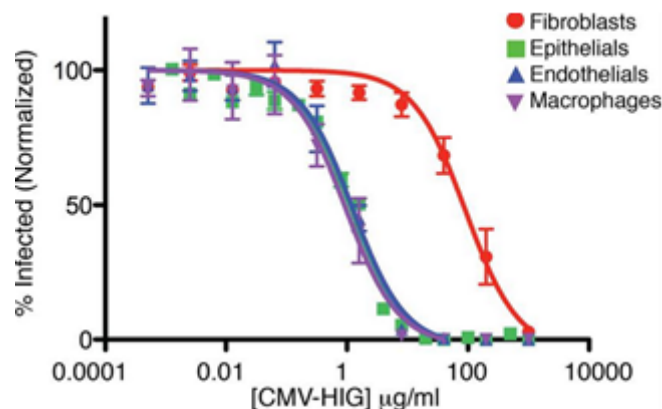
Figure 54: Results of the Tuebingen HIG study (Kagan et al., 2018)

The study of Kagan et al. had one viral transmission from mother to fetus in 40 cases (2.5%) in the prevention group, compared to the historic cohort with 35.2%. This result represented a significant difference between both groups ( $p < 0.0001$ ). The study showed, that HCMV-IgG treatment of pregnant women with HCMV primary infection in the first trimester of pregnancy could decrease the maternofetal transmission rate, compared to HIG untreated pregnant women. Therefore, the work of Kagan et al., demonstrated a promising treatment option for a defined cohort of HCMV-primary infected mothers during early gestation (<week 14). However, the improved study design, including a narrow HIG application interval and enrollment of pre-selected mothers has to be proven in further controlled studies to evaluate the results of the Kagan study and to confirm the collected data. Considering kinetics of HCMV-specific IgG, cumulative effects were noticed in all HIG-treated pregnant women, referring to the increasing baseline between the first to the last HIG application. A shorter HIG application interval of two weeks was applied in the Kagan study than in the studies of Nigro and Revello. An incorrect half-life time ( $t_{1/2}$ ) of IgG antibodies was assumed in both studies which was based on studies of Thurmann et al., 1995. The shorter HIG application interval indicates, that the HCMV-specific IgG was not completely eliminated by the mothers or spent for viral neutralization between the HIG doses. Additionally, the study of Revello reported signs of an increased rate of prematurity after HIG application to pregnant mothers. However, a recent paper contradicts with Revello and showed no evidence of obstetrical adverse events after HIG treatment to those mothers (Chiaie et al., 2018).

In order to characterize the used HIG preparation Cytotect® in the Kagan study and to understand the possible mode of action of administrated IgG-antibodies, further investigations were made in the presented PhD thesis. For the first analysis of NT-capacity of IgG preparations, *in vitro* plaque reduction assays were modified after a previous publication of Schampera et al., 2017 which based on NT protocols of Eggers et al., 2000 and Abai et al., 2007. The NT protocol was additionally adapted, depending on the respectively scientific investigation (Point 1.15).

For calibration, two serum pools were used as reference controls to define the reference conditions of the *in vitro* NT assay. Each serum pool contained sera of 100 women, who were either HCMV-seronegative or HCMV-latently infected at birth, measured concordantly with five different HCMV serological test systems. The NT reference pools represented two different cohorts of mothers at birth and were derived from the Tübingen congenital HCMV study. Two HIG preparations, Cytotect® and Cytogam®, as well as two standard immunoglobulins, Kiovig® and Octagam® were characterized via defined sample dilutions in the established PRA. On the base of the analyzed *in vitro* neutralization capacities, the corresponding  $NT_{50}$ -values were calculated and compared, using statistical programs for significance proofing (Wilcoxon rank sum test for equality on unmatched data) (Fig.33).

The first obtained results showed consistently higher *in vitro* NT-capacities in HIGs than in IVIGs. The HCMV-IgG<sup>+</sup>pool possessed the lowest NT-capacity. While the *in vitro* NT-capacities of HIGs were comparable, differences were found between the analyzed IVIGs. Octagam® showed generally higher NT<sub>50</sub>-values than Kiovig®. It might be suggested that Cytogam® could be used as alternative product to Cytotect® in the United States under the previously given permission of the American food and drug administration (FDA). On the base of the presented *in vitro* results, the administration of Cytogam® may result in prognostically comparable successes in therapy and prevention of maternofetal HCMV transmission, using the same study design of Kagan et al, 2018. The application of Kiovig® also increased the NT-titer against HCMV in pregnant women with a HCMV-primary infection, according to a study of Polilli et al., 2012. This result matched with the data in this study, that Kiovig® contained high HCMV-specific neutralization titer. The observation of higher NT<sub>50</sub> values in HIGs than IVIGs were found on both epithelial cells, as well as on human foreskin fibroblasts as target cells for viral infection via HCMV. But, IgG antibodies, directed against HCMV showed higher protective potential, combined general higher NT-titers to prevent viral infection and cell-to-cell spread in ARPE-19 cells than in HFF. The results of a former study confirmed these observations on different cell types (Fouts et al., 2012).



	EC <sub>50</sub> µg/ml	EC <sub>90</sub> µg/ml
Fibroblasts	157	590
Epithelials	1.3	9.1
Endothelials	1.3	9.1
Macrophages	1.1	7.4

**Figure 55: Percentage of infected cells (normalized) under the usage of HIG on 4 cell types. Cytogam® was incubated with the low-passage clinical HCMV strain VR1814 (Fouts et al., 2012)**

HCMV possesses two different mechanism of entry into different cells types. During a viral infection, HCMV uses gH/gL/gO to infect fibroblasts and the entry into epithelial and endothelial cells is mainly mediated via the pentameric complex (gH/gL-UL128L) (Adler et al., 2006; Vanarsdall et a.,2011; Hahn et al., 2004; Gerna et al., 2005; Wang et al., 2005; Sinzger et al., 2006).

In conclusion, different epitope-specific IgG antibodies are responsible for strong binding and effective neutralization in different target cells. In the study of Fouts et al., the HIG Cytogam® was incubated with low-passage clinical HCMV strain (VR1814) on four different cell types for 18h. The results confirmed comparable EC<sub>50</sub> and EC<sub>90</sub> values for epithelial and endothelial cells, as wells for macrophages. However, >100-fold higher concentration of Cytogam® was needed to bind and neutralize HCMV on fetal lung fibroblasts (MRC-5) as target cells (red line) (Fig.55). The results of the PC depletion experiments in the presented PhD thesis confirm the data of Fouts, because the depletion of PC-specific antibodies had no impact on HFF (Fig.46).

In another work of Cui et al., 2008, the impact on induced *in vitro* NT-activity through HCMV-specific antibodies was investigated using Cytogam® and Cytotect®, as well as sera from donors, who achieved a vaccination with recombinant gB/MF59 subunit or an attenuated equivalent of the Towne virus strain as. The samples were analyzed on MRC-5 fibroblasts and ARPE-19 cells (Fig.56).

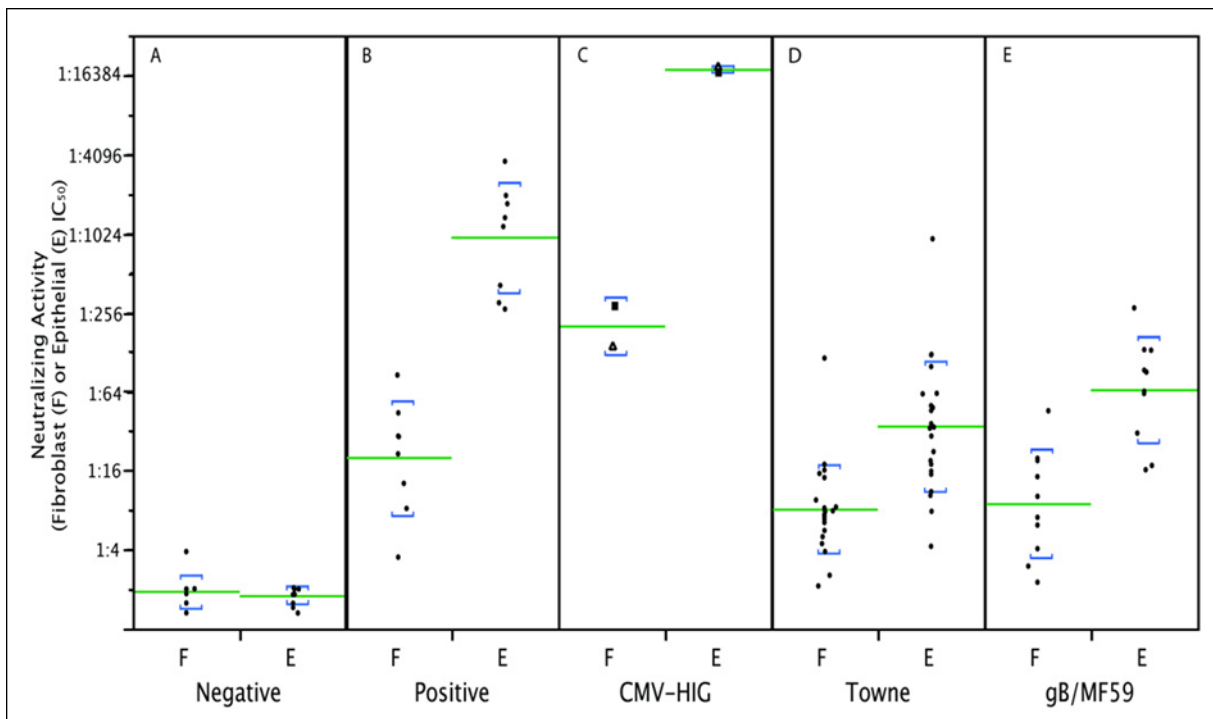


**Figure 56: Neutralizing activity of HIGs (Cytotect®▲, Cytogam®■) versus vaccination (gB/MF59; Towne), described as IC<sub>50</sub> titers on fibroblasts (F) and epithelial cells (E) (Cui et al., 2008)**

The results revealed a 48-fold increased NT-activity in epithelial cells than in fibroblasts which indicated that the humoral immune control of natural HCMV infections is mainly promoted by epithelial-specific neutralizing antibodies against the pentameric complex (Fig.56). In this context, both vaccines failed to induce HCMV-specific neutralizing antibodies which generated on average a 28-fold (Towne) and a 15-fold (gB/MF59) lower neutralization activity in comparison to HIGs on ARPE-19 cells. These results suggested that the effectivity of vaccination against HCMV may be improved by vaccines, based on the viral pentameric complex in the future. The UL130 peptide and PC depletion experiments in this work support this suggestion. A significant part of *in vitro* NT-capacity was reduced after PC-specific antibodies were removed from HIG (Fig.46).

The negative and positive control were represented by a cohort of randomized blood donors without HCMV infection and a cohort of randomized blood donors, who were HCMV-latently infected after a natural infection. The results of Ciu showed additionally a comparable NT-capacity between Cytotect® and CytoGam® on both cell types which confirmed the data in this thesis and a previous work of Frenzel et al., 2012 which suggested, that HCMV-specific infection rates and corresponding neutralization depend on the cell type.

A current paper published *in vitro* NT data, comparing Cytotect® and CytoGam® to 2 different IVIG preparations (Vena® and Flebogamma®) (Germer et al., 2017).

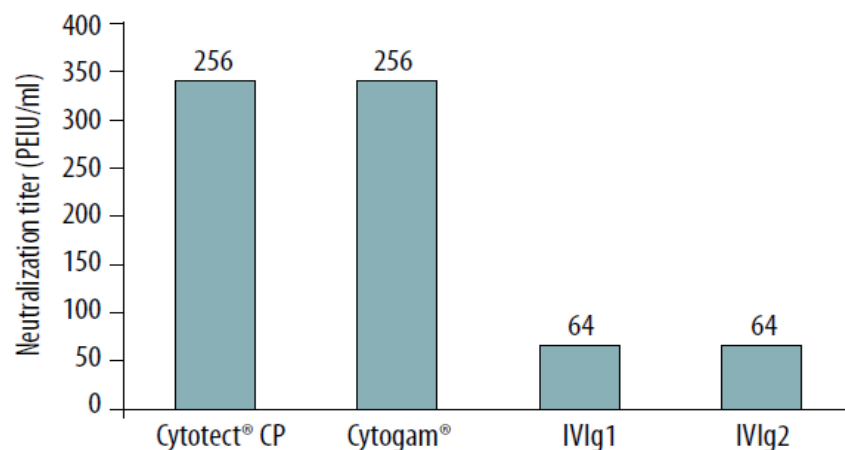


**Figure 57: Neutralization titers of HIG preparations Cytotect®/CytoGam® and IVIG preparations 1 and 2 (Germer et al., 2017).**

The data support both suppositions of this work, that the NT capacity of Cytotect® and CytoGam® are comparable and show higher neutralizing titers than IVIGs (Vena® and Flebogamma®) (Fig.57). The IgG of the products values were expressed using PEI Units/ml. Interestingly, the estimated PEI values of Cytotect® (101.8 PEI U/ml) and CytoGam® (112.5 PEI U/ml) were comparable to the PEI values, calculated in this work (Tab.19 and Fig.31).

The results of another paper confirmed, that HIGs contain higher concentrations of HCMV-specific IgG which also results in higher neutralizing antibodies than IVIGs (Fig.58) (Miescher et al., 2015)

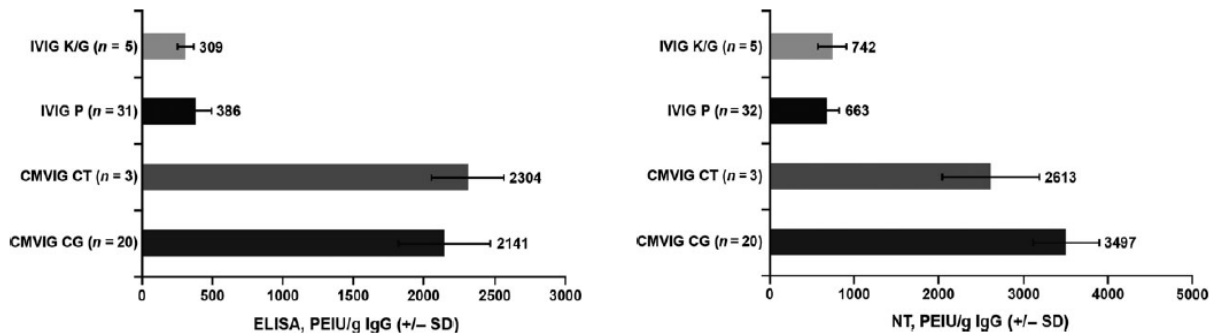


**Figure 58: (A) HCMV-specific IgG, detected by ELISA in PEI U/g IgG for HIGs and IVIGs; (B) Resulting NT activities of HIGs and IVIGs, expressed as PEI U/g IgG (modified after Miescher et al., 2015)**

The HIG preparations Cytotect® (CMVIG CT) and Cytogam® (CMV CG), as well as the IVIGs Privigen® (P), Kiovig® and Gammagrad® (K/G) were analyzed in this study, using IgG stock solutions. However, their results were only examined on fibroblasts.

Miescher et al., 2015 strongly contrasts to Planitzer et al., 2011 and postulated higher IgG subclass 3 concentration in Cytogam® than Kiovig®, paired with slightly higher NT-capacities for Cytogam® than Cytotect®. The mentioned observations were not confirmed by own investigations (Schampera et al., 2017). It has to be considered, that both studies of Miescher and Germer were funded by the manufactures of the HIGs Cytotect® (Germer et al., 2017; Miescher et al., 2015).

On the base of PEI Units, HCMV-specific IgG normalization was used to analyze the *in vitro* NT-capacity per PEI Unit for each IgG preparation in a following NT experiment (Fig.37). The IgG preparations were quantified for the ECLIA HCMV® Roche and a generated standard curve with a high correlation coefficient ( $R^2=0.99$ ). This allowed an excellent transformation of ECLIA® HCMV-IgG into to PEI Units (Fig.30). The results revealed no significant differences in the HCMV-specific neutralization activity on APRE-19 cells and HFF. It suggested for all investigated preparations that the same amount HCMV-specific IgG possess the same quality in terms of neutralization activity per PEI Unit and only the concentration HCMV-specific IgG might be important to prevent HCMV infection and maternofetal transmission. Furthermore, the PEI units and the corresponding NT-capacity showed an approximated-linearized course in the established NT assay after a  $\log_{10}$  adaption (Fig.37). The findings were contradictory to the data of Planitzer et al., 2011 (Fig.34/35). The authors postulated higher IgG3 concentrations in Kiovig® than Cytotect® which resulted also in higher *in vitro* NT-activity in Kiovig® than in Cytotect® during their investigations.



In contrast, the results in the presented work showed consistently significantly higher NT-capacities for Cytotect® than Kiovig® which was independent, considering IgG3 concentrations. The impact of IgG 3 antibodies on NT-capacity point will be further discussed in detail on the point 4.5.

In a next attempt, the TB40E variant (RV-TB40-BACKL7-SE-EGFP) was used to modify the PRA protocol to provide an alternative read out system via an intracellular-expressed eGF-protein instead of p72 staining (Fig.38) (Sinziger et al., 2008; Sampaio et al., 2017). The experiment was successful on HFF with more than 100 PFUs/well and showed comparable NT data to the H2497-11 strain for all IgG preparations. Sample images of TB40E-plaque formation in microculture were given in figure 39.

Unfortunately, the TB40E strain was not able to induce sufficient numbers of evaluable TB40E-PFUs in ARPE-19 cells. Repeated propagation of TB40E in ARPE-19 cells, following by generation of multiple viral stocks at different stages did not lead to valid results in the *in vitro* PRA. Therefore, the H2497 strain was used for further investigations.

Interestingly, multiple single infected cells were detectable (Fig.40). However, it might be suggested that either the viral cell-to cell spread in ARPE-19 cells is much slower than in HFF or the IgG preparations prevented the viral cell-to-cell spread in a more efficient way. The TB40E was investigated to offer an alternative readout system in contrast to p72 staining.

A previously published paper of Wang et al., 2017 considered the variations of NT-capacities between different Lots of one HIG and eight IVIG preparations using the TB40E and AD169 strain. Firstly, an ELISA was examined to determinate their binding activities and avidity (Tab.23)

**Table 23: Variations in Lots of HIG (A) and IVIG products (B –I), considering anti-HCMV binding activity and avidity index in comparison to the PEI reference standard 1996 (modified after Wang et al., 2017)**

Anti-CMV binding activity and avidity of IG products.

	IG Product	Specific ELISA Activity (PEI U/g IgG) <sup>a</sup>	Avidity Index 1:10	Avidity Index 1:20
HIGs	PEI Ref	2306	NT	NT
	A <sup>b</sup> Lot 1	3817	83.9%	83.5%
	A <sup>b</sup> , Lot 2	2821	82.8%	81.9%
	A <sup>b</sup> , Lot 3	3217	88.0%	80.5%
IVIGs	B, Lot 1	438	67.7%	64.5%
	B, Lot 2	562	69.3%	67.5%
	C, Lot 1	645	73.6%	69.3%
	C, Lot 2	692	73.2%	75.1%
	D, Lot 1	264	66.8%	75.4%
	E, Lot 1	353	69.0%	70.4%
	F, Lot 1	394	66.2%	69.8%
	G, Lot 1	317	72.0%	66.1%
	G, Lot 2	221	66.6%	66.9%
	H, Lot 1	540	66.5%	70.2%
I, Lot 1	386	63.1%	70.0%	

NT: Not tested.

<sup>a</sup> Calculated using activity of 110 U/mL and IgG concentration of 4.77% (PEI).

<sup>b</sup> CMV-specific IG product.

Lots of the same IgG product revealed comparable stable in NT-testing which indicates comparable concentrations of HCMV-specific IgG over multiple charges. The HIG showed the 10- to 20-fold higher HCMV-binding activity ( $\bar{X}$ :  $3285 \pm 501$  PEI U/g IgG) than the IVIG preparations ( $\bar{X}$ :  $437.5 \pm 153.9$  PEI U/g IgG) in all three Lots. However, the avidity was high in both the HIGs ( $\bar{X}$ :  $84.9 \pm 2.7\%$ ) as well as in the IVIGs ( $\bar{X}$ :  $68.5 \pm 3.2\%$ ).

While it was repeatedly shown, that HCMV-specific antibodies interact with a huge amount of HCMV proteins, binding of viral components does not necessarily result in viral neutralization (Britt et al., 1996 and Schoppel et al., 1997). The NT-capacity was subsequently analyzed via an RT-qPCR-based neutralization assays using PEI units for normalization (Wang et al., 2017). Therefore, the infected cells were lysed after viral inoculation for 6 h to 24 h, analyzing the transcript of the IE1 gene UL123 in a following RT-qPCR to make conclusions about the genome copy numbers of the virus and corresponding neutralization activity of the IgG products (Fig.59).

The experiments were performed to compare the NT capacities against TB40E-GFP strain to AD169<sup>wt131</sup> strain with a restored pentameric complex under the usage of several HIG and IVIG preparations. ARPE-19 cells and MRC-5 fibroblasts were used as target cells.

Usually, the high-passaged AD169 strain lost its ability to infect epithelial cells in cell culture through mutations in the UL131 gene which results in a non-functional pentameric complex, essential for the epithelial entry process.

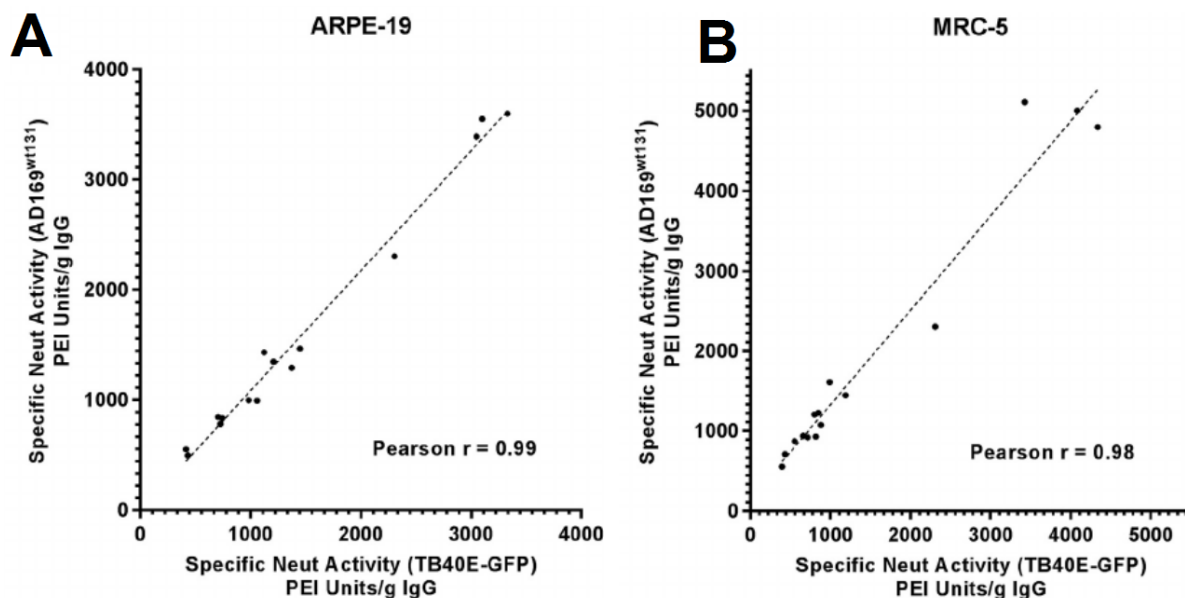


**Figure 59: Comparison of NT activity of HIG and IVIG preparations against the HCMV strains AD169<sup>wt131</sup> and TB40E-GFP on ARPE-19 (A) and MRC-5 cells (B) (modified after Wang et al., 2017)**

A correlation was found in the HCMV-specific neutralization activities of IgG products between the HCMV strains AD169<sup>wt131</sup> and TB40E-GFP in ARPE-19 cells and HFF. Each dot represented an analyzed Lot of different or the same IgG preparations. These results confirmed the data of *in vitro* NT-capacities in the HCMV strains H2479-11 and TB40E variant (RV-TB40-BACKL7-SE-EGFP) in this PhD thesis.

In addition, the RT-qPCR neutralization assay system was suitable to detect the NT-capacities, using the TB40E-GFP strain on APRE-19 cells which was not possible in this PhD thesis (Fig.40). This might be caused by a different read out system, compared to the established plaque reduction protocol which induced insufficient PFUs for TB40E in ARPE-19 cells to deliver valid test results.

Furthermore, variations were found in the viral stocks from vial to vial in this work, caused by freeze-thaw durability and resulted in different total numbers of HCMV-induced PFUs in the HCMV-IgG negative pool and in the analyzed IgG preparations. This phenomenon promoted different results, using different vials of the same viral stock and made a direct comparison of PFU numbers impossible between single performed experiments (Fig.35).

The viral isolates were frozen in 100 µL aliquots. It was observed, that variations were recognized within a box of the same viral isolate. Especially, greater variations occurred between edge-placed vials and vials, localized in the center of the box (up to ~15%). The freezing process took place at -80°C from the edges to the center of the boxes which could be an explanation for the differences of infectivity. However, the appearance of described effect was discovered early during this thesis and was reduced by preparing of a mixture of several vials before each NT experiment and the usage of the relative NT capacity in percentage instead of total HCMV-PFU numbers.

#### **4.2 Cytotect® neutralization activity against HCMV isolates, resistant to antiviral compounds**

The established *in vitro* PRA assay protocol was used to investigate the potential of Cytotect® to neutralize wildtype HCMV strains which were drug-resistant against GCV or/and CDV. It was clarified, whether the acquirement of a drug-resistance has an impact on the *in vitro* NT-capacity of IgG products, containing HCMV-neutralizing antibodies. The NT assays and the following statistical analysis via JMP software revealed no significant differences between the drug-resistant HCMV strains and a drug-sensitive strain (H2497-11) in relation to their infectivity in presence of defined concentrations of IgG preparations. The results of the experiments suggested, that the *in vitro* NT capacity of Cytotect® and other analyzed IgG preparations seemed to be not affected by drug-resistant HCMV strains against GCV and/or CDV under the selected parameters of the PRA assay protocol. For the interpretation of the collected NT data, the neutralization capacities of the analyzed IgG preparations showed general high potency to prevent viral infection and cell-to cell spread, independent of the wild type of HCMV. Due to the fact, that especially HIGs contain high numbers of different neutralizing antibodies against many relevant epitopes of HCMV which are important for successful infection and virus production. Furthermore, the mode of action and the involvement of defined target gene products differ between antibodies and anti-viral drugs.

### **4.3 Characterization of Cytotect® neutralization activities against HCMV isolates with different gB-genotypes**

Further investigation of this work analyzed HCMV strains with different gB types in context of *in vitro* neutralization. For this purpose, HCMV strains from different human materials of patients with different diagnoses were chosen to increase the number possible genetically variations. In addition, the AD169 strain was added as gB2-strain to represent a high-passage laboratory-strain in comparison to the other used low-passage clinical isolates, carrying gB1, gB3 and gB4. The H487-06 strain (gB4) was isolated from the same patient like the H815-06 strain which is drug-resistant.

However, the isolate was collected on a different time point during antiviral treatment, possessing the same multidrug resistance against GCV and CDV (UL97 [L595S] UL54 [V715M]) to evaluate already given results and put the presented results in context of these considered data. According to the results, Cytotect® and other IgG products are able to neutralize HCMV strains with different glycoprotein B genotypes at the same level of neutralization capacity. Therefore, the gB genotype seems not to be associated with a reduction or increase of HCMV-specific IgG NT capacity.

These results confirmed former data in this study which showed no difference in NT activity between drug-resistant and drug sensitive HCMV strains. In addition to the already given interpretation, the polyclonal neutralizing antibodies of Cytotect® and other IgG preparation were harvested from different donors which were infected with different HCMV variants. These variants possess most likely different gB types which could explain the universally high NT-capacity.

Interestingly, AD169 is a high passage laboratory strain mutant with a multitude of genetically modifications during cell culture adaption and propagation, but the infectivity-related genes and the expressing protein products for production seems to be highly conserved over all strains, resulting in comparable high NT-capacities of the investigated IgG preparations. However, HIGs contain a higher amount of these high-class neutralizing antibodies than IVIGs.

The biochemical analysis of the used IgG-preparations was previously described in the work of Schampera et al., 2017. In a summary, the results confirmed, that HIGs have a higher neutralizing potential against HCMV, compared to IVIGs. But HIGs contain lower concentrations of total IgG than IVIGs at stock solutions.

In addition, the results indicate that IgG antibodies need 100-fold higher concentrations to prevent viral cell-to-cell spread in cell cultures in comparison to cell-free virus infection (Murrell et al., 2017).

Murrell intensively investigated this phenomenon in different viral strains of HCMV (TB40 BACs and Merlin-GFP variants) and showed clearly, that viral cell-to-cell spread is more efficient than cell-free infection. Furthermore, the IC<sub>50</sub> values for the strains were similar under the usage of Cytotect® and HCMV-seropositive serum samples.

This observation agrees with results in this thesis, analyzing the NT-capacity of Cytotect® and other IgG preparations against different laboratory strains and clinical isolates. The lower consumption of IgG preparations for analysis of cell-free *in vitro* HCMV infection was one of the main reasons for the modification of the previous NT assay protocols (CFNT versus PRANT), described in Schampera et al., 2017 to establish a combined PRA protocol which covers both the cell-free viral infection, as well as the *in vitro* cell-to-cell spread of HCMV.

#### **4.4 Role of PC-specific antibodies in IgG preparations**

The viral trimer complex (gH/gL/gO) and pentamer complex (gH/gL-UL128L) are the two mayor viral glycoprotein complexes for mediating the tropism-dependent cell entry via the membrane fusion protein gB (Wang et al., 2005; Ryckman et al., 2008; Lilleri et al., 2013, Ciferri et al., 2015). An interesting fact, the gene products of the UL128-131 region and gB compete for binding to their common gH/gL subunit which affects the ratio of timer complex/pentameric complex on the viral surface and consequently the cell tropism (Zhou et al., 2013; Li et al., 2015).

The first antibody depletions experiments in this work were performed using a modified peptide of UL130 after Saccoccio et al., 2011 which induced highly HCMV-specific antibodies in rabbits. The TAN-peptide was analyzed via computer software analysis by Jose Arellano-Galindo (Infectious Diseases Laboratory (Virology) Children's Hospital Federico Gómez, México City, Mexico) and showed an increased probability for antibody binding than the original SWS-peptide, as well as optimal physical and chemical properties (Schampera et al., 2018). Subsequently, both UL130 peptides were used in a depletion strategy, involving magnetic beads. The potential of TAN- and SWS-peptides was analyzed to remove a relevant number of HCMV-neutralizing antibodies which are UL130-specific and resulting in decreases of *in vitro* NT-capacity in epithelial cells (ARPE-19). After HCMV-IgG-normalization, the TAN-peptide reached a maximal decrease of 16% which formed a significant difference in reduction of NT-capacity in comparison to the UL130 SWS peptide (Fig.45).

However, this result was not repeatable, using HIG/IVIG stock solutions (Fig.44). Nevertheless, a clear non-significant trend towards NT-reduction was visible in both UL130 peptides after IgG antibody depletion.

It has to be highlighted, that the PC-related depletion of HCMV-specific IgG antibodies revealed a much higher effect on NT reduction with 42% at its maximum than single UL130 peptides, due to a much higher amount of presenting linear and non-linear epitopes via secondary and tertiary protein folding (Fig.46). In this context, a work of Magacno et al., showed at least two expressed gene regions of UL128 locus are necessary to bind monoclonal antibodies which possess a high neutralizing activity against HCMV (Macagno et al., 2010).

This could be an explanation for the relative low reduction of neutralization capacity for the UL130 peptides in comparison to a complete pentameric complex.

Two papers investigated the impact of PC-specific antibody depletion on the infection rate of different HCMV strains, using Cytogam® instead of Cytotect® (Fouts et al., 2012; Loughney et al., 2015)

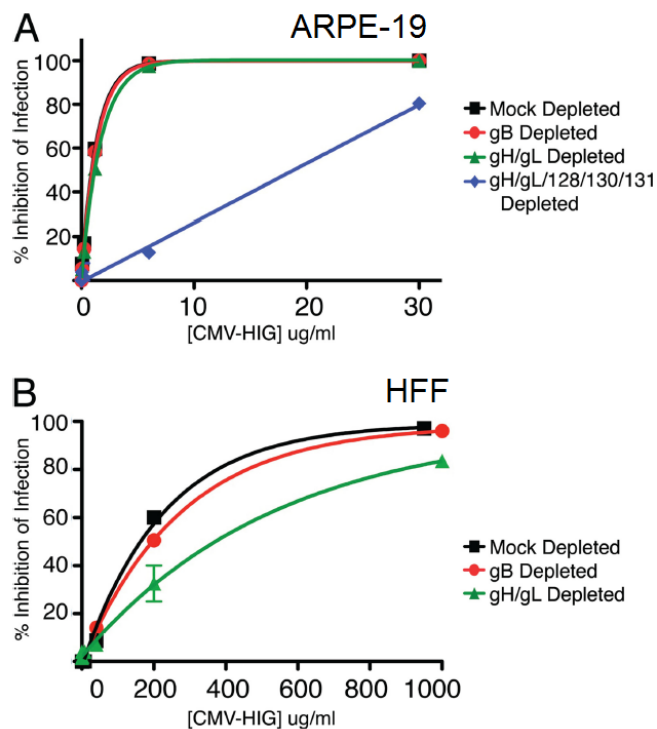


**Figure 60: Inhibition of infection after Mock, gB, gH/gL or PC antibody depletion on (A) ARPE-19 cells and (B) HFF using Cytogam® (Fouts et al., 2012)**

Using an adenovirus expression system, Fouts generated a membrane-bound pentameric complex as well as gB and a gH/gL subunit from the Merlin strain on the surface of ARPE-19 cells in order to deplete related antibodies. While 91% of the gB-specific antibodies were removed with this strategy, the depletions of gH/gL- and PC-specific antibodies were not as efficient as the gB-depletion with 67% and 79%. The IgG-depletion was determined by an ELISA. However, the gB-depletion (red) resulted in no remarkable decrease of “inhibition of infection (%)” (= identical to neutralization (%)) in following NT assay, using ARPE-19 or fibroblasts as target cells (Fig.60AB).

Interestingly, the same result was observed after gH/gL-depletion (green) in ARPE-19 cells. Only the PC-depletion (blue), involving a complete pentameric complex showed a strong reduction (85%) in inhibition of infection in ARPE-19 cells which underlines the connection between non-linear and neutralization-dependent epitopes once more. In addition, in HFF, a reduction of neutralization was observed using gH/gL subunit which is part of the trimer complex gH/gL/gO and responsible for fibroblast entry.

In summary, gB-specific antibodies revealed no or weak neutralizing potential which could be the reason for the failing of the vaccine candidate gB/MF59 (Pass et al., 2009), but it could be suggested that UL128-131 region are mainly important for neutralization in epithelial cells and a better candidate for vaccine development. The second study of Loughney et al., showed similar results to Fouts for the HIG Cytogam® and used a constructed soluble PC and gH/gL dimers which were produced in CHO (Chinese Hamster Ovary) cells after transfection with two vectors (pGS-gH-gL<sub>trn</sub> and pGSUL128-UL-130-131), presenting native epitopes on the base of the Merlin strain. The viral proteins were purified via Reversed Phase (RP)-HPLC and their conformations were analyzed using in-gel digestion, followed by Nano LC-MS/MS. Afterwards, 96-well microtiter plates were coated with soluble purified pentameric complex and gH/gL dimers for protein-specific IgG depletion of Cytogam®.

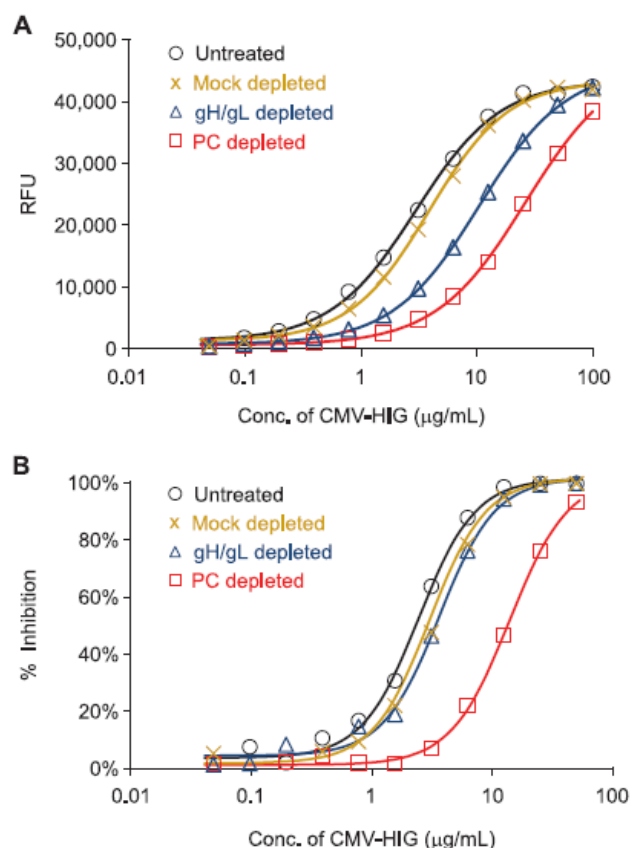


**Figure 61: (A) Reduction of binding activity after Mock, gH/gL and PC depletion of Cytogam®, measured in RFU (Relative Fluorescence Units) (B) Corresponding inhibition of infection in ARPE-19 cells (Loughney et al., 2015)**



The antibody depletion via gH/gL-fragment (blue triangles) induced a reduction in binding activity (Fig.61A), but hardly any reduction of neutralization activity (= inhibition (%)) in contrast to PC antibody depletion (red squares) (Fig.61B). The maximal noticeable NT reduction was 76% after PC depletion in Cytogam®.

The results in this thesis confirm the data of both described studies of Fouts and Loughney. The depletion via a recombinant PC resulted in higher reduction effects of NT capacity than single UL130 peptides. However, the depletion effects, expressed in percentage were lower than in both publications.

The reason might be the different strategies, used to deplete HCMV-related IgG antibodies from different HIGs of both publications and this thesis which may have different efficacies to remove these antibodies.

In addition, both publications investigated Cytogam®, while the results in this thesis are gained with Cytotect®. It may contain higher numbers of PC-specific antibodies than Cytogam®. The next point which must be considered critically, is the test resolution of the established PRA protocol which is reflected in the number of sample dilutions (here n= 6) of the investigated IgG preparation. The test resolution is limited to the number of wells in a microtiter plate (n= 96), as well as to the number of examined replica, dilutions steps and respective controls. An increased number of sample dilutions or a variation of dilution series may detect the highest peak of NT depletion effect for each analyzed IgG product.

Furthermore, both publications of Fouts and Loughney established own expression systems to generate a membrane bound or a soluble pentameric complex on the base of the Merlin strain, while the experiments in this thesis were performed with the first commercially available PC. It is a recombinant product of the VR1814 strain and generated in human cells (HEK293) by The Native Antigen Company, Oxfordshire UK. The different production methods may lead to different expressed PCs which may affect their natural conformation and therefore their potential to bind and deplete PC-specific neutralizing antibodies from polyclonal sera.

However, a commercially available pentameric complex has the potential to generate a standard for further investigations.

Considering monoclonal antibodies (mAbs) against HCMV-PC, a recent paper identified 4 immunogenic regions (IR1 to IR4) (Fig.62A). In a further analysis, generation of PC-specific mAbs were tested against 2 laboratory strains (VR1814, TB40/E) and 11 clinical isolates in comparison to HCMV-HIG on ARPE-19 cells (Fig.62B) (Ha et al., 2017).

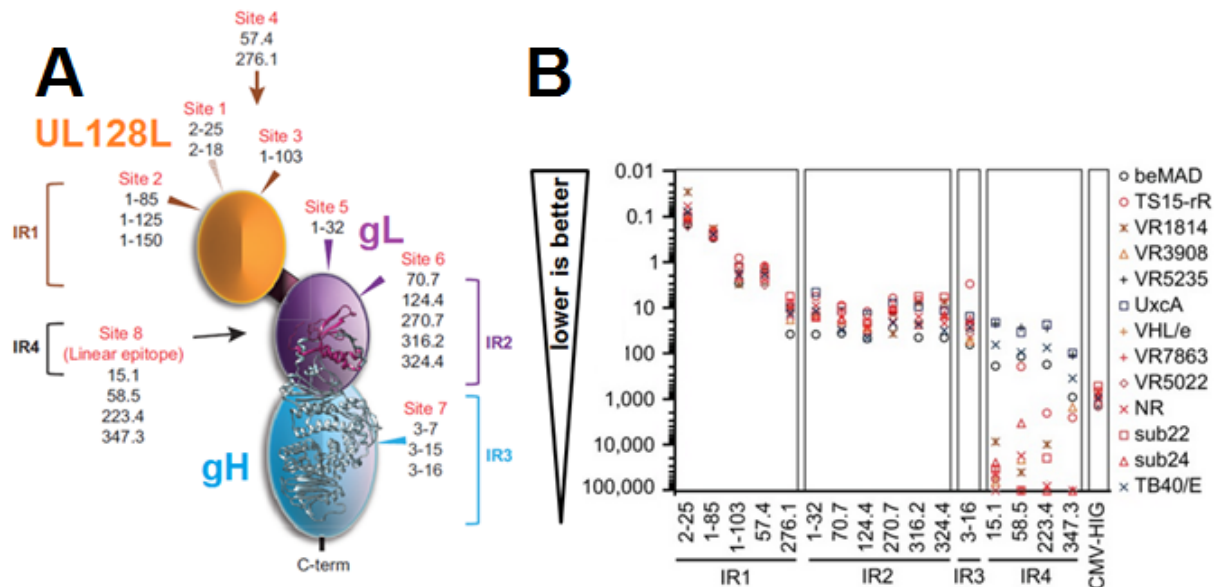


**Figure 62: (A) Visualized binding sites of PC-specific monoclonal antibodies, separated in 4 immunogenic regions (IRs) using an EM 3D reconstruction of pentameric complex; (B) IC<sub>50</sub> concentrations of generated monoclonal antibodies against the pentameric complex against 2 laboratory strains (VR1814, TB40/E) and 11 clinical isolates in comparison to HCMV-HIG on ARPE-19 (modified after Ha et al., 2017)**

The results revealed the neutralizing antibodies against the immunogenic regions 1 to 3 were highly potent against all HCMV strains which indicates that these immunogenic regions are highly conserved over all investigated strains. This observation confirmed data of this thesis which showed consistently, that HIG is effective against HCMV strains, possessing various genotypes. The most effective PC-mAbs emerged against IR1 which reflects the UL128-131 region. Impressively, PC-mAbs which are directed against IR1 to IR3 showed up to 25,000-fold higher IC<sub>50</sub> values than an HCMV-HIG. However, the HIG preparation which was used as reference during the NT experiments was not mentioned (Ha et al., 2017). Therefore, monoclonal antibodies showed remarkable advances in prevention of viral *in vitro* infection and could be a promising alternative treatment option to HCMV-HIG in the future.

The focus was placed on PC-specific antibodies, because of their potential ability to prevent viral transmission during pregnancy after HCMV-primary infection in contrast to gB-induced antibodies which are mostly non-neutralizing (Kabanova et al., 2014). In a former study, the antibody titers against gB and PC were compared between two groups of either maternofetal HCMV-Non-transmitters or HCMV-transmitters.

It suggested a correlation between a delay of PC-specific antibodies and an increased fetal HCMV-transmission during primary infection (Lilleri et al., 2013). The results indicated, that antibody titers against PC and dimers of gH/gL were significantly higher in HCMV-non-transmitters than in HCMV-transmitters after the first 30 dpi (days post infection).

However, in contrast to these findings, another publication characterized a monoclonal antibody against gB which prevented the infection of placenta-related trophoblast progenitor cells (TBPCs), but two monoclonal antibodies against the PC failed (Zydek et al., 2014).

In conclusion, the maternal HCMV primary infection during pregnancy, followed by a possible maternofetal transmission of HCMV through the placenta depends on known and still unknown factors which include manifold interactions of different cell types, as well as the maturity of immune system. It might be suggested that the divergent findings of the discussed publications are part of the multistep maternofetal transmission process (Schampera et al., 2018).

Additionally, latest findings showed that essential HCMV genes were reported to influence the formation of the trimer and pentameric complex. For post-entry tropism, the HCMV genes UL135 and UL136 were considered to be essential for HCMV replication in endothelial cells (Buglio et al., 2015). Modulating specific cell type tropism, the UL148 gene is suggested to manage the assembly of the trimer and pentameric complex into the virions through an encoding glycoprotein, localized in the cellular endoplasmic reticulum (Li et al., 2015).

Furthermore, an alternative variant of gH/gL was recently described, the gH/gC subunit which is encoded by UL116. Its function remains unclear and its role in context of cell tropism has to be further evaluated (Caló et al., 2016). The dysfunction of the US16 gene might be associated with a reduced ratio of expressed PCs on the viral surfaces, inhibiting HCMV infection of endothelial and epithelial cells (Luganini et al., 2017).

#### **4.5 Depletion of HCMV hyperimmunoglobulin IgG subclass 3 from Cytotect® and analysis of its functional activity**

Further antibody depletion experiments of this work analyzed the influence of IgG subclass 3 antibodies in HIGs and IVIGs (Schampera et al., 2018). In this context, Planitzer et al., 2011 postulated earlier the importance of IgG antibody subclass 3 to be mainly involved in viral neutralization of HCMV which based on former data of Gupta et al., 1996.

Furthermore, Planitzer used the increased concentration of IgG 3 antibodies in Kiovig® (Fig.63A) as argumentation to claim, that Kiovig® showed higher HCMV-specific NT-capacity (NT<sub>50</sub> values) than Cytotect® (Fig.63C). Although, the authors clearly demonstrated, that the HIG Cytotect® possesses more HCMV-specific IgG than Kiovig, measured in an ELISA HCMV system (Fig.63B) which was never properly considered in this publication.

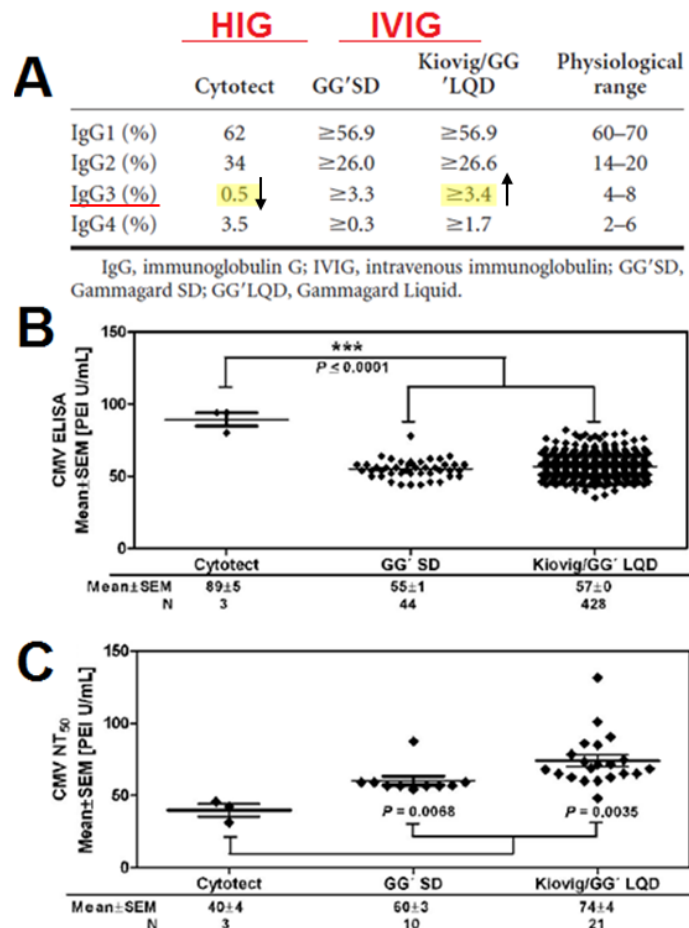


Figure 63: (A) IgG subclass distribution in HIG and IVIGs, (B) Corresponding HCMV-specific IgG and (C) HCMV NT<sub>50</sub> values, according to Planitzer et al., 2011

While, comparable results for IgG subclass 3 and HCMV-specific IgG concentrations for Cytotect® and Kiovig® were found during the investigations of Schampera et al, 2017, the publication of Miescher et al., determined the highest concentration of IgG 3 in Cytogam®. In contrast, higher IgG 3 concentrations were found in Cytogam® than in Cytotect®, but Cytogam® contained lower IgG 3 levels than Kiovig® (Schampera et al., 2017). At this point, the results of Schampera and Miescher are contradictory. As reminder, Miescher et al. showed in their results, that the IgG product Cytogam® had the highest concentration of IgG subclass 3 antibodies. HIGs and IVIGs are serum products, continuously made from hundreds to thousands of various human donors which indicates that there might be charge-dependent biological variations in composition of IgG sub classes.

Several time-differing charges of each product could be analyzed to clarify these different observations in context of IgG 3 antibodies. However, Schampera et al., 2017 showed that IVIGs contain the double amount of total IgG, compared to HIGs which should also have a beneficial impact on IgG3 for IVIGs, but not necessarily for HCMV-specific IgG binding and neutralization, as mentioned previously.

For NT-testing, the results in this PhD thesis strongly contrast to the findings of Planitzer et al., 2011. But not only in terms of functional NT-capacities of HIGs versus IVIGs, even the depletion of IgG subclass 3 antibodies showed any significantly difference in NT<sub>50</sub> values in both HFF and ARPE-19 cells for the investigated IgG preparations (Fig.47). The rebuttal was published in Schampera et al., 2018.

Furthermore, two important points have to be considered. Firstly, if the IgG class distribution is analyzed in detail, the concentrations of IgG subclass 3 antibodies are remarkably low (<2%), while the IgG subclass 1 is predominantly present with about 50–70% of all IgG subclasses (Schampera et al., 2017). This observation could influence the impact on NT-capacity between IgG subclass 1 to 4. As a following validation experiment, a depletion of IgG subclass 1, 2, 4 or combinations could be performed to deliver evidence for their neutralizing potentials.

On the other hand, it has to be exclusively highlighted, that the measured IgG subclass concentrations refer to the total IgG amounts of each IgG product and not inevitably to the particular concentrations of HCMV-specific IgG. It is not known, how the IgG subclasses are distributed for HCMV-specific IgG in particularly which has to be evaluated, if such tests are available in the future.

#### 4.6 T cell modulation via HIG administration after HCMV primary infection of pregnant women

In the attempt to prevent maternofetal HCMV transmission, high virus-specific antibody titers and strong neutralizing activity seemed to be the only relevant benchmarks which were considered to be predictable parameters for immune protection. But it was shown that HCMV-IgG concentrations and resulting neutralization did not necessarily correlate (Corrales-Aguilar et al., 2016). While highly-neutralizing antibodies play an important role to bind and effectively inactivate infectious HCMV virions as part of the humoral immune response, further immunological functions are induced by antibodies. The antibody-dependent natural killer (NK) cell activation (Chung et al., 2014), as well as the antibody-dependent complement deposition (ADCD) (Chung et al., 2015) are defense mechanisms which are also important to prevent viral infection. NK cells, especially the memory-like CD57<sup>+</sup>NKG2C natural killer cell subset are known to be the first line defense against HCMV as part of the innate immune system and were observed to expand during HCMV primary infection in adults, as well as in congenitally HCMV-infected infants (Costa-Garcia et al., 2015; Lopez-Vergès et al., 2011 and Noyola et al., 2012). Furthermore, the antibody-dependent cellular cytotoxicity (ADCC) plays an essential role in binding and lysis of HCMV-infected cells via effector cells of the innate immune system (Ackerman et al., 2011). The subsequent activation of Fc-γ receptors allows these receptors to act as linkers and modulators between the innate and adaptive immune response to provide various inflammatory and anti-inflammatory tasks (Fig.64) (Corrales-Aguilar et al., 2011; Schwab et al., 2013).

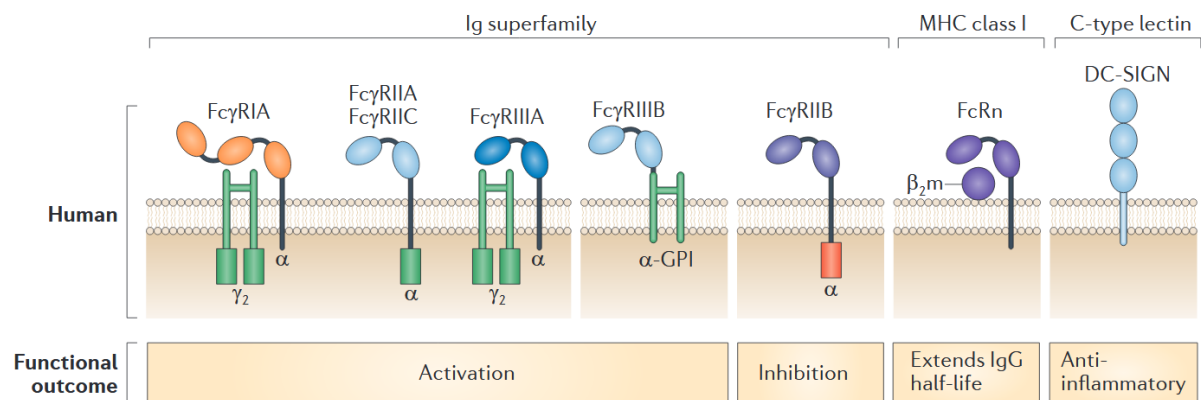


**Figure 64: Overview of the functional outcome of Fc-γ receptors: From activation over inhibition to anti-inflammatory activities (modified after Schwab et al., 2013).**

Further immunological investigations were performed in this PhD thesis to analyze, whether the HIG administration could beneficially modulate cellular immunomodulatory effects in pregnant women with a proven HCMV-primary infection.

This hypothesis based on an open question in development of an effective HCMV vaccine which describes the uncertainty about the establishment of a protective immunity that prevents virus transmission to the fetus through the placenta. Both the humoral, as well as the cellular immune system are necessary to protect from viral infection, but the influence of these two pathways in prevention of maternofetal transmission are still unknown (Schleiss et al., 2013). Therefore, the possible impact of HIG administrations on the cellular immunity in pregnant women was investigated, using indirect IFN- $\gamma$  secretions assays. IFN- $\gamma$  is generated during the adaptive immune response of CD4<sup>+</sup> and CD8<sup>+</sup> T-cells, as well as during the innate immune response of NK cells and NK-T cells (Lilleri et al., 2008; Jackson et al., 2014).

The IFN- $\gamma$  production was checked by stimulation of PBMCs with HCMV-specific peptides, following analysis via ELISA system QuantiFERON CMV® from Qiagen and EliSPOT HCMV® from Lophius. The *ex vivo* blood samples were derived from women of the Tuebingen HIG study (Kagan et al., 2018). Both different assays were used to clarify, whether IFN- $\gamma$  could be used as a predictable parameter for stimulated PBMCs and therefore might have a protective cell-mediated immunity (CMI) against HCMV in the HIG-treated mothers. While the HCMV-specific CMI protected from uncontrolled viral replication in healthy humans, the CMI is impaired in immune-suppressed patients after an organ transplantation. The IFN- $\gamma$  secretions assays are usually used for the monitoring of adaptive T-cell transfer immunotherapy in immunocompromised patients (Feucht et al., 2015 and Günther et al., 2015).

However, a recent report postulated the related appearance of functional impairment of CMI in pregnant women compared to non-pregnant women after HCMV infection (Reuschel et al., 2017). In this context, the administration of HIG, containing highly-neutralizing antibodies against HCMV might counteract the impairment of CMI by an improved opsonization through effective viral binding, neutralizing and Fc $\gamma$ -receptor activation.

The administration of HIG during this study seems to boost the secretion of IFN- $\gamma$  which is an indicator for an active cellular immune response in the treated women with a HCMV-primary infection. This suggestion is supported by the given results in the present work (Fig.53). All HIG-treated mothers, who were HCMV Non-transmitters showed rising levels of IFN- $\gamma$  concentrations and IFN- $\gamma$  reactive PBMCs within 7 days after the first HIG application, followed by longer-lasting increases after repeated HIG doses. Interestingly, it seems, that multiple applications of HIG are necessary to maintain the possible T-cell stimulus after the first intravenous HIG administrations in the pregnant mothers.

While the induced peak levels of IFN- $\gamma$  production and corresponding numbers of IFN- $\gamma$  reactive PBMCs strongly differed in each woman, the kinetics of IFN- $\gamma$  production were longitudinally comparable among these pregnant women. This observation matched with previous described data of Jackson et al., 2014, that the T-cell response can differ between individuals.

These observations were confirmed by *in vitro* data which were recently provided by PD Dr. Ludwig Deml, Chief Scientific Officer (CSO) at Lophius. The results were already represented at the ESOT2017 Barcelona Congress. After a formal permission of Lophius (Dr. Katharina Eder -Key-Account Manager Lophius), their officially presented *in vitro* data are available to discuss in this PhD thesis (Fig.65).

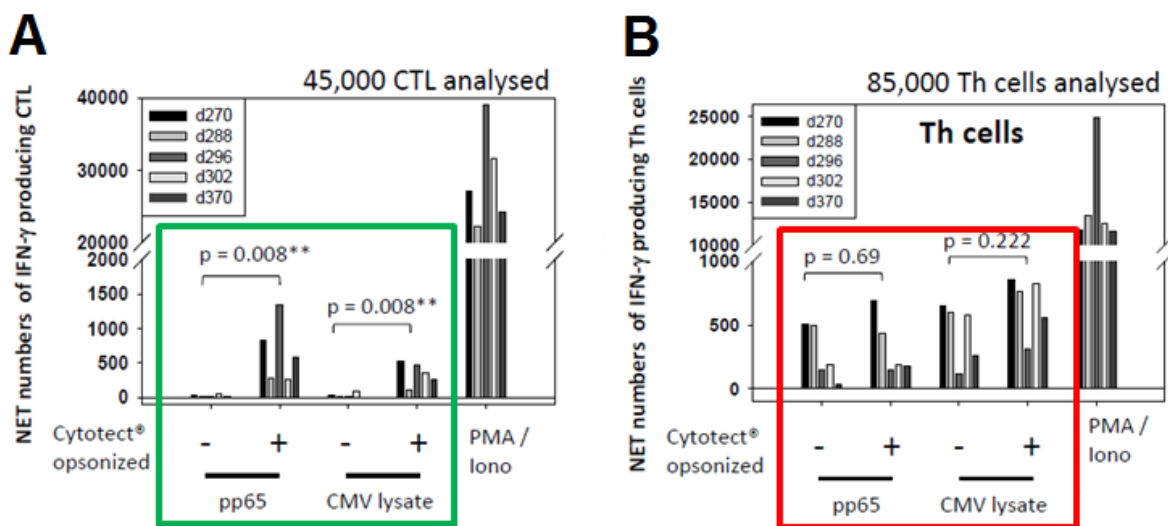


**Figure 65:** *In vitro* stimulation of PBMCs with viral antigens in the presence of HIG Cytotect® (A) CB8+ Cytotoxic T-cells (B) CD4+ T-helper (modified after Deml et al., 2017; ESOT2017 Barcelona Congress, Lophius)

Deml et al., stimulated CD8<sup>+</sup> T-cells and CD4<sup>+</sup> T-cells with and without an HCMV pp65 peptide mixture or HCMV lysate in the presence of HIG Cytotect® for 6h. After incubation the number of corresponding IFN- $\gamma$  reactive T-cells were determined with EliSPOT HCMV®.



On the one hand, the induced numbers of CD8<sup>+</sup> T-cells (green square) which produced IFN- $\gamma$  was significantly higher than the number of CD4<sup>+</sup> T-cells (red square) which identified cytotoxic T-cells, mainly involved in CMI and not T-helper cells, according to IFN- $\gamma$  secretion. This confirmed the *in vivo* boosting effect of the cellular immune system via HIG which was observed in the HIG-treated pregnant mothers. On the other hand, the given results also revealed that the presence of viral antigens is necessary for immunogenic processing which resulted in IFN- $\gamma$  production. HIG Cytotect® alone was not able to trigger the cellular immune response vice versa.

Finally, the results showed various numbers of IFN- $\gamma$  producing PBMCs between different patients (d270, d288, d296, d302 and d370) which matched with the different IFN- $\gamma$  responses in the investigated HCMV-primary infected pregnant women, who achieved HIG administrations during the Tuebingen HIG study (Kagan et al., 2018) (Fig.53).

An important point that has to be critically considered during the study of induced IFN- $\gamma$  production in HCMV-primary infected pregnant women is the absence of control cohorts. It was not possible to compare the data of the HIG-treated women with a group of HCMV-primary infected women, who achieved no HIG or placebo. These negative controls were not enrolled in the Tuebingen HIG study (Kagan et al., 2018), since the study was not placebo controlled for ethical reasons.

However, in the absence of a placebo control group, data of van de Berg are available for the correlation of viral load to IFN- $\gamma$  production (Fig.66).

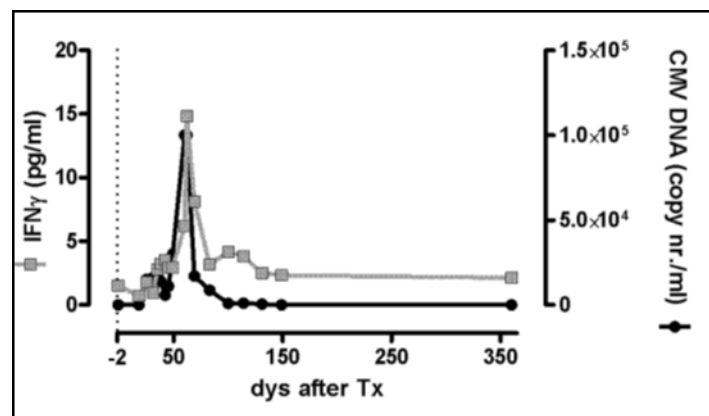


**Figure 66: Unstimulated course of IFN- $\gamma$  after HCMV primary infection compared with HCMV DNA viral load in blood of an immunocompetent patient (van de Berg et al., 2010)**

Van de Berg demonstrated, that an HCMV primary infection of an immune competent patient induced a clear proinflammatory response during a natural infection which was maintained during latency. This response was characterized by increased levels of IFN- $\gamma$  levels and other cytokines.

Figure 66 shows the kinetic of IFN- $\gamma$  levels during a natural infection of HCMV in relation to the viral load in blood. The authors found only one major increase of IFN- $\gamma$  between day 50 and 70 which was downregulated afterwards through T-cell suppression of the immune system. These findings correspond with the observations of IFN- $\gamma$  concentrations after the second HIG application, expect for the IFN- $\gamma$  boosting after the first HIG administration.

Additionally, the administration of HIG might improve the HCMV antigen recognition and thus it could support the cellular immune response. However, the detection of viral load was not observed in each individual woman of the HIG cohort during the Tuebingen HIG study. Only in a minority of women (6/40), low viral loads were found at the initial detection of HCMV primary infection in pregnancy (Kagan et al., 2018). The viral exposition to the cellular immune system might be detectable only in placental cytotrophoblasts and syncytiotrophoblasts (Palmeira et al., 2012).

The increased number of Fc-fragments in blood of the women could also trigger the cellular immune system by Fc $\gamma$ -receptor binding and could promote the IFN- $\gamma$  production through IL-2 secretion (Klenerman et al., 2016). Further HIG administrations had no longer stimulating effect on the IFN- $\gamma$  secretion (Fig.53). This can be explained by the intrinsic cellular and humoral immune response which suppressed usually the T-cell reaction during the progress of a HCMV primary infection or reactivation (van de Berg et al., 2010).

One pregnant woman of the HIG cohort (1/40) was an HCMV-transmitter in the Kagan study and was investigated in this PhD thesis. She showed a different kinetic pattern of IFN- $\gamma$  parameters than all other maternal HCMV non-transmitters. Interestingly, the HCMV-transmitting mother showed an already strong IFN- $\gamma$  reactivity at the beginning of the HIG treatment in both assays (Fig.52). The IFN- $\gamma$  activity weakly increased during the first two HIG applications and constantly decreased afterwards. It seems that the IFN- $\gamma$  secretion was already reactive on a high level and was not further simulated by further HIG administration, while the serological parameter clearly indicated an early HCMV-primary infection with low concentration of HCMV-specific IgG and low IgG avidity, paired with high HCMV-specific IgM index.

This interesting case contributes to a currently published paper of Saldan et al., 2015 which described this specific constellation of immunological parameters in HCMV-primary infected pregnant women. The Saldan study enrolled 80 pregnant women, including 57 HCMV-primary and 23 non-primary infected mothers. The median age of pregnant women was 31 years with a range of 17-42 years which correlates with the median age in the present study. The maternal HCMV IgM and IgG were determined via Immulite® Siemens, Germany and the HCMV IgG avidity was measured, using a TGS TA ELISA assay from Technogenetics KHB group, Italy.

The number of IFN- $\gamma$  reactive PBMCs was analyzed with an EliSPOT from Autimmun Diagnostika, Germany (Fig.67).

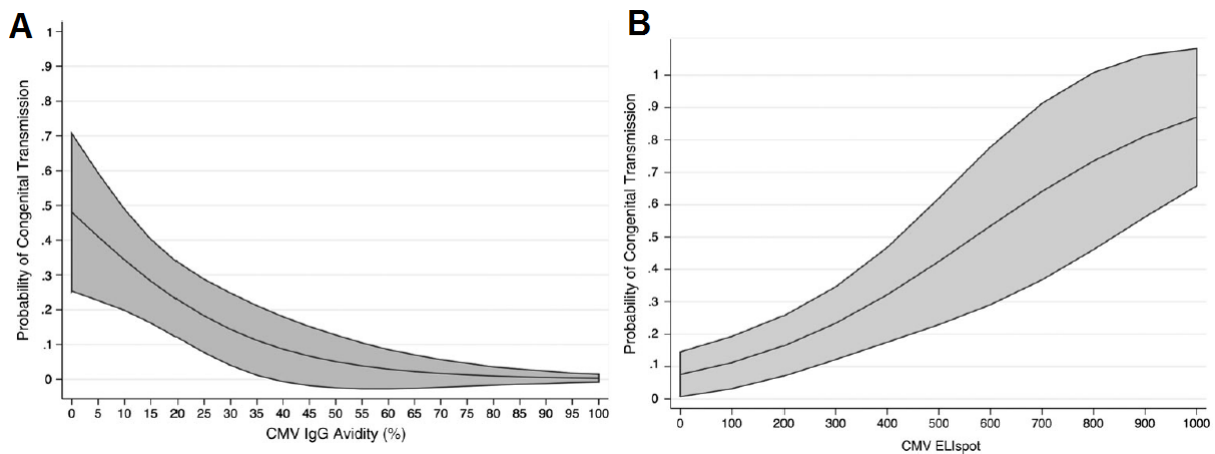


**Figure 67: (A) Correlation between HCMV low IgG avidity and high congenital transmission rate; (B) Correlation between high number of IFN $\gamma$ -reactive PBMCs and and high congenital transmission rate (Saldan et al., 2015)**

The HCMV-primary infections occurred during the first and second trimester of pregnancy (median GA= 6 weeks; Range: 0-20 weeks). The given results of Saldan showed an increased risk for a congenital transmission at lower IgG avidity and higher numbers of IFN- $\gamma$  reactive PBMCs at the same time. The authors further suggested that a combination of HCMV EliSPOT and low HCMV IgG avidity could reach a higher diagnostic validity to estimate the risk of maternofetal transmission after HCMV-primary infection of the mothers than either method alone. However, the reasons for the association between high IFN- $\gamma$  PBMC numbers and increased risk of HCMV congenital transmission is unknown.

But two hypotheses were addressed to this issue until now. First, during HCMV-primary infection, the duration and degree of the maternal viremia, corresponding to higher viral loads transient in blood and urine may induce a faster and stronger CMI response (Lazzarotto et al., 2000) which was detected in the IFN- $\gamma$  secretion assay (Saldan et al., 2015). However, a stronger maternal viremia in combination with an increased risk of HCMV-transmission was not reported during the Tuebingen HIG study (Kagan et al., 2018), since the presence of viral DNA in blood has been reported to be not associated with a greater risk of maternofetal transmission (Lazzarott et al., 2011)

The second hypothesis described an indirect caused damage by the CMI which promotes a local proinflammatory process in the placenta and leads to unintendedly supported viral transmission to the fetus (Fischer et al., 2000; Tabata et al., 2008). However, these hypotheses have to be proven in controlled studies.

In this context, the impact of early inflammatory events in the placenta on the risk of HCMV transmission should be further investigated which could be the initial trigger and door opener for viral transmission to the fetus. Therefore, more inflammatory factors should be identified which especially reflect the status of the placenta. This could enhance the significance of HCMV diagnostics and evaluate the efficacy of HIG treatment during pregnancy.

The results in the presented work correlate with the observation in the paper of Saldan et al., 2015. However, it has to be critically considered, that only one woman was monitored with a HCMV-maternofetal transmission in the present study, although it was a simultaneous success for the HIG treatment of HCMV-primary infected women.

Longitudinal samples have to be analyzed via IFN- $\gamma$  production, using T-Track EliSPOT CMV® and/or QuantiFERON CMV® assay when more data on maternal transmitters are available, who underwent HIG treatment. Further studies have also to improve the understanding of the HCMV-specific cell-mediated immunity in context of HCMV-primary infections.

In a conclusive comparison, both IFN- $\gamma$  secretion assays revealed comparable results for the statistical median and mean in the HIG-treated women. However, there were test-dependent variations noticeable for single points of measurement between both assays. In detail, the QuantiFERON CMV® showed more single outliers than the EliSPOT HCMV® (Fig.53A versus Fig.53B). Saldan et al., 2016, confirmed in another paper the correlation between both test systems (Fig. 68).

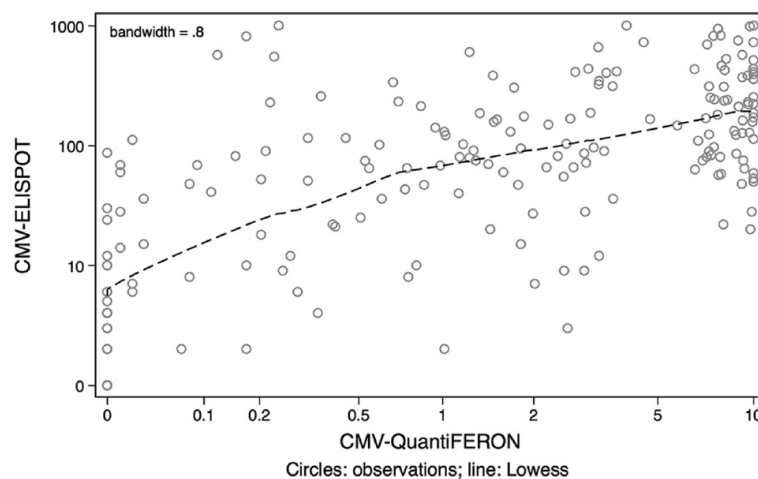


**Figure 68: Comparison between QuantiFERON CMV® and HCMV EliSPOT collected data of pregnant women with and without HCMV primary infection. Bandwidth was 0.8 (modified after Saldan et al., 2016).**

The data were collected from 195 Caucasian women, who included 57 HCMV-primary and 23 HCMV-nonprimary infected pregnant mothers, as well as 7 HCMV-seropositive and 4 HCMV-seronegative nonpregnant women. The correlation between both assays was determined with a bandwidth of 0.8, using a “local regression-smoothing model”.

Interestingly, Saldan et al., 2016 reported, that the QuantiFERON CMV® seemed to fail to detect the difference between HCMV-primary and non-primary infected mothers in contrast to a used EliSPOT assay (AID Autimmun Diagnostika, Germany), while the detection of HCMV-seronegative pregnant women was concordantly accurate in both assays.

Furthermore, the results of Saldan showed less outliers in the EliSPOT assay than QuantiFERON HCMV® which matched with the given results in this PhD thesis. Concerning the collected data of EliSPOT HCMV® and QuantiFERON HCMV®, the different read out systems have always to be considered in the background of repeated HIG administrations. While the results of EliSPOT HCMV® based on the given number of PBMCs which were purified from 15 ml LiHep-blood samples via density gradient, the QuantiFERON CMV® detects the produced amount of IFN- $\gamma$  concentration of 1ml whole blood. The stimulation of IFN-secretion also differs in both test assays.

Recently, Bialas et al., 2015 underline the importance of an active CMI in a relevant primate model. Using pregnant rhesus macaques, Bialas depleted CD4<sup>+</sup> T-cells these animals via specific anti-CD4<sup>+</sup> T-cell antibodies. The CD4<sup>+</sup> T-cell depletion resulted in an increased number of placental infections and fetal transmission which led to fetal death, myocarditis and hepatic calcination in a combination with viral load in maternal plasma and amniotic fluid. Furthermore, it was demonstrated, that an impaired CD8<sup>+</sup> T-cell response was caused by the induced lack of CD4<sup>+</sup> T-cells which was also the reason for a delayed maturation and production of HCMV-neutralizing antibodies via B-cells.

Another work group also worked with CD4<sup>+</sup> T cell-depleted, rhesus macaques which achieved either rhIVIG or rhHIG (Nelson et al., 2017) after primary infection during early pregnancy. Both IgG preparations were made from rhCMV-seropositive monkeys. The dose-optimized rhHIG administration completely prevented the placental rhCMV transmission after infection of pregnant macaques. At this point, the calculated rhHIG half-life time ( $t_{1/2}$ ) of about 7 days supports initial observations by Hamprecht et al., 2014 and Kagan et al., 2018. However, the pregnant rhesus macaques achieved rhHIG one hour after the rhCMV infection which is a point of criticism of the study and cannot be transferred to clinical routine practice in the detection of HCMV-primary infected pregnant women, with an HCMV exposition at least 6 to 8 weeks prior to start of HIG treatment.

In summary, the exact mode of action of HCMV-specific immunoglobulin preparations is not known in detail. The interaction of both, the innate and the adaptive immune response, directed against HCMV in pregnancy is not completely understood. Therefore, the possible beneficial effects of HIG on both pathways of the CMI were addressed in this work.

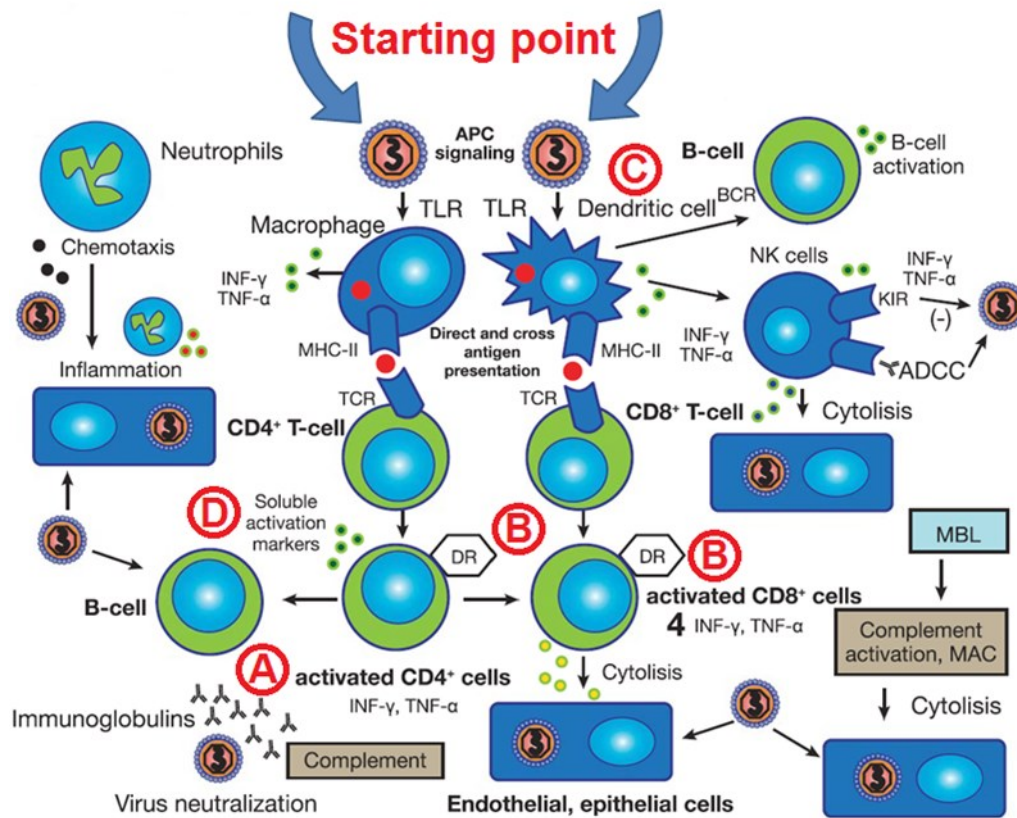


**Figure 69: Summarized response of the immune system to HCMV and potential HIG modes of action: (A) responsible for viral neutralization; (B) potential effect on T-cell stimulation; (C) possible modulation of DC maturation; (D) Suggested impact on cytokine secretion (modified after Carbone et al., 2016)**

In a summarized overview, the response of the immune system to HCMV and possible interactions between HIG and the cellular immune response are shown in (Fig.69). At the starting point, HCMV is initially detected by pathogen recognition receptors. In this context, Toll-like receptors (TLR) were reported to recognize the HCMV glycoprotein B which results in proinflammatory IFN type I and further cytokines (Boehme et al., 2006). The viral antigens are presented on antigen-presenting cells (APCs), including dendritic cells (DC) and macrophages, while TLR-4/5 stimulate the production of IL-6 and IL-8, as well as TNF- $\alpha$ . Further, CD4<sup>+</sup> and CD8<sup>+</sup> T-cells activation is performed by the antigen presentation via MHC-II binding which is followed by cell signaling via IFN- $\gamma$  and TNF- $\gamma$  (Smith et al., 2014). This cascade ends in the cytolysis of infected cells and initiates HCMV-specific antibody production of B-cells and IgG maturation. In addition, there is an interaction of dendritic cells with NK cells, including IFN- $\gamma$  production and ADCC, as well as a reported activation of B-cells through DCs.

Independently, HCMV antigens are detected by NK cells which induce the secretion of IFN- $\gamma$ . Especially, the already mentioned CD57<sup>+</sup>NKG2C natural killer cells play an important role during the first two weeks after onset of infection, following viremia (Stern et al., 2008; Lopez-Vergès et al., 2011).

Interestingly, in murine HCMV, neutrophils were identified to act as potent antiviral effector cells which limited viral replication and viral associated symptoms by an induced inflammation (Stacey et al., 2014). While the impact of complement on the regulation of HCMV infections is poorly characterized, an enhancing neutralizing effect of added complement on serum was demonstrated in the presence of HCMV particles (Spiller et al., 1997).

HIG has several potential interaction points with the innate and adaptive immune system. Administrated HCMV-specific antibodies effectively bind and neutralize free-circulating virions, as well as intracellular localized virions with reduced efficacy (Fig.69A). The binding of viral antigens may improve their opsonization to the innate immune systems (Fig.69B). A faster recognition of the virus after an HCMV-primary infection may boost the innate NK cells as well as adaptive CD4<sup>+</sup> and CD8<sup>+</sup> T-cell response in terms of reaction time and strength through specific IFN- $\gamma$  receptor activation (Fig.69C). In the presented work, an indirectly-detected modulation of T-cell activity was demonstrated by IFN- $\gamma$  secretion, as well as IFN- $\gamma$  reactive PBMCs (Fig.53).

Importantly, divergent results were also published in context of HIG administrations and their impact on T-cell and B-cell regulation in SOT patients. According to these publications, HIG was suggested to inhibit cytokine expression and suppress T-cell proliferation which could be associated with lower rates of allograft rejection. The increase of naïve B-cells levels may be also induced by HIG administration (Fig.69D) (Hoetzenecker et al., 2007; van Gent et al., 2014). However, another group did not observe such inhibitory effects after solid organ transplantations (Bonaros et al., 2008).

In conclusion, in the absence of an effective vaccination against HCMV, the focus should be set on the early identification of HCMV-primary infections in pregnant women, as well as on the determination of risk factors for maternofetal transmission. The results in this PhD thesis suggested, that the determination of IFN- $\gamma$  secretion could be useful to estimate the risk of maternofetal HCMV transmission after maternal primary infection. Furthermore, the PC depletion experiments in this presented work encourage the vaccine development on the base of the viral pentameric complex which might lead to a potent vaccine in the future.

## 5 Zusammenfassung

Die maternale Primärinfektion mit dem Humanen Cytomegalievirus ist die häufigste intrauterine Infektion weltweit. Der Krankheitsverlauf ist bei werdenden Müttern meist asymptomatisch und ist in seltenen Fällen von unspezifischen grippe-ähnlichen Symptomen begleitet. Jedoch kann das erhöhte Risiko einer diaplazentären Übertragung auf den Fetus zu schwerwiegenden Entwicklungsstörungen des Zentralen Nervensystems führen, sowie im Verlauf der ersten Lebensjahre Hörschädigungen verursachen (Picone et al., 2013).

In der Abwesenheit eines effektiven Impfstoffes gegen das Virus, haben mehrere Studien verschiedene Präventionsmaßnahmen untersucht um das Risiko einer HCMV-Transmission auf den Feten zu reduzieren. Die Hygieneberatung von seronegativen Frauen hat sich als sehr effektive Methode erwiesen, dieses Risiko um bis zu 50% zu senken. Die Untersuchung der Serostatuses der Schwangeren ist Grundvoraussetzung, um die werdende Mutter entsprechend medizinisch aufzuklären. Dabei ist der bewusste Umgang mit Kleinkindern im Umfeld der Frau von besonderer Bedeutung. So sollte beispielhaft der körperliche Kontakt vermieden und gemeinsam benutzte Gegenstände und Oberflächen entsprechend gereinigt werden. Das routinemäßige Händewaschen hat sich dabei als erfolgreiches Werkzeug erwiesen (Revello et al., 2015).

Des Weiteren konnte eine Therapie mit HCMV-spezifischen Hyperimmunoglobulinen nach einer bestätigten Primärinfektion der Mutter, die Übertragungsrate nachweislich reduzieren (Nigro et al., 2005; Visentin et al., 2012). Hyperimmunoglobuline sind gepoolte Seren von gesunden Spendern, die einen erhöhten HCMV-spezifischen Titer aufweisen. Jedoch sind die Ergebnisse verschiedener Studien, hinsichtlich der Effektivität der HIG Behandlung widersprüchlich. In diesem Zusammenhang konnte die einzige randomisierte kontrollierte Studie keinen signifikanten Unterschied zwischen der Präventions- und Placebogruppe feststellen (Revello et al., 2014). Jedoch konnte eine Meta-Analyse der Nigro- und Revello-Studie einen signifikanten Trend, im Bezug auf die Reduktion der maternofetalen Transmission feststellen (Rawlinson et al., 2016). Es gibt allerdings keine offizielle Empfehlung für die Behandlung von schwangeren Frauen mit Hyperimmunoglobulinen außerhalb von klinischen Studien (Rawlinson et al., 2017).

Die Untersuchungen dieser Dissertation wurden im Hintergrund einer in Tübingen durchgeführten HIG Studie zur Prävention von maternofetalen Transmissionen im ersten Trimenon der Schwangerschaft durchgeführt (Kagan et al., 2018). Parallel zu dieser Studie, war das Ziel, der vorliegenden Arbeit, die *in vitro* Evaluierung des verwendeten Hyperimmunoglobulin-Präparates Cytotect® (Biotest AG) durchzuführen.



In den ersten Experimenten konnte gezeigt werden, dass Cytotect® in der Lage ist, verschiedene HCMV Stämme effektiv in *in vitro* Untersuchungen zu neutralisieren. Dies könnte darauf zurückzuführen sein, dass essentielle Strukturen des Virus genetisch konserviert sind, die für eine erfolgreiche Infektion, Vermehrung und Verbreitung des Virus notwendig sind und sich dies durch Hyperimmunoglobuline verhindern lässt.

Im Folgenden wurden HCMV-spezifische Antikörper weiter untersucht, die in HIG vorhanden sind und sich gegen gezielte Strukturen des Virus richten – den Pentamerkomplex (gHgL-UL128-131). Dieser virale Komplex ermöglicht dem Virus den Eintritt in Epithel- und Endothelzellen und scheint auch bei Dendritischen Zellen und Monozyten von Bedeutung zu sein (Hahn et al., 2004; Gerna et al., 2005; Wang et al., 2005). Zwei UL130 Peptide und ein rekombinanter Pentamerkomplex wurden verwendet, um Epitop-spezifische Antikörper aus Cytotect® zu depletieren und deren Einfluss auf die *in vitro* Neutralisationskapazität in retinalen Pigment-Epithelzellen (ARPE-19) zu untersuchen. Während die Depletion mit UL130 Peptiden zu einer niedrigeren Reduktion der *in vitro* Neutralisationskapazität führte (maximale Differenz: 16%), konnte unter der Verwendung des rekombinanten Pentamerkomplex ein beachtlicher Anteil der *in vitro* Neutralisationskapazität (maximale Differenz: 42%) entfernt werden. Diese Ergebnisse bestätigen Studien von Fouts et al., 2012 und Loughney et al., 2015. Sie zeigen, zusammen mit den Ergebnissen in dieser Dissertation die mögliche, vielversprechende Anwendung des Pentamerkomplex als Zielstruktur für die Impfstoff-Entwicklung, da viele polyklonale HCMV-neutralisierende Antikörper in HIGs gegen den Pentamerkomplex gerichtet sind.

In weiteren *in vivo* Untersuchungen wurden longitudinale LiHep-Blutproben von 9 schwangeren Frauen untersucht, die Teil der Patientenkohorte der Tübinger HIG Studie waren. Die Proben wurden mit dem Ziel analysiert, die mögliche Stimulation von HIG Administrationen auf die zelluläre Immunantwort nach einer HCMV-Primärinfektion zu untersuchen. Für diesen Zweck, wurden zwei IFN- $\gamma$  Release Assays parallel durchgeführt, um die indirekte IFN- $\gamma$  Sekretion zu messen. Dabei erfasste der QuantiFERON CMV® (Qiagen) die IFN- $\gamma$  Konzentrationen und der T-Track EliSPOT CMV® (Lophius) bestimmte die Anzahl der IFN- $\gamma$  produzierenden mononukleären Zellen des peripheren Blutes. Die *in vivo* Untersuchungen in beiden Tests zeigten, dass mehrfache, zweiwöchentliche Applikationen von Cytotect® in wiederholten Stimuli der IFN- $\gamma$  Produktion bei 8 behandelten Schwangeren resultierten, die HCMV-Non-Transmitterinnen waren. Die erfassten IFN- $\gamma$  Messwerte schwankten stark zwischen den untersuchten Frauen und zeigten jeweils eine unterschiedliche Kinetik für IFN- $\gamma$ , beginnend bei variierenden IFN- $\gamma$  Ausgangsniveaus. Diese Beobachtung deckt sich mit Untersuchungen von Jackson et al., 2014, welche beschreiben, dass die individuelle zelluläre Immunantwort stark schwanken kann.

Im Allgemeinen kann die Verabreichung von HCMV-spezifischen hochaviden Antikörpern an mehreren Stellen in die zelluläre Immunantwort eingreifen und beispielhaft die Opsonierung verbessern durch effektives Binden und Neutralisieren des Virus, sowie Fc $\gamma$ -Rezeptor Aktivierung (Corrales-Aquilar et al., 2011; Schwab et al., 2013).

Eine HCMV-Transmitterin wurde während der Tübinger HIG Studie erfasst und in dieser Dissertation untersucht. Sie zeigte eine bereits erhöhte IFN- $\gamma$  Produktion mit einer zeitgleich frischen HCMV-Primärinfektion zu Beginn der HIG Therapie. Interessanterweise bringt eine Studie von Saldan et al., 2015 erhöhte IFN- $\gamma$  Messwerte und korrespondierende niedrige HCMV IgG Avidität in Zusammenhang mit einem erhöhten Risiko einer maternofetalen Transmission während der Schwangerschaft und bestätigt damit die Daten der analysierten HCMV-Transmitterin. Darüber hinaus waren die Ergebnisse aller untersuchten Schwangeren bei beiden IFN- $\gamma$  Tests im proportionalen Verhältnis gesehen miteinander vergleichbar, auch wenn sie unterschiedliche Ausleseparameter besitzen. Aus den gewonnenen Daten lässt sich ableiten, dass IFN- $\gamma$  möglicherweise als Surrogat-Marker in Kombination mit einer serologischen Auswertung dienen kann, um ein potenziell-erhöhtes Risiko für eine HCMV-Transmission zum Feten nach einer Primärinfektion der Mutter abzuschätzen. Jedoch müssen weitere Untersuchungen diese These bestätigen.

## Declaration on Oath

I assure that I have written this dissertation independently and have not used any other sources and aids than those indicated.

### Funding

Matthias Stefan Schampera received a Grant from Biotest AG, Preclinical Research (Dr. M Germer). Cytotect® was provided from Biotest AG.

---

Date

---

Signature

## 6 References

### 6.1 Literatures

**Abai AM, Larry R, Smith LR, Wloch MK.** Novel Microneutralization Assay for HCMV Using Automated Data Collection and Analysis J Immunol Methods. 2007 Apr 30;322(1-2):82-93.

**Ackerman ME, Moldt B, Wyatt RT, Dugast AS, McAndrew E, Tsoukas S, Jost S, Berger CT, Sciaranghella G, Liu Q, Irvine DJ, Burton DR, Alter G.** A robust, high-throughput assay to determine the phagocytic activity of clinical antibody samples. J Immunol Methods 2011; 366:8–19.

**Adland E, Klenerman P, Goulder P, Matthews PC.** Ongoing burden of disease and mortality from HIV/CMV coinfection in Africa in the antiretroviral therapy era. Front Microbiol. 2015 Sep 24; 6:1016.

**Adler B, Scrivano L, Ruzcics Z, Rupp B, Sinzger C, Koszinowski U.** Role of human cytomegalovirus UL131A in cell type-specific virus entry and release. J Gen Virol. 2006 Sep;87(Pt 9):2451-60.

**Adler SP.** Molecular epidemiology of cytomegalovirus: viral transmission among children attending a day care center, their parents, and caretakers. J Pediatr. 1988 Mar;112(3):366-72.

**Adler SP, Manganello AM, Lee R, McVoy MA, Nixon DE, Plotkin S, Mocarski E, Cox JH, Fast PE, Nesterenko PA, Murray SE, Hill AB, Kemble G.** A phase 1 study of 4 live, recombinant human cytomegalovirus Towne/Toledo chimera vaccines in cytomegalovirus-seronegative men. J Infect Dis. 2016 Nov 1; 214(9):1341-1348.

**Anderholm KM, Bierle CJ, Schleiss MR.** Cytomegalovirus Vaccines: Current Status and Future Prospects. Drugs. 2016 Nov;76(17):1625-1645.

**Banas B, Böger CA, Lückhoff G, Krüger B, Barabas S, Batzilla J, Schemmerer M, Köstler J, Bendfeldt H, Rascle A, Wagner R, Deml L, Leicht J, Krämer BK.** Validation of T-Track® HCMV to assess the functionality of cytomegalovirus-reactive cell-mediated immunity in hemodialysis patients. BMC Immunol. 2017 Mar 7;18(1):15.

**Barabas S, Spindler T, Kiener R, Tonar C, Lugner T, Batzilla J, Bendfeldt H, Rascle A, Asbach B, Wagner R, Deml L.** An optimized IFN- $\gamma$  ELISpot assay for the sensitive and standardized monitoring of HCMV protein-reactive effector cells of cell mediated Immunity. BMC Immunology. 2017; 18:14

**Benoist G, Leruez-Ville M, Magny JF, Jacquemard F.** Management of Pregnancies with Confirmed Cytomegalovirus Fetal Infection. Fetal Diagn. 2013; 33:203-214

**Benoist G, Salomon LJ, Jacquemard F, Daffos F, Ville Y.** The prognostic value of ultrasound abnormalities and biological parameters in a group of fetuses infected with cytomegalovirus. *BJOG*. 2008;114: 823-829

**Berencsi K, Gyulai Z, Gonczol E, Pincus S, Cox WI, Michelson S, Kari L, Meric C, Cadoz M, Zahradnik J, Starr S, Plotkin S.** A canarypox vector-expressing cytomegalovirus (HCMV) phosphoprotein 65 induces long-lasting cytotoxic T cell responses in human HCMV-seronegative subjects. *J Infect Dis*. 2001 183:1171–1179.

**Bernstein DI, Munoz FM, Callahan ST, Rupp R, Wootton SH, Edwards KM, Turley CB, Stanberry LR, Patel SM, McNeal MM, Pichon S, Amegashie C, Bellamy AR.** Safety and efficacy of a cytomegalovirus glycoprotein B (gB) vaccine in adolescent girls: a randomized clinical trial. *Vaccine* 34. 2016: 313-319.

**Bernstein DI, Reap EA, Katen K, Watson A, Smith K, Norberg P, Olmsted RA, Hoepfer A, Morris J, Negri S, Maughan MF, Chulay JD.** Randomized, double-blind, phase 1 trial of an alphavirus replicon vaccine for cytomegalovirus in HCMV seronegative adult volunteers. *Vaccine*. 2009 Dec 11; 28(2):484-93.

**Bialas KM, Tanaka T, Tran D, Varner V, Cisneros De La Rosa E, Chiuppesi F, Wussow F, Kattenhorn L, Macri S, Kunz EL, Estroff JA, Kirchherr J, Yue Y, Fan Q, Lauck M, O'Connor DH, Hall AH, Xavier A, Diamond DJ, Barry PA, Kaur A, Permar SR.** Maternal CD4+ T cells protect against severe congenital cytomegalovirus disease in a novel nonhuman primate model of placental cytomegalovirus transmission. *Proc Natl Acad Sci U S A*. 2015 Nov 3; 112(44):13645-50.

**Bilavsky E, Pardo J, Attias J, Levy I, Magny JF, Ville Y, Leruez-Ville M, Amir J.** Clinical Implications for Children Born With Congenital Cytomegalovirus Infection Following a Negative Amniocentesis. *Clin Infect Dis*. 2016 Jun 10; 63(1):33–8.

**Blundell C, Tess ER, Schanzer AS, Coutifaris C, Su EJ, Parry S, Huh D.** A microphysiological model of the human placental barrier. *Lab Chip*. 2016 Aug 2; 16(16):3065-73.

**Boeckh M, Geballe AP.** Cytomegalovirus: pathogen, paradigm, and puzzle. *J Clin Invest*. 2011 May; 121(5):1673-80.

**Boehme KW, Guerrero M, Compton T.** Human cytomegalovirus envelope glycoproteins B and H are necessary for TLR2 activation in permissive cells. *J Immunol*. 2006; 177:7094–7102.

**Bonalumi S, Trapanese A, Santamaria A, D'Emidio L, Mobili L.** Cytomegalovirus infection in pregnancy: review of the literature. *J Prenat Med*. 2011 Jan; 5(1):1-8.

**Bonaros N, Mayer B, Schachner T, Laufer G, Kocher A.** CMV-hyperimmune globulin for preventing cytomegalovirus infection and disease in solid organ transplant recipients: a meta-analysis. *Clin Transplant.* 2008 Jan-Feb; 22(1):89-97.

**Bonin O.** Quantitativ-virologische Methodik. Georg Thieme Verlag Stuttgart 1973; 183-186.

**Boppana, SB, Pass, RF, Britt, WJ.** Symptomatic congenital cytomegalovirus infection: neonatal morbidity and mortality. *Pediatr Infect Dis J.* 1992 Feb; 11(2):93-9.

**Brito LA, Chan M, Shaw CA, Hekele A, Carsillo T, Schaefer M, Archer J, Seubert A, Otten GR, Beard CW, Dey AK, Lilja A, Valiante NM, Mason PW, Mandl CW, Barnett SW, Dormitzer PR, Ulmer JB, Singh M, O'Hagan DT, Geall AJ.** A cationic nanoemulsion for the delivery of nextgeneration RNA vaccines. *Mol Ther.* 2014 Dec; 22(12):2118-29.

**Britt WJ, Auger D.** Human cytomegalovirus virion-associated protein with kinase activity. *J Virol.* 1986 Jul; 59(1):185-8.

**Britt WJ, Mach M.** Human cytomegalovirus glycoproteins. *Intervirology.* 1996; 39 (5-6):401-12.

**Britt WJ, Vugler L, Butfiloski EJ, Stephens EB.** Cell surface expression of human cytomegalovirus (HCMV) gp55-116 (gB): use of HCMV-recombinant vaccinia virus-infected cells in analysis of the human neutralizing antibody response. *J Virol.* 1990 Mar; 64(3):1079-85.

**Bruce MC.** Human Embryology and Developmental Biology (Fifth Edition): Placenta and Extraembryonic Membranes Chapter 7. 2013; Elsevier Inc.

**Bughio F, Umashankar M, Wilson J, Goodrum F.** Human cytomegalovirus UL135 and UL136 genes are required for postentry tropism in endothelial cells. *J Virol* 2015; 89:6536-6550.

**Burstone MS.** Histochemical demonstration of cytochrome oxidase with new amine reagents. *J. Histochem. Cytochem.* 1960; 8: 63-70.

**Buxmann H, Hamprecht K, Meyer-Wittkopf M, Friese K.** Primary Human Cytomegalovirus (HCMV) Infection in Pregnancy. *Dtsch Arztebl Int.* 2017; 114(4):45-52.

**Buxmann H, Stackelberg OM, Schlößer RL.** Use of cytomegalovirus hyperimmunoglobulin for prevention of congenital cytomegalovirus disease: a retrospective analysis. *J. Perinat. Med.* 2012; 40(4): 439-46.

**Caló S, Cortese M, Ciferri C, Bruno L, Gerrein R, Benucci B, Monda G, Gentile M, Kessler T, Uematsu Y, Maione D, Lilja AE, Carfi A, Merola M.** The human cytomegalovirus UL116 gene encodes an envelope glycoprotein forming a complex with gH independently from gL. *J Virol.* 2016 Apr 29; 90(10):4926-38.

**Capretti MG, Lanari M, Lazzarotto T, Gabrielli L, Pignatelli S, Corvaglia L, Tridapalli E, Faldella G.** Very low birth weight infants born to cytomegalovirus-seropositive mothers fed with their mother's milk: a prospective study. *J Pediatr.* 2009 Jun; 154(6):842-8.

**Carbone J.** The Immunology of Posttransplant HCMV Infection: Potential Effect of HCMV Immunoglobulins on Distinct Components of the Immune Response to HCMV. *Transplantation.* 2016 Mar; 100 Suppl 3:11-8.

**Carlson BM.** Human Embryology and Developmental Biology (Fifth Edition): Placenta and Extraembryonic Membranes Chapter 7. 2013, Elsevier Inc.:117-135.

**Cayatte C, Schneider-Ohrum K, Wang Z, Irrinki A, Nguyen N, Lu J, Nelson C, Servat E, Gemmell L, Citkowicz A, Liu Y, Hayes G, Woo J, Van Nest G, Jin H, Duke G, McCormick AL.** Cytomegalovirus vaccine strain Towne-derived dense bodies induce broad cellular immune responses and neutralizing antibodies that prevent infection of fibroblasts and epithelial cells. *J Virol.* 2013 Oct; 87(20):11107-20.

**Chee MS, Bankier AT, Beck S.** Analysis of the protein-coding content of the sequence of human cytomegalovirus strain AD169. *Curr Top Microbiol Immunol.* 1990; 154:125-69.

**Chiaie LD, Neuberger P, Vochem M, Lihs A, Karck U, Enders M.** No evidence of obstetrical adverse events after hyperimmune globulin application for primary cytomegalovirus infection in pregnancy: experience from a single centre. *Arch Gynecol Obstet.* 2018 Jun; 297(6):1389-1395.

**Chou SW, Dennison KM.** Analysis of interstrain variation in cytomegalovirus glycoprotein B sequences encoding neutralization-related epitopes. *J Infect Dis.* 1991 Jun; 163(6):1229-34.

**Chung AW, Ghebremichael M, Robinson H, Brown E, Choi I, Lane S, Dugast AS, Schoen MK, Rolland M, Suscovich TJ, Mahan AE, Liao L, Streeck H, Andrews C, Rerks-Ngarm S, Nitayaphan S, de Souza MS, Kaewkungwal J, Pitisuttithum P, Francis D, Michael NL, Kim JH, Bailey-Kellogg C, Ackerman ME, Alter G.** Polyfunctional Fc-effector profiles mediated by IgG subclass selection distinguish RV144 and VAX003 vaccines. *Sci Transl Med* 2014; 6:228–238.

**Chung AW, Kumar MP, Arnold KB, Yu WH, Schoen MK, Dunphy LJ, Suscovich TJ, Frahm N, Linde C, Mahan AE, Hoffner M, Streeck H, Ackerman ME, McElrath MJ, Schuitemaker H, Pau MG, Baden LR, Kim JH<sup>10</sup>, Michael NL, Barouch DH, Lauffenburger DA, Alter G.** Dissecting polyclonal vaccine-induced humoral immunity against HIV using systems serology. *Cell* 2015; 163:988-998.

**Ciferri C, Chandramouli S, Donnarumma D, Nikitin PA, Cianfrocco MA, Gerrein R, Feire AL, Barnett SW, Lilja AE, Rappuoli R, Norais N, Settembre EC, Carfi A.** Structural and

biochemical studies of HCMV gH/gL/gO and Pentamer reveal mutually exclusive cell entry complexes. *Proc Natl Acad Sci U S A*. 2015 Feb 10; 112(6):1767-72.

**Ciu X, Meza BP, Adler SP, McVoy MA.** Cytomegalovirus vaccines fail to induce epithelial entry neutralizing antibodies comparable to natural infection. *Vaccine*. 2008 Oct 23; 26(45):5760-6.

**Cohen JI, Corey GR.** Cytomegalovirus infection in the normal host. *Medicine (Baltimore)*, 1985; 64: 100-114.

**Compton T, Nepomuceno RR, Nowlin DM.** Human cytomegalovirus penetrates host cells by pH-independent fusion at the cell surface. *Virology*. 1992; 191(1):387–395.

**Connolly SA, Jackson JO, Jardetzky TS, Longnecker R.** Fusing structure and function: a structural view of the herpesvirus entry machinery. *Nat Rev Microbiol*. 2011 May; 9(5):369-81.

**Corrales-Aguilar E, Hoffmann K, Hengel H.** HCMV-encoded Fcγ receptors: modulators at the interface of innate and adaptive immunity. *Semin Immunopathol* 2014; 36:627–640.

**Corrales-Aguilar E, Trilling M, Reinhard H, Falcone V, Zimmermann A, Adams O, Santibanez S, Hengel H.** Highly individual patterns of virus-immune IgG effector responses in humans. *Med Microbiol Immunol*. 2016 Oct; 205(5):409-24.

**Costa-Garcia M, Vera A, Moraru M, Vilches C, López-Botet M, Muntasell A.** Antibody-mediated response of NKG2CbrightNK cells against human cytomegalovirus. *J Immunol* 2015; 194:2715–2724.

**Crough T, Khanna R.** Immunobiology of human cytomegalovirus: from bench to bedside. *Clin Microbiol Rev*. 2009 Jan;22(1):76-98,

**Cui X, Meza BP, Adler SP, McVoy MA.** Cytomegalovirus vaccines fail to induce epithelial entry neutralizing antibodies comparable to natural infection. *Vaccine*. 2008 Oct 23;26(45):5760-6.

**Davison AJ, Eberle R, Fauquet CM, Mayo MA.** Eighth Report of the International Committee on Taxonomy of Viruses. London/ San Diego 2004; 193–212.

**De Vries JJ, Vossen AC, Kroes AC.** Implement neonatal screening for congenital cytomegalovirus: addressing the deafness of policy makers. *Rev Med Virol*. 2011 Jan; 21(1):54-61.

**Deml L.** Modulatory effects of cytomegalovirus hyperimmunoglobulins on HCMV protein-mediated activation of different effector cell populations of cell-mediated immunity. ESOT2017 Barcelona Congress.



**Dolan A, Cunningham C, Hector RD, Hassan-Walker AF, Lee L, Addison C, Dargan DJ, McGeoch DJ, Gatherer D, Emery VC, Griffiths PD, Sinzger C, McSharry BP, Wilkinson GW, Davison AJ.** Genetic content of wild-type human cytomegalovirus. *J Gen Virol.* 2004 May; 85(Pt 5):1301-12.

**Douglas AJ, Cheryl E, Dunn JP, Forman M.** Cytomegalovirus Retinitis and Viral Resistance: Ganciclovir Resistance, *Journals of the Royal Society if Tropical Medicine and Hygiene* 1997; 177: 770-773.

**Douglas AJ, Cheryl E, Forman M, Dunn JP.** Incidence of Foscarnet Resistance and Cidofovir Resistance in Patients Treated for Cytomegalovirus Retinitis. *Antimicrob Agents Chemother* 1998; 42(9): 2240–2244.

**Dunn KC, Aotaki-Keen AE, Putkey FR, Hjelmeland LM.** ARPE-19, A human retinal pigment epithelial cell line with differentiated properties. *Exp. Eye Res.* 1996; 62: 155-169.

**Eggers E, Bäder U, Enders G.** Combination of microneutralization and avidity assays: Improved diagnosis of recent primary human cytomegalovirus infection in single serum sample of second trimester pregnancy. *J Med Virol.* 2000 Mar; 60(3):324-30.

**Enders G, Daiminger A, Bäder U, Exler S, Enders M.** Intrauterine transmission and clinical outcome of 248 pregnancies with primary cytomegalovirus infection in relation to gestational age. *Journal of Clinical Virology.* Elsevier B.V; 2011 Nov; 52(3):244–6.

**Enders G, Jahm G, Hamprecht K.** HCMV-Screening während der Schwangerschaft. *Frauenarzt* 2006; 47: 910-911.

**Fabbri E, Revello MG, Furione M.** Prognostic markers of symptomatic congenital human cytomegalovirus infection in fetal blood. *BJOG.* 2011 Mar; 118(4):448-56.

**Feucht J, Opherk K, Lang P, Kayser S, Hartl L, Bethge W, Matthes-Martin S, Bader P, Albert MH, Maecker-Kolhoff B, Greil J, Einsele H, Schlegel PG, Schuster FR, Kremens B, Rossig C, Gruhn B, Handgretinger R, Feuchtinger T.** Adoptive T-cell therapy with hexon-specific Th1 cells as a treatment of refractory adenovirus infection after HSCT. *Blood.* 2015 Mar 19; 125(12):1986-94.

**Filipovich AH, Peltier MH, Bechtel MK, Dirksen CL, Strauss SA, Englund JA.** Circulating cytomegalovirus (HCMV) neutralizing activity in bone marrow transplant recipients: comparison of passive immunity in a randomized study of four intravenous IgG products administered to HCMV-seronegative patients. *Blood* 1992; 80(10):2656-60.

**Fisher SJ, Genbace O, Maidji E, Pereira L.** Human cytomegalovirus infection of placental cytotrophoblasts in vitro and in utero: implications of transmission and pathogenesis. *J Virol.* 2000 Aug; 74(15):6808-20.

**Fouts AE, Chan P, Stephan JP, Vandlen R, Feierbach B.** Antibodies against the gH/gL/UL128/UL130/UL131 complex comprise the majority of the anti-cytomegalovirus (anti-HCMV) neutralizing antibody response in HCMV hyperimmune globulin. *J Virol.* 2012 Jul; 86(13):7444-7

**Fouts AE, Comps-Agrar L, Stengel KF, Ellerman D, Schoeffler AJ, Warming S, Eaton DL, Feierbach B.** Mechanism for neutralizing activity by the anti-HCMV gH/gL monoclonal antibody MSL-109. *Proc Natl Acad Sci U S A.* 2014 Jun 3; 111(22):8209-14.

**Fowler KB, Stagno S, Pass RF, Britt WJ, Boll TJ, Alford CA.** The outcome of congenital cytomegalovirus infection in relation to maternal antibody status. *N Engl J Med.* 1992 Mar 5; 326(10):663-7.

**Freed DC, Tang Q, Tang A, Li F, He X, Huang Z, Meng W, Xia L, Finnefrock AC, Durr E, Espeseth AS, Casimiro DR, Zhang N, Shiver JW, Wang D, An Z, Fu TM.** Pentameric complex of viral glycoprotein H is the primary target for potent neutralization by a human cytomegalovirus vaccine. *Proc Natl Acad Sci U S A.* 2013 Dec 17; 110(51):E4997-5005.

**Frenzel K, Ganepola S, Michel D, Thiel E, Krüger DH, Uharek L, Hofmann J.** Antiviral function and efficacy of polyvalent immunoglobulin products against HCMV isolates in different human cell lines. *Med Microbiol Immunol.* 2012 Aug; 201(3):277-86.

**Fu TM, An Z, Wang D.** Progress on pursuit of human cytomegalovirus vaccines for prevention of congenital infection and disease. *Vaccine.* 2014 May 7; 32(22):2525-33.

**Garty BZ, Ludomirsky A, Danon YL, Peter JB, and Douglas SD.** Placental transfer of immunoglobulin G subclasses. *Clin Diagn Lab Immunol.* 1994 Nov; 1(6): 667–669.

**Germer M, Herbener P, Schüttrumpf J.** Functional Properties of Human Cytomegalovirus Hyperimmunoglobulin and Standard Immunoglobulin Preparations. *Ann Transplant.* 2016 Sep 6; 21:558-64.

**Gerna G, Percivalle E, Lilleri D, Lozza L, Fornara C, Hahn G, Baldanti F, Revello MG.** Dendritic-cell infection by human cytomegalovirus is restricted to strains carrying functional UL131–128 genes and mediates efficient viral antigen presentation to CD8+ T cells. *J Gen Virol.* 2005 Feb; 86(Pt 2):275-84.

**Gerna G, Percivalle E, Perez L, Lanzavecchia A, Lilleri D.** Monoclonal Antibodies to Different Components of the Human Cytomegalovirus (HCMV) Pentamer gH/gL/pUL128L and Trimer gH/gL/gO as well as Antibodies Elicited during Primary HCMV Infection Prevent Epithelial Cell Syncytium Formation. *J Virol.* 2016 Jun 24; 90(14):6216-6223.

**Gerna G, Revello MG, Baldanti F, Percivalle E, Lilleri D.** The pentameric complex of human Cytomegalovirus: cell tropism, virus dissemination, immune response and vaccine development. *J Gen Virol.* 2017 Sep; 98(9):2215-2234.

**Gerna G, Sarasini A, Patrone M, Percivalle E, Fiorina L, Campanini G, Gallina A, Baldanti F, Revello MG.** Human cytomegalovirus serum neutralizing antibodies block virus infection of endothelial/epithelial cells, but not fibroblasts, early during primary infection. *J Gen Virol.* 2008 Apr; 89(Pt 4):853-65.

**Gilbert C, Azzi A, Goyette N, Lin SX, Boivin G.** Recombinant phenotyping of cytomegalovirus UL54 mutations that emerged during cell passages in the presence of either ganciclovir or foscarnet. *Antimicrob Agents Chemother.* 2011 Sep; 55(9):4019-27

**Giulieri S, Manuel O.** QuantiFERON(R)-CMV assay for the assessment of cytomegalovirus cell-mediated immunity. *Expert Rev Mol Diagn.* 2011 Jan;11(1):17-25.

**Göhring K, Wolf D, Bethge W, Mikeler E, Faul C, Vogel W, Vöhringer MC, Jahn G, Hamprecht K.** Dynamics of coexisting HCMV-UL97 and UL54 drug-resistance associated mutations in patients after hematopoietic cell transplantation. *J Clin Virol.* 2013 May; 57(1):43-9.

**Goodpasture EW, Talbot FB.** Concerning nature of „protozoan like“ cells in certain lesions of infancy. *J Infect Dis* 1920; 26: 347-350.

**Griffiths PD, Stanton A, McCarrell E, Smith C, Osman M, Harber M, Davenport A, Jones G, Wheeler DC, O'Beirne J, Thorburn D, Patch D, Atkinson CE, Pichon S, Sweny P, Lanzman M, Woodford E, Rothwell E, Old N, Kinyanjui R, Haque T, Atabani S, Luck S, Prideaux S, Milne RS, Emery VC, Burroughs AK.** Cytomegalovirus glycoprotein-B vaccine with MF59 adjuvant in transplant recipients: a phase 2 randomised placebo-controlled trial. *Lancet.* 2011 Apr 9; 377(9773):1256-63.

**Guerra B, Simonazzi G, Puccetti C, Lanari M, Farina A, Lazzarotto T, Rizzo N.** Ultrasound prediction of symptomatic congenital cytomegalovirus infection. *Am J Obstet Gynecol.* 2008 Apr; 198(4):380.e1-7.

**Günther PS, Peper JK, Faist B, Kayser S, Hartl L, Feuchtinger T, Jahn G, Neuenhahn M, Busch DH, Stevanović S, Dennehy KM.** Identification of a Novel Immunodominant HLA-B\*07: 02-restricted Adenoviral Peptide Epitope and Its Potential in Adoptive Transfer Immunotherapy. *J Immunother.* 2015 Sep; 38(7):267-75.

**Gupta CK, Leszczynski J, Gupta RK, Siber GR.** IgG subclass antibodies to human cytomegalovirus (HCMV) in normal human plasma samples and immune globulins and their neutralizing activities. *Biologicals.* 1996 Jun; 24(2):117-24.

**Ha S, Li F, Troutman MC, Freed DC, Tang A, Loughney JW, Wang D, Wang IM, Vlasak J, Nickle DC, Rustandi RR, Hamm M, DePhillips PA, Zhang N, McLellan JS, Zhu H, Adler SP5, McVoy MA, An Z, Fu TM.** Neutralization of Diverse Human Cytomegalovirus Strains Conferred by Antibodies Targeting Viral gH/gL/pUL128-131 Pentameric Complex. *J Virol.* 2017 Mar 13; 91(7). pii: e02033-16.

**Hahn G, Revello MG, Patrone M, Percivalle E, Campanini G, Sarasini A, Wagner M, Gallina A, Milanesi G, Koszinowski U, Baldanti F, Gerna G.** Human cytomegalovirus UL131-128 genes are indispensable for virus growth in endothelial cells and virus transfer to leukocytes. *J Virol.* 2004 Sep; 78(18):10023-33.

**Hamilton ST, van Zuylen W, Shand A, Scott GM, Naing Z, Hall B, Craig ME, Rawlinson WD.** Prevention of congenital cytomegalovirus complications by maternal and neonatal treatments: a systematic review. *Rev Med Virol.* 2014 Nov;24(6):420-33.

**Hamprecht K, Goelz R, Maschmann J.** Breast milk and cytomegalovirus infection in preterm infants. *Early Hum Dev.* 2005 Dec; 81(12):989-96.

**Hamprecht K, Kagan KO, Goelz R.** Comment on: a randomized trial of hyperimmune globulin to prevent congenital cytomegalovirus. *N Engl J Med* 2014; 370(26):2543

**Hamprecht K, Maschmann J, Vochem M, Dietz K, Speer CP, Jahn G.** Epidemiology of transmission of cytomegalovirus from mother to preterm infant by breastfeeding. *Lancet.* 2001 Feb 17; 357(9255):513-8.

**Hansen SG, Sacha JB, Hughes CM.** Cytomegalovirus vectors violate CD8+Z cell recognition paradigms. *Science.* 2013 May 24; 340(6135):1237874.

**Heldwein EE.** gH/gL supercomplexes at early stages of herpesvirus entry. *Curr Opin Virol.* 2016 Jun; 18:1-8.

**Ho M.** Cytomegalovirus: Biology and infection. New York Plenum 1991.

**Hofmann I, Wen Y, Ciferri C, Schulze A, Fühner V, Leong M, Gerber A, Gerrein R, Nandi A, Lilja AE, Carfi A, Laux H.** Expression of the human cytomegalovirus pentamer complex for vaccine use in a CHO system. *Biotechnol Bioeng.* 2015 Dec; 112(12):2505-15.

**Huber MT, Compton T.** Characterization of a novel third member of the human cytomegalovirus glycoprotein H-glycoprotein L complex. *J Virol.* 1997 Jul; 71(7):5391-8.

**Huber MT, Compton T.** The human cytomegalovirus UL74 gene encodes the third component of the glycoprotein H-glycoprotein L-containing envelope complex. *J Virol.* 1998; 72(10):8191-8197.

**Isaacson MK, Compton T.** Human cytomegalovirus glycoprotein b is required for virus entry and cell-to-cell spread but not for virion attachment, assembly, or egress. *J Virol.* 2009 Apr; 83(8):3891-903.

**Jacob CL, Lamorte L, Sepulveda E, Lorenz IC, Gauthier A, Franti M.** Neutralizing antibodies are unable to inhibit direct viral cell-to-cell spread of human cytomegalovirus. *Virology.* 2013 Sep; 444(1-2):140-7.

**Jacquemard F, Yamamoto M, Costa JM, Romand S.** Maternal administration of valaciclovir in symptomatic intrauterine cytomegalovirus infection. *BJOG.* 2007 Sep; 114(9):1113-21.

**Jahn G, Scholl BC, Traupe B, Fleckenstein B.** The two major structural phosphoproteins (pp65 and pp150) of human cytomegalovirus and their antigenic properties. *J Gen Virol.* 1987 May; 68 (Pt 5):1327-37.

**Jean Beltran PM, Cristea IM.** The life cycle and pathogenesis of human cytomegalovirus infection: lessons from proteomics. *Expert Rev Proteomics.* 2014 Dec; 11(6):697-711.

**Jim WT, Shu CH, Chiu NC, Kao HA, Hung HY, Chang JH, Peng CC, Hsieh WS, Liu KC, Huang FY.** Transmission of cytomegalovirus from mothers to preterm infants by breast milk. *Pediatr Infect Dis J.* 2004 Sep; 23(9):848-51.

**Jordan MC, Rousseau W, Stewart JA, Noble GR, Chin TD.** Spontaneous cytomegalovirus mononucleosis. Clinical and laboratory observations in nine cases. *Ann Intern Med.* 1973 Aug; 79(2):153-60.

**Kabanova A, Perez L, Lilleri D, Marcandalli J, Agatic G, Becattini S, Preite S, Fuschillo D, Percivalle E, Sallusto F, Gerna G, Corti D, Lanzavecchia A.** Antibody-driven design of a human cytomegalovirus gHgLpUL128L subunit vaccine that selectively elicits potent neutralizing antibodies. *Proc Natl Acad Sci U S A.* 2014 Dec 16; 111(50):17965-70.

**Kagan KO, Enders M, Schampera MS, Baeumel E, Hoopmann M, Geipel A, Berg C, Goelz R, De Catte L, Wallwiener D, Brucker S, Adler SP, Jahn G, Hamprecht K.** Prevention of maternal-fetal transmission of HCMV by hyperimmunoglobulin (HIG) administered after a primary maternal HCMV infection in early gestation. *Ultrasound Obstet Gynecol.* 2018 Jun 26.

**Kahl M, Siegel-Axel D, Stenglein S, Jahn G, Sinzger C.** Efficient Lytic Infection of Human Arterial Endothelial Cells by Human Cytomegalovirus Strains. *J Virol.* 2000 Aug; 74(16):7628-35.

**Kharfan-Dabaja MA, Boeckh M, Wilck MB, Langston AA, Chu AH, Wloch MK, Guterwill DF, Smith LR, Rolland AP, Kenney RT.** A novel therapeutic cytomegalovirus DNA vaccine in allogeneic haemopoietic stem-cell transplantation: a phase 2 randomised placebo-controlled trial. *Lancet Infect Dis.* 2012 Apr; 12(4):290-9.

**Kimberlin DW.** Antiviral therapies in children: has their time arrived? *Pediatr Clin North Am.* 2005 Jun; 52(3):837-67.

**Kirchmeier M, Fluckiger AC, Soare C, Bozic J, Ontsouka B, Ahmed T, Diress A, Pereira L, Schodel F, Plotkin S, Dalba C, Klatzmann D, Anderson DE.** Enveloped virus-like particle expression of human cytomegalovirus glycoprotein B antigen induces antibodies with potent and broad neutralizing activity. *Clin Vaccine Immunol.* 2014 Feb; 21(2):174-80.

**Klenerman P, Oxenius A.** T cell responses to cytomegalovirus. *Nature Reviews Immunology* 2016; 16: 367–377.

**Knowles NJ, Buckley HG, Pereira L.** Classification of porcine enteroviruses by antigenic analysis and cytopathic effects in tissue culture: Description of 3 new serotypes. *Arch Virol.* 1979;62(3):201-8.

**Kobayashi T, Sato JI, Ikuta K, Kanno R, Nishiyama K, Koshizuka T, Ishioka K, Suzutani T.** Modification of the HCMV-specific IFN- $\gamma$  release test (QuantiFERON-HCMV) and a novel proposal for its application. *Fukushima J Med Sci.* 2017 Aug 9; 63(2):64-74.

**Koffron AJ, Patterson BK, Yan S, Kaufman DB, Fryer JP, Stuart FP, Abecassis MI.** Latent human cytomegalovirus: a functional study. *Transplant Proc.* 1997 Feb-Mar; 29(1-2):793-5.

**Kwon JS, Kim T, Kim SM, Sung H, Shin S, Kim YH, Shin EC, Kim SH, Han DJ.** Comparison of the Commercial QuantiFERON-HCMV and Overlapping Peptide-based ELISPOT Assays for Predicting HCMV Infection in Kidney Transplant Recipients. *Immune Netw.* 2017 Oct; 17(5):317-325.

**La Rosa C, Longmate J, Martinez J, Zhou Q, Kaltcheva TI, Tsai W, Drake J, Carroll M, Wussow F, Chiappesi F, Hardwick N, Dadwal S, Aldoss I, Nakamura R, Zaia JA, Diamond DJ.** MVA vaccine encoding HCMV antigens safely induces durable expansion of HCMV-specific T cells in healthy adults. *Blood.* 2017 Jan 5; 129(1):114-125.

**Landolfo S, Gariglio M, Gribaudo G, Lembo D.** The human cytomegalovirus. *Pharmacol Ther.* 2003 Jun; 98(3):269-97.

**Lang DJ, Krummer JF.** Cytomegalovirus in semen: observations in selected populations. *J Infect Dis.* 1975 Oct; 132(4):472-3.

**Lazzarotto T, Guerra B, Gabrielli L, Lanari M, Landini MP.** Update on the prevention, diagnosis and management of cytomegalovirus infection during pregnancy. *Clin Microbiol Infect.* 2011 Sep; 17(9):1285-93.

**Lazzarotto T, Varani S, Guerra B, Nicolosi A, Lanari M, Landini MP.** Prenatal indicators of congenital cytomegalovirus infection. *J Pediatr* 2000; 137:90–5.

**Leruez-Ville M, Ghout I, Bussi eres L, Stirnemann J, Magny JF, Couderc S, Salomon LJ, Guillemintot T, Aegerter P, Benoist G, Winer N, Picone O, Jacquemard F, Ville Y.** In utero treatment of congenital cytomegalovirus infection with valgacyclovir in a multicenter, open-label, phase II study. *Am J Obstet Gynecol.* 2016 Oct; 215(4).

**Li G, Nguyen CC, Ryckman BJ, Britt WJ, Kamil JP.** A viral regulator of glycoprotein complexes contributes to human cytomegalovirus cell tropism. *Proc Natl Acad Sci USA* 2015; 112:4471–4476.

**Li L, Nelson JA, Britt WJ.** Glycoprotein H-related complexes of human cytomegalovirus: Identification of a third protein in the gCIII complex. *J Virol.* 1997 Apr; 71(4):3090-7.

**Lilleri D, Fornara C, Revello MG, Gerna G.** Human cytomegalovirus-specific memory CD8+ and CD4+ T cell differentiation after primary infection. *J Infect Dis.* 2008 Aug 15; 198(4):536-43.

**Lilleri D, Kabanova A, Revello MG.** Fetal human cytomegalovirus transmission correlates with delay to gH/gL/ pUL128-130-131 complex during primary infection. *PLoS One.* 2013; 8(3):e59863.

**Lilleri D, Kabanova A, Lanzavecchia A, Gerna G.** Antibodies against neutralization epitopes of human cytomegalovirus gH/gL/pUL128-130-131 complex and virus spreading may correlate with virus control in vivo. *J Clin Immunol.* 2012 Dec; 32(6):1324-31.

**Lipitz S, Yinon Y, Malinger G, Yagel S, Levit L, Hoffman C, Rantzer R, Weisz B.** Risk of cytomegalovirus-associated sequelae in relation to time of infection and findings on prenatal imaging. *Ultrasound Obstet Gynecol.* 2013 May; 41(5):508-14.

**Liu B, Stinski MF.** Human cytomegalovirus contains a tegument protein that enhances transcription from promoters with upstream ATF and AP-1 cisacting elements. *J Virol.* 1992 Jul; 66(7):4434-44.

**Ljungman P, Reusser P, de la Camara R, Einsele H, Engelhard D, Ribaud P, Ward K; European Group for Blood and Marrow Transplantation.** Management of CMV infections: recommendations from the infectious diseases working party of the EBMT. *Bone Marrow Transplant.* 2004 Jun ;33(11):1075-81.

**Lopez-Verg es S, Milush JM, Schwartz BS, Pando MJ, Jarjoura J, York VA, Houchins JP, Miller S, Kang SM, Norris PJ, Nixon DF, Lanier LL.** Expansion of a unique CD57+ NKG2Chi natural killer cell subset during acute human cytomegalovirus infection. *Proc Natl Acad Sci U S A.* 2011 Sep 6; 108(36):14725-32.

**Loughney JW, Rustandi RR, Wang D, Troutman MC, Dick LW Jr, Li G, Liu Z, Li F, Freed DC, Price CE, Hoang VM, Culp TD, DePhillips PA, Fu TM, Ha S.** Soluble human

cytomegalovirus gH/gL/pUL128-131 pentameric complex, but not gH/gL, inhibits viral entry to epithelial cells and presents dominant native neutralizing epitopes. *J Biol Chem*. 2015 Jun 26; 290(26):15985-95.

**Luganini A, Cavaletto N, Raimondo S, Geuna S, Gribaudo G.** Loss of the human cytomegalovirus US16 protein abrogates virus entry into endothelial and epithelial cells by reducing the virion content of the pentamer. *J Virol*. 2017 May 12; 91(11). pii: e00205-17.

**Lurain NS, Chou S.** Antiviral drug resistance of human cytomegalovirus. *Clin Microbiol Rev*. 2010 Oct; 23(4):689-712.

**Macagno A, Bernasconi NL, Vanzetta F, Dander E, Sarasini A, Revello MG, Gerna G, Sallusto F, Lanzavecchia A.** Isolation of human monoclonal antibodies that potently neutralize human cytomegalovirus infection by targeting different epitopes on the gH/gL/UL128-131A complex. *J Virol*. 2010 Jan; 84(2):1005-13.

**Maidji E, McDonagh S, Genbacev O, Tabata T, Pereira L.** Maternal Antibodies Enhance or Prevent Cytomegalovirus Infection in the Placenta by Neonatal Fc Receptor-Mediated Transcytosis. *Am J Pathol*. 2006 Apr; 168(4): 1210–1226.

**Manicklal S, Emery VC, Lazzarotto T, Boppana SB, Gupta RK.** The “Silent” Global Burden of Congenital Cytomegalovirus. *Clin Microbiol Rev*. 2013 Jan; 26(1):86-102.

**Marty FM, Ljungman P, Chemaly RF, Maertens J, Dadwal SS, Duarte RF, Haider S, Ullmann AJ, Katayama Y, Brown J, Mullane KM, Boeckh M, Blumberg EA, Einsele H, Snyderman DR, Kanda Y, DiNubile MJ, Teal VL, Wan H, Murata Y, Kartsonis NA, Leavitt RY, Badshah C.** Letermovir Prophylaxis for Cytomegalovirus in Hematopoietic-Cell Transplantation. *N Engl J Med*. 2017 Dec 21; 377(25):2433-2444.

**Maschmann J, Hamprecht K, Dietz K, Jahn G, Speer CP.** Cytomegalovirus infection of extremely low-birth weight infants via breast milk. *Clin Infect Dis*. 2001 Dec 15; 33(12):1998-2003.

**McGeoch DJ, Cook S, Dolan A, Jamieson FE, Telford EA.** Molecular phylogeny and evolutionary timescale for the family of mammalian herpesviruses. *J Mol Biol*. 1995 Mar 31; 247(3):443-58.

**Miescher SM, Huber TM, Kühne M, Lieby P, Snyderman DR, Vensak JL, Berger M.** In vitro evaluation of cytomegalovirus-specific hyperimmune globulins vs. standard intravenous immunoglobulins. *Vox Sang*. 2015 Jul;109(1):71-8.

**Mocarski ES, Courcelle CT.** Cytomegaloviruses and their Replication. In *Fields Virology* 2001; 4: 2629-2673.

**Mocarski, ES, Shenk T, Pass RF.** Cytomegaloviruses. In *fields Virology* 2007;5: 2701-2772.



**Mostoufi-zadeh M, Driscoll SG, Bianco SA, Kundsinn RB.** Placental evidence of cytomegalovirus infection of the fetus and neonate. *Arch Pathol Lab Med.* 1984 May; 108(5):403-6.

**Murrell I, Bedford C, Ladell K, Miners KL, Price DA, Tomasec P, Wilkinson GWG, Stanton RJ.** The pentameric complex drives immunologically covert cell-cell transmission of wild-type human cytomegalovirus. *Proc Natl Acad Sci U S A.* 2017 Jun 6; 114(23):6104-6109.

**Murthy S, Hayward GS, Wheelan S, Forman MS, Ahn JH, Pass RF, Arav-Boger R.** Detection of a single identical cytomegalovirus (CMV) strain in recently seroconverted young women. *PLoS One.* 2011 Jan 10; 6(1):e15949

**Nakamura R, La Rosa C, Longmate J, Drake J, Slape C, Zhou Q, Lampa MG, O'Donnell M, Cai JL, Farol L, Salhotra A, Snyder DS, Aldoss I, Forman SJ, Miller JS, Zaia JA, Diamond DJ.** Viraemia, immunogenicity, and survival outcomes of cytomegalovirus chimeric epitope vaccine supplemented with PF03512676 (HCMVPepVax) in allogeneic haemopoietic stem-cell transplantation: randomised phase 1b trial. *Lancet Haematol.* 2016 Feb; 3(2):e87-98.

**Nigro G, Adler SP, La Torre R, Best AM.** Congenital Cytomegalovirus Collaborating Group. Passive immunization during pregnancy for congenital cytomegalovirus infection. *N Engl J Med.* 2005 Sep 29; 353(13):1350-62.

**Noyola DE, Fortuny C, Muntasell A, Noguera-Julian A, Muñoz-Almagro C, Alarcón A, Juncosa T, Moraru M, Vilches C, López-Botet M.** Influence of congenital human cytomegalovirus infection and the NKG2C genotype on NK-cell subset distribution in children. *Eur J Immunol.* 2012 Dec; 42(12):3256-66.

**Palmeira P, Quinello C, Silveira-Lessa AL, Zago CA, Carneiro-Sampaio M.** IgG Placental Transfer in Healthy and Pathological Pregnancies. *Clin Dev Immunol.* 2012;2012:985646.

**Pass RF.** Development and evidence for efficacy of CMV glycoprotein B vaccine with MF59 adjuvant. *J Clin Virol.* 2009 Dec;46 Suppl 4:S73-6.

**Pereira L, Maidji E, McDonagh S, Genbacev O, Fisher S.** Human cytomegalovirus transmission from uterus to placenta correlates with the presence of pathogenic bacteria and immunity. *J Virol.* 2003 Dec;77(24):13301-14.

**Picone O, Vauloup-Fellous C, Cordier AG, Guitton S, Senat MV, Fuchs F, Ayoubi JM, Grangeot Keros L, Benachi A.** A series of 238 cytomegalovirus primary infections during pregnancy: description and outcome. *Prenat Diagn.* 2013 Aug; 33(8):751-8.

**Picone O, Vauloup-Fellous C, Cordier AG, Parent Du Châtelet I, Senat MV, Frydman R, Grangeot-Keros L.** A 2-year study on cytomegalovirus infection during pregnancy in a French hospital. *BJOG*. 2009 May;116(6):818-23.

**Plachter B.** Prospects of a vaccine for the prevention of congenital cytomegalovirus disease. *Med Microbiol Immunol*. 2016 Dec; 205(6):537-547.

**Planitzer CB, Saemann MD, Gajek H, Farcet MR, Kreil TR.** Cytomegalovirus neutralization by hyperimmune and standard intravenous immunoglobulin preparations. *Transplantation*. 2011 Aug 15; 92(3):267-70.

**Plotkin SA, Higgins R, Kurtz JB.** Multicenter trial of Towne strain attenuated virus vaccine seronegative renal transplant recipients. *Transplantation*. 1994 Dec 15; 58(11):1176-8.

**Plotkin SA, Smiley ML, Friedman HM, Starr SE, Fleisher GR, Wlodaver C, Dafoe DC, Friedman AD, Grossman RA, Barker CF.** Towne-vaccine-induced prevention of cytomegalovirus disease after renal transplants. *Lancet* 1984; 528-530.

**Polilli E, Parruti G, D'Arcangelo F, Tracanna E, Clerico L, Savini V, D'Antonio F, Rosati M, Manzoli L, D'Antonio D, Nigro G.** A preliminary evaluation of safety and efficacy of standard intravenous immunoglobulins in pregnant women with primary Cytomegalovirus infection. *Clin Vaccine Immunol*. 2012 Dec;19(12):1991-3.

**Prix L, Hamprecht K, Holzhüter B, Handgretinger R, Klingebiel T, Jahn G.** A comprehensive restriction analysis of the UL97 region allows early detection of ganciclovir-resistant human cytomegalovirus in an immunocompromised child. *J Infect Dis*. 1999 Aug;180(2):491-5.

**Puliyanda DP, Silverman NS, Lehman D, Vo A, Bunnapradist S, Radha RK, Toyoda M, Jordan SC.** Successful use of oral ganciclovir for the treatment of intrauterine cytomegalovirus infection in a renal allograft recipient. *Transpl Infect Dis*. 2005 Jun;7(2):71-4.

**Rawlinson WD, Hamilton ST, van Zuylen WJ.** Update on treatment of cytomegalovirus infection in pregnancy and of the newborn with congenital cytomegalovirus. *Curr Opin Infect Dis*. 2016 Dec; 29(6):615-624.

**Rawlinson WD, Boppana SB, Fowler KB, Kimberlin DW, Lazzarotto T, Alain S, Daly K, Doutré S, Gibson L, Giles ML, Greenlee J, Hamilton ST, Harrison GJ, Hui L, Jones CA, Palasanthiran P, Schleiss MR, Shand MW, van Zuylen WJ.** Congenital cytomegalovirus infection in pregnancy and the neonate: consensus recommendations for prevention, diagnosis, and therapy. *Lancet Infect Dis*. 2017 Jun;17(6):e177-e188.

**Revello MG, Gerna G.** Pathogenesis and prenatal diagnosis of human cytomegalovirus infection. *J Clin Virol*. 2004 Feb;29(2):71-83.

**Reynolds DW, Stagno S, Hosty TS, Tiller M, Alford CA Jr.** Maternal cytomegalovirus excretion and perinatal infection. *Engl. J. Med.* 1973 ;289: 1-5.

**Rieder F, Steininger C.** Cytomegalovirus vaccine: phase II clinical trial results. *Clin Microbiol Infect.* 2014 May; 20 Suppl 5:95-102

**Rinaldo CR Jr, Black PH, Hirsch MS.** Interaction of cytomegalovirus with leukocytes from patients with mononucleosis due to cytomegalovirus. *J. infect. Dis.* 1977; 136(5): 667-678

**Roizmann B, Carmichael LE, Deinhardt F.** Herpesviridae Definition, provisional nomenclature, and taxonomy. The herpes virus study group, the international committee on taxonomy of viruses. *Intervirology.* 1981; 16: 201-217.

**Ross DS, Dollard SC, Victor M, Sumartojo E, Cannon MJ.** The epidemiology and prevention of congenital cytomegalovirus infection and diseases: activities of the centers for diseases control and Prevention Workgroup. *J. Womens Health (Larchmt).* 2006 Apr; 15(3):224-9.

**Rowe WP, Hartley JW, Waterman S, Turner HC, Huebner RJ.** Cytopathogenic agent resembling human salivary gland virus recovered from tissue cultures of human adenoids. *Proc Soc Exp Biol Med.* 1956; 92: 418-424.

**Ryckman BJ, Rainish BL, Chase MC, Borton JA, Johnson DC.** Characterization of the Human Cytomegalovirus gH/gL/UL128-131 Complex that mediates entry into epithelial and endothelial cells. *J Virol.* 2008 Jan;82(1):60-70. Epub 2007 Oct 17.

**Ryckman BJ, Chase MC, Johnson DC.** HCMV gH/gL/UL128-131 interferes with virus entry into epithelial cells: evidence for cell type-specific receptors. *Proc Natl Acad Sci U S A.* 2008 Sep 16; 105(37):14118-23.

**Saccoccio FM, Sauer AL, Cui X, Armstrong AE, Habib el-SE, Johnson DC, Ryckman BJ, Klingelutz AJ, Adler SP, McVoy MA.** Peptides from cytomegalovirus UL130 and UL131 proteins induce high titer antibodies that block viral entry into mucosal epithelial cells. *Vaccine.* 2011 Mar 24; 29(15):2705-11.

**Saldan A, Forner G, Mengoli C, Gussetti N, Palù G, Abate D.** Strong Cell-Mediated Immune Response to Human Cytomegalovirus Is Associated With Increased Risk of Fetal Infection in Primarily Infected Pregnant Women. *Clin Infect Dis.* 2015 Oct 15; 61(8):1228-34.

**Saldan A, Forner G, Mengoli C, Tinto D, Fallico L, Peracchi M, Gussetti N, Palù G, Abate D.** Comparison of the Cytomegalovirus (HCMV) Enzyme-Linked Immunosorbent Spot and HCMV QuantiFERON Cell-Mediated Immune Assays in HCMV-Seropositive and -Seronegative Pregnant and Nonpregnant Women. *J Clin Microbiol.* 2016 May; 54(5):1352-6.

**Sampaio KL, Weyell A, Subramanian N, Wu Z, Sinzger C.** A TB40/E-derived human cytomegalovirus genome with an intact US-gene region and a self-excisable BAC cassette for immunological research. *Biotechniques*. 2017; 63(5):205-214.

**Schampera MS, Arellano-Galindo J, Kagan KO, Adler SP, Jahn G, Hamprecht K.** Role of pentamer complex-specific and IgG subclass 3 antibodies in HCMV hyperimmunoglobulin and standard intravenous IgG preparations. *Med Microbiol Immunol*. 2018 Sep 10.

**Schampera MS, Schweinzer K, Abele H, Kagan KO, Klein R, Rettig I, Jahn G, Hamprecht K.** Comparison of cytomegalovirus (HCMV)-specific neutralization capacity of hyperimmunoglobulin (HIG) versus standard intravenous immunoglobulin (IVIG) preparations: Impact of HCMV IgG normalization. *J Clin Virol*. 2017 May; 90:40-45.

**Schleiss MR.** Cytomegalovirus in the neonate: immune correlates of infection and protection. *Clin Dev Immunol*. 2013; 501801.

**Schleiss MR, Berka U, Watson E, Aistleithner M, Kiefmann B, Mangeat B, Swanson EC, Gillis PA, Hernandez-Alvarado N, Fernandez-Alarcon C, Zabeli JC, Pinschewer DD, Lilja AE, Schwendinger M, Guirakhoo F, Monath TP, Orlinger KK.** Additive protection against congenital cytomegalovirus conferred by combined glycoprotein B/pp65 vaccination using a lymphocytic choriomeningitis virus vector. *Clin Vaccine Immunol*. 2017 Jan 5;24(1).

**Schoppel K, Kropff B, Schmidt C, Vornhagen R, Mach M.** The humoral immune response against human cytomegalovirus is characterized by a delayed synthesis of glycoprotein-specific antibodies. *J Infect Dis*. 1997 Mar; 175(3):533-44.

**Schwab I, Nimmerjahn F.** Intravenous immunoglobulin therapy: how does IgG modulate the immune system? *Nat Rev Immunol*. 2013 Mar;13(3):176-89.

**Seidel V, Feiterna-Sperling C, Siedentopf JP, Hofmann J, Henrich W, Bühner C, Weizsäcker K.** Intrauterine therapy of cytomegalovirus infection with valganciclovir: review of the literature. *Med Microbiol Immunol*. 2017 Oct; 206(5):347-354.

**Shedlock DJ, Talbott KT, Wu SJ, Wilson CM, Muthumani K, Boyer JD, Sardesai NY, Awasthi S, Weiner DB.** Vaccination with synthetic constructs expressing cytomegalovirus immunogens is highly T cell immunogenic in mice. *Hum Vaccin Immunother*. 2012 Nov 1; 8(11):1668-81.

**Shimamura M, Mach M, Britt WJ.** Human cytomegalovirus infection elicits a glycoprotein M (gM)/gN-specific virus-neutralizing antibody response. *J Virol*. 2006 May;80(9):4591-600.

**Sinzger C, Eberhardt K, Cavignac Y, Weinstock C, Kessler T, Jahn G, Davignon JL.** Macrophage cultures are susceptible to lytic productive infection by endothelial-cell-propagated human cytomegalovirus strains and present viral IE1 protein to CD4+ T cells

despite late downregulation of MHC class II molecules. *J Gen Virol.* 2006 Jul; 87(Pt 7):1853-62.

**Sinzger C, Schmidt K, Knapp J, Kahl M, Beck R, Waldman J, Hebart H, Einsele H, Jahn G.** Modification of human cytomegalovirus tropism through propagation in vitro is associated with changes in the viral genome. *J Gen Virol.* 1999 Nov; 80 (Pt 11):2867-77.

**Sinzger C, Plachter B, Grefte A, The TH, Jahn G.** Tissue macrophages are infected by human cytomegalovirus in vivo. *J Infect Dis.* 1996 Jan;173(1):240-5.

**Sinzger C, Grefte A, Plachter B, Gouw AS, The TH, Jahn G.** Fibroblasts, epithelial cells, endothelial cells and smooth muscle cells are major targets of human cytomegalovirus infection in lung and gastrointestinal tissues. *J Gen Virol.* 1995 Apr; 76 (Pt 4):741-50.

**Sinziger C, Jahn G.** Human cytomegalovirus cell tropism and pathogenesis. *Intervirology.* 1996; 39(5-6):302-19.

**Smith LR, Wloch MK, Chaplin JA, Gerber M, Rolland AP.** Clinical development of a cytomegalovirus DNA vaccine: from product concept to pivotal phase 3 trial. *Vaccines (Basel).* 2013 Sep 25; 1(4):398-414.

**Smith PD, Shimamura M, Musgrove LC, Dennis EA, Bimczok D, Novak L, Ballestas M, Fenton A, Dandekar S, Britt WJ, Smythies LE.** Cytomegalovirus enhances macrophage TLR expression and MyD88-mediated signal transduction to potentiate inducible inflammatory responses. *J Immunol.* 2014 Dec 1; 193(11):5604-12.

**Smith MG.** Propagation in tissue cultures of a cytopathogenic virus from human salivary gland virus (SGV) disease. *Proc Soc Exp Biol Med.* 1956; 92: 424-430.

**Snaar SP, Vincent M, Dirks RW.** RNA polymerase II localizes at sites of human cytomegalovirus immediate-early RNA synthesis and processing. *J Histochem Cytochem.* 1999 Feb; 47(2):245-54.

**Spiller OB, Hanna SM, Devine DV, Tufaro F.** Neutralization of cytomegalovirus virions: the role of complement. *J Infect Dis.* 1997 Aug;176(2):339-47.

**Stacey MA, Marsden M, Pham N TA, Clare S, Dolton G, Stack G, Jones E, Klenerman P, Gallimore AM, Taylor PR, Snelgrove RJ, Lawley TD, Dougan G, Benedict CA, Jones SA, Wilkinson GW, Humphreys IR.** Neutrophils recruited by IL-22 in peripheral tissues function as TRAIL-dependent antiviral effectors against MCMV. *Cell Host Microbe.* 2014 Apr 9;15(4):471-83.

**Stagno S, Pass RF, Dworsky ME, Henderson RE, Moore EG, Walton PD, Alford CA.** Congenital cytomegalovirus infection: The relative importance of primary and recurrent maternal infection. *N Engl J Med.* 1982 Apr 22;306(16):945-9.

**Stegmann C, Abdellatif ME, Laib Sampaio K, Walther P, Sinzger C.** Importance of Highly Conserved Peptide Sites of Human Cytomegalovirus gO for Formation of the gH/gL/gO Complex. *J Virol.* 2016 Dec 16; 91(1).

**Stern M, Elsässer H, Hönger G, Steiger J, Schaub S, Hess C.** The number of activating KIR genes inversely correlates with the rate of CMV infection/reactivation in kidney transplant recipients. *Am J Transplant.* 2008; 8:1312–1317.

**Stern-Ginossar N, Weisburd B, Michalski A, Le VT, Hein MY, Huang SX, Ma M, Shen B, Qian SB, Hengel H, Mann M, Ingolia NT, Weissman JS.** Decoding human cytomegalovirus. *Science.* 2012 Nov 23; 338(6110):1088-93.

**Stinski MF, Thomsen DR, Stenberg RM.** Organization and expression of the immediate early genes of human cytomegalovirus. *J Virol.* 1983; 46: 1-14.

**Tabata T, Kawakatsu H, Maidji E, Sakai T, Sakai K, Fang-Hoover J, Aiba M, Sheppard D, Pereira L.** Induction of an epithelial integrin alphavbeta6 in human cytomegalovirus-infected endothelial cells leads to activation of transforming growth factor-beta1 and increased collagen production. *Am J Pathol.* 2008 Apr; 172(4):1127-40.

**Tarragó D, Quereda C, Tenorio A.** Different cytomegalovirus glycoprotein B genotype distribution in serum and cerebrospinal fluid specimens determined by a novel multiplex nested PCR. *J Clin Microbiol.* 2003 Jul; 41(7):2872-7.

**Thurmann PA, Sonnenburg-Chatzopoulos C, Lissner R.** Pharmacokinetic characteristics and tolerability of a novel intravenous immunoglobulin preparation. *Eur J Clin Pharmacol* 1995; 49:237-242.

**Tooze J, Hollinshead M, Reis B, Radsak K, Kern H.** Progeny vaccinia and human cytomegalovirus particles utilize early endosomal cisternae for their envelopes. *Eur J Cell Biol.* 1993 Feb; 60(1):163-78.

**Tugizov S, Maidji E, Xia J, Zheng Z, Pereira L.** Human cytomegalovirus glycoprotein b contains autonomous determinants for vectorial targeting to apical membranes of polarized epithelial cells. *J Virol.* 1998 Sep; 72(9):7374-86.

**van de Berg PJ, Heutinck KM, Raabe R, Minnee RC, Young S., van Donselaar-van der Pant KA, Bemelman FJ, van Lier RA, ten Berge IJ.** Human cytomegalovirus induces systemic immune activation characterized by a type 1 cytokine signature. *J Infect Dis.* 2010 Sep 1; 202(5):690-9.

**Vanarsdall AL, Chase MC, Johnson DC.** Human cytomegalovirus glycoprotein gO complexes with gH/gL, promoting interference with viral entry into human fibroblasts but not entry into epithelial cells. *J Virol.* 2011 Nov;85(22):11638-45.

**Varnum SM, Streblow DN, Monroe ME, Smith P, Auberry KJ, Pasa-Tolic L, Wang D, Camp DG, Rodland K, Wiley S., Brit W, Shenk T, Smith RD, Nelson JA.** Identification of proteins in human cytomegalovirus (HCMV) particles: the HCMV proteome. *J Virol.* 2004 Oct; 78(20):10960-6.

**Vauloup-Fellous C, Picone O, Cordier AG, Parent-du-Châtelet I, Senat MV, Frydman R, Grangeot-Keros L.** Does hygiene counseling have an impact on the rate of HCMV primary infection during pregnancy? Results of a 3-year prospective study in a French hospital. *J Clin Virol.* 2009 Dec;46 Suppl 4:S49-53.

**Visentin S, Manara R, Milanese L, Da Roit A, Forner G, Salviato E.** Early Primary Cytomegalovirus Infection in Pregnancy: Maternal Hyperimmunoglobulin Therapy Improves Outcomes Among Infants at 1 Year of Age. *Clin Infect Dis.* 2012 Aug;55(4):497-503. doi: 10.1093/cid/cis423.

**Vochem M, Hamprecht K, Jahn G, Speer CP.** Transmission of cytomegalovirus to preterm infants through breast milk. *Pediatr Infect Dis J.* 1998 Jan; 17(1):53-8.

**Wang D, Shenk T.** Human cytomegalovirus virion protein complex required for epithelial and endothelial cell tropism. *Proc Natl Acad Sci U S A.* 2005 Dec 13; 102(50):18153-8.

**Wang D, Shenk T.** Human cytomegalovirus UL131 open reading frame is required for epithelial cell tropism. *J Virol.* 2005 Aug; 79(16):10330-8.

**Weller TH, Craig JM, Macauley JC, Wirth P.** Isolation of intranuclear inclusion producing agents from infants with illnesses resembling cytomegalic inclusion disease. *Proc Soc Exp Biol Med.* 1957 Jan; 94(1):4-12.

**Wilkinson GW, Davison AJ, Tomasec P, Fielding CA, Aicheler R, Murrell I, Seirafian S, Wang EC, Weekes M, Lehner PJ, Wilkie GS, Stanton RJ.** Human cytomegalovirus: taking the strain. *Med Microbiol Immunol.* 2015 Jun; 204(3):273-84.

**Wilson SR, Wilson JH, Buonocore L, Palin A, Rose JK, Reuter JD.** Intranasal immunization with recombinant vesicular stomatitis virus expressing murine cytomegalovirus glycoprotein B induces humoral and cellular immunity. *Comp Med.* 2008 Apr; 58(2):129-39.

**Zaia JA.** Prevention and treatment of cytomegalovirus pneumonia in transplant recipients. *Clin Infect Dis.* 1993 Nov; 17 Suppl 2:S392-9.

**Zhong J, Rist M, Cooper L, Smith C, Khanna R.** Induction of pluripotent protective immunity following immunisation with a chimeric vaccine against human cytomegalovirus. *PLoS One.* 2008 Sep 22;3(9):e3256.

**Zhou M, Yu Q, Wechsler A, Ryckman BJ.** Comparative analysis of gO isoforms reveals that strains of human cytomegalovirus differ in the ratio of gH/gL/gO and gH/gL/UL128-131 in the virion envelope. *J Virol.* 2013; 87(17):9680–9690.

**Zhou M, Lanchy JM, Ryckman BJ.** Human Cytomegalovirus gH/gL/gO Promotes the Fusion Step of Entry into All Cell Types, whereas gH/gL/UL128-131 Broadens Virus Tropism through a Distinct Mechanism. *J Virol.* 2015 Sep; 89(17):8999-9009.

**Zydek M, Petitt M, Fang-Hoover J, Adler B, Kauvar LM, Pereira L, Tabata T.** HCMV infection of human trophoblast progenitor cells of the placenta is neutralized by a human monoclonal antibody to glycoprotein B and not by antibodies to the pentamer complex. *Viruses.* 2014 Mar 19; 6(3):1346-64.



## 6.2 Uniform Resource Locator

URL: Celeromics documents (date 02.08.2018):

<http://celeromics.com/en/resources/docs/Articles/Cell-counting-Neubauer-chamber.pdf>

URL: Roche HCMV IgG (date: 06.09.2018):

[http://www.rochecanada.com/content/dam/roche\\_canada/en\\_CA/documents/package\\_inserts/HCMV%20IgG-04784596190-EN-CAN.pdf](http://www.rochecanada.com/content/dam/roche_canada/en_CA/documents/package_inserts/HCMV%20IgG-04784596190-EN-CAN.pdf)

URL: Roche HCMV IgM (date: 06.06.2018):

[http://www.rochecanada.com/content/dam/roche\\_canada/en\\_CA/documents/package\\_inserts/HCMVIGM-04784618190-En-V8-Can.pdf](http://www.rochecanada.com/content/dam/roche_canada/en_CA/documents/package_inserts/HCMVIGM-04784618190-En-V8-Can.pdf)

URL: Model of a HCMV virion (date: 04.07.2018)

[http://education.expasy.org/images/Herpesviridae\\_virion.jpg](http://education.expasy.org/images/Herpesviridae_virion.jpg)

URL: EliSPOT test principle (date:05.05.2018)

<http://www.mstechno.co.jp/html/protocolFile/ms56bd9af284fb2/IFNg%E3%83%88%E3%83%A9%E3%82%A4%E3%82%A2%E3%83%AB%E3%82%AD%E3%83%83%E3%83%88.pdf>